PhD THESIS OF THE UNIVERSITY OF Lille

University of Lille

Ecole Doctorale Biologie Santé
EDBSL

PhD Specialization: Structural Biology
Discipline: Molecular and Cellular Aspects of Biology

Public defense on November 6, 2024, by:

Lea El Hajjar

Post-Translational Modifications and Their Role in Tau Aggregation in Alzheimers Disease

---

In front of the jury composed of:

Pascale Barbier Professor, Aix Marseille Université	**Reviewer**
Stephanie Olivier-Van Stichelen Associate Professor, Medical College of Wisconsin	**Reviewer**
Cláudio Gomes Professor, University of Lisbon	**Examiner**
Ikram El Yazidi-Belkoura Professor, University of Lille	**Examiner**
Caroline Smet-Nocca Professor, University of Lille	**Thesis Supervisor**

THÈSE DE DOCTORAT DE L'UNIVERSITÉ DE Lille

Université de Lille

École Doctorale Biologie Santé
EDBSL

Spécialité : Biologie Structurale
Discipline : Aspects Moléculaires et Cellulaires de la Biologie

Soutenue publiquement le 6 novembre 2024 par :

Léa El Hajjar

Modifications Post-Traductionnelles et leur Rôle dans l'Agrégation de Tau dans la Maladie dAlzheimer

---

Devant le jury composé de :

Pascale Barbier Professeure, Aix Marseille Université	**Rapporteur**
Stephanie Olivier-Van Stichelen Professeure Associée, Medical College of Wisconsin	**Rapporteur**
Cláudio Gomes Professeur, Université de Lisbonne	**Examinateur**
Ikram El Yazidi-Belkoura Professeure, Université de Lille	**Examinatrice, Présidente du jury**
Caroline Smet-Nocca Professeure, Université de Lille	**Directrice de thèse**

Part I

Acknowledgments

I would like to take this opportunity to express my heartfelt thanks to those who have supported and guided me throughout my PhD journey.

I would like to begin by expressing my sincere gratitude to the jury members for agreeing to evaluate my thesis: Dr. Pascale Barbier and Dr. Stephanie Olivier-Van Stichelen, as reviewers, and Pr. Cláudio Gomes and Dr. Ikram Yazidi, as examiners.

My thanks go to Isabelle Landrieu, the head of the team. I am especially grateful for the opportunity she gave me by being the first to interview and accept me for this position. Her leadership, and encouragement have enriched my experience, providing me with numerous opportunities to attend conferences and participate in collaborations.

I would also like to express my deepest gratitude to my PhD supervisor, Pr. Caroline Smet-Nocca, for always being there to listen and believe in me, even during times when progress seemed slow. Her encouragement, valuable advice, and support made a big difference, giving me the trust and opportunities to work on multiple projects under her guidance. She consistently cared about my professional growth, helping me gain more experience and supporting my efforts to secure a post-PhD position. She is truly an exceptional supervisor.

Special thanks to the Dr. Elian Dupré, the hero of the lab, who always had a line of people waiting to seek his advice on experiments. He dedicated so much time to explaining experiments to me, listening during tough times, and always made every effort to save our experiments. Your guidance to help made a significant impact on my work.

I want to thank the NMR team, François-Xavier Cantrelle and Emmanuelle Boll, for all the time we spent together explaining protein NMR, assignments, and everything I needed for my thesis. Thank you F-X for the countless hours you dedicated to ensuring I truly understood the workings and assignments of NMR spectra. Your patience and support have been invaluable in my training and the progress of my work.

I would like to thank Dr. Clément Danis for all his advice and for sharing his personal experiences as a previous PhD student. I appreciate your efforts to help me whenever I faced a problem, and I am grateful for our discussions and the moments we shared while talking about and analyzing results on LLPS.

Thanks also to Dr. Xavier Hanoulle for his advice, and relevant comments.

Also thank you Justine, a truly invaluable presence in the lab. She is always there to lend a helping hand to everyone and consistently lifts my spirits whenever I am feeling tired or stressed.

I would like to thank Pr. Cláudio Gomes and his team at the Protein Folding and Misfolding Lab in Lisbon. First, I would like to express my gratitude to Cláudio Gomes, with whom I spent three weeks in his lab, learning various techniques. I am also grateful to Margarida C. Simões for her assistance during this internship and for training me in the use of AmyloFit. A special thanks to Guilherme Morera, who greatly helped me understand the mechanism of LLPS and for the good times we shared during his internship in Lille. I would also like to thank the entire team of Cláudio Gomes for all the meals we shared and for our engaging discussions.

I would like to thank Pr. Christian Hackenberger and Bingjia Yan from the Chemical Biology II Lab at the FMP in Berlin for collaborating with us and providing the opportunity to work together on the

semi-synthetic Tau project. Thank you, Bingjia, for the moments we shared discussing Tau aggregation and the benefits of using semi-synthetic Tau. It was a pleasure working with you.

Thanks to the incredible "pause café" team, whose support has been invaluable throughout my PhD journey. Clarisse, thank you for always being there to listen, even when I'm stressed in the office. Marine, you've been my lifesaver whenever I needed help. To Lucy, my PhD partner, with whom I've shared so many wonderful memories in training sessions, conferences, practical schools, and stressful timeswe truly made the best of every moment together, and I wish you all the best for the remainder of your PhD journey. Thanks to Marion, who has always been there to lend an ear and is always ready for a coffee break. And of course, to Bastien, our "friend who doesnt exist" but was always there to disrupt our experiments and never missed a chance to leave a lab coat on my bench. Beyond being coworkers, I had the chance to make wonderful friends and create lasting memories.

I would like to thank Frédérique Dewitte for our discussions and her help with the mission orders.

I would like to sincerely thank the Integrative Structural Biology team for their support throughout my journey.

I would like to thank Nicolas Barois for the countless hours we spent together at the electron microscope and for his explanations of its use and operation.

I want to thank my special friends in Lebanon, who are not just friends but also family, for supporting me throughout my entire journey. Specially my girls, Nour, Yara and rim! Your support from start to finish means the world to me, and I love you all.

I want to thank my cousins, whom I call my sistersRim, Douaa, and Layane. You are my source of strength and have been there for me more than I have been for myself. Your love and support are incredibly special to me, and I am deeply grateful for everything youve done.

I would also like to thank my special cousin, and big brother, Jad. You have always been like a second brother to me, constantly caring and ensuring that I receive the best education.

I would like to express my heartfelt gratitude to my incredible friends in Lille: Mahdi, Ramy, Tamara, Mohamad, Khaled, Salmen, Céline, Hussein, Wassim, Rami, Moussa, Dalia and Sara. You have been my pillars of support, always there whenever I needed help, and you helped me survive many stressful moments. Thank you for the countless memories we've shared, for all our evenings together, and for your love and friendship. You will forever hold a special place in my life, and I am deeply grateful to each of you for making this journey so much more bearable and meaningful.

I would like to thank my best friend and future Dr. Farah Mansour. Your support and encouragement have been an essential part of this journey. You have always been there through every challenge, offering advice and motivation. I am incredibly fortunate to have you by my side, and I look forward to seeing all the incredible things you will achieve in your own career. Thank you for being an irreplaceable part of my life.

I would like to thank my uncle Haitham for his constant support and for always following my scientific journey.

A special thank you to my aunt, Dana El Hajjar, for her generosity, wise advice, and support throughout this journey. You have been like a sister and a second mother in my life, someone I can always

count on without a second thought. Your kindness and willingness to listen have been a great comfort to me. I love you so much, Aamto!

My deepest gratitude goes to my parents, my heros, Badia and Louay, whose support and encouragement have been the cornerstone of my journey. Their belief in my potential, even during the most challenging times, has been a source of motivation. From nurturing my curiosity in science at a young age to standing by me through countless late nights and setbacks, they have been my greatest champions. Their sacrifices, guidance, and endless patience have made this achievement possible. Thank you for teaching me the values of perseverance, dedication, and resilience. This accomplishment is as much yours as it is mine.

My gratitude goes also my brother, Chafic, who has always been there to help me during my most difficult moments. He has consistently offered his advice, listened to me when I was stressed, and always made every effort to make me happy.

Finally, I would like to express my deepest gratitude to my (we can finally now say) fiancé, Nadim, whose support, encouragement, and understanding have been invaluable throughout this journey. You are always here to help me, and to solve my problems. Your belief in me, even during the most challenging times, has been a constant source of motivation. Thank you for your patience, love, and for always being my greatest cheerleader. I couldnt have done this without you by my side.

I would like to thank the Labex Distalz for funding my three years of PhD studies. I am also very grateful to the Lille Doctoral School for the wide range of training opportunities provided throughout this journey. A special thanks to the Graduate School, Precision Health for the valuable training and seminars, as well as for the financial support provided for part of my internship in Lisbon.

I dedicate my thesis to my beloved uncle, Khalo Bassel. I wish you were here today to see me achieve my greatest dream. I know you would have been so proud and happy for me. I love you and miss you dearly, Khalo Bassel.

"Perseverance is the key to success"

Part II

Abstract

Abstract

Alzheimers disease (AD) is a neurodegenerative disorder characterized by the accumulation of amyloid plaques and neurofibrillary tangles composed of hyperphosphorylated Tau protein. Tau aggregation plays a central role in the progression of tauopathies, a group of age-related neurodegenerative disorders, by disrupting microtubule stability and promoting the spread of Tau pathology through seeding mechanisms. Glycogen synthase kinase 3 beta (GSK3β) is one of the key kinases implicated in Tau hyperphosphorylation, and its dysregulation is closely associated with the pathogenesis of AD. This study explores the complex regulation of GSK3β activity through post-translational modifications, including phosphorylation and O-GlcNAcylation, and their impact on Tau function and aggregation. We found that Akt inhibits GSK3β kinase activity in a phosphorylation-independent manner. Akt-mediated phosphorylation at Ser9 inhibits GSK3β activity on unprimed Tau substrates, while selectively restoring its activity on primed Tau, highlighting a differential regulatory mechanism. GSK3β is also extensively O-GlcNAcylated at multiple sites, including Ser9, which does not significantly alter kinase activity but reduces Ser9 phosphorylation by Akt, indicating a crosstalk between these modifications that may influence GSK3β function.

Additionally, we investigated the functional and seeding properties of Tau fragments, R2Ct and R3Ct, which encompass key aggregation-prone regions and the PHF-1 epitope (S396, S400, S404). The R3Ct fragment demonstrated a greater loss of microtubule-stabilizing function and an increased propensity for toxic seeding compared to R2Ct, with these effects being exacerbated by GSK3β phosphorylation. We further tackled the impact of specific phosphorylation events on Tau behavior, through a semi-synthetic strategy to produce homogeneous, site-specifically phosphorylated full-length 2N4R Tau, including PHF1-3P Tau with three phosphorylation sites (pS396, pS400, pS404). Our results indicate that PHF1-3P Tau significantly impairs microtubule assembly and, while reducing heparin-induced aggregation, promotes the formation of long PHF-like fibrils via cross-seeding.

Furthermore, we explored the use of nanobodies as potential therapeutic agents for inhibiting Tau aggregation. Nanobodies, which are single-domain antibodies derived from camelid species, offer unique advantages due to their small size, high stability, and ability to bind to specific epitopes with high affinity. By targeting key regions within Taus intrinsically disordered domains, nanobodies can effectively inhibit aggregation and prevent the formation of neurofibrillary tangles. In our studies, we identified nanobodies that specifically bind to the PHF6 and PHF6* motifs within Tau, critical sites for fibril formation, and demonstrated that these nanobodies can reduce Tau aggregation *in vitro*.

This research provides critical insights into the regulation of GSK3β by phosphorylation and O-GlcNAcylation to modulate Tau hyperphosphorylation, the differential effects of Tau phosphorylation on seeding and aggregation, and the use of semi-synthetic approaches to study complex PTM interactions on Tau. Additionally, the identification of nanobodies as inhibitors of Tau aggregation opens new avenues for therapeutic intervention in AD. These findings enhance our understanding of the molecular mechanisms driving Tau pathology in AD and highlight potential therapeutic targets for mitigating Tau aggregation and propagation in tauopathies.

Résumé

La maladie d'Alzheimer (AD) est une maladie neurodégénérative caractérisée par l'accumulation de plaques amyloïdes et d'enchevêtrements neurofibrillaires composés de la protéine Tau hyperphosphorylée. L'agrégation de Tau joue un rôle central dans la progression des tauopathies, un groupe de troubles neurodégénératifs liés à l'âge, en perturbant la stabilité des microtubules et en favorisant la propagation de la pathologie Tau par des mécanismes de seeding. La glycogène synthase kinase 3 bêta (GSK3β) est l'une des kinases clés impliquées dans l'hyperphosphorylation de Tau, et sa dérégulation est étroitement associée à la pathogénèse de l'AD. Cette étude explore la régulation complexe de l'activité de GSK3β par des modifications post-traductionnelles, y compris la phosphorylation et l'O-GlcNAcylation, et leur impact sur la fonction et l'agrégation de Tau. Nous avons découvert que la phosphorylation de GSK3β par Akt sur Ser9 inhibe l'activité de GSK3β sur les substrats Tau non-primés, tout en restaurant sélectivement son activité sur les substrats primés, soulignant un mécanisme de régulation différentiel. GSK3β est également fortement O-GlcNAcylée à plusieurs sites, y compris Ser9, ce qui n'altère pas significativement l'activité kinase mais réduit la phosphorylation de Ser9 par Akt, indiquant une interaction complexe entre ces modifications qui pourrait influencer la fonction de GSK3β.

En outre, nous avons étudié les propriétés fonctionnelles et de seeding des fragments de Tau, R2Ct et R3Ct, qui englobent des régions critiques pour l'agrégation et l'épitope PHF-1 (S396, S400, S404). Le fragment R3Ct a montré une plus grande perte de fonction de stabilisation des microtubules et une propension accrue à l'agrégation toxique par seeding par rapport au fragment R2Ct, ces effets étant exacerbés par la phosphorylation de GSK3β. Pour mieux comprendre l'impact des événements de phosphorylation spécifiques sur le comportement de Tau, nous avons développé une stratégie semi-synthétique pour produire une protéine Tau 2N4R complète et homogène, phosphorylée de manière site-spécifique, incluant la Tau PHF1-3P avec trois sites de phosphorylation (pS396, pS400, pS404). Nos résultats indiquent que Tau PHF1-3P altère significativement l'assemblage des microtubules et, tout en réduisant l'agrégation induite par l'héparine, favorise la formation de longues fibrilles de type PHF via le cross-seeding.

De plus, nous avons exploré l'utilisation de nanocorps comme agents thérapeutiques potentiels pour inhiber l'agrégation de Tau. Les nanocorps, qui sont des anticorps à domaine unique dérivés d'espèces camélidés, offrent des avantages uniques grâce à leur petite taille, leur grande stabilité et leur capacité à se lier à des épitopes spécifiques avec une grande affinité. En ciblant des régions clés au sein des domaines intrinsèquement désordonnés de Tau, les nanocorps peuvent inhiber efficacement l'agrégation et empêcher la formation d'enchevêtrements neurofibrillaires. Dans nos études, nous avons identifié des nanocorps qui se lient spécifiquement aux motifs PHF6 et PHF6* au sein de Tau, des sites critiques pour la formation des fibrilles, et démontré que ces nanocorps peuvent réduire l'agrégation de Tau *in vitro*.

Cette recherche apporte des connaissances essentielles sur la régulation de GSK3β par phosphorylation et O-GlcNAcylation, les effets différentiels de la phosphorylation de Tau sur le seeding et l'agrégation, et l'utilisation d'approches semi-synthétiques pour étudier les interactions complexes des modifications post-traductionnelles sur Tau. De plus, l'identification des nanocorps comme inhibiteurs de l'agrégation de Tau ouvre de nouvelles perspectives pour l'intervention thérapeutique dans l'AD. Ces résultats améliorent notre compréhension des mécanismes moléculaires conduisant à la pathologie Tau dans l'AD et mettent en évidence des cibles thérapeutiques potentielles pour atténuer l'agrégation et la progression de Tau dans les tauopathies.

Contents

List of Figures

List of Tables

List of Abbreviations

MAPT	Microtubule-Associated Protein Tau
Aβ	Amyloid Beta Peptide
AcetylCoA	Acetyl-coenzyme A
AD	Alzheimer's disease
AGD	Argyrophilic grain disease
APP	Amyloid Precursor Protein
ARTAG	Aging-Related Tau Astrogliopathy
BBB	Blood-Brain Barrier
BiFC	Bimolecular Fluorescence Complementation
CAA	Cerebral Amyloid Angiopathy
CBD	Corticobasal degeneration
CDK	Cyclin-dependent kinase
CNS	Central Nervous System
Cryo-EM	Cryo-Electron Microscopy
EPL	Expressed Protein Ligation
ETD	Electron Transfer Dissociation
FRET	Fluorescence Resonance Energy Transfer
FTA	Filter Trap Assay
GalNAz	N-azidoacetylglucosamine
GGT	Globular glial tauopathy
GSK3β	Glycogen synthase kinase 3 beta
GWAS	Genome-Wide Association Studies
HCD	Higher-energy Collisional Dissociation
IDP	Intrinsically Disordered Protein
IDR	Intrinsically Disordered Region

kDa	kiloDalton
LC-MS/MS	Liquid Chromatography-Tandem Mass Spectrometry
LLPS	Liquid Liquid Phase Separation
MALDI-TOF	Matrix-Assisted Laser Desorption - Ionisation-Time of Flight
MS	Mass Spectrometry
NCL	Native Chemical Ligation
NFT	Neurofibrillary tangles
NP	Neuritic Plaques
NPFs	Narrow Pick Filaments
OBP	OGT Binding Peptide
OGA	O-GlcNAcase
OGA-L	OGA-Long
OGA-S	OGA-Short
OGT	O-GlcNAc transferase
PCA	Posterior Cortical Atrophy
PD	Pick disease
PET	Positron-emission tomography
PHF	Paired Helical Filament
PKB	Protein Kinase B
PSP	Progressive supranuclear palsy
PTMs	Post-Traductional Modifications
SDS	Sodium Dodecyl-Sulfate
SP	senile plaques
TAMRA	Tetramethylrhodamine
Tau	Tubulin Associated Unit
TEM	Transmission electron microscopy
TEnTR	Trans-Entorhinal Region
ThT	Thioflavin T
UDP-GlcNAc	Uridine Diphosphate N-acetylglucosamine
VHH	Variable Heavy domain of Heavy chain
WHO	World Health Organization
WPFs	Wide Pick Filaments

Table 1: Amino Acids and Their Codes

Amino Acid	Three-Letter Code	One-Letter Code
Alanine	Ala	A
Arginine	Arg	R
Asparagine	Asn	N
Aspartic Acid	Asp	D
Cysteine	Cys	C
Glutamine	Gln	Q
Glutamic Acid	Glu	E
Glycine	Gly	G
Histidine	His	H
Isoleucine	Ile	I
Leucine	Leu	L
Lysine	Lys	K
Methionine	Met	M
Phenylalanine	Phe	F
Proline	Pro	P
Serine	Ser	S
Threonine	Thr	T
Tryptophan	Trp	W
Tyrosine	Tyr	Y
Valine	Val	V

Part III

General Introduction to Protein Biochemistry

1. Protein biochemistry

Proteins are complex macromolecules essential to life, often constituting more than 50 % of the dry weight of living organisms. They play a crucial role in a wide range of biological processes, from maintaining cellular structure to facilitating biochemical reactions. Proteins are composed of one or more polypeptide chains, which are copolymers made up of approximately 20 different amino acids known as "proteinogenic" amino acids, linked together by peptide bonds.
The structural organization of proteins is a key aspect of their function and is categorized into several levels: primary, secondary, tertiary, and quaternary structures. The three-dimensional (3D) structure of proteins is determined by the interactions between the unique side chains (R groups) of the amino acids, and this 3D structure is intimately linked to the protein's specific function.

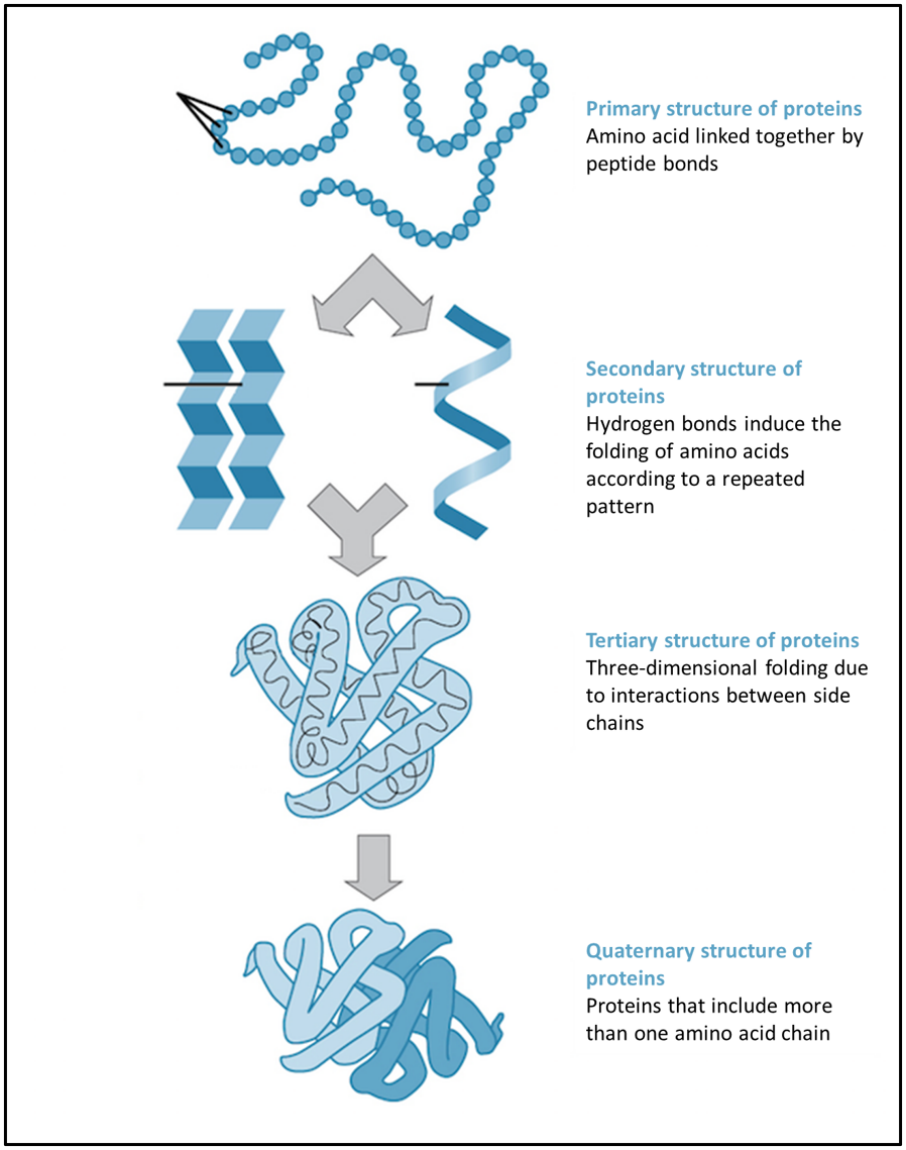

Figure 1: The amino acid chain can be analyzed to predict the secondary, tertiary, and quaternary structures of a protein

Proteins exhibit a remarkable diversity in their roles within biological systems. They can function as enzymes, catalyzing biochemical reactions; as hormones, regulating various physiological processes; as structural components, forming tissues; as transport molecules, carrying substances across cell membranes; and as defensive agents in the immune system, among other roles. The physicochemical properties of proteins, such as sizewhich can range from a few thousand to several million daltonssolubility, and isoelectric point, are determined by their specific amino acid composition and structural

conformation.
The study of protein biochemistry involves a range of techniques to explore the structure and function of these molecules. This includes methods for protein production, purification, and structural and functional characterization. Techniques like chromatography, electrophoresis, and mass spectrometry are commonly used to analyze proteins.
The biological importance of proteins is underscored by their involvement in nearly all cellular processes, making them fundamental to the understanding of life at the molecular level. The study of protein biochemistry is not only essential for basic biological research but also has significant applications in medicine, biotechnology, and industry. This field is continually evolving, integrating approaches from chemistry, biophysics, molecular biology, and cell biology to uncover the molecular mechanisms that underpin life Cuq 2024; Sanvictores and Farci 2024.
In this work, we will be focusing on one protein named Tau.

2. Regulation of Protein Expression

Protein expression regulation is a crucial process that allows cells within the same organism to express different sets of proteins despite having an identical genome. Epigenetic regulation modifies chromatin structure and gene accessibility to the transcriptional machinery, with key modifications including DNA methylation, where methyl groups are added to cytosines often associated with gene repression, and histone modifications such as acetylation, methylation, and phosphorylation, which influence DNA compaction and accessibility. These modifications can be inherited and are influenced by environmental factors, allowing cells to adapt (Ramírez-Clavijo and Montoya-Ortíz 2013). Transcriptional regulation is often the primary point of gene expression control, involving transcription factors that bind to specific DNA sequences called cis-regulatory elements, including promoters, which are sequences located upstream of a gene that initiate transcription, and enhancers, which increase transcription efficiency from a distance. Extracellular signals, such as hormones, can activate or inhibit these transcription factors, modulating gene expression in response to stimuli (Casamassimi and Ciccodicola 2019). Post-transcriptional regulation occurs after transcription, where mRNA undergoes various maturation and regulatory processes, such as splicing, which generates multiple protein isoforms from a single gene to enhance protein diversity, and mRNA stability, where the lifespan of mRNA in the cytoplasm affects protein production, with regulatory elements in the mRNA influencing its degradation (Zhao, Roundtree, and He 2017). Translational regulation is another critical regulatory point, particularly at the initiation of translation, which can be modulated by protein factors that bind to mRNA to either inhibit or stimulate translation, and regulatory RNAs, such as antisense RNAs or microRNAs, that can bind to mRNA and block translation. Translation consumes a significant amount of cellular energy, representing up to 90% of the energy used for protein synthesis, highlighting its regulatory importance (Sonenberg and Hinnebusch 2009). Cells also respond to internal and external signals through signaling pathways that modulate gene expression, activating transcription factors or directly influencing the translation machinery, for example, in response to stress, cells may induce the transcription of specific genes while globally inhibiting translation to prioritize proteins essential for survival.

3. Regulation Mechanisms of Post-Translational Modifications (PTMs)

Post-translational modifications (PTMs) are chemical changes that occur after protein synthesis. These modifications include phosphorylation, which involves adding phosphate groups often through kinases, altering enzymatic activity and protein function, such as the crucial role of eIF2-α phosphorylation in translation initiation. Acetylation of lysines affects protein interactions and stability, while ubiquitination marks proteins for degradation by the proteasome, regulating protein levels within the

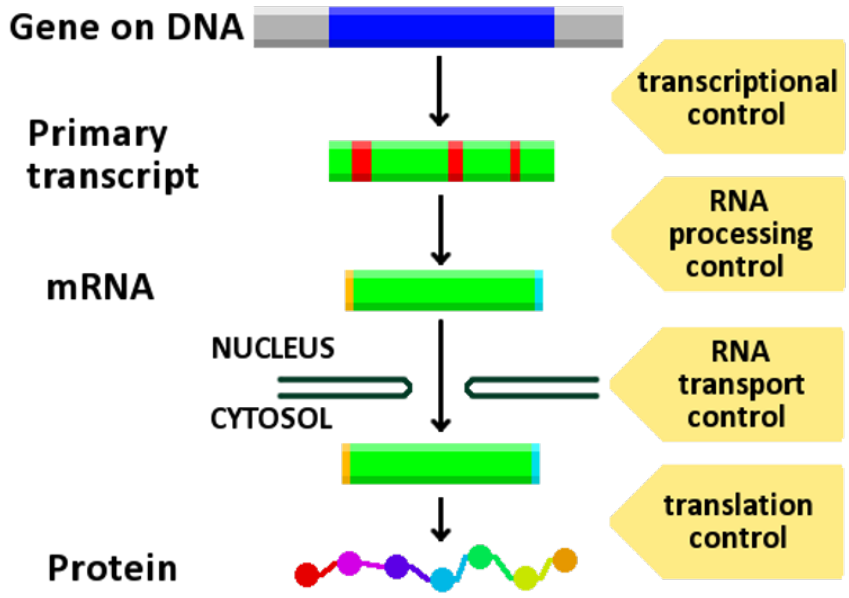

Figure 2: Regulation of gene expression

cell. Glycosylation, the addition of carbohydrate chains, impacts protein structure and function, particularly in cellular signaling. PTMs enable cells to rapidly respond to environmental changes without the need for new protein synthesis.

Cellular adaptability largely depends on the dynamic nature of PTMs. Cells can quickly adjust their responses to stimuli through rapid and reversible modifications of proteins. For instance, during cellular stress, specific proteins may be phosphorylated or dephosphorylated, altering their functions within minutes.

Characterizing PTMs presents several challenges. The complexity arises from multiple and interacting modifications, making it difficult to pinpoint the specific effects of each modification. Additionally, the dynamic nature of PTMs requires sensitive and rapid detection techniques to capture real-time changes. Cellular specificity further complicates the establishment of universal models, as responses to stimuli can vary significantly between different cell types.

4. The Relationship Between Protein Structure and Function

The relationship between the structure and function of proteins is fundamental in biology, as the specific three-dimensional shapes of proteins dictate their roles in cellular processes. Proteins are macromolecules composed of chains of amino acids that fold into specific three-dimensional structures. This structural complexity can be understood through four hierarchical levels: primary, secondary, tertiary, and quaternary structures. The primary structure refers to the linear sequence of amino acids in the polypeptide chain, which ultimately dictates how the protein will fold. Secondary structures, such as alpha helices and beta sheets, arise from local folding patterns stabilized by hydrogen bonds between backbone atoms. The tertiary structure represents the overall three-dimensional conformation of the entire polypeptide, driven by interactions among side chains, including hydrophobic interactions, ionic bonds, and disulfide bridges. Finally, the quaternary structure involves the assembly of multiple polypeptide subunits into a larger functional complex, as seen in proteins like hemoglobin (*Structure des protéines* 2024).

The function of a protein is intimately connected to its structure, as the shape and folding of a protein determine how it interacts with other molecules. For example, enzymes have active sites with specific

shapes that fit their substrates precisely, enabling them to catalyze chemical reactions with high specificity and efficiency. This specificity is a direct result of the proteins three-dimensional conformation, which is tailored to recognize and bind certain molecules while excluding others. Similarly, antibodies have variable regions that bind to specific antigens, and their structure is key to their function in the immune response. If the protein's structure is disrupted, such as through denaturation caused by heat, pH changes, or chemical agents, the protein often loses its functional capabilities. This loss of function upon structural alteration underscores the importance of maintaining the integrity of protein folding for biological activity (*Structure des protéines* 2024; *Protein Structural Analysis* 2019).

Structural similarity often correlates with functional similarity, a concept known as structural homology. Proteins with similar amino acid sequences and three-dimensional structures usually perform similar functions, even if they are found in different organisms. This allows scientists to predict the function of newly discovered proteins based on their resemblance to known proteins. Structural biology techniques such as X-ray crystallography, nuclear magnetic resonance (NMR) spectroscopy, and cryo-electron microscopy are invaluable for determining the structures of proteins and understanding their functions at the molecular level. Insights gained from these techniques can help elucidate how proteins interact with other biomolecules, such as DNA, RNA, lipids, and other proteins (*Protein Structural Analysis* 2019).

Understanding the structure-function relationship in proteins is crucial for therapeutic development. Detailed knowledge of protein structures enables the design of drugs that specifically target proteins involved in disease processes. For example, enzyme inhibitors can be crafted to bind precisely to the active sites of enzymes, thereby blocking their activity. This approach is widely used in the development of treatments for diseases such as cancer, where overactive enzymes drive cell proliferation, or in infectious diseases, where viral or bacterial enzymes are targeted to inhibit pathogen replication. By studying the structures of disease-related proteins, researchers can develop molecules that precisely interfere with their function, offering a pathway to highly specific and effective therapies (*Structure des protéines* 2024).

This section underscores the importance of protein structure in determining function and highlights how structural insights can drive scientific and medical advancements. Understanding the intricate details of protein folding, stability, and interaction capabilities not only reveals fundamental biological principles but also opens avenues for targeted therapeutic interventions.

5. Structural Biology and Determining Protein Structure

Structural biology is a crucial field dedicated to understanding the three-dimensional architecture of biological macromolecules, including proteins and nucleic acids. Determining protein structures provides insights into their functions, interactions, and roles in various biological processes. A variety of techniques are employed to achieve high-resolution structures, each with its own strengths, applications, and limitations.

X-ray crystallography is a widely used method that relies on the diffraction of X-rays through crystallized proteins to determine atomic positions. The resulting diffraction pattern is analyzed to generate electron density maps, from which the positions of atoms are deduced, providing detailed insights into the proteins three-dimensional structure. This technique excels at revealing high-resolution structures of individual proteins and complexes, but it requires high-quality crystals, which can be challenging to obtain for certain proteins, such as membrane proteins or highly flexible proteins.

Nuclear Magnetic Resonance (NMR) spectroscopy leverages the magnetic properties of atomic nuclei to determine the structure of proteins in solution. By applying a strong magnetic field and radiofrequency pulses, NMR detects interactions between atomic nuclei, providing information on distances and angles between them. This allows the determination of protein structures in conditions that closely mimic the physiological environment, making it ideal for studying protein dynamics, conformational changes, and interactions in solution. However, NMR is limited by the size of the protein; it becomes less effective for larger proteins or complexes due to spectral complexity and reduced signal quality.

Cryo-electron microscopy (cryo-EM) has gained prominence as a powerful tool for determining the structures of large and complex macromolecular assemblies without the need for crystallization. In cryo-EM, proteins are rapidly frozen in a thin layer of vitreous ice, preserving their native conformation, and then imaged using a beam of electrons. High-resolution structures are obtained by averaging thousands of images, allowing the visualization of proteins at near-atomic resolution, especially suited for large complexes, membrane proteins, and transient states. The preparation of cryo-EM samples can be technically demanding, and the interpretation of data requires sophisticated computational techniques.

Neutron diffraction uses neutrons instead of X-rays to probe protein structures. Neutrons interact with atomic nuclei rather than the electron cloud, making them particularly sensitive to light atoms such as hydrogen, which are often invisible in X-ray diffraction data. This technique is valuable for studying hydrogen bonding and hydration shells around proteins, but it requires specialized facilities like nuclear reactors or spallation sources, making it less accessible than other methods.

Small-angle X-ray scattering (SAXS) is a solution-based technique used to obtain low-resolution information about the overall shape, size, and conformational changes of proteins in solution. SAXS measures the scattering of X-rays at small angles as they pass through the sample, providing data on the global structure and dynamics of proteins and complexes under various conditions. Although SAXS does not provide atomic resolution, it is highly useful for studying flexible proteins, conformational changes, and protein-ligand interactions in a more native-like environment.

Mass spectrometry is primarily used to determine the mass, composition, and post-translational modifications of proteins. While it does not directly provide three-dimensional structural information, mass spectrometry can reveal the stoichiometry of protein complexes, identify interaction partners, and map the locations of modifications such as phosphorylation, glycosylation, and acetylation. Advanced techniques like cross-linking mass spectrometry can also provide distance constraints between specific residues, contributing to the understanding of protein topology and interactions.

AlphaFold, represents a revolutionary advancement in artificial intelligence for predicting protein structures from amino acid sequences, significantly enhancing structural biology. By integrating deep learning with biological and physical knowledge, AlphaFold provides highly accurate predictions that rival experimental methods like X-ray crystallography, NMR spectroscopy, and cryo-electron microscopy. Its AlphaFold Protein Structure Database (AlphaFold DB) now includes over 214 million predicted structures, vastly increasing the available protein structural data. Key features include confidence metrics, such as the predicted local distance difference test (pLDDT), which indicates the reliability of specific regions, and Predicted Aligned Error (PAE), which helps assess positional accuracy. This extensive resource supports high-throughput structural bioinformatics, aids in structure-based drug discovery, and offers insights into disease mechanisms by elucidating the structures of proteins related to various conditions. The database is set to expand further, promising to enhance its value for the scientific community.

Studying the structural impact of post-translational modifications (PTMs) on proteins remains a significant challenge in structural biochemistry, despite advances in analytical techniques. This complexity arises from several factors: technical challenges associated with sample heterogeneity make it difficult to obtain homogeneous preparations, as a single protein can exhibit various combinations of PTMs, complicating data interpretation. Techniques such as X-ray crystallography may have insufficient resolution to detect subtle modifications, and PTMs can increase protein flexibility, making it harder to achieve high-resolution structures. Additionally, PTMs can exert structural effects distally from the modification site, and their impact on protein-protein interactions and temporal dynamics further complicates their study. Nevertheless, emerging approaches are addressing these challenges, including the use of complementary techniques (such as crystallography, NMR, and cryo-EM), computational methods and molecular simulations, single-molecule analysis techniques, and the development of specific enrichment and purification methods for modified forms. These integrative approaches are gradually enhancing our understanding of how PTMs modulate protein structure and function, even as many challenges remain in this evolving field.

Understanding protein structures and their interactions is essential for elucidating the mechanisms of proteinopathies, where misfolded proteins can form toxic aggregates or lose their normal functions, as seen in diseases like Alzheimers, where beta-amyloid aggregates into plaques and Tau protein into neurofibrillary tangles. Detailed structural knowledge allows the identification of therapeutic targets, guiding the design of molecules that stabilize native protein conformations, prevent misfolded protein aggregation, or promote the clearance of toxic aggregates. This approach also supports precision medicine by identifying different strains of misfolded proteins, enabling tailored treatments for neurodegenerative diseases. Furthermore, early structural insights can lead to sensitive biomarkers for diagnosing proteinopathies before clinical symptoms appear, and understanding the molecular mechanisms of misfolding could help develop preventive strategies. Finally, this knowledge fosters innovative therapies, such as pharmacological chaperones for correct protein folding, immunotherapies targeting misfolded proteins, and molecules that modulate pathological protein-protein interactions, underscoring the critical role of structural biology in addressing proteinopathies (family=Canada 2015).

Part IV

Introduction

Chapter 1: Alzheimer's Disease

1. History and Definition of Alzheimer's Disease

The meeting between the German psychiatrist and neurologist Alois Alzheimer (Figure 1.1a) and his patient Auguste Deter (Figure 1.1b) in 1901 marked a historic and foundational moment in the scientific understanding of dementia. At the time, the young clinician could not anticipate that his discoveries about the connection between brain and mental illnesses would make him world-famous. In 1901, Auguste Deter, at the age of 50, exhibited symptoms of memory loss and relational difficulties. After her death in 1906, Alzheimer examined her brain, as well as that of another patient, John F., using silver staining. He observed the presence of amyloid plaques and neurofibrillary tangles, although these terms were not used at the time. These discoveries marked the beginning of a significant advancement in the understanding of brain diseases (Möller and Graeber 1998).

(a) Portraits of Alois Alzheimer

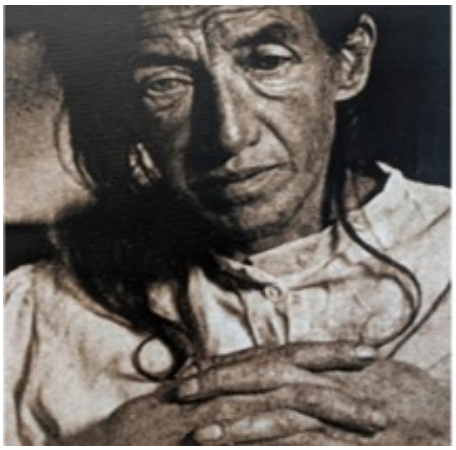

(b) Portrait of Auguste Deter

Figure 1.1: Portraits of Alois Alzheimer and Auguste Deter

On November 3, 1906, the young physician Alois Alzheimer delivered a lecture describing the psychiatric symptoms and histological changes in the brain of his patient Auguste Deter. This moment marked the first publication of what would become one of the most tragically famous conditions, the disease that now bears his name: Alzheimer's disease (AD) (Dahm 2006).

2. Symptoms of Alzheimer's Disease

Today, Alzheimer's disease has been declared a "global public health priority" by the World Health Organization (WHO) , as there is no permanent cure for Alzheimer's disease. So far, there are only well-established concepts and hypotheses regarding the causes and drug targets of Alzheimer's disease. Based on this concept, medications help reduce the progression of the disease pathology (Downer et al. 2021).
Alzheimer's disease is the most common form of dementia, affecting memory, thinking, and behavior. It is a progressive brain disorder that slowly destroys memory and cognitive skills, eventually

impairing the ability to carry out daily tasks. The disease may initially appear after the age of 60, and the risk increases with age, but it can also affect younger individuals, although less frequently.
Symptoms of AD can vary from person to person but the most common ones include memory loss, difficulty performing tasks, decreased judgment, and changes in mood or behavior (*What Is Alzheimer's Disease?* 2019; *Alzheimer's Disease* 2018). Symptoms evolve as the disease progresses through different stages.

3. Factors Influencing Alzheimer's Disease

AD is considered a multifactorial disease associated with several risk factors such as age, genetic factors, head injuries, vascular diseases, infections, and environmental factors. Additionally, there are also molecular causes which will be detailed in the subsequent manuscript.

3.1. Environmental Factors

Age is the most significant risk factor for Alzheimer's disease (Coria, Rubio, and Bayón 1994), with risk increasing as individuals age (*Risk Factors for Alzheimer's Disease | Alzheimer's Society* 2023; *Causes and Risk Factors for Alzheimer's Disease* 2024). Individuals over 65 are more likely to develop Alzheimer's disease, with the risk doubling every five years after this age. Although most people with Alzheimer's disease are over 65, about 1 in 20 people with the disease are under 65, known as early-onset or younger-onset Alzheimer's disease (*Early-Onset Dementia and Alzheimer's Rates Grow for Younger American Adults* 2021).

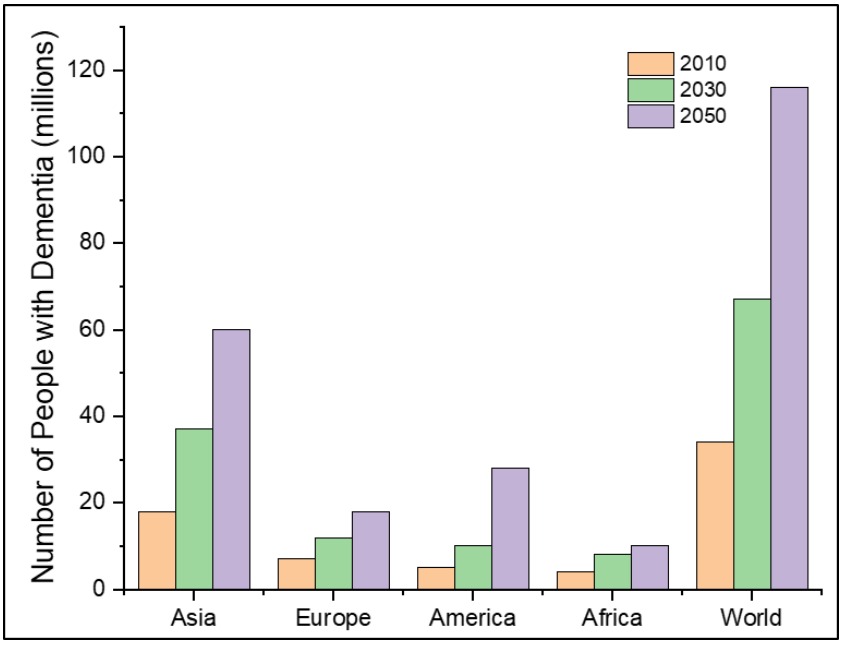

Figure 1.2: Projected Prevalence of Alzheimer's Disease in 2050. (Figure adapted from *Alzheimer's Disease* 2017)

3.2. Genetic Factors

Alzheimer's disease (AD) is impacted by various genetic factors that play a crucial role in its development.
The *APOE* gene, specifically the *APOE* $\epsilon 4$ allele, is widely recognized as a major genetic risk factor for Alzheimer's disease. Individuals carrying the *APOE* $\epsilon 4$ allele have an increased risk of developing

Alzheimer's disease and may exhibit an early onset of the disease (Silva et al. 2019). In contrast, the APOE $\epsilon 2$ allele may offer some protection against Alzheimer's disease, delaying its onset compared to the $\epsilon 4$ allele (Raber, Huang, and Ashford 2004). Since 2022, genome-wide association studies (GWAS) have identified about 75 genetic susceptibility loci (Grupe et al. 2007; Bellenguez et al. 2022). These studies initially confirmed the APOE gene as the most significant risk factor for Alzheimer's disease (Coon et al. 2007). Furthermore, the initial GWAS revealed the following susceptibility loci: BIN1 (Bridging integrator 1), CLU (Clusterin), PICALM (Phosphatidylinositol-binding clathrin assembly protein), and CR1 (Cell-surface receptor 1) (Chapuis et al. 2013; Harold et al. 2009; Lambert et al. 2009).
Regarding other genetic factors, rare forms of early-onset Alzheimer's disease (EO-FAD) are closely related to mutations in genes such as APP (amyloid precursor protein) and PSEN1/2 (presenilin) (A Armstrong 2019).

3.3. Increased Alzheimer's Risk in Women

Women may face a greater risk of developing Alzheimer's disease compared to men due to a combination of genetic, biological, hormonal, psychiatric, and psychosocial factors, as well as increased longevity. Genetically, women carrying the APOE-$\sigma 4$ allele, a significant risk factor for Alzheimer's, are nearly twice as likely to develop the disease compared to women without the allele. In contrast, men with this allele have only a slightly elevated risk (Podcasy and Epperson 2016). Additionally, some genes pose risks for Alzheimer's exclusively in women or men, indicating sex-specific genetic influences (*Women and Alzheimer's Disease | Lifespan* 2024).
Biologically, brain imaging studies show that toxic tau protein spreads more rapidly and extensively in women's brains, potentially accelerating disease progression. Womens brains may also metabolize sugar more efficiently, masking early Alzheimer's symptoms and delaying diagnosis. Hormonal changes, especially declining estrogen levels during menopause, increase women's vulnerability to Alzheimer's. The Women's Health Initiative Memory Study found that postmenopausal hormone therapy with estrogen and progesterone doubled the risk of dementia in women aged 65-79 (*Women and Alzheimer's Disease | Lifespan* 2024).
Psychiatric conditions such as depression and insomnia, which are more prevalent in women, are linked to a higher risk of Alzheimer's. Pregnancy-related hypertensive disorders, like gestational hypertension and preeclampsia, may elevate the risk of dementia later in life. Psychosocial factors, such as lower educational levels common in previous generations of women, are associated with a higher risk of Alzheimer's due to reduced cognitive reserve. Additionally, the traditional caregiving roles often assumed by women can lead to increased stress levels, potentially influencing their risk (O'Neal 2024).
Finally, women generally live longer than men, and since older age is the greatest risk factor for Alzheimer's, this increases the overall prevalence of the disease in women (*Women and Alzheimer's* 2019).

3.4. Low Education

Low education is a significant risk factor for developing Alzheimer's disease (AD).
Case-control studies consistently show that individuals with low educational attainment (typically defined as 6 years or less of formal schooling) have a higher prevalence of AD compared to those with higher education levels (Gatz et al. 2001; Schmand et al. 1997).
Meta-analyses and systematic reviews have quantified this increased risk, with summary odds ratios ranging from 1.59 to 1.89 for developing any dementia, including AD, in individuals with low education. Longitudinal studies following cognitively healthy individuals over time have found that low education is associated with a higher incidence and risk of developing AD and other dementias.

A continuous meta-analysis found that each additional year of education reduces the risk of AD by around 8% (95% CI: 5-12%). Furthermore, a dichotomous meta-analysis showed an 85% increased risk (95% CI: 56-118%) of developing AD for individuals with low education compared to those with higher education levels. While the definition of "low education" varies across studies (ranging from 0 to 12 years), the evidence consistently points to an inverse relationship between years of education and risk of AD(Maccora, Peters, and Anstey 2020).
The proposed mechanisms linking low education to increased AD risk include reduced cognitive reserve, lifestyle factors associated with lower socioeconomic status, and potential interactions with genetic and vascular risk factors (Ngandu et al. 2007). .

3.5. Cardiovascular Risk Factors

Cardiovascular risk factors play a significant role in the development of Alzheimer's disease, influencing brain and cognitive health. Studies have demonstrated that conditions such as hypertension, diabetes, hypercholesterolemia, obesity, smoking, and lack of physical activity can contribute to cognitive impairment and the progression of Alzheimer's disease. Additionally, high cardiovascular risk is associated with an increased risk of developing Alzheimer's disease, underscoring the importance of controlling these factors to maintain brain health. To reduce this risk, it is recommended to monitor and control blood pressure, cholesterol, body weight, and adopt a healthy lifestyle including a balanced diet and regular physical activity. Furthermore, quitting smoking, managing type 2 diabetes, and engaging in stimulating cognitive activity can also contribute to reducing the risk of developing Alzheimer's disease associated with cardiovascular factors. In summary, by taking measures to control cardiovascular risk factors, it is possible to reduce the risk of developing Alzheimer's disease, highlighting the importance of a proactive approach to maintaining good cardiovascular and brain health throughout life (Leszek et al. 2021).

4. Neuropathological lesions

4.1. Macroscopic Features

The brain affected by AD often shows a decrease in weight and atrophy, at least moderate cortical atrophy, more marked in the medial temporal lobes (MTL), with relative preservation of the primary motor, somatosensory, and visual cortices, as well as widening of the lateral ventricles (ex vacuo hydrocephalus). Cerebral atrophy often affects posterior cortical areas, including the precuneus and posterior cingulate gyrus, in the preclinical stage of AD (Zhou et al. 2010) (Figure 1.3). However, none of the macroscopic features are specific to Alzheimer's disease, and healthy older individuals often exhibit moderate cortical atrophy, notably affecting the frontal lobes (Piguet et al. 2009), with a loss of white matter volume. Medial temporal atrophy affecting the amygdala and hippocampus with temporal horn enlargement is typical of Alzheimer's disease. However, this is also observed in other age-related disorders, such as hippocampal sclerosis (Serrano-Pozo et al. 2011).

4.2. Microscopic Aspects

The definitive diagnosis of Alzheimer's disease requires microscopic examination of several brain regions with a semi-quantitative assessment of lesion density and their topographic distribution.
In 1906, Alzheimer used silver staining techniques, then recent, to examine the autopsy of the brain of his patient Auguste Deter (Figure 1.1b). The results revealed the presence of senile plaques (SP) extracellularly and of intracellular neurofibrillary tangles (NFT) 1.4, which are now recognized as the primary lesions causing Alzheimer's disease (Mufson et al. 2015).

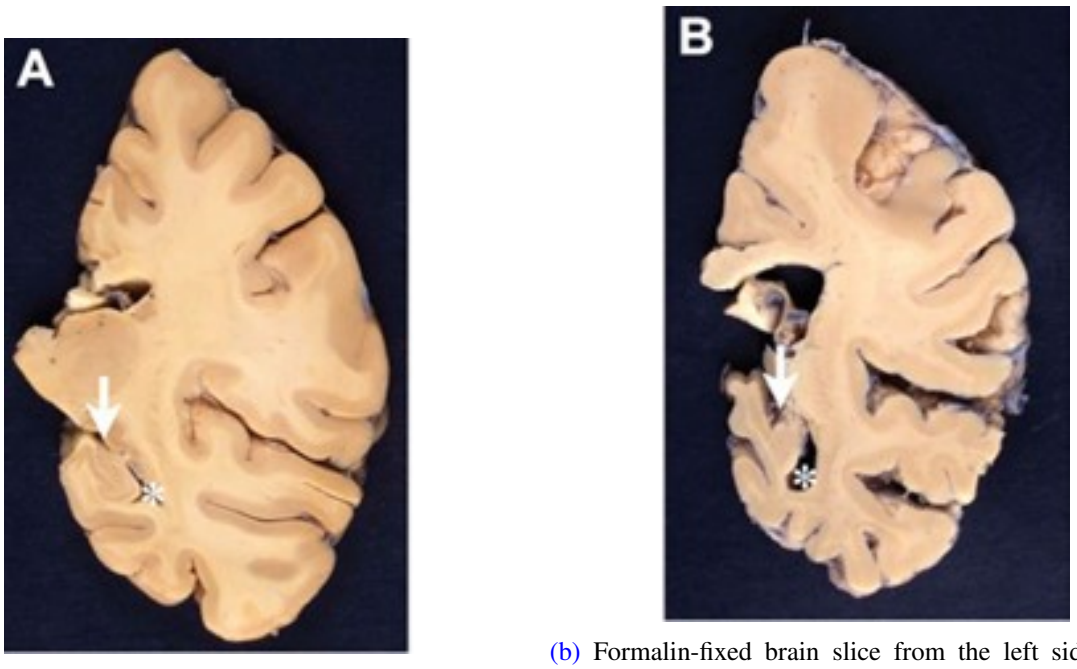

(a) Formalin-fixed brain slice from the left side, at the level of the posterior hippocampus, of a non-demented individual

(b) Formalin-fixed brain slice from the left side, at the level of the posterior hippocampus, of an individual with Alzheimer's disease

Figure 1.3: Comparision of Formalin-Fixed Brain Slices (Jellinger 2020)

Extracellular SPs and intracellular NFTs, essential for neuropathological diagnosis, are associated with tau-positive neuropil threads (NT), dystrophic neurites, and neuritic plaques (NP) , cerebral amyloid angiopathy , reactive astrocytes and activated microglia, as well as neuroinflammation. These lesions result in synaptic and neuronal loss in vulnerable regions, leading to cerebral atrophy and the characteristic clinical picture of the disease. Hirano bodies, granulovacuolar degeneration (GVD), TDP-43 deposits, and other lesions may also be present (DeTure and Dickson 2019; Tomé et al. 2020).

Amyloid Plaques

Amyloid plaques result from the extracellular accumulation of Aβ peptides with a molecular weight of approximately 4.5 kDa. This peptide is the result of proteolytic cleavage of amyloid precursor protein (APP) (Kang et al. 1987–0025). APP is a large transmembrane protein encoded by the *APP* gene located on chromosome 21 (Goldgaber et al. 1987). APP can undergo two different degradation pathways: the non-amyloidogenic pathway and the amyloidogenic pathway, and other alternative pathways (Figure 1.5). In the non-amyloidogenic processing pathway, membrane-bound mature APP is cleaved by α-secretase within the amyloid-β (Aβ) region (indicated in red), releasing soluble α-APP (sAPPα) and C-terminal fragment α (CTF-α). CTF-α is then cleaved by γ-secretase to generate P3 and the APP intracellular domain (AICD). In the amyloidogenic pathway, which occurs preferentially in acidic environments such as endosomes, internalized APP is sequentially cleaved by β- and γ-secretases to produce soluble β-APP (sAPPβ), Aβ, and AICD. C-terminal fragment β (CTF-β) is an intermediate product of β-secretase cleavage. An example of alternative pathways is achieved by cleavage at the β-site of APP by the enzymatic activity of the secretase BACE1, a transmembrane enzyme with aspartyl protease activity. Cleavage by β-secretase yields a slightly shorter soluble fragment (sAPPβ) and a longer corresponding C-terminal fragment (CTFβ) or C99 (Zheng and Koo 2011).
Cleavage of APP by α-secretases releases the soluble ectodomain of APP named sAPPα and a membrane-bound intracellular C-terminal fragment named CTFα and C83 (Jellinger 2020). This pathway is also known as neuroprotective because the sAPPα peptide possesses neuroprotective

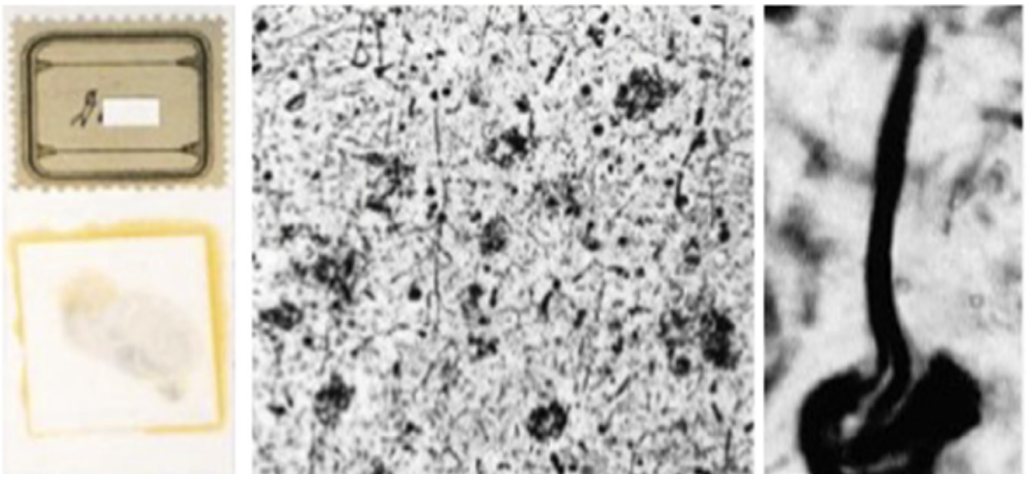

Figure 1.4: Image of original post-mortem histological slides showing silver-impregnated neuritic plaques and a neurofibrillary tangle in the brain of Auguste Deter (Mufson et al. 2015)

properties, preventing the formation of Aβ peptides formed in the amyloidogenic pathway (Hick et al. 2015).
In the amyloidogenic pathway, Aβ peptides are produced. These peptides vary in size: Aβ-40, composed of 40 amino acids, and Aβ-42, composed of 42 amino acids, resulting from the sequential cleavage of a protein by β- and γ-secretases (O'Brien and Wong 2011).
In the context of Alzheimer's disease (AD), the amyloidogenic cleavage process of APP directly competes with the neuroprotective pathway. This competition can lead to dysregulation of the neuroprotective pathway, thus favoring the amyloidogenic pathway and contributing to disease development. In this hypothesis, mutations in genes encoding APP, presenilins 1 and 2 (enzymes in the γ-secretase activation pathway) also play a role (Kojro and Fahrenholz 2005; Jellinger 2020).
γ-Secretases cleave the C-terminal fragments of APP such as C83 or C99 releasing 3 or 4 amino acids from the transmembrane fragment. This pathway is only active after cleavage by α or β-secretase. The products of γ-secretase cleavage of C83 are a 3 kDa peptide, called p3, and an intracellular domain of amyloid precursor protein (AICD), while cleavage by γ-secretase of C99 produces the famous Aβ peptide and an identical AICD fragment (Haass et al. 2012).

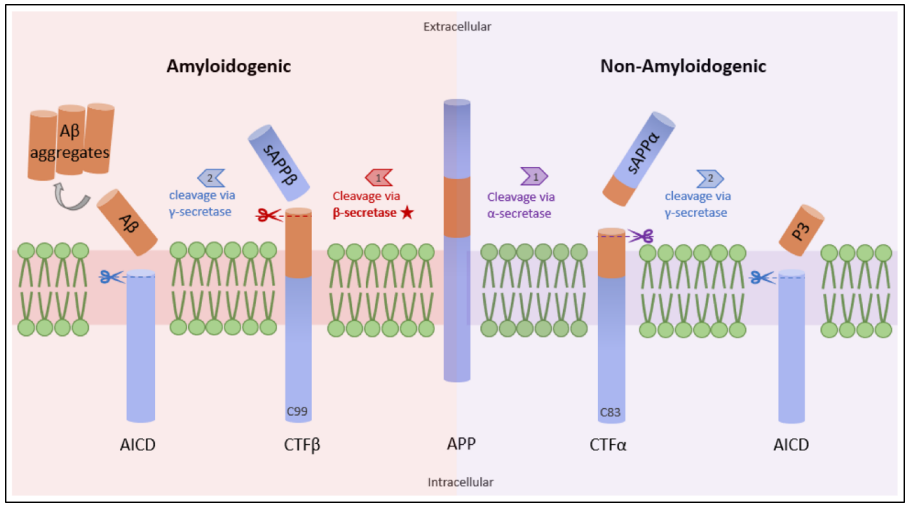

Figure 1.5: Proteolytic cleavage of amyloid precursor protein (APP) by non-amyloidogenic (left) and amyloidogenic (right) processing pathways (Sun et al. 2022)

Regarding distribution, amyloid plaque deposits are mainly found in the gray matter of the brain and are associated with degenerative neuronal elements as well as an abundance of microglia and astrocytes. Amyloid plaques vary in size and appearance, ranging from small accumulations to denser or

diffuse masses. "Classic plaques" include a compact core of Aβ amyloid surrounded by a less dense crown. They also include abnormal neuronal processes, activated astrocytes, and microglia (Jellinger 2020). Studies have shown a positive correlation between the distribution of amyloid plaques and different brain regions, highlighting an association between these deposits and specific regions of the brain in the pathogenesis of Alzheimer's disease (Tsui et al. 2022). Amyloid plaques progress in brain regions according to the Thal stages, with an initial presence in the neocortex, then in the entorhinal cortex, hippocampus, and deeper regions such as the thalamus and hypothalamus (Figure 1.6) (Hampel et al. 2021).

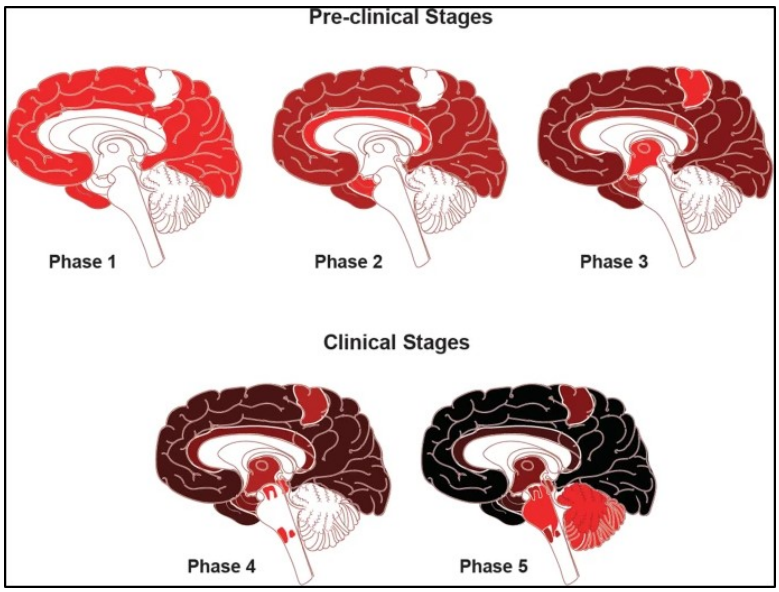

Red areas in phase 1 represent cortical regions with initial amyloid-β accumulation during early preclinical stage. The continued deposition in the same areas is represented by darker colors in subsequent phases, with new areas showing amyloid-β in red at each phase. Neocortical regions with initial amyloid-β accumulation in phase 1 include associative cortices. Additional accumulation is observed in allocortical regions and the mesencephalon (phases 2 and 3), with the cerebellum and brainstem showing amyloid-β accumulation in late clinical stages. The transition to darker shading indicates continued Aβ accumulation (Hampel et al. 2021)

Figure 1.6: The five phases of amyloid pathology development in Alzheimer's disease

4.3. Neurofibrillary Tangles

After being initially identified using silver staining, examination of neurofibrillary tangles (NFTs) by electron microscopy revealed their fibrillary structure. Indeed, as early as 1963, it was discovered that NFTs exhibit paired helical filaments (PHFs) (Kidd 1963). A few years later, through biochemical analysis of PHFs isolated from the brains of Alzheimer's disease patients, the composition of NFTs was elucidated. It was established that NFTs were primarily composed of aggregates of Tau proteins (Figure 1.7), as well as Aβ peptide, MAP2, and ubiquitin (Brion et al. 1985; Kosik et al. 1989; Masters et al. 1985; Perry et al. 1987). For the first time in 1986, the Grundke-Iqbal group observed that Tau protein in PHFs is in a hyperphosphorylated form (Grundke-Iqbal et al. 1986).
The Braak staging system is a method used to assess the progression of neurofibrillary tangles (NFTs) associated with Alzheimer's disease (Braak et al. 2006).
Braak stages are hierarchical, meaning that a given stage encompasses the abnormalities observed in previous stages. Stages I and II are marked by involvement of the transentorhinal and entorhinal cortices, respectively. By stage III, moderate damage is observed in the hippocampus, amygdala, and adjacent neocortical areas. Stage IV defines the initial extension of the pathological process to neocortical association areas, including the insular cortex and basal frontal areas. Stage V shows

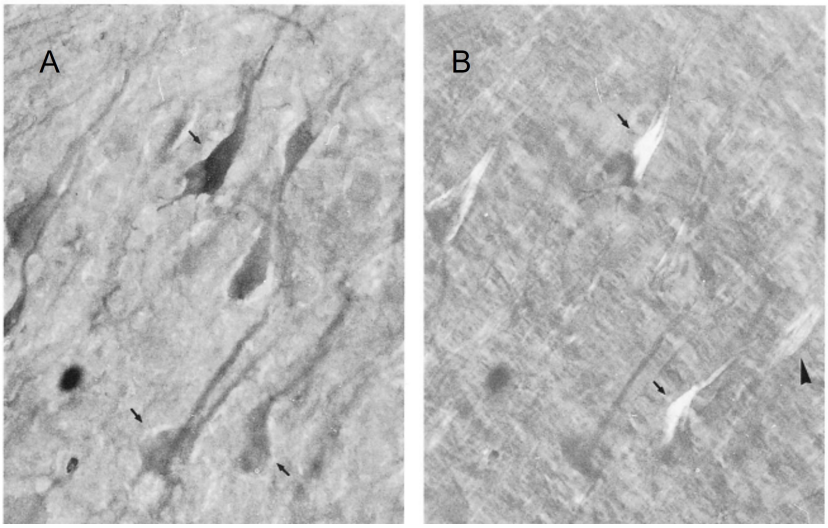

(A) Microtubule labeling by a serum produced from the thermostable fraction of MAPs (B) Counterstaining with Congo red (PHFs identification). This shows that anti-microtubular protein serum also recognise PHFs (Brion et al. 1985)

Figure 1.7: Immunolabeling on hippocampal section of AD patients

impairment of neocortical association areas, particularly in the temporal, parietal, and occipital associative regions. By stage VI, degeneration spreads to primary motor and sensory fields (Figure 1.8) (Macedo et al. 2023).

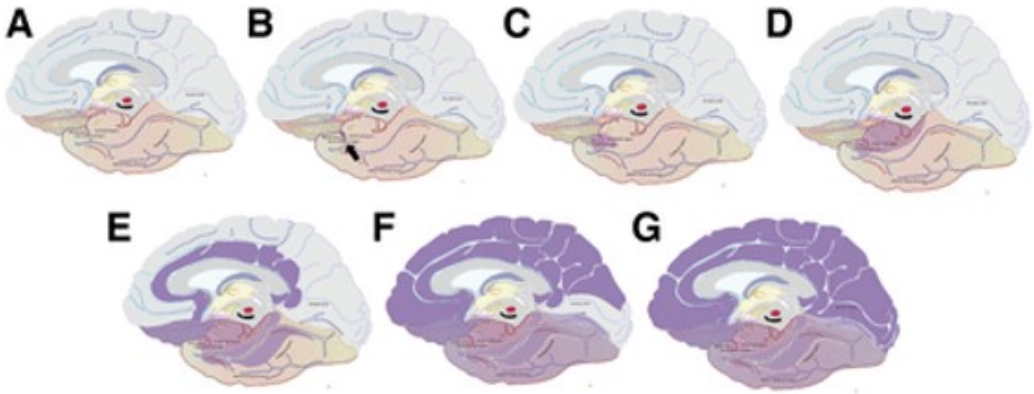

(A), I (B), II (C), III (D), IV (E), V (F), and VI (G) according to original histopathological descriptions, displaying a median sagittal brain section. Affected brain regions are colored in different shades of purple (Macedo et al. 2023)

Figure 1.8: Topographical representation of Braak stages 0 (absence of Tau accumulation)

In the following chapter (Chapter 2), details on the structure and function of the Tau protein will be elaborated.

Relationship between the two lesions

Many studies have established a link between Aβ and Tau and raised the possibility that protein-protein interactions are key to both the spread and toxicity of these two abnormal proteins (Kara, Marks, and Aguzzi 2018). Several models have been described: (1) *Seeding* of toxic Tau is enhanced by the presence of Aβ; (2) Aβ toxicity depends on the presence of Tau; (3) Aβ and Tau mutually reinforce their toxicity (Figure 1.9).
The first hypothesis is ex'ed by the fact that the presence of amyloid-beta (Aβ) significantly enhances the seeding of toxic Tau, as evidenced by several key points. Direct interaction between Aβ and

Tau proteins facilitates pathological cross-seeding, with the Aβ core region binding specific areas of Tau and promoting its aggregation via a shared epitope (Tripathi and Khan 2020). According to the amyloid cascade hypothesis, the accumulation of Aβ is an early event in Alzheimer's disease that triggers subsequent Tau pathology, with Aβ deposits leading to the formation of neurofibrillary tangles composed of hyperphosphorylated Tau. Aβ also influences the spatial distribution of Tau pathology, potentially causing a shift towards neuritic dystrophy or tangles depending on the disease stage. In mouse models, amyloid deposition accelerates and broadens Tau propagation, with Aβ promoting the formation of specific pathological Tau forms (Paul et al. 2024). Furthermore, pre-aggregated Aβ can act as a template for Tau aggregation by increasing the hydrophobic surface area, thereby facilitating template-assisted growth of Tau protein. The rate of Tau fibril formation in vitro is enhanced in a dose-dependent manner with increasing concentrations of Aβ seeds (*Aβ Plaques: Breeding Ground for Toxic Tau? | ALZFORUM* 2017). The molecular interaction between Aβ and Tau involves oxidative stress induced by Aβ, which upregulates RCAN1, thereby inhibiting calcineurin (a Tau dephosphorylating phosphatase) and activating GSK3β, leading to increased Tau phosphorylation and toxicity (Lloret et al. 2011). Aβ also promotes pathological Tau formation by affecting kinases and phosphatases that regulate Tau, resulting in its misfolding (Bloom 2014).
The second hypothesis is supported by research suggesting that, even though the "amyloid cascade" hypothesis posits that neurodegeneration in Alzheimer's disease is caused by the abnormal accumulation of beta-amyloid (Aβ) plaques in the brain, neurofibrillary degenerations (NFDs) have been observed to manifest before the appearance of amyloid plaques. According to the amyloid cascade hypothesis, the initial event triggering neuronal degradation in Alzheimer's disease is an increase in amyloid plaque accumulation.
The toxicity of amyloid-beta (Aβ) in Alzheimer's disease (AD) is critically influenced by the presence of Tau protein, as highlighted by several key points. Experimental evidence supports this relationship, with studies in Tau knockout mouse models showing reduced Aβ-induced neurodegeneration and synaptic dysfunction, indicating that Tau is necessary for Aβ toxicity (Ng et al. 2024). In vitro experiments further demonstrate that Tau enhances the toxic effects of Aβ on neurons (Zhang et al. 2021). A feedback loop has been observed, wherein Aβ not only triggers Tau pathology, but toxic Tau can also amplify Aβ toxicity, worsening the neurodegenerative process (Bloom 2014).
The two initial hypotheses lead to the third hypothesis: the mutual reinforcement of toxicity between amyloid-beta (Aβ) and Tau proteins in Alzheimer's disease (AD). This relationship is well-supported by various studies. Aβ and Tau proteins directly interact, facilitating pathological cross-seeding, where the core region of Aβ interacts with specific regions of Tau, promoting Tau aggregation through a shared epitope, indicating common binding regions (Tripathi and Khan 2020). This cross-seeding mechanism means that the presence of Aβ can enhance Tau aggregation and vice versa, significantly contributing to their mutual toxicity (Kim et al. 2023).
These findings suggest that therapeutic strategies targeting both Aβ and Tau may be more effective than those focusing on a single protein, with some inhibitors showing promise in reducing the aggregation and toxicity of both proteins by binding to their common epitope (Tripathi and Khan 2020).

5. Therapies for AD

As of now, only a few immunotherapies targeting amyloid-beta (Aβ) peptides have been approved by the FDA in the United States for the treatment of Alzheimer's disease (AD). Aducanumab (Aduhelm) received accelerated approval in 2021, though its development was halted by Biogen in 2024 for commercial reasons rather than issues with safety or efficacy (*Aducanumab to Be Discontinued as an Alzheimer's Treatment* 2022; *Biogen Walks Away From Aducanumab to Prioritize Lecanemab and Alzheimer Disease Pipeline* 2024). Lecanemab (Leqembi) was granted accelerated approval in

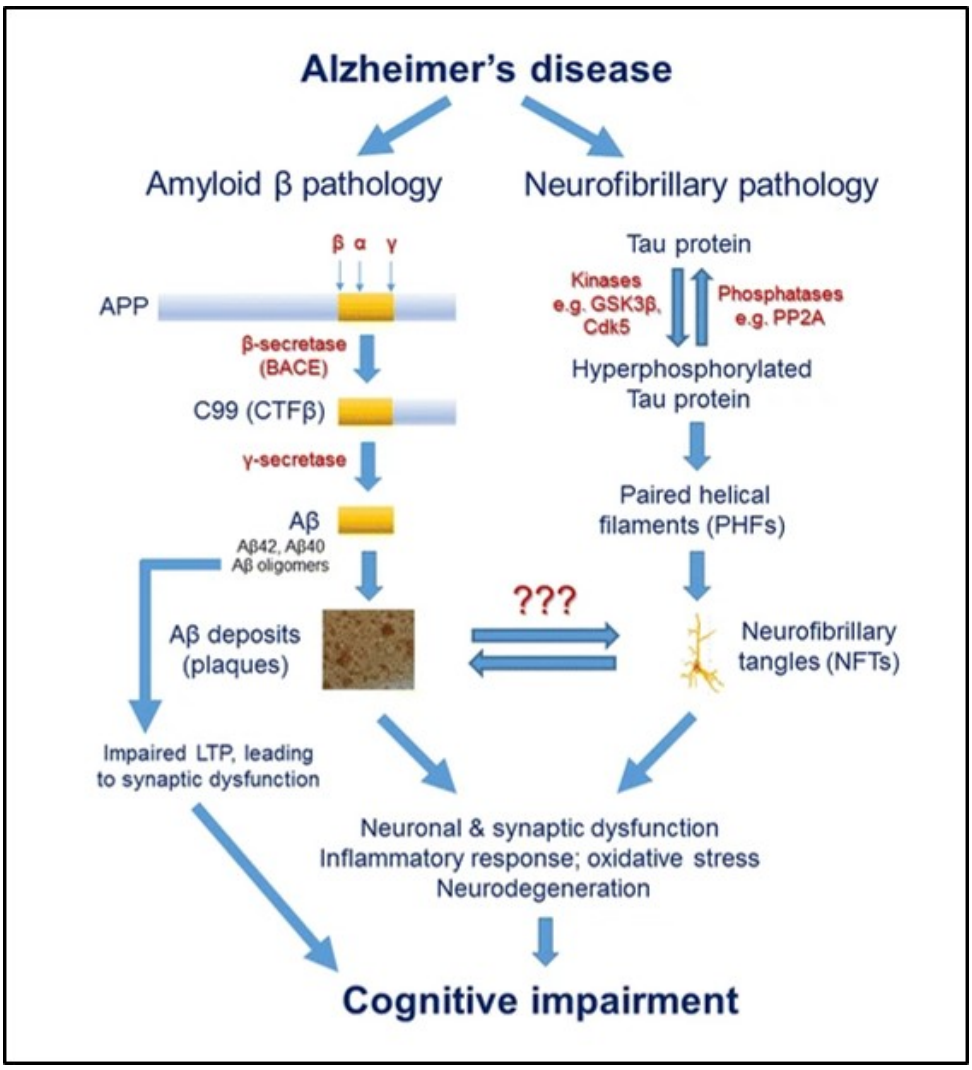

Figure 1.9: Aβ plaques and NFTs as features of AD

January 2023, followed by traditional approval in July 2023, demonstrating a 27% reduction in cognitive and functional decline compared to placebo over 18 months in the phase 3 CLARITY AD trial (*Lecanemab Approved for Treatment of Early Alzheimer's Disease* 2021). Donanemab is currently under FDA review for potential approval (*Donanemab Approved for Treatment of Early Alzheimer's Disease* 2023). These therapies employ different mechanisms to target Aβ: both aducanumab and lecanemab bind to the N-terminal of Aβ, while donanemab targets a central epitope of Aβ. Their mode of action involves the removal of soluble Aβ from the peripheral nervous system, following the "peripheral sink therapeutic strategy," which reduces soluble Aβ levels in the plasma, thus facilitating the clearance of Aβ from the brain via the blood-brain barrier. However, these treatments do not directly target the amyloid plaques that accumulate outside neurons in the brain, and their efficacy remains modest, with about a 25-30% reduction in cognitive decline compared to placebo. Looking forward, while these immunotherapies mark progress in AD treatment, further research is crucial to developing more effective therapies. Additional approaches, such as tau kinase inhibitors and agents that enhance tau protein clearance, are also under investigation. In summary, Aβ-targeting immunotherapies currently represent the only approved therapeutic options for AD, but their limited efficacy underscores the need for continued research to develop more effective treatments and address other pathological mechanisms involved in Alzheimer's disease.

The exploration of Tau antibodies in Alzheimer's disease (AD) has provided valuable insights into their mechanisms of action and therapeutic potential. Research indicates that antibodies targeting the mid-region of Tau are more effective at blocking Tau's seeding activity than those targeting

the N-terminal region. Studies, including those presented at the 2021 International Conference on Alzheimer's and Parkinson's Diseases, have shown that mid-region antibodies, such as those targeting amino acids 235250, can significantly inhibit the propagation of Tau aggregates, which is crucial for preventing the spread of Tau pathology in the brain. Despite the lower efficacy of N-terminal antibodies in blocking seeding activity, several of these antibodies, including semorinemab, tilavonemab, zagotenemab, and gosuranemab, have progressed to clinical development due to their high affinity for Tau and ability to clear neurofibrillary tangles in model systems (Song et al. 2023). The choice of epitope is critical for the efficacy of therapeutic anti-Tau antibodies, with mid-region antibodies showing superior performance in preventing *seeding* and limiting the spread of Tau pathology. This is especially significant given the recent clinical trial failures of N-terminally directed antibodies, which have cast doubt on their effectiveness in treating tauopathies (Song et al. 2023; Albert et al. 2019). The findings underscore the importance of epitope selection in antibody development for AD, with mid-region antibodies offering a more promising avenue for therapeutic intervention. Ongoing research continues to investigate the mechanisms by which these antibodies exert their effects and their potential in clinical settings, aiming to develop more effective immunotherapies for Alzheimer's disease (Song et al. 2023).

Here's a concise summary of the current clinical trials for Tau immunotherapies, both active and passive, indicating the phase of each study and the companies involved:

Various Tau-targeting immunotherapies are under clinical investigation for treating Alzheimer's disease (AD) and related tauopathies. These include both active and passive immunotherapy approaches. Active immunotherapies such as AADvac1 and ACI-35 are in advanced stages, with AADvac1 undergoing Phase 2 trials for AD and Progressive Nonfluent Aphasia. ACI-35, developed by AC Immune and Janssen, is in Phase 2/3 trials for AD. On the other hand, several passive immunotherapies, including Bepranemab, BMS-986446, and E2814, are in different stages of clinical trials. Bepranemab is in Phase 2 for AD and Phase 1 for Progressive Supranuclear Palsy, while BMS-986446 and E2814 are in Phase 2 and Phase 1/2 trials for AD, respectively. Some therapies, like Gosuranemab and Zagotenemab, have been discontinued, highlighting the challenges in this area of research. Overall, these immunotherapies represent a promising approach, although further studies are required to fully establish their therapeutic efficacy (*Therapeutics Search | ALZFORUM* 2019).

Chapter 2: Tau Protein

Tau protein is a microtubule-associated protein primarily found in neurons, where it plays a crucial role in stabilizing microtubules, which are part of the cell's cytoskeleton. Structurally, Tau is characterized by several domains, including an N-terminal projection domain, a proline-rich region, a microtubule-binding domain, and a C-terminal tail. The microtubule-binding domain, consisting of three or four repeat regions, is essential for its interaction with microtubules. Tau's ability to promote the assembly and stabilization of microtubules is vital for maintaining the structural integrity and proper function of neurons, including axonal transport. However, in pathological conditions such as Alzheimer's disease, Tau can become hyperphosphorylated, leading to its dissociation from microtubules and aggregation into neurofibrillary tangles, contributing to neurodegeneration.

1. Tau: An intrinsically Disordered Protein

1.1. Definition of Intrinsically Disordered Proteins

Structure-Function Paradigm

In the early stages, protein research focused on the study of globular (structured) proteins, so the principles of biochemistry explained that protein structure is rather specific to globular proteins. These fundamental bases defining protein structures continued to receive experimental support in the 20th century given the large number of protein structures deposited in repositories such as the Protein Data Bank (PDB) (Huang, Rose, and Hsu 2015). There was no doubt about the structure-function relationship: "a protein requires a structured native structure to perform its biological function" was the philosophy of structural biology of the time. Proteins were initially considered rigid molecules. This idea of the static property of proteins comes from one of the most important functions: catalysis (Fischer 1894). Later, Koshland proposed the need for a certain degree of flexibility in protein structures to perform their roles, and this was accepted (Koshland 1958). The three-dimensional (3D) structure of the protein, the center of the structure-function paradigm, is already encoded in the primary structure of the protein formed by its sequence of amino acids. This is thus defined by the different types of interactions between amino acids. This 3D structure of the protein allows for specific ligand binding sites as well as ensuring functions. On the other hand, with the increase in cases of structure-function deviating from the classic structure-function paradigm, a proposal for a disorder-function paradigm has been presented.

Disorder-Function Paradigm

Abnormal behaviors of proteins such as missing electron densities in PDB structures, high sensitivity to proteolysis, peculiar behaviors during purification, etc., have always been observed but considered as artifacts in the shadow of classic structural biology. The study of this unknown part of structural biology resulted in the discovery of intrinsically disordered proteins (IDPs). The IDPs are characterized by the absence of stable 3D structure under physiological conditions. In this case, the absence of 3D structure is directly encoded by the amino acid sequence of the protein (primary structure) (Trivedi

and Nagarajaram 2022). Several servers allow predicting the disordered nature of the protein (Figure 2.3 B for example). The absence of 3D structure does not equate to the absence of biological function in this case. Several IDPs have been discovered, and various functions as well as mechanisms of action have been deciphered. Our protein (Tau), studied in this thesis, also belongs to the family of IDPs, and we will see in the following of this chapter the properties of this protein.

Disorder to order transition

We can describe a continuum of structural rigidity/flexibility existing between very rigid globular proteins on one end and more flexible or disordered proteins on the other (Figure 2.1). At the far left

Figure 2.1: Schematic representation of the continuum existing between very rigid globular proteins (on the left) and completely disordered proteins, lacking any structuring (on the right) (Habchi et al. 2014)

of this continuum are the classical globular proteins, which have a highly compact and rigid tertiary structure. These proteins adopt a very stable spherical or spheroidal shape, with a buried hydrophobic core and hydrophilic side chains exposed on the surface. This rigid globular structure is essential for their enzymatic, transport, or signaling functions (*Protéine globulaire* 2024). Moving towards the center of the continuum, we find proteins that combine well-structured globular domains with more flexible or disordered regions. The tertiary structure of a globular protein appears as a succession of ordered regions, either in α-helix or β-sheet form, connected by more flexible segments. As we move further to the right of the continuum, proteins become increasingly intrinsically disordered or flexible, lacking a well-defined tertiary structure. Proteins are not rigid macromolecules. They are flexible, and their ability to deform is often essential for their biological function. At the far right, we find completely disordered proteins or protein regions, existing as highly flexible ensembles of conformations in solution, without a stable tertiary structure (Habchi et al. 2014).

1.2. Expression and Structure of Tau

Tau is an intrinsically disordered protein (Figure 2.3 B) encoded by a single gene: *MAPT* . This gene is located on the long arm of chromosome 17 (17q21) (Holper, Watson, and Yassi 2022) and consists of 16 exons. Exons 0 (-1) and 14 out of the 16 exons that compose the gene *MAPT* are transcribed but not translated (Figure 2.2).
In the central nervous system (CNS), Tau is translated from a 6 kb mRNA transcript in the human brain to produce a variety of six Tau isoforms ranging in size from 37 to 46 kDa (Figure 2.2). These isoforms are distinguished by the presence of 0, 1, or 2 N-terminal amino acid inserts and the presence of 3 or 4 repeat domains (R1-R4) in the C-terminal part (Goedert and Jakes 1990). Exons 2 and 3 of *mapt* each encode an N-terminal insertion of 29 amino acids leading to the 0N, 1N, or 2N isoforms (exon 3 is not translated in the absence of exon 2), while alternative splicing of exon 10 leads to the presence or absence of the R2 repeat domain resulting in the 3R and 4R isoforms. The longest isoform of Tau in the CNS is thus 2N4R composed of two N-terminal inserts, a proline-rich region (PRR), 4 repeat domains: R1, R2, R3, and R4, and a C-terminal domain (Figure 2.2). Unlike the repeats that form a microtubule-binding region, the N-terminal part of Tau represents a projection domain away from microtubules into the cytoplasm and may be involved in microtubule spacing (Chen et al. 1992). Tau 2N4R is composed of 441 amino acids that adopt a positive overall charge at physiological pH. The overall amino acid composition is hydrophilic, consistent with the unfolded nature of the protein (Figure 2.3). Tau 2N4R is composed of 80 serines (S) or threonines (T), 56 glutamic (E) and aspartic

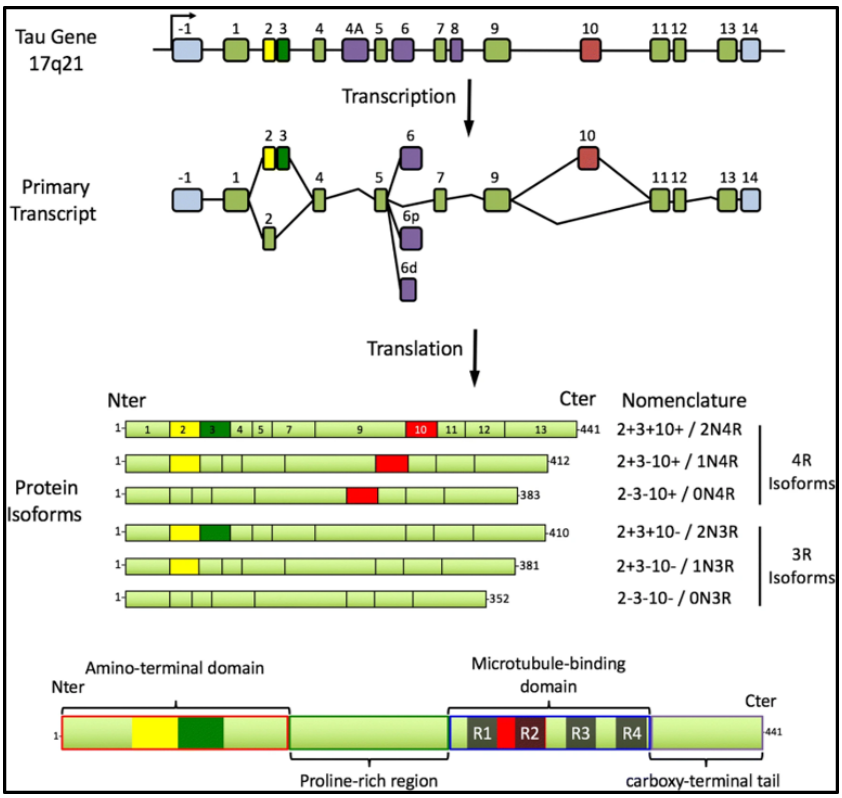

Figure 2.2: Gene structure and its primary transcript of the Tau protein

acids (D), 58 arginines (R) and lysines (K), and 8 aromatics: 5 tyrosines (Y), 3 phenylalanines (F), and no tryptophan (W), and relatively low quantities of hydrophobic residues, making the entire protein hydrophilic (Mandelkow and Mandelkow 2012).

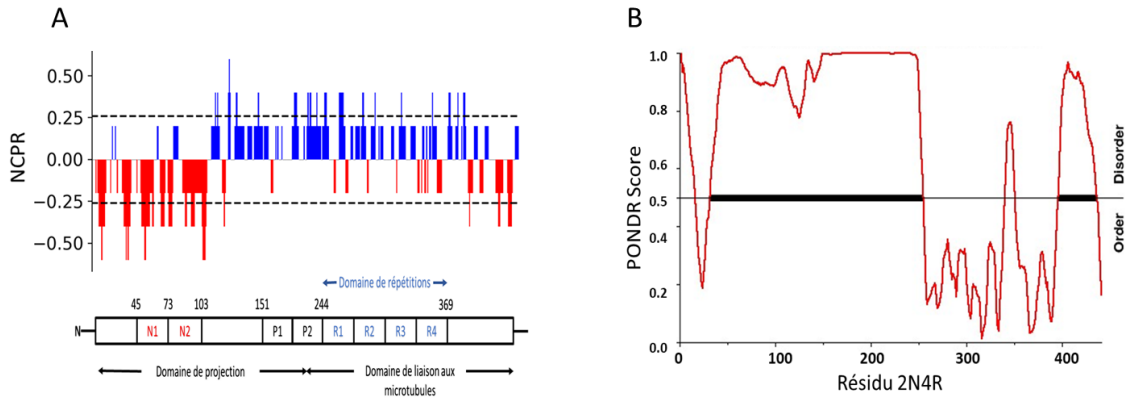

(A) Distribution of charge of Tau 2N4R protein (Figure created using the CIDER server) (B) Disorder prediction of Tau 2N4R protein (Figure created using the PONDR server)

Figure 2.3: Sequence and structural property of Tau 2N4R

The exons 4a, 6, and 8 originate from a 9 kb *MAPT* transcript that is expressed only in the peripheral nervous system (PNS). These exons are then translated into a series of larger Tau proteins, ranging in size from 110 to 120 kDa.
There is substantial evidence that the intrinsically disordered Tau protein can adopt a compact, paperclip-like conformation in solution.

Global Folding and Paperclip Conformation

Fluorescence resonance energy transfer (FRET) and antibody binding studies initially suggested that Tau can form a double hairpin structure, bringing the N- and C-terminal domains into proximity with the repeat domain, resembling a paperclip shape. NMR studies using paramagnetic relaxation enhancement (PRE) provided high-resolution structural insights, revealing that Tau adopts a much more compact conformation than previously thought from electron microscopy images (Jeganathan et al. 2008).

Structural Features

The paperclip model shows Tau in a loosely packed but highly flexible form, exchanging between numerous conformations consistent with its intrinsically disordered nature. The repeat domain (R1-R4) and flanking regions are proposed to form a semi-rigid, transiently folded core, with the N- and C-terminal domains folding back and making long-range interactions with this core. Specific sequences like the VQIINK and VQIVYK motifs in R2 and R3 are prone to forming β-sheet structures and are implicated in the paperclip folding (Jeganathan et al. 2008; Mukrasch et al. 2009; Zabik, Imhof, and Martic-Milne 2017).

Functional Implications

The paperclip conformation is thought to regulate Tau's interactions with microtubules and other binding partners by modulating the accessibility of key binding sites. Pathogenic mutations or post-translational modifications that disrupt this native paperclip folding could potentially expose aggregation-prone regions and promote pathological Tau aggregation (Jeganathan et al. 2008; Mukrasch et al. 2009).

Conformational Dynamics

The paperclip structure is not a single, rigid conformation but rather represents an ensemble of compact conformations in dynamic equilibrium. Binding of Tau to partners like microtubules or molecular chaperones like Hsp90 can induce conformational opening and unfolding of the paperclip (Mukrasch et al. 2009; Zabik, Imhof, and Martic-Milne 2017; Weickert et al. 2020).

2. Functions of Tau

The configuration of Tau is important for its normal functioning. The N-terminal part of Tau extends away from microtubules, and although it does not directly bind to these structures, it plays a role in regulating microtubule dynamics, influencing microtubule attachment and spacing relative to other cellular components (Sillen 2007). The specific function of the N-terminal region is still poorly understood, but it has significant implications for distinguishing between the 0N, 1N, and 2N isoforms, which exhibit distinct subcellular localizations in the brains of mice (Kanaan et al. 2011).
The proline-rich domain contains four P-XX-P motifs that can bind to proteins containing the SH3 (Src homology-3) domain, such as Src family kinases like Lck, Fgr, Fyn, as well as other diverse proteins such as Bin1 (Bridging integrator 1) and peptidylprolyl cis/trans isomerases. Direct interactions between Tau and SH3 domain-containing proteins play a crucial role in regulating Tau's signaling functions (Flanagan et al. 1997). Similarly, this domain has been demonstrated to interact with DNA and RNA, which may explain the presence of Tau in the nucleus (Bukar Maina, Al-Hilaly, and Serpell 2016).
Tau binds to microtubules through the repeat domain, and the part separating the repeats has a regulatory role. The presence of different amino acids in the repeats shows that there is some difference

in the affinities of the repeats to microtubules (Sillen 2007). Other proteins also bind to Tau through the repeat domain, such as F-actin, α-synuclein, histone deacetylase, apolipoprotein E, and presenilin (Guo, Noble, and Hanger 2017). Regarding the C-terminal region of Tau, neither its function nor the proteins that bind to this domain have been determined. However, studies have revealed that modifications in this region can influence other domains of Tau, thus affecting their interactions with other proteins and their availability for phosphorylation. These observations highlight the potential importance of the C-terminal region in the overall regulation of Tau and suggest its involvement in complex regulatory processes.

The functions and localizations of Tau will be detailed in Section 3.

3. Localization and roles of Tau in Neurons

The cellular distribution of Tau is regulated during development. In young neurons, Tau is evenly distributed in the cell body as well as in neurites. Later, as axons emerge and neurons polarize, Tau enriches in axons, with minor amounts found in dendrites and nuclei (Wang and Mandelkow 2016).

3.1. Cytoskeletal Localization

Recognized as a Microtubule Associated Protein (MAP), the essential role of Tau protein is in the regulation of microtubules. In adult neurons, Tau is mainly localized in axons where it interacts with microtubules.

Microtubules (MTs) are cytoskeletal fibers approximately 25 nm in diameter. Their length varies due to the dynamic balance between polymerization and depolymerization at each end. Microtubules are composed of a unique type of globular proteins: tubulin. Tubulin is a dimer consisting of two similar polypeptides called α-tubulin and β-tubulin. Tubulin dimers polymerize end-to-end via GTP hydrolysis catalyzed by the β subunit, to form microtubules composed of 13 protofilaments that come together to form a hollow cylinder (Figure 2.4). The protofilaments forming the microtubules are arranged in parallel, allowing them to have a well-polarized structure. Indeed, microtubules have two different ends: a positive end (β-tubulin end) called the fast-growing end, and a negative end (α-tubulin end) called the slow-growing end. These two ends then give the image of a conveyor belt during the elongation phase (Cooper 2000).

Tau stabilizes microtubules either by direct binding or by acting as a bridge that allows microtubules to interconnect with cytoskeletal components such as actin and neurofilaments(Qiang et al. 2018). Inactivation of Tau protein reduces neuronal growth (Liu, Lee, and Jay 1999), alters the repulsive response of growth cones (Biswas and Kalil 2018), disrupts axonal extension (Caceres and Kosik 1990), delays neuronal maturation (Caceres, Potrebic, and Kosik 1991), and reduces the density of microtubules (Harada et al. 1994). Tau also recruits end-binding (EB) proteins to the stable microtubule bundle, preventing them from targeting the microtubule ends where they increase the frequency of catastrophes (Ramirez-Rios et al. 2016).

Microtubule dynamic instability is a fundamental feature of the microtubule cytoskeleton, characterized by the rapid alternation between growth (polymerization) and shortening (depolymerization) at microtubule ends. This dynamic behavior is driven by GTP hydrolysis on β-tubulin subunits following their incorporation into the microtubule lattice. A key aspect of this instability is the occurrence of catastrophes, where microtubules switch from a phase of growth to rapid shrinkage, and rescues, where they transition back from shrinkage to growth. Catastrophes are not random single-step events but involve multiple intermediate steps. The rates of microtubule growth and shrinkage are influenced differently by tubulin concentration, with growth scaling linearly while shrinkage remains largely unaffected. Interestingly, the frequency of catastrophes shows low sensitivity to tubulin concentration. Additionally, microtubule aging plays a role, as older microtubules exhibit a higher probability of undergoing catastrophe compared to younger ones (Bowne-Anderson 2013)

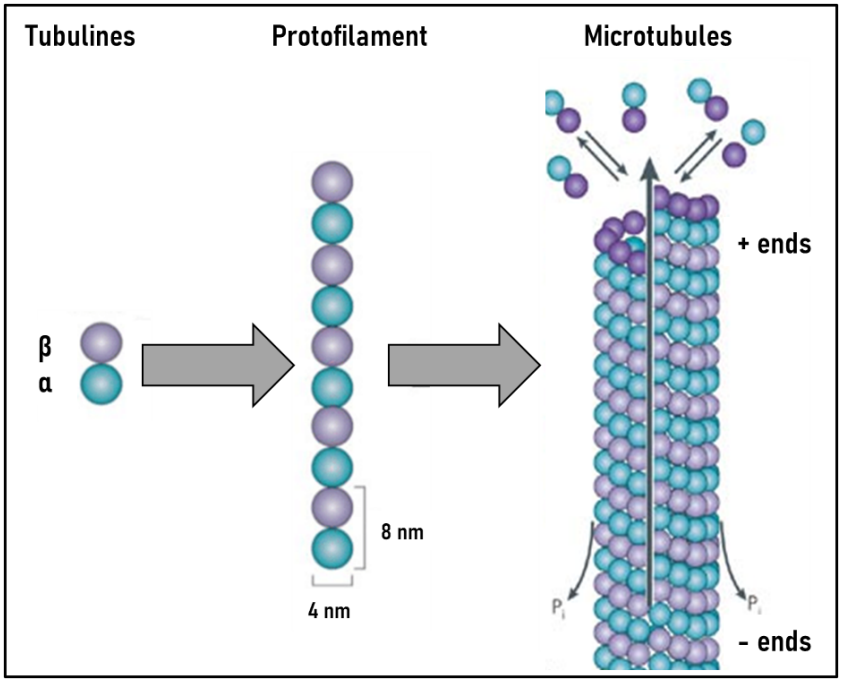

Figure 2.4: Structure and assembly of microtubules. (Figure adapted from Akhmanova and Steinmetz 2008)

3.2. Axonal Localization

Under physiological conditions, Tau is mainly expressed in neurons and, to a lesser extent, in oligodendrocytes and astrocytes. Intraneuronal Tau is concentrated in the axons of neurons, with some quantities of this protein also found in somatodendritic compartments, plasma membranes, nucleus, and mitochondria.
The distribution of Tau is polarized in neurons. Specifically, Tau mRNA is directed to axons by the axonal localization signal in the 3' untranslated region of *mapt*. Subsequently, mRNA translation can be regulated. Cytosolic Tau can also be translocated to axons either by free diffusion between different compartments or by motor transport mediated by proteins. The retention of Tau in axons is ensured by maintaining a low level of Tau phosphorylation in axons, which increases the capacity for binding to axonal microtubules, as well as an axon initial segment (AIS), which forms a retrograde barrier allowing Tau to enter axons but preventing its return (Guo, Noble, and Hanger 2017).

3.3. Dendritic and Synaptic Localization

The role of Tau in dendrites is still not well understood. However, studies have shown the role of Tau in regulating synaptic plasticity in hippocampal neurons. Similarly, Tau plays a role in the synaptic and morphological maturation of new hippocampal granule neurons. Tau is required for the proper formation of postsynaptic densities, dendritic spines, and mossy fiber terminals. Knocking out Tau also results in the sensitivity of new neuronal granules to neurogenesis modulators (Guo, Noble, and Hanger 2017).

3.4. Tau and Neuronal Membrane

The N-terminal domain of Tau projects toward the plasma membrane of neurons, suggesting roles in intracellular signaling pathways, particularly within lipid-rich microdomains (Pooler and Hanger 2010). Tau's binding to the plasma membrane is influenced by its phosphorylation state: dephosphorylated Tau strongly associates with the membrane, as demonstrated in neuronal cells. When kinases are inhibited, reducing Tau phosphorylation, Tau rapidly translocates from the cytosol to the membrane. Conversely, inhibiting the phosphatase PP2A increases Tau phosphorylation and prevents its

membrane interaction (Pooler et al. 2012). This membrane association of dephosphorylated Tau is further supported by studies showing increased Tau release from brain slices during neuronal depolarization, which correlates with a rise in membrane-bound dephosphorylated Tau (Croft et al. 2017). Although Tau's primary role in stabilizing microtubules may seem at odds with its membrane association when dephosphorylated, this behavior can be understood as part of Tau's dynamic regulation. Phosphorylation reduces Tau's affinity for microtubules, allowing it to associate with other cellular structures like membranes. This suggests that dephosphorylated Tau's membrane binding may facilitate cellular signaling or vesicle formation, playing a role in intercellular communication through processes such as exosome release. This dynamic regulation is disrupted in pathological conditions like Alzheimers disease, leading to abnormal Tau accumulation (Arrasate, Pérez, and Avila 2000; Croft et al. 2017).

3.5. Nuclear Localization

A number of studies have shown that Tau protein is present in the nucleus and nucleolus of many cell lines (Maina et al. 2018). Post-translational modifications, such as phosphorylation, impact the nuclear localization of Tau protein and its ability to bind to DNA and protect it (Diez and Wegmann 2020). Additionally, it has been discovered that nuclear Tau undergoes stress-triggered redistribution, suggesting its involvement in the nucleolar stress response (Maina et al. 2018). The relevance of Tau extends beyond its conventional cytoplasmic localization, as evidenced by its presence in the nucleus and its possible involvement in DNA and RNA homeostasis. Thus, research on the nuclear localization of Tau and its possible role in neurodegenerative diseases is ongoing and could lead to a better understanding of the pathophysiology of these diseases (Ulrich et al. 2018).

4. Tau and Post-translational modifications

4.1. Post-translational modifications

Post-translational modifications (PTMs) refer to covalent processing occurrences altering the characteristics of a protein either through proteolytic cleavage or the addition of modifying groups to one or more amino acids. Far from being merely decorative, PTMs play crucial roles in determining a protein's activity state, localization, turnover, and interactions with other proteins (Mann and Jensen 2003).There are numerous distinct post-translational modifications, each with specific functions. The most common modifications include phosphorylation, glycosylation, acetylation, methylation, ubiquitinylation and sulfonation.

4.2. Tau and PTMs

Approximately 35 percent of the amino acid residues in tau are susceptible to modification peri- or post-translationally. These residues are serine (S), threonine (T), tyrosine (Y), lysine (K), arginine (R), asparagine (N), histidine (H), and cysteine (C) (Alquezar, Arya, and Kao 2021). As an intrinsically disordered protein, Tau is prone to a variety of PTMs, such as phosphorylation on S, T, or Y, acetylation, ubiquitination, SUMOylation on K, methylation on K or R, oxidation on sulfur (M,C) , O-GlcNAcylation on S and T, and N-glycosylation on N. These PTMs regulate the structural properties, stability, or cellular localization of Tau, as well as its interaction network with targets, thereby influencing the aggregation propensity or function of Tau. Consequently, alterations in PTMs have been considered as crucial indicators for the pathogenesis of neurodegenerative diseases (Ye et al. 2022). Tau can also undergo protonation on histidine residues and proteolytic cleavage (or truncation), although these modifications are often not considered alongside traditional PTMs.

In my thesis, I will focus on two primary post-translational modifications affecting Tau, namely phosphorylation and O-GlcNAcylation.

4.3. Phosphorylation

Phosphorylation is a crucial process of post-translational modification of proteins, playing a significant role in regulating their function and localization within the cell. This process is highly regulated and specific, and defects in phosphorylation processes are linked to human pathologies.

Tau phosphorylation

Phosphorylation is the most studied post-translational modification in Tau. Being a disordered protein with numerous phosphorylation sites, Tau is a target for several kinases. The longest isoform of Tau, 2N4R, has 85 potential phosphorylation sites for serine, threonine, or tyrosine residues (Rawat et al. 2022).
Three types of kinases can phosphorylate Tau:

- Proline-Directed Protein Kinases, which phosphorylate Ser/Thr-Pro motifs such as GSK3β (Pelech 1995)
- Non-Proline-Dependent Protein Kinases, which phosphorylate serines and threonines without the need for proline, such as casein kinase 1 and 2 (Singh et al. 1996)
- Tyrosine kinases, which phosphorylate five tyrosines of Tau, such as kinases from the Src family (Lebouvier et al. 2009).

Phosphorylation is a reversible post-translational modification through the action of phosphatases targeting either phosphorylated Ser/Thr, such as PP-1, PP-2A, PP2-B, and PP-5, or tyrosines, such as STEP (Braithwaite, Stock, and Mouradian 2012). Normal phosphorylation of Tau is represented by 2-3 moles of phosphate per mole of protein (Ksiezak-Reding, Liu, and Yen 1992). Phosphorylation of Tau at specific sites is the predominant mechanism by which Tau and its functions are regulated.
The first significant role of Tau phosphorylation lies in regulating Tau's binding to microtubules. Phosphorylation of the KXGS motif, found in the three or four repeat domains, reduces Tau's binding to microtubules in vitro and likely in vivo. In vitro studies have shown that phosphorylation of Tau at Ser262 alone is sufficient to significantly attenuate Tau's ability to bind to microtubules (Schneider et al. 1999). Additionally, in situ phosphorylation of two or more other sites within the KXGS motif is necessary for the reduced binding of Tau to microtubules and to facilitate cellular processes. Thus, several other studies have demonstrated the importance of Tau phosphorylation in its binding to microtubules (Johnson and Stoothoff 2004) (Figure 2.5).
During axonogenesis, the function of Tau appears to be locally regulated by phosphorylation. Interestingly, there is a proximodistal gradient of Tau protein phosphorylation at Ser199/202 and Thr205 along the nascent axon: Tau protein in the cell body and proximal axon is phosphorylated at 80 % at these sites, while Tau in the growth cone is phosphorylated at 20 % (Mandell and Banker 1996). Moreover, neurite outgrowth appears to require spatial and temporal specific phosphorylation of Tau at KXGS motifs, likely by MARK or PKA (Biernat and Mandelkow 1999; Biernat et al. 2002). Conversely, there are hypotheses indicating that GSK3-mediated phosphorylation of Tau could facilitate neurite retraction (Sayas, Ávila, and Wandosell 2002). Tau regulates axonal transport in the central nervous system. When the protein is overexpressed in mouse models, axonal and myelin degeneration is observed, with axonal swellings containing cytoskeletal elements, particularly in spinal cord neurons (Ishihara et al. 1999; Probst et al. 2000; Spittaels et al. 1999).
Tau protein can inhibit fast axonal transport by reducing the motor attachment frequency, but it has no effect on the speed or run length of kinesin once it is attached to microtubules. Phosphorylation of

Tau modulates its affinity for microtubules and therefore its ability to regulate motor activity. GSK3β overexpression in transgenic mice expressing human Tau protein significantly increases Tau protein phosphorylation and reduces axonopathy compared to mice overexpressing only human Tau protein, likely because increased phosphorylation of Tau decreases its affinity for microtubules and makes it less effective in competing with kinesin for attachment sites, thereby increasing kinesin attachment and restoring anterograde axonal transport (Johnson and Stoothoff 2004). Hyperphosphorylation,

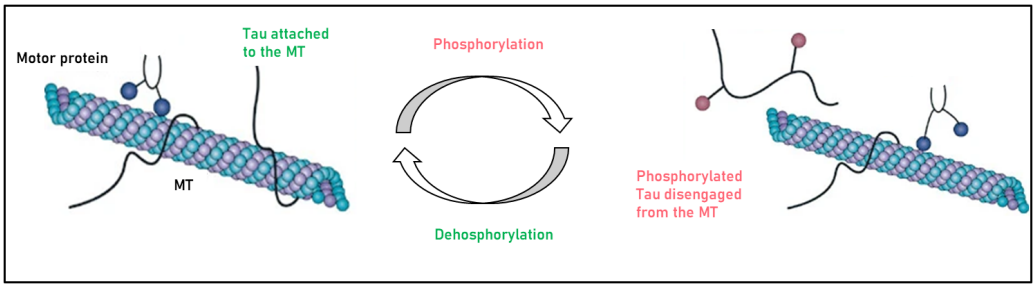

Figure 2.5: Dynamic equilibrium of Tau-microtubule binding regulated by Tau phosphorylation (Figure adapted from Ballatore, Lee, and Trojanowski 2007)

however, possesses the ability to disturb this dynamic Tau balance. Subsequently, the hyperphosphorylated proteins totally separate from the microtubules, causing them to become unstable and preventing axonal transmission. Furthermore, the amount of free proteins in the cells are greatly enhanced as a result (Figure 2.6).

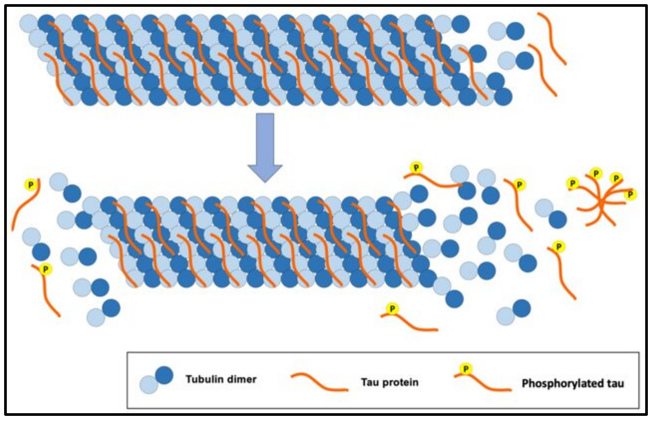

Figure 2.6: Consequences of Tau protein hyperphosphorylation for the structure of tubulin microtubules, a classic pathology of AD (García-Morales et al. 2021).

4.4. O-GlcNAcylation

Glycosylation is an important post-translational modification of proteins, which can affect their function, stability, and localization within the cell. It is catalyzed by specific glycosyltransferases that add carbohydrates to specific amino acid residues.
There are two main types of glycosylation: N-glycosylation and O-glycosylation. N-glycosylation involves adding carbohydrates to a specific asparagine in the consensus motif N-X-S/T, where X can be any amino acid except proline. O-glycosylation involves adding carbohydrates to specific serine or threonine residues in various motifs (Figure 2.7).
Glycosylation is involved in numerous physiological processes, and defects in glycosylation can lead to serious diseases, such as congenital disorders of glycosylation (CDG), which affect enzymes involved in N-glycan synthesis of N-glycosyl-proteins (Huynh and Boyce 2023).
A variant of O-glycosylation is O-β-GlcNAcylation, which involves adding a single O-β-N-acetylglucosamine

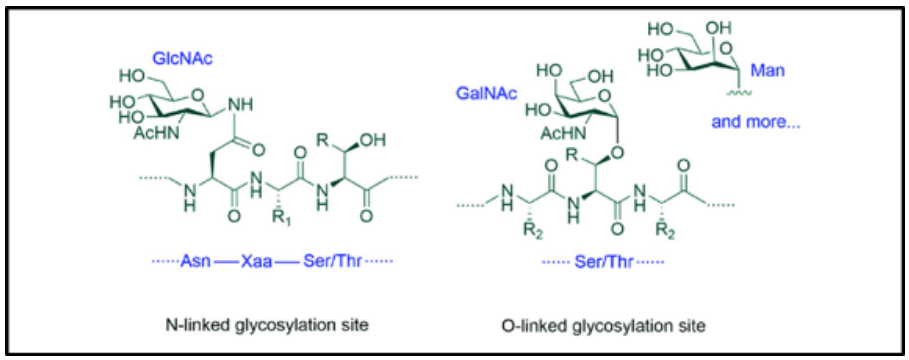

Figure 2.7: The two main types of glycosylation (Ma et al. 2020)

group to serine and threonine residues of hundreds of nuclear, cytoplasmic, and mitochondrial proteins, representing the major form of intracellular glycosylation.
35 years ago, Hart and Torres discovered protein O-GlcNAcylation by using bovine milk galactosyltransferase to attach tritiated UDP-galactose onto GlcNAc residues on murine lymphocytes (Torres and Hart 1984).
O-GlcNAcylation occurs through the hexosamine biosynthetic pathway (HBP) (Figure 2.8), which integrates the metabolism of glucose, amino acids, fatty acids, and nucleotides to produce uridine diphosphate N-acetylglucosamine (UDP-GlcNAc), the substrate for O-GlcNAcylation. O-GlcNAc signaling is influenced not only by nutrient availability but also by various cellular stresses, such as heat shock, hypoxia, and nutritional deprivation. The precise mechanisms underlying this response are still under investigation (Hart et al. 2011).
Unlike phosphorylation, which is regulated by hundreds of kinases and phosphatases, O-GlcNAcylation is regulated by only two enzymes: O-GlcNAc transferase (OGT),responsible for transferring GlcNAc derived from UDP-GlcNAc to protein S/T residues upon the release of UDP, and O-GlcNAcase (OGA) that removes GlcNAc from proteins (Huynh and Boyce 2023) (Figure 2.9). Protein structures of OGT and OGA are described in Section 4.5. and Section 4.6. respectively.
O-GlcNAcylation controls many cellular processes and is essential in mammals, as deletion of the OGT gene has been shown to be lethal in mice. It also influences all types of tissues, such as the brain, where there is high expression of the OGT gene, and O-GlcNAcylation is abundant in postsynaptic densities and synapses. OGT utilizes UDP-GlcNAc to add a GlcNAc group to the serine or threonine amino acid residues of intracellular proteins, while OGA catalyzes the hydrolysis of this group (Huynh and Boyce 2023).

4.5. OGT : Role, gene and protein structure

OGT, or O-GlcNAc transferase, belongs to the Leloir-type glycosyltransferase family. Leloir enzymes utilize nucleotide-based molecules as substrates, specifically nucleotide sugars (as UDP-GlcNAc) which serve as high-energy donors, facilitating glycosylation processes. This mechanism enables the transfer of sugar moieties onto specific target molecules, thereby modulating their function and activity within the cell (Ross, Davis, and Fridovich-Keil 2004).
Human OGT is encoded by a single gene situated on chromosome X, specifically at the locus Xq13.1, which is in close proximity to the X-inactivation center (Shafi et al. 2000). Alternative splicing of this gene gives rise to three distinct isoforms of OGT (Lazarus et al. 2011):

- A full-length nucleocytoplasmic form weighing approximately 110 kDa, often referred to as OGT.
- A shorter form with a molecular weight of around 75 kDa, known as sOGT.
- A mitochondrial form weighing about 103 kDa, termed mOGT.

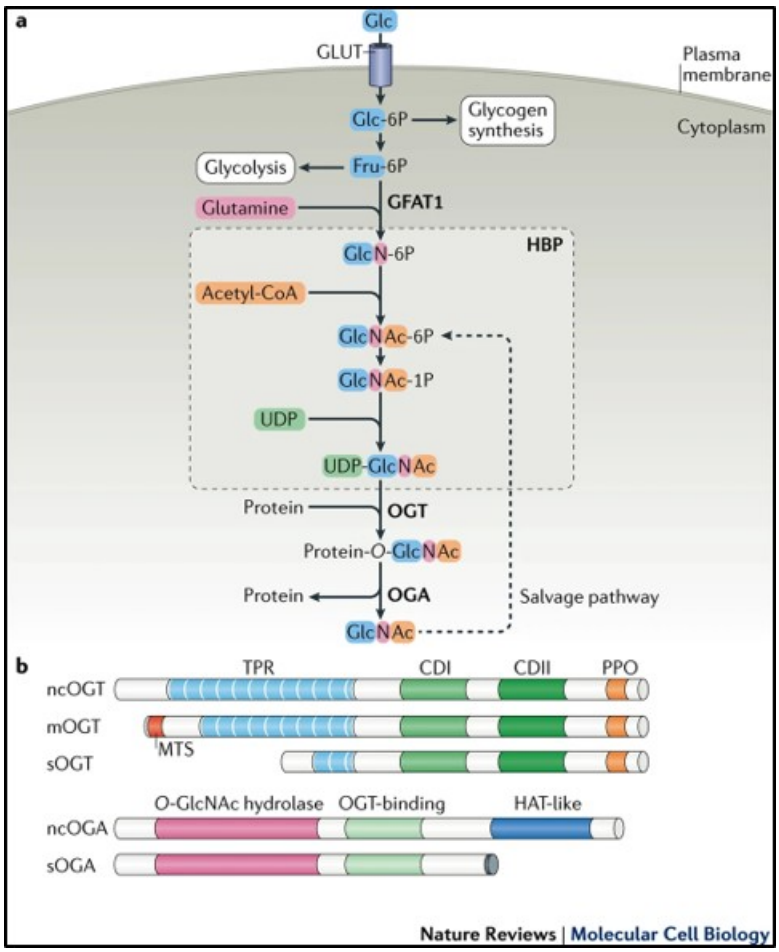

Figure 2.8: The flow of nutrients through the hexosamine biosynthetic pathway governs protein O-GlcNAcylation (**qiangTauDoesNot2018**)

These isoforms exhibit differential subcellular localization and may have distinct roles or functions within the cell.
OGT (O-GlcNAc Transferase) recognizes and modifies its protein substrates through multiple modes involving its TPR (Tetratricopeptide Repeat) domain and catalytic site.

TPR Domain and Substrate Recognition

The TPR domain of OGT binds to intrinsically disordered regions (IDRs) of substrates, forming a superhelical structure. This domain contains an "Asn-ladder" and "Asp-ladder" of asparagine and aspartate residues, which interact functionally with the stalk and catalytic domains of substrates like OGA. Specific TPR residues spanning TPRs 3-13.5, primarily on the concave surface, form a binding tunnel leading to the active site and are crucial for substrate recognition. These residues can be categorized into four types based on their effects on OGT-substrate interactions: those affecting binding, those affecting catalysis, those affecting both binding and catalysis, and those with no effect (Kositzke et al. 2021; Lu et al. 2023).

Catalytic Site and Substrate Recognition

The catalytic site of OGT relies mainly on backbone interactions with various peptide substrates, enabling promiscuous substrate recognition. The GlcNAc moiety of substrates forms abundant conserved interactions with the OGT catalytic pocket. Additionally, substrate peptide side chains and backbones interact with surface residues in the substrate-binding cleft near the active site (Li et al. 2017a).

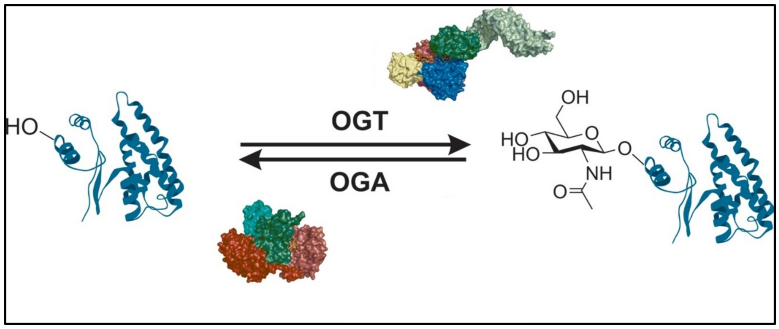

Figure 2.9: O-GlcNAcylation process (Figure adapted from Alteen, Tan, and Vocadlo 2021)

4.6. Substrate recognition by OGT

There is various mechanisms by which O-GlcNAc transferase (OGT) recognizes and binds its substrates.

Substrate Selection: Consensus Sequence

Finding a consensus sequence that determines the location of the O-GlcNAc modification is a desirable prospect since consensus sequences control a significant portion of the N-linked glycosylation in the secretory pathway. Over the years, 7,002 O-GlcNAcylation sites have been identified across 1,803 proteins, with 58.4 % located on serine residues and 41.6 % on threonine residues, reflecting the natural abundance of these amino acids in the human proteome, where serine makes up 60.9 % and threonine 39.1 %. The analysis of amino acid sequences around these O-GlcNAcylation sites has led to the identification of a semi-consensus sequence, which suggests a preference for certain amino acids, such as proline, valine, and alanine, adjacent to the modified serine or threonine residues. These specific amino acids within the semi-consensus sequence may enhance the likelihood of O-GlcNAcylation, potentially influencing the structural conformation of proteins and their interaction with OGT, thereby impacting their biological functions and aiding in the prediction of O-GlcNAcylation sites in other proteins (Wulff-Fuentes et al. 2021; Wu et al. 2014).

According to analysis carried out after the OGT enzyme was discovered, glycosylation may need substantial enrichment of S/T residues, proline, and acidic residues close to the glycosylation site. Early characterisation of O-GlcNAc-modified peptides revealed common "PVST" and "TTA" patterns close to the glycosylation site, which are somewhat similar to "mucin domains" for O-GalNAc modification in the secretory route. Further analysis of phosphorylation/O-GlcNAcylation crosstalk has identified a frequently occurring motif involving Ser/Thr proline-directed phosphorylation sitesi.e., sites targeted by proline-directed kinasesthat are enriched in the phospho-proteome. This suggests a significant overlap between phosphorylation sites and potential O-GlcNAcylation sites, further influencing substrate selection and modification patterns (Leney et al. 2017).

Based on structural evidence provided by crystallising OGT with synthetic peptides, subsequent work discovered a degenerate consensus sequence, [TS][PT][VT][ST][RLV][ASY] (Pathak et al. 2015). Many OGT substrates feature positively charged residues (R/K) 710 residues upstream of the glycosylation site that interact with Asp residues in the TPR domain, according to additional studies based on comparative sequence analysis and mutational evidence (Joiner et al. 2021). Later structural research looked for consistent secondary structures of OGT substrates, but it was unable to find any patterns in the structure, order, or disorder of the substrates that were known to exist (Stephen, Adams, and Wells 2021).

Substrate selection: selection by OGTs catalytic domain

A plausible hypothesis regarding OGT's potential to attain substrate selectivity is the employment of its dual domains, namely the catalytic and TPR domains. Research has also been done on the function of the catalytic domain itself in substrate selection, even if the TPR domain is still the more widely used option for substrate selectivity. It was proposed that OGT possessed a distinct PIP3-

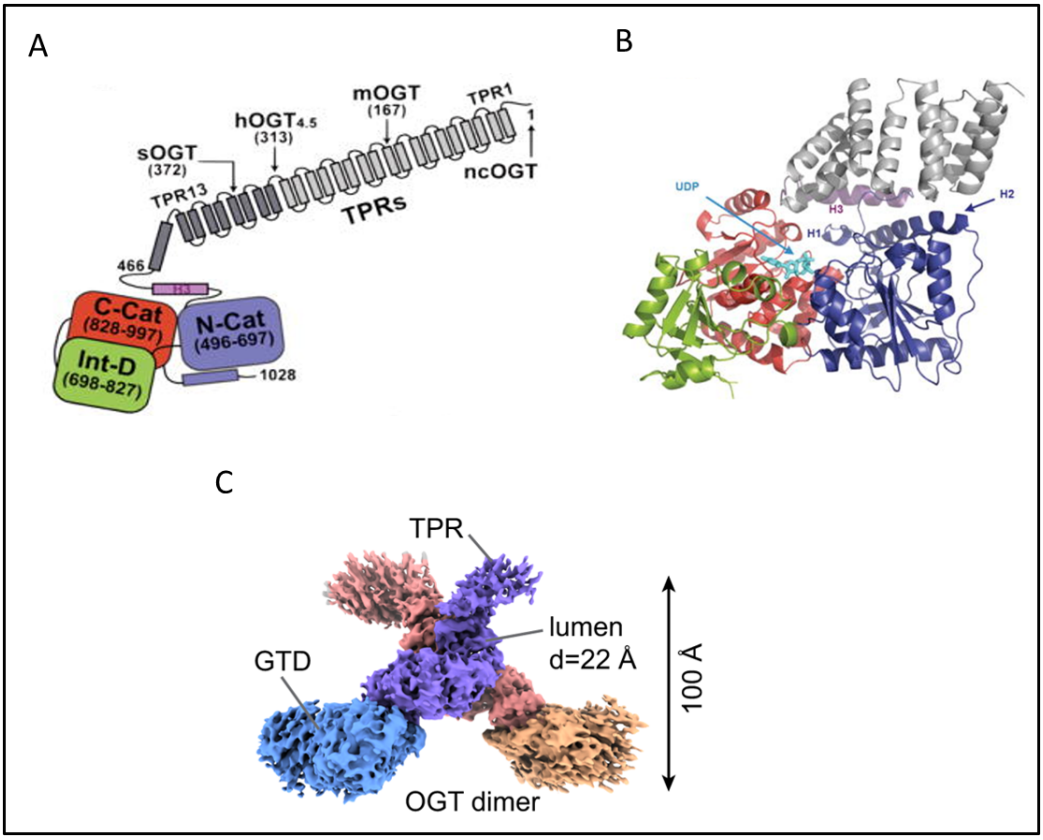

(A) Schematic representation of OGT domains: TPR units (gray), transitional helix H3 (purple), N-Cat domain (blue), Int-D domain (green), and C-Cat domain (red). The native isoforms (sOGT, mOGT, ncOGT) and the crystallization construct differ in the number of TPRs (Lazarus et al. 2011), (B) Crystal structure of OGT binding to the metabolite UDP (Lazarus et al. 2011), (C) Cryo-EM map of human OGT dimer (left panel). GTD, glycosyltransferase family B domain (Lu et al. 2023)

Figure 2.10: OGT protein structure

binding domain on its C terminus that could bind phosphoinositides, and that OGT modified insulin signaling-related proteins as a result of this interaction. Nevertheless, subsequent research has not been able to replicate this binding activity (Lazarus et al. 2011).
One interesting finding is that the catalytic domain of OGT is the only thing that p38, a particular OGT inhibitor, interacts with. The proteins that OGT interacts with were shown to be unaffected by this contact, however OGT was induced to O-GlcNAc alter the constitutive interactor neurofilament-H. As far as we are aware, this is the only protein interactor that has been demonstrated to work exclusively with OGT's catalytic domainthe TPR domain being excluded.

Substrate Recognition by the TPR Domain of OGT

The TPR domain can bind to unstructured regions of substrate proteins, facilitating their glycosylation by OGT. It recognizes disordered segments of the substrates, providing a compositional bias in amino acids for OGT targets. Additionally, the TPR domain interacts with globular parts of the substrates through unidentified regions of OGT, beyond the active site. It can also bind to specific peptide sequences of the substrates, as demonstrated with the HCF-1 peptide, which significantly extends into the TPR domain, anchored by numerous interactions.
OGT plays a crucial role in sensing and responding to glucose levels in cells. When glucose concentrations are high, OGT modifies various nuclear and cytoplasmic proteins. This modification affects the activity of these proteins, influencing important cellular processes such as gluconeogenesis regulation and insulin-like signaling pathways (Pathak et al. 2015).
Additionally, OGT appears to have a significant impact on cellular kinase signaling cascades, as

many sites where O-GlcNAcylation occurs overlap with sites of phosphorylation. This suggests a complex interplay between O-GlcNAcylation and phosphorylation in regulating cellular signaling (Wells, Vosseller, and Hart 2001).
Dysregulation of OGT activity, leading to hyper-O-GlcNAcylation, is associated with conditions such as diabetes and cancer. In these conditions, prolonged hyperglycemia or excessive glucose uptake results in elevated levels of O-GlcNAcylation, which can have detrimental effects on cellular function (Goldberg et al. 2006).
Given the role of OGT in these diseases, regulating its activity could potentially be a therapeutic target. By modulating OGT activity, it may be possible to mitigate the adverse effects of hyper-O-GlcNAcylation and potentially treat or manage conditions such as cancer and diabetes (Yang et al. 2008).

OGA: Role, gene and protein structure

In humans, OGA (O-GlcNAcase) is encoded by the gene *MGEA5* (for meningioma-expressed antigen 5) since it was identified as an antigen expressed in meningioma patients), which is located on chromosome 10 at the locus 10q24.1-q24.3. Interestingly, this genetic locus overlaps with the genetic locus associated with Alzheimer's disease. This suggests a potential link or involvement of OGA in the pathogenesis or susceptibility to Alzheimer's disease (Zhu and Hart 2021).
Human OGA (hOGA) is a 103-kDa nucleocytoplasmic protein comprising three distinct regions: an N-terminal catalytic domain (residues 60366) responsible for O-GlcNAc removal, a stalk domain (residues 367706), and a C-terminal pseudohistone acetyltransferase (HAT) domain (residues 707916), lacking key residues for binding acetyl-coenzyme A (acetylCoA) , necessitating clarification of its precise role (Figure 2.11) (Li et al. 2017b).
Similarly to OGT, two isoforms of OGA exist that differ in their cellular localization.

- OGA-L, the long, full length form, located predominantly in the cytoplasm and the nucleus (Gao et al. 2001; Toleman et al. 2004)
- OGA-S, the short form, located predominantly at the nucleus (Comtesse, Maldener, and Meese 2001)

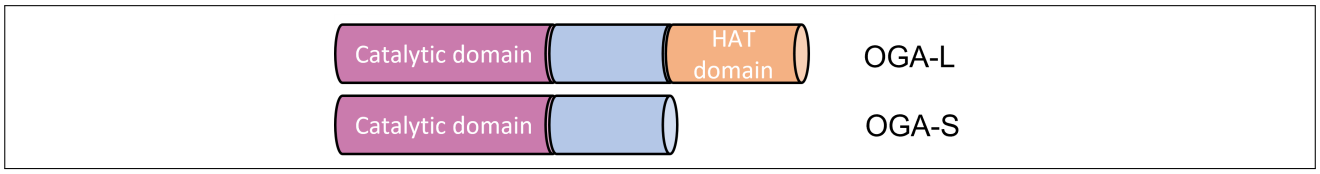

Figure 2.11: OGA isoforms

In 2017, Li and collaborators utilized a simplified version of hOGA, comprising residues 60704 of hOGA, named OGA_{Cryst} and in which the unstructured insert residues 401552 were replaced by a 15-residue glycine-serine (GS) linker (GS15linker), to elucidate the crystal structure of OGA. This structure was elucidated because structural predictions indicate that hOGA features two low-complexity regions, with one situated at the N-terminus and the other inserted within the stalk domain. These regions are projected to exhibit flexibility and lack structural order, presenting a significant hurdle in the generation of protein crystals suitable for diffraction studies, that can be overcomed by using OGA_{Cryst}.

Tau O-GlcNAcylation

Like phosphorylation, Tau protein is a target for O-GlcNAcylation. Tau O-GlcNAcylation was first described in 1996 (Arnold et al. 1996), with the level initially estimated to be around four O-GlcNAc

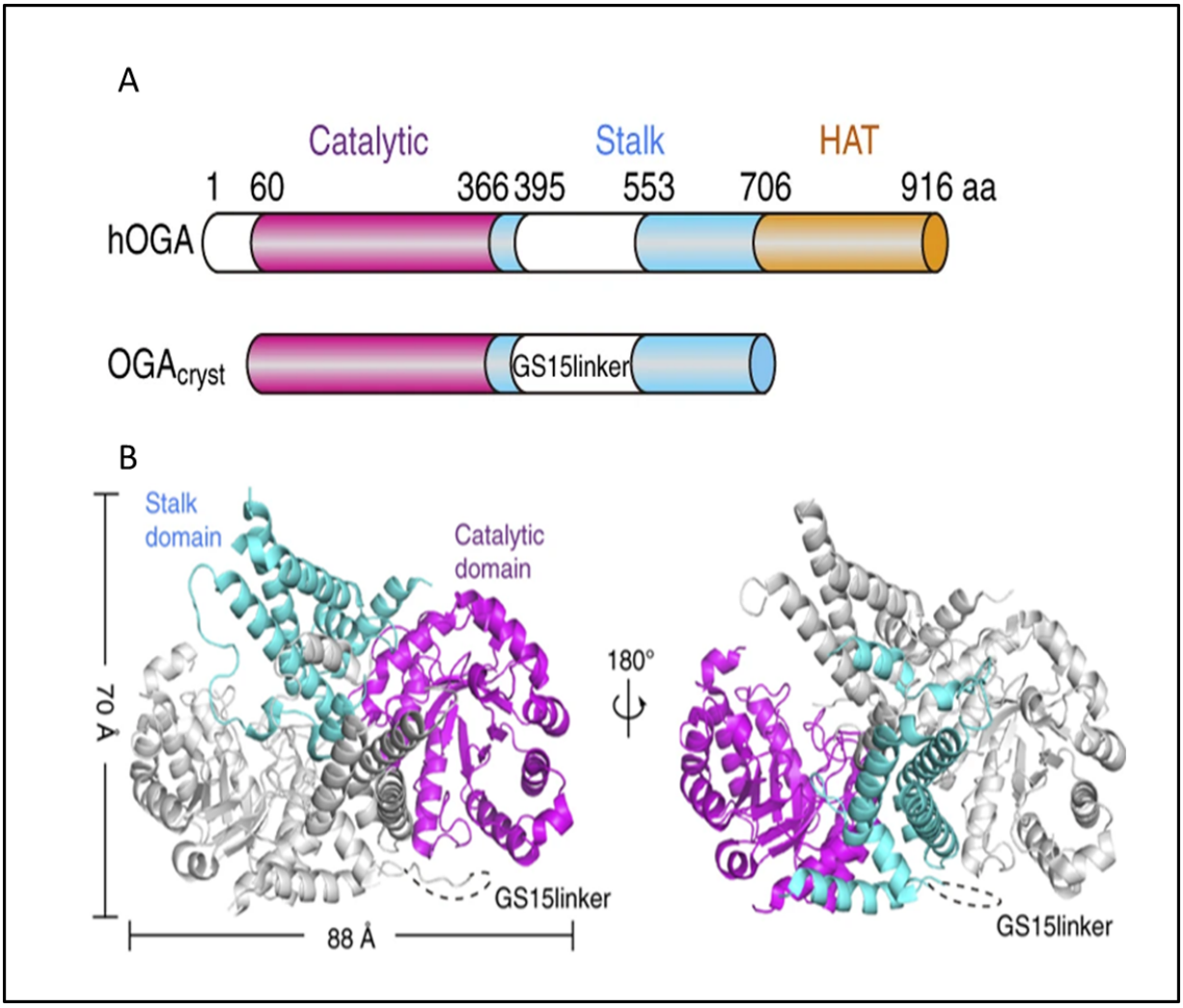

(A) Schematic of the domain architecture of the hOGA and OGA$_{cryst}$ constructs used in the study of Li et al. 2017b. Catalytic domain (residues 60366), stalk domain (residues 367706), HAT domain (residues 707916), and low-complexity regions are highlighted in magenta, cyan, orange and white, respectively. GS15linker represents amino acid (aa) residues 401552, which were replaced by a 15-residue glycine and serine linker in OGAcryst (Lazarus et al. 2011) (B) Ribbon representation of the OGA$_{c}ryst$ homodimer in two different views. The OGA-α monomer is colored gray; the catalytic domain and stalk domain of OGA-β are colored magenta and cyan, respectively. GS15linker is shown as a dashed line

Figure 2.12: OGA protein structure

groups per molecule on at least 12 Ser/Thr sites. Tau O-GlcNAcylation sites were first identified in 2010 where O-GlcNAc-modified peptides undergo tagging using a unique biotinylation reagent and enriched through affinity chromatography then subsequently liberated from the solid support via photochemical cleavage. Finally, the liberated peptides are subjected to analysis using electron transfer dissociation mass spectrometry (Wang et al. 2010a). Several Tau GlcNAcylation sites have been described, including T123, S185, S191, S208, S238, S400, S412, and S413 (Morris et al. 2015; Yuzwa et al. 2012; Smet-Nocca et al. 2011). These sites were identified using O-GlcNAcylated recombinant Tau. The S400 site was identified as the sole endogenous Tau O-GlcNAcylation site in mouse brains (Yuzwa et al. 2012; Morris et al. 2015). In vivo, identification of O-GlcNAc sites is often challenging due to their low stoichiometry. Therefore, it requires enrichment procedures such as lectins, antibodies, and/or solid-phase extraction (Calle et al. 2021; Kim 2011). In 2023, new strategies aimed at either increasing OGT activity or improving O-GlcNAcylation detection led to the identification of new O-GlcNAc sites. Li et al. identified 19 O-GlcNAcylation sites, 13 of which were new, while

Bijttebier et al. identified low-abundance sites such as S208, S191, and S184 or S185 in a transgenic mouse model expressing human Tau protein treated with Thiamet-G (an OGA inhibitor), using immunoprecipitation combined with LC-MS/MS analysis (Li et al. 2023b; Bijttebier et al. 2023).
Many studies have shown that Tau O-GlcNAcylation may play a regulatory role by reducing the protein's phosphorylation level, potentially inhibiting its aggregation and the formation of NFT-type deposits in tauopathies. Additionally, it has been shown that O-GlcNAcylation has an intrinsic inhibitory role in Tau aggregation without altering its microtubule polymerization function (Yuzwa et al. 2008; Yuzwa et al. 2012; Yuzwa et al. 2014). This part will be detailed in the section 3.

4.7. Other PTMs

Tau protein undergoes PTMs that regulate its normal functions. Other than phosphorylation and O-GlcNAcylation, acetylation, primarily on lysine residues, which regulates Tau's stability and function; methylation, where mono-methylation of lysines plays a role in Tau regulation; and ubiquitination, which is involved in the normal degradation and turnover of Tau. These PTMs regulate Tau's affinity for microtubules, modulate protein-protein interactions, control its subcellular localization, and manage its turnover and degradation. Tau's PTMs are dynamic and finely regulated; for example, the half-life of Tau in hippocampal neurons is about 9.4 days, and there is a complex interplay between different PTMs, with some influencing or competing with others (Alquezar, Arya, and Kao 2021). PTMs also play a role in pathological functions, as discussed in Chapter 4.

Chapter 3: Tau and tauopathies

1. Generalities about Tauopathies

Neurodegenerative disorders characterized by the aggregation of abnormal Tau protein in the brain are grouped under the single umbrella term 'tauopathies'. Tau lesions in tauopathies display heterogeneity in their isoform composition, morphology, involvement of cell types, and the specific brain regions predominantly affected (Chung et al. 2021).
Two types of tauopathies are described : primary and secondary tauopathies.
Primary tauopathies are conditions characterized by the prominent accumulation of abnormal Tau protein. Examples include Pick's disease, progressive supranuclear palsy, corticobasal degeneration, and argyrophilic grain disease. Secondary tauopathies encompass diseases in which Tau pathology arises from diverse underlying causes. For instance, in Alzheimer's disease and chronic traumatic encephalopathy, Tau aggregation occurs as a response to other primary pathological processes, such as amyloid-beta accumulation or repetitive brain injury (Zhang et al. 2022; Chung et al. 2021).

2. Tauopathies classifications

2.1. Isoform classification

Primary tauopathies

Primary tauopathies are rare and heterogeneous. It include aging-related Tau astrogliopathy (ARTAG), argyrophilic grain disease (AGD), corticobasal degeneration (CBD), primary age-related tauopathy (PART), and progressive supranuclear palsy (PSP), among others (Irwin 2016). While many primary tauopathies are believed to be influenced by genetic factors to some extent, certain tauopathies are more distinctly associated with environmental triggers or exposures.

Secondary tauopathies

The most common example of a secondary tauopathy is AD, where tau pathology is thought to be driven or accelerated by beta-amyloid (Aβ) (See chapter 1 for more details). Other examples worth mentioning are Down syndrome, For instance, chronic traumatic encephalopathy (CTE) is linked to repetitive concussions or subconcussions, and Guam Parkinsonism-dementia complex (PDC), associated with exposure to environmental neurotoxins (McGeer and Steele 2011; Mackenzie and Neumann 2016).

2.2. *MAPT* Mutations: Coding and Non-Coding Variants and Their Effects on Tau Isoform Composition

MAPT mutations can be broadly categorized into coding and non-coding mutations, each exerting distinct influences on tau mRNA splicing and the isoform composition of tau inclusions

Non-coding Mutations

Non-coding mutations, particularly those located in the intronic regions such as the splice donor site of intron 10 (e.g., +3, +16), disrupt the regulatory elements responsible for tau exon 10 splicing. This disruption results in the increased inclusion of exon 10, leading to an overproduction of 4R tau isoforms, which contain the additional microtubule-binding repeat encoded by exon 10. Consequently, the Tau filaments formed exhibit distinct structural folds, such as the argyrophilic grain disease (AGD) fold, which is observed in cases with the +3 mutation (Strang, Golde, and Giasson 2019; Bhagat et al. 2023)..

Coding Mutations

Coding mutations, typically exonic missense mutations within the microtubule-binding repeat domain (e.g., P301L, S320F), are present in both 3R and 4R tau isoforms. These mutations enhance tau aggregation kinetics by destabilizing local structures and exposing amyloidogenic motifs, thereby promoting the formation of pathological tau aggregates. Additionally, these mutations reduce the ability of tau to bind and stabilize microtubules, impairing their essential role in maintaining neuronal integrity (Strang, Golde, and Giasson 2019; Bhagat et al. 2023)..
Furthermore, certain exonic mutations such as S305N and the silent S305S mutation can also affect exon 10 splicing. The S305N mutation induces stem-loop instability, which alters the 3R:4R ratio and reduces lysosomal Tau degradation. Conversely, the S305S mutation increases exon 10 inclusion, leading to an overproduction of 4R tau isoforms (**daCostaTaumRNAMetabolism2022**).

2.3. Structure-based classification of tauopathies

Another classification of tauopathies is based on the primary Tau isoforms found in the aggregates, namely the 3-repeat (3R) and 4-repeat (4R) Tau isoforms (Figure 2.2), which can be detected using isoform-specific antibodies or by analyzing the Western blot pattern of sarcosyl-insoluble Tau (Höglinger, Respondek, and Kovacs 2018).
Primary tauopathies can be categorized as either 3R tauopathy (such as Pick disease, abbreviated as PD), 4R tauopathy (such as Progressive supranuclear palsy, PSP; Corticobasal degeneration, CBD; Globular glial tauopathy, GGT; Argyrophilic grain disease, AGD), or 3R+4R tauopathy (such as Primary age-related tauopathy, PART) .
Secondary tauopathies are all classified as 3R+4R tauopathies such as Alzheimer's disease (AD) and Chronic traumatic encephalopathy (CTE) (Holper, Watson, and Yassi 2022).
The presence of various filament morphologies in human tauopathies has prompted the notion that different molecular conformations of aggregated Tau may exist.

Tau filaments in Alzheimer's disease

In Alzheimer's disease (AD), Tau undergoes abnormal self-assembly to form paired helical filaments (PHFs) and straight filaments (SFs), which accumulate in the brain as neurofibrillary tangles.
In 2017, cryo-electron microscopy (Cryo-EM) studies conducted by Fitzpatrick et al. 2017 have shown that paired helical filaments (PHFs) and straight filaments (SFs), purified from the brain of a 74-year-old AD patient, are ultrastructural polymorphs, characterized by differences in their interprotofilament packing. The sarkosyl-insoluble fraction of the patients neocortex contained numerous PHFs and SFs, which consisted of full-length, hyperphosphorylated Tau, as confirmed by immunogold electron microscopy. In line with earlier discoveries, both PHFs and SFs consist of two protofilaments with C-shaped subunits, as observed consistently.
The cores of both PHFs and SFs are composed of residues $V_{306}F_{378}$ (that is, all of R3 and R4) as well as 10 amino acids C-terminal to the repeats, and are comprised of eight β-sheets (β18) that extend

along the length of the protofilament, forming a C-shaped architecture. Each C structure includes a β-helix region, where three β-sheets are arranged in a triangular fashion, and two regions characterized by a cross-β architecture, where pairs of β-sheets align antiparallel to each other.
Around the region that constitutes the core of the fibers, as observed in cryo-EM (with PHFs having a width ranging from 7 to 15 nm and a longitudinal periodicity of 65 to 80 nm), the rest of the protein forms a "fuzzy coat" - a disordered layer approximately 16 nm thick, that resembles a polyelectrolyte brush which extends from both the N- and C-terminal domains of the fibril core (Figure 3.1). These regions represent together the largest portion of PHF-Tau (more than 70% considering the longest human Tau protein). The extreme N-terminal sequence consists of an unstructured, negatively charged domain while the remaining N-terminal sequence, attached to the fibril core, is positively-charged. This long N-terminal domain forms a two-layer polyelectrolyte brush together with the short, neutral C-terminal sequence around the fibril core, keeping a high degree of flexibility and potentially accessibility (to PTM enzymes, for example). Together, these layers create a 16-nm-thick fuzzy coat, which exhibits specific adhesive and mechanical properties, and is believed to play a critical role in the aggregation and stability of Tau fibrils, as well as in their interactions with other proteins and the physiological environement (Wegmann et al. 2013).

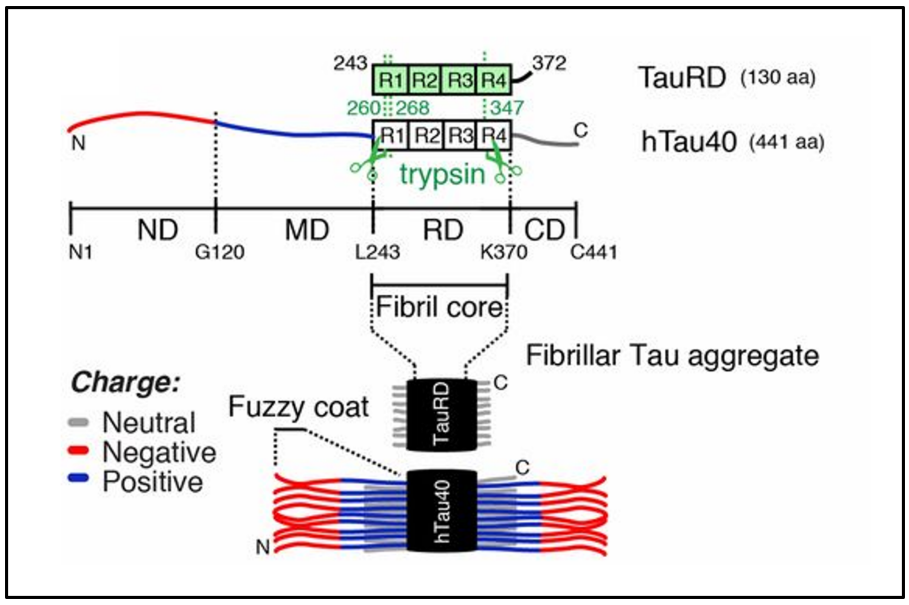

Figure 3.1: Fuzzy coat of Tau fibrils.

The ultrastructural polymorphism between PHFs and SFs arises from variances in the lateral contacts between the two protofilaments.
In PHFs, both protofilaments adopt identical structures, which are helically symmetrical, and their interface is characterized by the anti-parallel stacking of residues $_{332}$PGGGQ$_{336}$ (Figure 3.2 C). In SFs, the two protofilaments exhibit asymmetric packing (Figure 3.2 D). A less pronounced β-sheet-like density at the N-terminal end of the structured core is observed in one protofilament due to steric hindrance at the protofilament interface, hindering the formation of a peripheral β-strand on the other protofilament. While the β-helices of both protofilaments seem to share a similar chemical environment, the β-helix of the second protofilament appears to be more disordered.

Tau filaments in chronic traumatic encephalopathy

Chronic traumatic encephalopathy (CTE) is a neurodegenerative condition marked by the abnormal buildup of hyperphosphorylated Tau protein in the brain, defining it as a tauopathy (Dickstein et al. 2016).Repetitive head impacts (RHI) from contact sports or military service stand as the primary risk factor for developing chronic traumatic encephalopathy (CTE) (Butler et al. 2022).

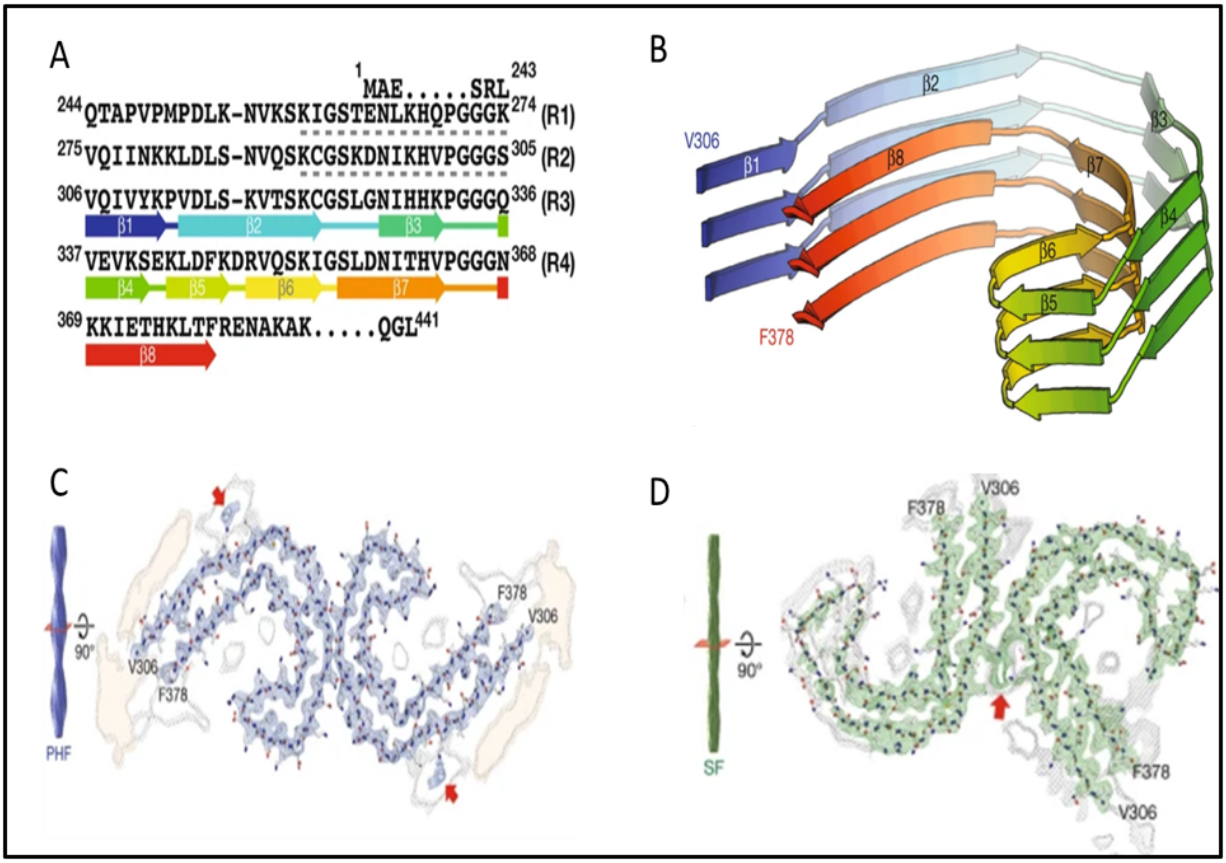

(A) Sequence alignment of the four MTBR with the eight β-strand regions from blue to red.
(B) Details of the C-form secondary structure of a protofilament.
(C) Cryo-EM density and atomic models of PHFs.
(D) Cryo-EM density and atomic models of SFs.

Figure 3.2: Cryo-EM structure of PHFs and SFs in Alzheimer's disease

In 2019, Falcon et al. 2019 determined the structures of Tau filaments from the brain of three individuals with CTE using cryo-EM. As a 3R+4R tauopathy, CTE exhibits the presence of all Tau isoforms within its filaments. Two types of filaments were identified, with type I comprising 90 % of the observed filaments, and type II representing the remaining 10 %.
Type I filaments consist of two protofilaments, where residues K_{274}-R_{379} of the 3R Tau isoform and S_{305}-R_{379} of the 4R Tau isoform constitute the core of the C-shaped protofilaments (Figure 3.3 A). Type I filaments differ from AD filaments due to a distinct β-helix region that forms a hydrophobic cavity, which is absent in AD filaments. Type II filaments resembled PHFs, and had pronounced helical twists (Figure 3.3 B).

Tau filaments in Pick's Disease

Pick's disease is a specific type of frontotemporal dementia (FTD), a degenerative brain disease that usually affects people under 65. It is characterized by the abnormal accumulation of Tau proteins, called Pick bodies, in the brain (Pippin and Gupta 2024). Pick's disease is the 3R only tauopathy that only contain 3R Tau isoforms.
In 2018, Falcon et al. 2018a used cryo-EM to determine the structure of Tau filaments from a patient having pick's disease. Two types of filaments could be distinguished: Narrow Pick Filaments (NPFs) representing 93 % of filaments, and Wide Pick Filaments (WPFs) representing 7 % of filaments .
Similar to AD, a fuzzy coat composed of the disordered N- and C-terminal regions of Tau surrounded the filament cores.

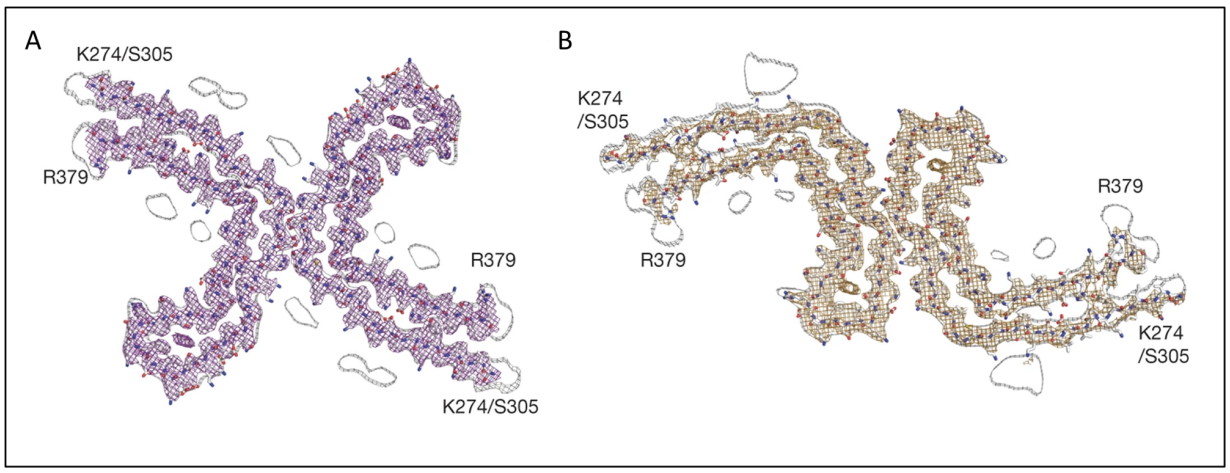

(A) Cryo-EM density and atomic models of type I Tau filaments, (B) Cryo-EM density and atomic models of type II Tau filaments

Figure 3.3: Cryo-EM structure of CTE type I and II Tau filaments

NPFs consist of a single protofilament with an elongated structure, which contrasts significantly with the C-shaped protofilament of PHFs and SFs typically observed in AD. WPFs are formed by the association of two NPF protofilaments at their distal tips.

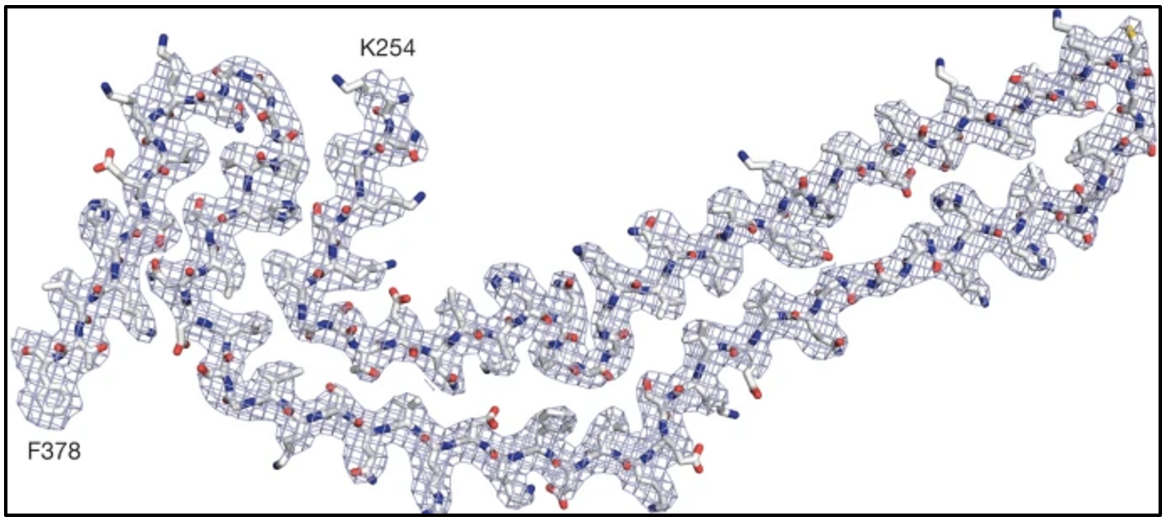

Figure 3.4: Cryo-EM structure of the NPF

Tau filaments in corticobasal degeneration

Corticobasal degeneration (CBD) is an infrequent, progressive neurodegenerative condition marked by the abnormal buildup of hyperphosphorylated Tau (p-tau) protein within the brain. It is classified as a primary 4-repeat (4R) tauopathy, indicating that the Tau filaments exclusively consist of Tau isoforms with four microtubule-binding repeats (Kouri et al. 2011).
In 2020, Zhang et al. 2020 used cryo-EM to analyze the structures of Tau filaments extracted from the brains of three individuals diagnosed with CBD based on neuropathological confirmation. The cores of the Tau filaments include the hole R1, R3 and R4 repeats. Narrow and wide filaments were observed, named as Type I and Type II, respectively. All Type I filaments extracted from the three individuals consisted of only one protofilament adopting a four-layered fold, while Type II filaments comprised two protofilaments of Type I. The core structure of the protofilaments consisted of residues K_{274}-E_{380}, corresponding to the last residue of the R1 repeat, the entire sequence of R2-

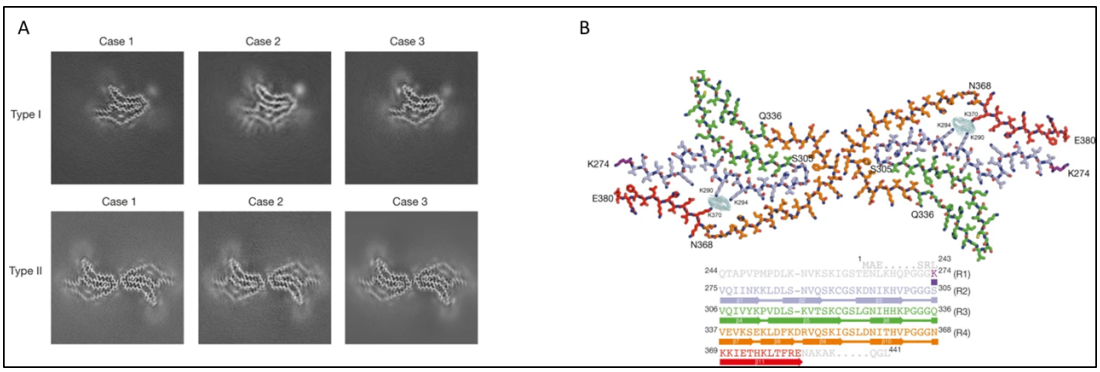

(A) Cryo-EM maps of type I and type II tau filaments (B) Atomic models of type II Tau filaments and the R1R4 region of Tau and the sequence after R4 that is present in the core of CBD filaments

Figure 3.5: Cryo-EM structure of CBD type I and II Tau filaments

R4, and an additional 12 residues following the R4 repeat. Eleven β-strands were identified, with β_1-β_3 corresponding to the R2 repeat, β_4-β_6 originating from the R3 repeat, β_7-β_{10} stemming from the R4 repeat, and β_{11} arising from the sequence following the R4 repeat.
The central four layers consist of β_7, β_4, β_3, and β_{10}. Strands β_3 and β_4 are connected by a sharp turn, while β_7 and β_{10} are connected through β_8 and β_9, which wrap around the turn. On the opposite side, β_2, β_5, and β_6 form a three-layered structure. β_2 packs against one end of β_5, and β_6 packs against the other end. The first and last strands, β_1 and β_{11}, interact with each other, closing a hydrophilic cavity formed by residues from β_2, β_3, β_{10}, β_{11}, and the connections between β_1 and β_2, as well as between β_2 and β_3. All interfaces in the CBD fold have mixed compositions of polar and hydrophobic groups. In CBD type II tau filaments, the two protofilaments are related by C2 symmetry. The interface between protofilaments is formed by antiparallel stacking of $_{343}$KLDFKDR$_{349}$. Besides van der Waals interactions between the antiparallel side chains of K_{347} from each protofilament, the side chain of K_{347} is positioned to form hydrogen bonds with the carboxyl group of D_{348} and the backbone carbonyl of K_{347} on the opposite protofilament (Figure 3.5).
These filaments were consistent across all cases but differed from those found in Alzheimers disease, Picks disease, and CTE.

Tau filaments in PART

In 2021, Shi et al. 2021a utilized extracts from the frontal cortex of PART patients to elucidate the filament structure of Tau bound to a PET ligand (APN-1607). We can find a mix of PHFs and SFs. These filaments were found to be identical to those observed in posterior cortical atrophy (PCA) (an AD variant) (see Figure 3.6).

Tau filament in other tauopathies

In 2021, Shi et al. 2021b aimed to elucidate the structures of filaments in resting tauopathies for comparison both within this group and with the filaments observed in AD.
As observed in the preceding sections, the structures of Tau filaments in AD differ from those in PD, CTE, and CBD, but are identical to those found in PART diseases.
By Shi et al. 2021b, 4R tauopathies are described as being subclassified into two classes: Tauopathies with three-layered core regions, where R2 and R4 pack on either side of R3, as seen in PSP and GGT, and four-layered tauopathies where the packing of the C-terminal region against a portion of R2 provides a fourth layer for the folds observed in CBD and AGD.

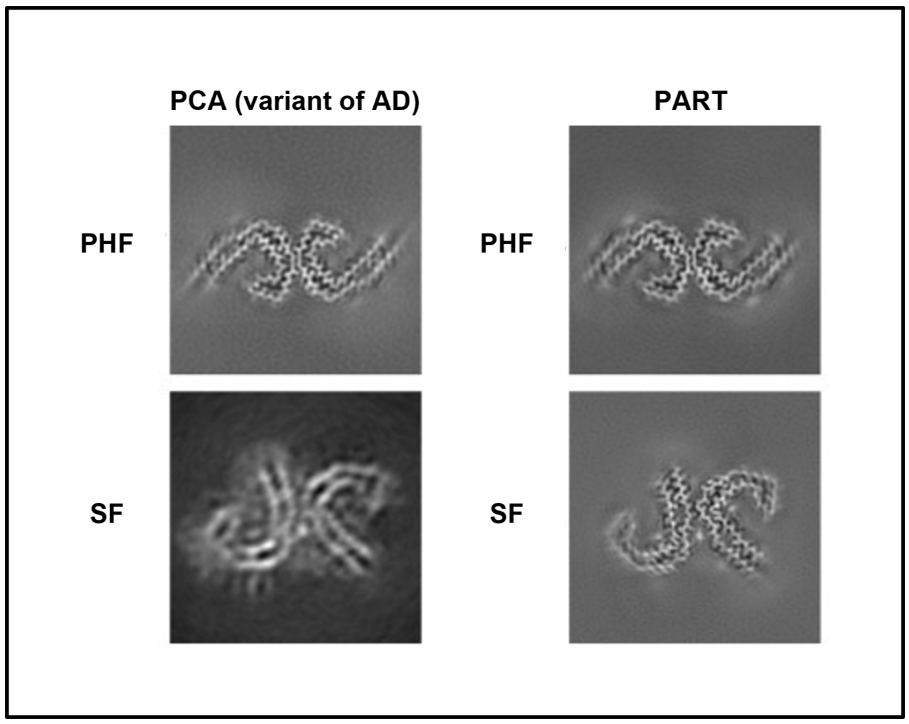

Figure 3.6: Cryo-EM maps of Tau filaments from PCA and PART

3. Mechanism of Tau Aggregation

The abnormal aggregation of Tau protein is a key feature of tauopathies, including Alzheimer's disease. This complex process involves several distinct steps that have been elucidated through in vitro and in vivo studies.The aggregation of Tau protein follows a nucleation-elongation kinetic mechanism, similar to other amyloidogenic proteins. This process involves several key steps: nucleation, elongation, fragmentation, and secondary nucleation.

3.1. General mechanism of amyloid aggregation

The general mechanism of amyloid aggregation can be summarized as follows: Monomeric proteins undergo a conformational change to an aggregation-prone state, facilitated by factors such as mutations, post-translational modifications, and interactions with cofactors. These misfolded monomers then assemble into oligomeric nuclei or seeds through a nucleation process, which is the rate-limiting step of aggregation. Nucleation can occur via primary nucleation from monomers or secondary nucleation on the surfaces of existing aggregates. Once nuclei are formed, they can rapidly grow by elongation through the addition of monomers, following a nucleation-polymerization mechanism. This elongation results in the formation of protofibrils and eventually mature amyloid fibrils with a characteristic cross-β structure (Figure 3.8). Different aggregate species like oligomers, protofibrils, and fibrils coexist and can interconvert or propagate further aggregation via secondary nucleation. Fragmentation of fibrils can also generate new growth nuclei, amplifying aggregation. Additionally, cell-to-cell propagation of aggregates can occur, spreading the aggregation process. Finally, amyloid aggregates can escape degradation pathways like autophagy, leading to their accumulation within cells (Almeida and Brito 2020; Linse 2019).

3.2. Mechanism of Tau Aggregation

3.3. Initiation

The initiation step involves the conformational conversion of normally soluble monomeric Tau into an aggregation-prone misfolded state, a key initial step that allows Tau aggregation to proceed. Tau monomers must undergo a conformational change or partial unfolding to expose aggregation-prone regions and form aggregation-competent conformations. This conversion can be induced or promoted by various factors such as mutations (e.g., P301L), post-translational modifications like hyperphosphorylation, oxidative stress, interactions with cofactors like heparin, RNA (that is more physiological than the heparin) or metal ions, or changes in the cellular environment (Fichou et al. 2018a). The formation of the earliest small oligomers from the aggregation-prone monomeric Tau is considered the rate-limiting, critical nucleation step (Limorenko and A. Lashuel 2022; Goedert and Spillantini 2017). Liquid-liquid phase separation of Tau into droplets has also been proposed as an initiating process that can lead to Tau aggregation over time (Wegmann et al. 2018).

3.4. Nucleation

The rate-limiting and critical initial step is the nucleation phase, that allows Tau aggregation to proceed. It involves the formation of small oligomeric nuclei or seeds from monomeric Tau that has transitioned into an aggregation-competent conformation. Nucleation follows a "nucleation-conversion" model, where Tau monomers must first misfold into aggregation-prone conformations before assembling into the initial nuclei. The formation of these first aggregation-competent Tau oligomers is the rate-limiting step in the overall aggregation process. This nucleation process can be induced or promoted by factors like mutations, cellular stress, post-translational modifications (PTMs) like hyperphosphorylation, or interactions with cofactors like RNA or heparin. The Hsp70 chaperone inhibits Tau nucleation in a dose-dependent manner, particularly reducing the formation of the earliest small Tau oligomers (<10-mers). Single-molecule FRET experiments have shown that Hsp70 decreases the number of early Tau oligomers formed upon nucleation. A study using highly sensitive techniques demonstrated that the P301L mutation in tau actually increases the nucleation rate by favoring the formation of the initial aggregation nuclei. Once the nuclei are formed, further elongation can rapidly occur by the addition of Tau monomers in an energetically favorable polymerization process (Shammas et al. 2015; Limorenko and A. Lashuel 2022).

3.5. Elongation

The elongation process occurs after the initial nucleation step, where oligomeric nuclei or seeds have already formed from the aggregation-prone monomeric Tau. Once nuclei are formed, they can rapidly grow by elongation through the addition of Tau monomers to the ends of the existing seeds, following a nucleation-polymerization mechanism. The elongation process is relatively rapid and energetically favorable compared to the initial nucleation step. The Hsp70 chaperone inhibits Tau fibril elongation in a dose-dependent manner, even at substoichiometric levels. Kinetic studies showed that Hsp70 decreases the relative elongation rate constants when added to pre-formed Tau seeds in seeding experiments. Electron microscopy revealed that in the presence of Hsp70, the resulting Tau aggregates appeared smaller and less elongated compared to controls. The P301L mutation in Tau was found to increase not just nucleation rates but also favor elongation by enhancing fibril growth and stability. During elongation, unmodified Tau monomers can incorporate into the growing fibrils and then undergo conformational changes and abnormal post-translational modifications like hyperphosphorylation (Goedert and Spillantini 2017; Limorenko and A. Lashuel 2022; Dimou et al. 2023). Different cofactors like heparin, RNA, or fatty acids can promote elongation by stabilizing and templating the growth of tau fibrils from the initial nuclei (Dominguez-Meijide, Vasili, and Outeiro 2020).

4. Tauopathies: Prion-like diseases?

Emerging evidence indicates a common pathogenic feature among neurodegenerative disorders: the accumulation of misfolded proteins with altered physicochemical properties in the Central Nervous System. While lacking infectivity, experimental findings suggest that the replication and spread of proteins associated with neurodegenerative diseasessuch as amyloid-β (Aβ), tau, α-synuclein, and the transactive response DNA-binding protein of 43 kDa (TDP-43)follow a similar pathological mechanism to prions.

4.1. Definition of Prion

The term "prions" denotes abnormal, transmissible agents capable of inducing the aberrant folding of specific normal cellular proteins called prion proteins, predominantly located in the brain. While the precise functions of these normal prion proteins remain incompletely understood, they are believed to play roles in cellular processes such as synaptic transmission and neuronal signaling. Abnormal folding of prion proteins leads to poor degradation, accumulation, and the formation of deposits inside and outside brain cells.
Despite extensive research efforts, there is still much to learn about prions and prion diseases, including their exact mechanisms of transmission, factors influencing susceptibility, and potential therapeutic interventions. However, advancements in understanding prion biology have led to improved diagnostic techniques and potential avenues for the development of novel treatments (rédaction 2019).

Prion protein

The discovery of the prion protein is attributed to Dr. Stanley B. Prusiner, an American biochemist. In the 1980s, Prusiner proposed the revolutionary hypothesis that the infectious agent responsible for transmissible spongiform encephalopathies (TSEs), such as mad cow disease (bovine spongiform encephalopathy) and Creutzfeldt-Jakob disease in humans, was not a conventional virus but a protein. Prusiner proposed that these diseases were caused by an abnormal form of a naturally occurring protein in cells, known as the cellular prion protein (PrPc) (Liautard et al. 2002).
The prion protein (PrP), encoded by the *PRNP* gene (also known as CD230), is highly conserved across mammals (Makrinou, Collinge, and Antoniou 2002). Human PrP consists of 253 amino acids before post-translational modifications, resulting in a mature length of 208 amino acids. Structurally, it comprises a globular domain with 3 α-helices and 2 β-strands, an N-terminal tail featuring octapeptide repeats that bind copper, and a C-terminal GPI anchor attaching it to cell membranes.
PrP exists in two main isoforms: PrPc (cellular prion protein), the normal, predominantly α-helical isoform found in healthy cells, and PrPSc (scrapie prion protein), the abnormal, β-sheet-rich, protease-resistant isoform associated with prion diseases. While the precise function of PrPc remains unknown, proposed roles include copper transport, neuroprotection, cell signaling, and synapse formation, with its ability to bind copper ions via octapeptide repeats potentially related to its function. In prion diseases, PrPsc serves as a template to convert normal PrPc into the misfolded PrPsc isoform through a seeded aggregation process. The accumulation of PrPsc aggregates in the brain leads to neurodegeneration and the formation of sponge-like vacuoles, resulting in the symptoms of prion diseases. Polymorphisms in *PRNP*, particularly at codon 129 (Met/Val), can influence the risk and onset of prion diseases.
In summary, the prion protein plays a central role in the pathogenesis of prion diseases through its ability to misfold and propagate the abnormal PrPsc isoform, leading to neurodegeneration and the characteristic features of these disorders.

Prion-like diseases

Prion-like diseases belong to a category of neurodegenerative disorders akin to prion diseases, where misfolded proteins have the ability to replicate and spread pathology across the brain. These diseases are also known as proteinopathies or protein misfolding disorders. In various disorders, misfolded proteins accumulate and form aggregates, which can trigger further misfolding of normal proteins, perpetuating a self-reinforcing cycle (Scialò et al. 2019).
Some examples of prion-like diseases include AD, FTDP, PD, PSP... As we can realise that those diseases are part of the tauopathies (Han et al. 2023).

4.2. Tau: a prion-like protein

The growing body of research indicates that Tau, a protein implicated in various neurodegenerative disorders, shares striking similarities with prions in its ability to spread pathology throughout the brain. Like prions, misfolded Tau aggregates can serve as *seeds*, prompting the misfolding and aggregation of normal Tau proteins in a templated manner. This process of *seeding* and templating occurs both within cells and between them, facilitating the propagation of Tau pathology across interconnected brain regions (Han et al. 2023; Holmes and Diamond 2014). Features defining prion-like behavior include the stable propagation of misfolded protein conformations. Notably, native Tau filaments extracted from Alzheimers disease (AD) brains, which bear all posttranslational modifications, efficiently induce endogenous Tau seeding in cultured cells (Falcon et al. 2015), after intracerebral injection in Tau transgenic mice (Jackson et al. 2016), and even in wild-type mice (Audouard et al. 2016). Furthermore, studies have revealed the existence of distinct conformational strains of misfolded Tau, each exhibiting unique biochemical and neuropathological features. These different Tau strains can influence the patterns of pathology, rates of disease progression, and vulnerability of specific brain regions, akin to the strain phenomena observed in prion diseases (Dujardin and Hyman 2019). There is also circumstantial evidence that prion-like Tau seeds are present in brain tissues in tauopathies and can promote Tau aggregation. For instance, the injection of brain homogenates from different tauopathies into the brains of mice expressing non-aggregated human Tau led to the formation of inclusions specific to the corresponding tauopathy (Clavaguera et al. 2013). Additionally, Sarkosyl-insoluble paired helical filaments (PHFs) extracted from AD brain tissues have been shown to induce seeding in cultured cells and wild-type mice. Moreover, widespread seeding activity has been measured in regions predicted to be free of phospho-Tau deposition and in detergent-insoluble fractions lacking Tau, indicating early transcellular propagation of Tau seeds prior to histopathological changes, which then triggers the subsequent development of neuropathology. This seeding activity correlates positively with Braak stages in the frontal and parietal lobes (Furman et al. 2017). Emerging evidence also suggests that Tau oligomers and aggregates can be released from cells, possibly via exosomes, and taken up by neighboring cells, thus initiating further *seeding* and propagation. This intercellular transmission mirrors mechanisms observed in prion diseases, although tauopathies are not considered infectious or transmissible between individuals (Brunello et al. 2020) (Figure 3.9). While the prion-like concept offers valuable insights into the mechanisms underlying tauopathies, ongoing research is imperative to fully grasp the extent to which prion-like mechanisms contribute to the development and progression of these neurodegenerative diseases (Han et al. 2023; Holmes and Diamond 2014; Dujardin and Hyman 2019).

4.3. Definition of *seed*-competence of Tau aggregation

The ability of some Tau aggregates to encourage the aggregation of more Tau monomers is referred to as "*seed* competence." *Seed*-competent aggregates have the ability to start an aggregation chain reaction, which is essential for the spread of Tau pathology in neurodegenerative disorders (Lo 2021a). Recent studies have made significant strides in identifying the composition and structure of Tau

monomers, particularly focusing on the distinction between inert and *seed*-competent forms in Tau aggregation. Tau monomers have been classified into two distinct types: inert (M_i) and *seed*-competent (M_s). While inert Tau monomers do not promote aggregation, *seed*-competent monomers have the ability to induce aggregation and self-assemble into larger structures, a key factor in the onset of tauopathies. The structural differences between these monomer types have been elucidated using techniques such as crosslinking mass spectrometry, revealing that M_s possesses specific structural features that enable it to act as a template for aggregation, whereas M_i remains stable and non-aggregative. Factors like heparin can facilitate the conversion of M_i into M_s, highlighting the potential triggers for Tau aggregation in disease contexts. Additionally, seed-competent Tau monomers have been successfully isolated from both recombinant sources and human brain tissue using mild purification techniques, underscoring their existence in vivo and their role in the pathological aggregation observed in tauopathies (Mirbaha et al. 2018).

4.4. Propagation and *Seeding* of Tau in Alzheimer's Disease

The conclusion drawn from the previous sections is that the development of prion diseases involves at least two distinct steps: (1) the transport of the misfolded prion, allowing contact with still-normal prionsand (2) the induction of misfolding. The first step is referred to as propagation, while the second step is known as *Seeding*. This mechanisme is the same for Tau propagation.

Intercellular Propagation of Tau

Intercellular Tau propagation is a critical aspect of tauopathies, and while 90% of Tau is secreted as a free form, this mode of transfer is likely not the most efficient (De La-Rocque et al. 2021). The majority of Tau is released into the extracellular space as a soluble protein, but this free form may not effectively propagate Tau pathology between neurons. The prion-like propagation hypothesis suggests that Tau can induce misfolding in neighboring cells, and this process is more efficient when Tau is in aggregated forms, such as oligomers or fibrils, which can seed further aggregation in recipient cells. Studies indicate that Tau can be internalized by neurons through various mechanisms, including endocytosis of Tau aggregates or extracellular vesicles. This internalization is crucial for the spread of Tau pathology. The synaptic environment may facilitate Tau transfer, as Tau has been shown to be enriched in synaptic fractions of brain-derived materials from Alzheimer's disease patients, suggesting that synaptic connections may play a significant role in intercellular propagation. Various in vivo and in vitro models have been developed to study Tau propagation, including those that utilize intracranial delivery of Tau aggregates or the use of transgenic mice expressing human Tau, helping to elucidate the mechanisms of Tau transfer and its implications in neurodegenerative diseases (De La-Rocque et al. 2021; Colin et al. 2020). Other potential pathways for Tau secretion have been proposed based on experimental studies. Tau could be secreted via ectosomes, which are extracellular vesicles derived from the plasma membrane. Another possibility is the exosomal pathway, where Tau is released into the extracellular space through exosomes, vesicles originating from multivesicular bodies. Additionally, studies suggest that Tau might spread along synaptic connections between neurons. Direct transfer via membrane nanotubes linking cells is another proposed mechanism. Moreover, a recent study indicated that hyperphosphorylated Tau could be secreted through direct translocation across the plasma membrane, a process mediated by sulfated proteoglycans (Sayas et al. 2019) (Figure 3.9). The evidence supporting the prion-like propagation of tau in Alzheimer's disease (AD) and other tauopathies is substantial and multifaceted.

There is now compelling evidence that Tau seeds are released and taken up by neurons where Tau seeds induce aggregation of non-aggregated Tau, across synaptically linked neuronal networks spreading through neuroanatomically linked brain regions (as described below). However, to be relevant to the mechanism by which Tau pathology spreads in humans, one would need evidence that this occurs

in patient brains. Braak staging is not an evidence for trans-synaptic spread of Tau pathology. It may simply reflect a spatio-temporal vulnerability of different neuroanatomical regions to Tau aggregation.

Templated *Seeding*

The concept of "templated seeding" refers to the process by which Tau aggregates (seeds) induce the misfolding and aggregation of normal Tau proteins, central to the propagation of Tau pathology in Alzheimer's disease (AD) and other tauopathies. This mechanism involves Tau aggregates acting as templates that recruit and convert nearby monomeric Tau into an aggregated form, similar to a crystallization process where a small number of misfolded proteins initiate a chain reaction of aggregation in normal proteins (Mudher et al. 2017). The aggregates produced through templated seeding must physically resemble the parental seeds, a structural similarity essential for their ability to effectively induce further aggregation (Kaufman et al. 2017) (Figure 3.10).
Tau seeds can be derived from various sources, including brain homogenates from tauopathy models, recombinant Tau proteins, or synthetic Tau fibrils, and these seeds exhibit unique conformations and post-translational modifications (PTMs) that influence their seeding ability (Mudher et al. 2017). Larger oligomers or aggregates of Tau have been found to have greater seeding capacity compared to monomeric Tau, with oligomers composed of 10 to 100 Tau units displaying enhanced ability to induce aggregation in recipient cells (Kaufman et al. 2017). Experimental evidence supports the efficacy of templated seeding, as Tau aggregates injected into animal models have been shown to propagate Tau pathology. For example, injecting Tau seeds from transgenic mice into wild-type mice results in the induction of tau aggregation in the recipient animals (Clavaguera et al. 2013). Understanding the mechanisms of templated seeding is critical for developing therapeutic strategies aimed at halting or reversing Tau propagation in tauopathies, as targeting this seeding process may help prevent the spread of Tau-related neurodegeneration (Mudher et al. 2017).

Cellular absorption of Tau seeds

The cellular absorption of Tau seeds, which are pathological aggregates involved in tauopathies such as Alzheimers disease, is crucial for the spread of Tau pathology. This process primarily begins with endocytosis, including macropinocytosis and receptor-mediated endocytosis, which allows cells to internalize these aggregates and induce the aggregation of normal Tau within the cell (Perea, Bolós, and Avila 2020; Asai et al. 2015). Internalized Tau seeds are mostly located in endosomal and lysosomal vesicles, with studies showing that modified Tau seeds, such as those with the P301L mutation, are found in fractions enriched with endosomal and lysosomal markers, indicating specific intracellular processing (Tseng et al. 2021). Additionally, the modifications of Tau seeds vary by cell type, with changes such as acetylation and phosphorylation observed in primary neurons and immune cells, but not in all cell lines (Asai et al. 2015). Tau seeds associated with disease tend to accumulate in autophagic vesicles, which can affect Tau aggregation dynamics and the spread of pathology (Cabrera-Pastor 2024). Lastly, internalization appears to be more efficient for Tau aggregates or oligomers than for soluble monomers, highlighting the importance of aggregated forms of Tau for its propagation (Gibbons, Lee, and Trojanowski 2019; Takeda et al. 2015).

Tau *seeds* properties

Tau *seeds*, derived from various sources such as brain homogenates from tauopathy patients or symptomatic Tau transgenic mice, viral vector-injected rodent brain extracts, Tau-aggregate-bearing transfected cells, and recombinant Tau incubated with aggregation inducers in vitro, present a diversity that allows researchers to explore their distinct properties and effects in different contexts. Native Tau filaments, which are more efficient at inducing *seeding* than preformed filaments, exhibit this efficiency through unclear post-translational modifications or conformational changes (Hou et al. 2021).

Moreover, the human brain may harbor multiple Tau species with *seeding* abilities, contributing to a complex landscape of Tau pathology (Tseng et al. 2021). Conflicting reports on the minimal Tau units required for efficient *seeding* indicate a need for further research, as some studies suggest that Tau trimers or monomers can initiate aggregation, while others propose that larger oligomers or insoluble Tau aggregates are necessary (Mirbaha et al. 2015). Interestingly, more stable Tau aggregates may exhibit lower *seeding* activity, suggesting that the dynamics of Tau aggregation influence their pathogenic potential. Beta-pleated sheet content, which correlates with *seeding* efficiency, highlights the importance of structural characteristics in Tau pathology (Mate De Gerando et al. 2023). Additionally, Tau *seeds* can be isolated from both soluble and insoluble fractions of Alzheimer's disease brain tissue, indicating that Tau pathology encompasses a range of species with varying biochemical properties (Furman et al. 2017). Pathological Tau species might utilize distinct mechanisms of toxicity, with some evidence suggesting that Taus harmful effects may be independent of its aggregation state. Despite the central role of Tau aggregation in tauopathies, the direct relationship between Tau aggregate propagation and neurodegeneration remains an area of ongoing investigation (Mudher et al. 2017).

Internalisation and *seeding* of Tau

The internalization of pathological Tau species is a critical step in the propagation of Tau pathology across cells and brain regions in tauopathies like Alzheimer's disease.
Major pathways for Tau internalization into recipient cells include macropinocytosis, clathrin-mediated endocytosis, and lipid raft-dependent endocytosis, with heparan sulfate proteoglycans (HSPGs) being predominant mediators. Additionally, Tau can be internalized through tunneling nanotubes, which are transient membrane channels directly connecting neighboring cells. Phagocytosis, particularly by microglial cells, has also been proposed as a potential mechanism (Zhao, Wu, and Tang 2021). The specific internalization pathway may depend on the conformation of Tau fibrils (monomers, oligomers, or larger fibrils) and the type of recipient cell, as live imaging studies show that different Tau antibodies can exhibit distinct spatiotemporal patterns of internalization into neuron-like cells (Shamir et al. 2020).
After internalization, the imbalance between Tau secretion, internalization, and clearance mechanisms may lead to the propagation of misfolded Tau species, contributing to the spreading of Tau pathology in the brain during tauopathies.

4.5. Trans-cellular propagation of Tau seeds

The transcellular transfer of Tau aggregates, central to neurodegenerative diseases such as Alzheimers, has been extensively studied using microfluidic chamber systems. These systems allow for the investigation of neuron-to-neuron interactions by separating neuronal populations while maintaining direct connections via microgrooves. Research has demonstrated that human Tau aggregates can propagate from one group of neurons to another through these connections, suggesting a mechanism of trans-synaptic transfer (Wu et al. 2016; Katsikoudi et al. 2020; Takeda et al. 2015). Effective Tau transfer is closely linked to synaptic connectivity, as evidenced by experiments showing positive Tau immunoreactivity in neurons with established axonal connections (Takeda et al. 2015; Wang et al. 2017a). Exosomes have also been identified as a mechanism for Tau transfer, carrying Tau aggregates between neurons and facilitating their spread without direct cell-to-cell contact (Wang et al. 2017a; Sala-Jarque et al. 2022).
Tau aggregates spread through synaptic connections in a hierarchical manner, following the brains anatomical pathways (Schoonhoven et al. 2023; Hu et al. 2022). Exosomes, small extracellular vesicles, play a significant role in this process by transporting Tau between neurons, as observed in experimental models such as organotypic hippocampal slices and microfluidic devices (Wang et al. 2017a). The extent of Tau spread is influenced by neuronal connectivity, with research showing Tau migration

from the entorhinal cortex to regions like the hippocampus (Colom-Cadena et al. 2023).
Tau uptake by various cell types, including neurons and immune cells, is mediated by specific receptors such as heparan sulfate proteoglycans (HSPGs) (Kim et al. 2024). Tau binds to these receptors, facilitating its internalization and promoting the transmission of Tau aggregates between cells (Wang et al. 2017b; Morozova et al. 2019). In neuronal cultures, Tau uptake can be blocked by muscarinic receptor antagonists, indicating the role of these receptors in Tau internalization, while immune cells may utilize different pathways (Morozova et al. 2019). Additionally, amyloid beta (Aβ) has been shown to enhance Tau uptake in neurons, with Aβ pretreatment increasing Tau internalization and potentially exacerbating Tau pathology in Alzheimer's disease (Kim et al. 2024).
The trans-synaptic spread of Tau pathology has also been observed in transgenic mice using various techniques. Studies show that Tau aggregation in the rodent brain, induced by intracerebral injections of brain homogenates containing Tau seeds, results in time-dependent development of Tau pathology in anatomically connected regions (Clavaguera et al. 2013). Other research highlights Tau pathology appearing in areas connected to Tau seed or viral vector injection sites (Liu et al. 2012). Interestingly, Tau propagation can occur even without the templated misfolding of endogenous Tau, as seen in a P301L model where abnormal Tau spreads without endogenous Tau expression (Wegmann et al. 2015). Moreover, Tau spread might not rely solely on trans-synaptic propagation but could also involve interstitial diffusion and microglial contribution. For instance, reducing microglial cells or inhibiting exosome production by these cells significantly reduces the spread of AT8-positive oligomers in rodent models (Asai et al. 2015).

Braak stages

6 stages are defined for the propagation of misfolded Tau in the AD. The regions affected at various stages of Alzheimer's disease progression reflect a pattern of pathological changes in the brain. In the initial stages (Stage I), the pathology manifests predominantly in the transentorhinal and entorhinal regions, which are crucial for memory and early cognitive functions. As the disease advances into Stages I-II, it spreads to involve associative areas of the brain, contributing to deficits in higher cognitive processes such as language, perception, and executive function. Finally, in the later stages (Stages III-VI), the pathology extends to affect the neocortical regions, which are integral for complex cognitive functions, leading to profound cognitive decline and functional impairment characteristic of advanced Alzheimer's disease. This sequential involvement of brain regions mirrors the progressive nature of the disease, starting from areas closely associated with memory and spreading to encompass broader cognitive domains as the pathology spreads throughout the brain.

4.6. Selective Neuron Vulnerability as an Alternative to the Prion-like Propagation of Tau Pathology

The propagation of Tau pathology in neurodegenerative diseases, particularly Alzheimer's disease, has traditionally been explained by the "prion-like" spreading hypothesis, where Tau aggregates transmit their misfolded state from one neuron to another. However, it is crucial to highlight that this may not be the sole mechanism at play. An alternative model, known as the selective neuron vulnerability hypothesis, has been proposed to explain Tau pathology in a different light. This model suggests that certain populations of neurons are inherently more susceptible to Tau pathology due to intrinsic factors or external stressors. According to this view, neurons that already harbor Tau aggregates or oligomers can induce stress in neighboring neurons, leading them to produce aggregates in response to these adverse stimuli (Chung, Lee, and Lee 2018; Walsh and Selkoe 2016).
Importantly, the selective neuron vulnerability hypothesis does not necessarily exclude the prion-like mechanism. Instead, it proposes that both mechanisms may coexist, potentially working together in the progression of Tau pathology. While the prion-like propagation may be responsible for the trans-

mission of Tau aggregates across neuronal networks, selective vulnerability could determine which neurons are affected and how they respond to Tau pathology. This dual mechanism model suggests a more complex interaction, where the prion-like spread facilitates aggregate transmission, and selective vulnerability influences the susceptibility and response of individual neurons (Landrieu et al. 2022).

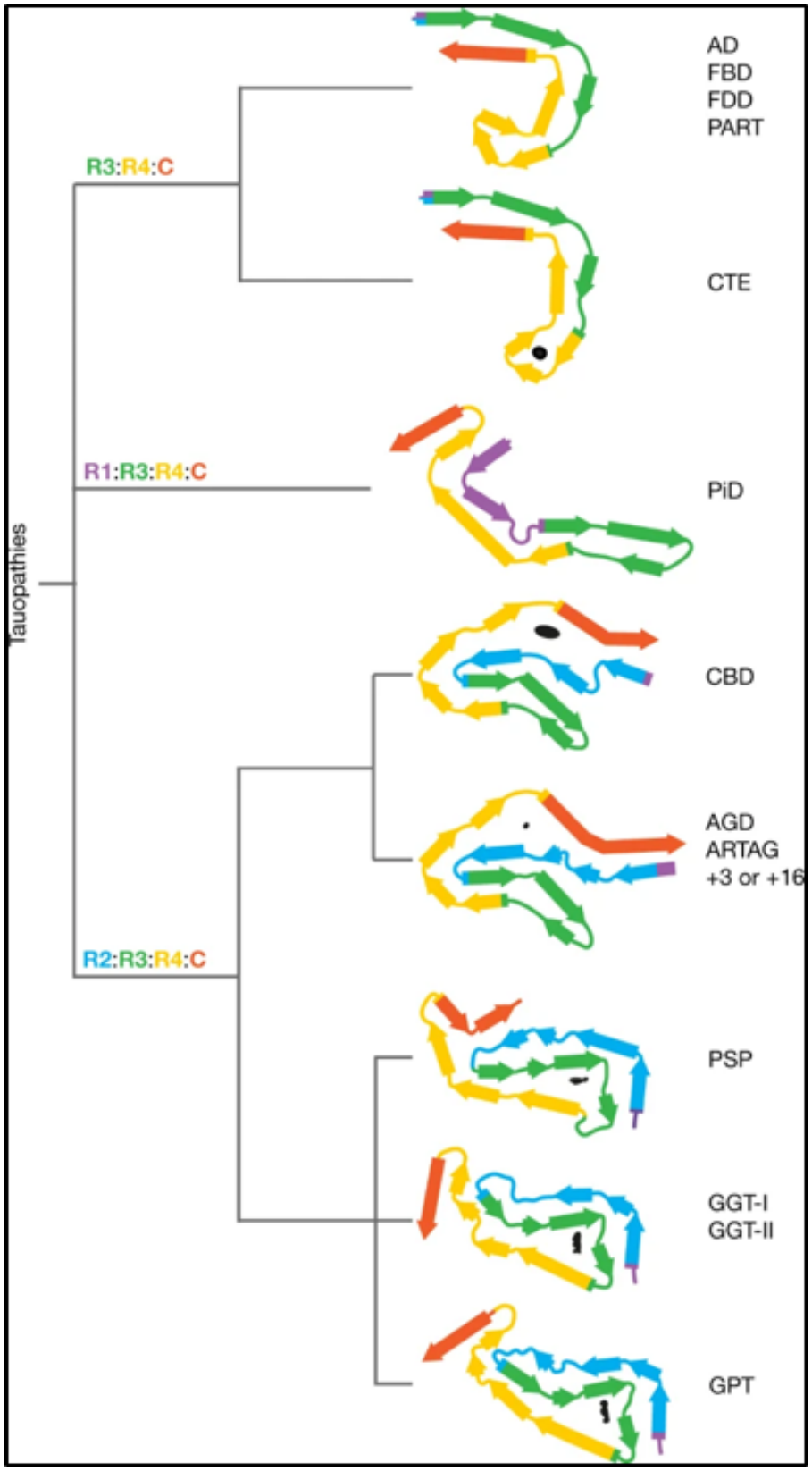

Figure 3.7: Structure-based classification of tauopathies

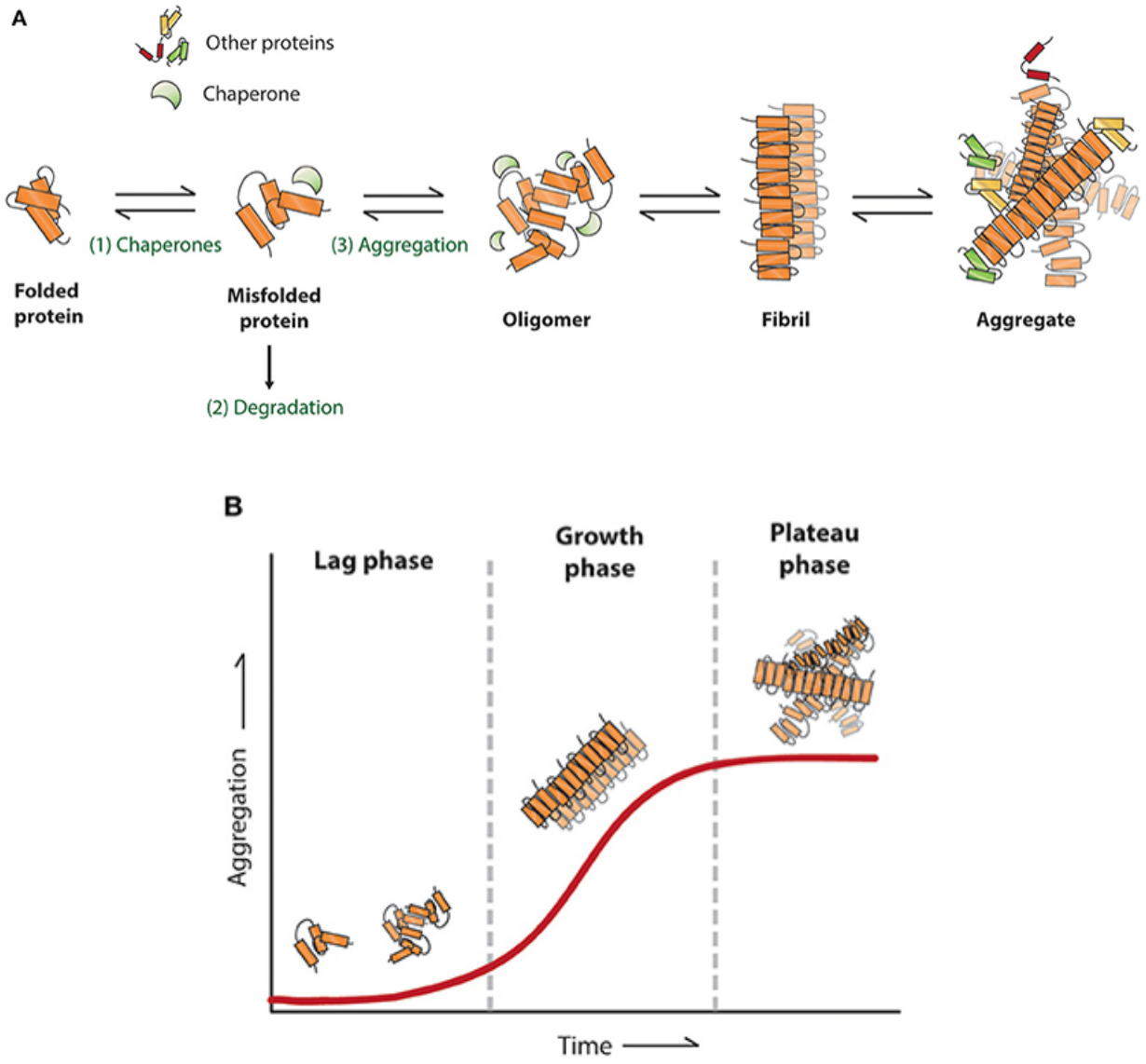

Figure 3.8: Proposed mechanism for amyloid formation

(A) Misfolded protein can be refolded (1), degraded (2), or aggregated (3),where the first step involves oligomers, followed by fibril formation around the fibril axis until the initial aggregates (B) Schematic view of an in vitro assay with the corresponding aggregation stages for each phase (Stroo et al. 2017)

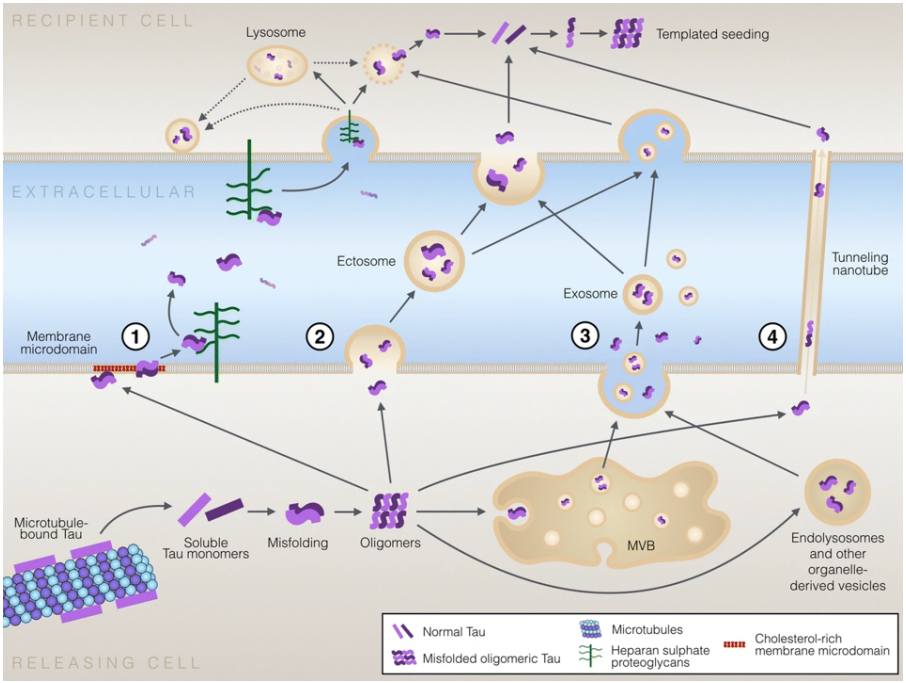

Figure 3.9: Mechanisms of cell-to-cell transfer of pathological Tau protein

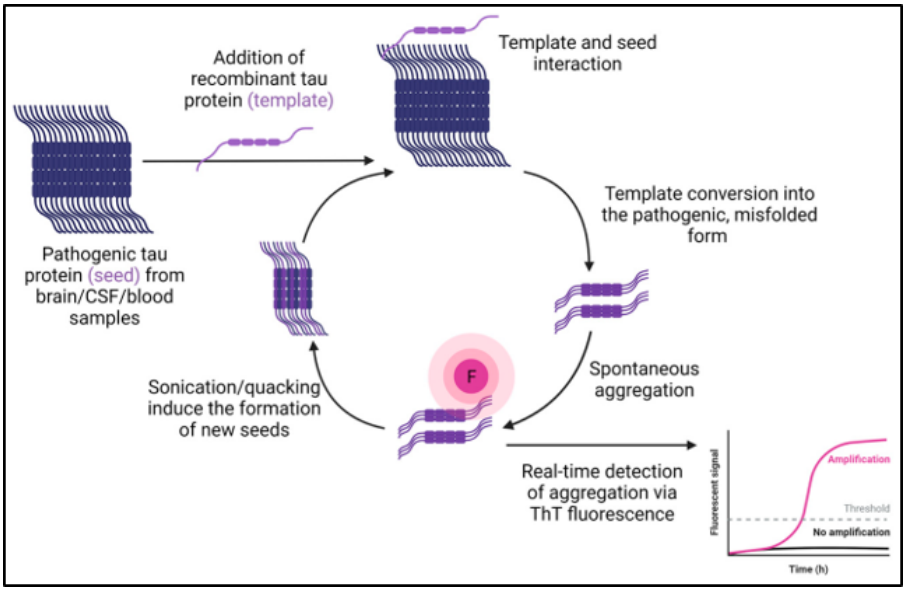

Figure 3.10: Templated seeding process (Figure from Tamvaka et al. 2023)

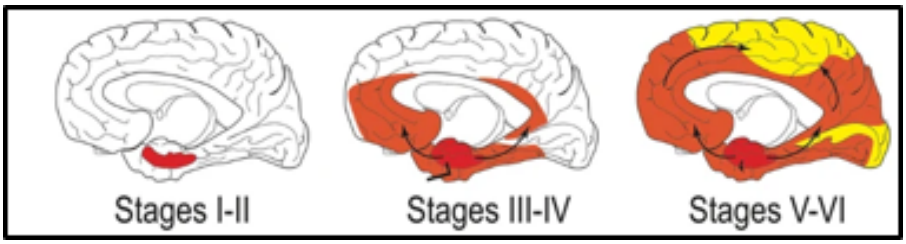

Figure 3.11: Staging of Tau pathology in AD

Chapter 4: Hyperphosphorylation, O-GlcNAcylation and Tau Aggregation

Tau's clearance, conformation, and aggregation potential can all be changed by the same PTMs that control Tau function (Park et al. 2018). Not every Tau PTM is "pathological," though. Numerous PTMs have been found in Tau that was isolated from healthy brains, indicating that PTMs normally play a role in Tau function (Haj-Yahya and Lashuel 2018). Phosphorylation is the most researched Tau PTM, and it was previously believed that elevated phosphorylation was the cause of Tau intracellular aggregation (Hanger, Anderton, and Noble 2009). Nonetheless, an increasing amount of data indicates that additional PTMs may also significantly control Tau function and may even come before phosphorylation in the chain of events that results in the creation of Tau inclusions.
Given that certain alterations have only been discovered in the disease-related Tau aggregates (Cohen et al. 2011; Hanger, Anderton, and Noble 2009) , it has been proposed that these alterations might be controlling Tau dysfunction.

1. Hyperphosphorylation in non-pathological conditions

Hyperphosphorylation of Tau protein is a crucial element in the development of tauopathies, but it can also occur in non-pathological and reversible contexts, such as during hypothermia, anesthesia, and hibernation. In certain physiological conditions, like brain development and hibernation, Tau undergoes transient hyperphosphorylation, a modification that is quickly reversed, as observed in hibernating animals where Tau returns to its normal state upon awakening, preventing permanent pathological alterations. Similarly, hypothermia can trigger Tau hyperphosphorylation; however, this alone is insufficient, as additional regulatory mechanisms play a role, underscoring the tightly controlled nature of Tau phosphorylation and its sensitivity to environmental factors (Duquette et al. 2021).

2. Tau hyperphosphorylation and aggregation

There are 85 possible phosphorylation sites in the longest Tau isoform, 2N4R Tau, which includes 44 S, 35 T, and 5 Y sites (Reynolds et al. 2000). Over 20% of Tau has the capacity to become phosphorylated.
In Tau isolated from healthy brains, it has been discovered that about 20 residues of these locations are phosphorylated (Morishima-Kawashima et al. 1995; Cook et al. 2014). On the other hand, hyperphosphorylated Tau have been found in the PHFs (Grundke-Iqbal et al. 1986).Hyperphosphorylation of Tau might play a role in modulating propagation of Tau pathology: in mice expressing wild-type Tau, intracerebral injection of dephosphorylated AD-derived hyperphosphorylated Tau strongly reduced Tau propagation (Hu et al. 2016). Individuals with a tauopathy have been discovered to have approximately 44 residues that are "abnormally" hyperphosphorylated, some of which overlap with residues present in Tau from healthy brains (Hanger, Anderton, and Noble 2009).
According to certain hypotheses, Tau protein loses its ability to attach to microtubules and aid in their

stabilisation, which leads to cytoskeleton destabilisation, especially in neurons. As a result, a build-up of hyperphosphorylated Tau protein would occur, promoting its aggregation and NFT production (Li, Yin, and Kuret 2004) (Figure 4.1).
Other proposed hypothesis is that hyperphosphorylation of Tau protein precipitates Tau aggregation through several interrelated mechanisms, ultimately contributing to the formation of NFTs, characteristic of AD and other tauopathies. Firstly, hyperphosphorylation induces conformational changes in Tau, making it more prone to aggregation by altering its structure to facilitate interactions with other Tau molecules. Secondly, the phosphorylation enhances Tau's ability to bind to other Tau proteins, thus promoting aggregate formation. Thirdly, hyperphosphorylated Tau exhibits a propensity for self-assembly, leading to the formation of small, amorphous aggregates via spontaneous liquid-liquid phase separation (Avila 2006; Meng et al. 2022).
Finally, the increased stability of hyperphosphorylated Tau, due to its heightened resistance to degradation, allows it to accumulate and form aggregates more readily (Avila 2006).
The 1998 mass spectrometry study by Hanger et collaborateurs (Hanger et al. 1998) on PHFs isolated from Alzheimer patients allowed for the identification of the primary "pathological" phosphorylation sites that characterise the disease. Based on this, antibodies that specifically recognise pathological phospho-épitopes have been developed, enabling, among other things, the post-mortem detection of Alzheimer's disease.

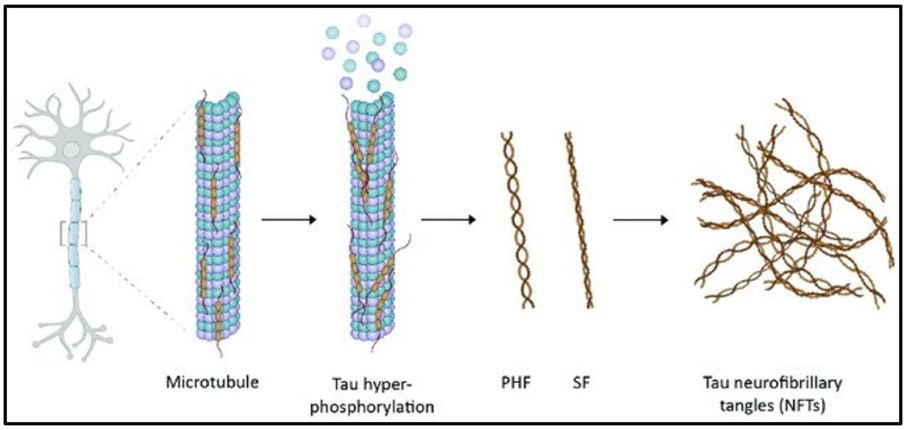

Figure 4.1: Hypothesis of hyperphosphorylation and Tau aggregation (Jie et al. 2021)

The neuroanatomist Heiko Braak examined the spatiotemporal evolution of specific phospho-epitopes in brain slices from AD patients and identified the epitope AT8 (pS202/pT205) as the preferred marker of pathological development enabling the determination of various stages and verification of the post-mortem diagnosis (Braak and Braak 1991; Braak and Braak 1995; Braak et al. 2006). In 100 μm polyethylene glycol-embedded hemisphere sections immunostained for hyperphosphorylated Tau (AT8, Innogenetics), cortical neurofibrillary pathology progresses through stages I to VI, revealing a temporal and spatial pattern of lesion development in Alzheimer's disease. Initially, at stage I, minimal involvement is observed, mainly confined to the transentorhinal region on the medial surface of the rhinal sulcus, in a non-demented 80-year-old female. Progressing to stage II, additional immunoreactivity extends into the entorhinal region, with lesions encroaching into the hippocampus, noted in a non-demented 80-year-old male. By stage III, the lesions worsen, spreading through the transentorhinal region into adjacent temporal neocortex areas in a 90-year-old female. Stage IV exhibits involvement of Ammon's horn sectors and insular cortex, reaching up to the medial temporal gyrus but sparing primary neocortical fields. In stage V, lesions extend into the superior temporal gyrus and affect premotor and sensory association areas, with varying degrees of involvement in the occipital lobe peristriate region, observed in a 90-year-old female with dementia. Finally, in stage VI, strong immunoreactivity is evident in primary neocortical areas, including first order sensory association areas and even the occipital neocortex, in severely demented 70-year-old female Alzheimer

patients, showcasing the progression of neurofibrillary pathology (Figure 4.2, Braak et al. 2006).

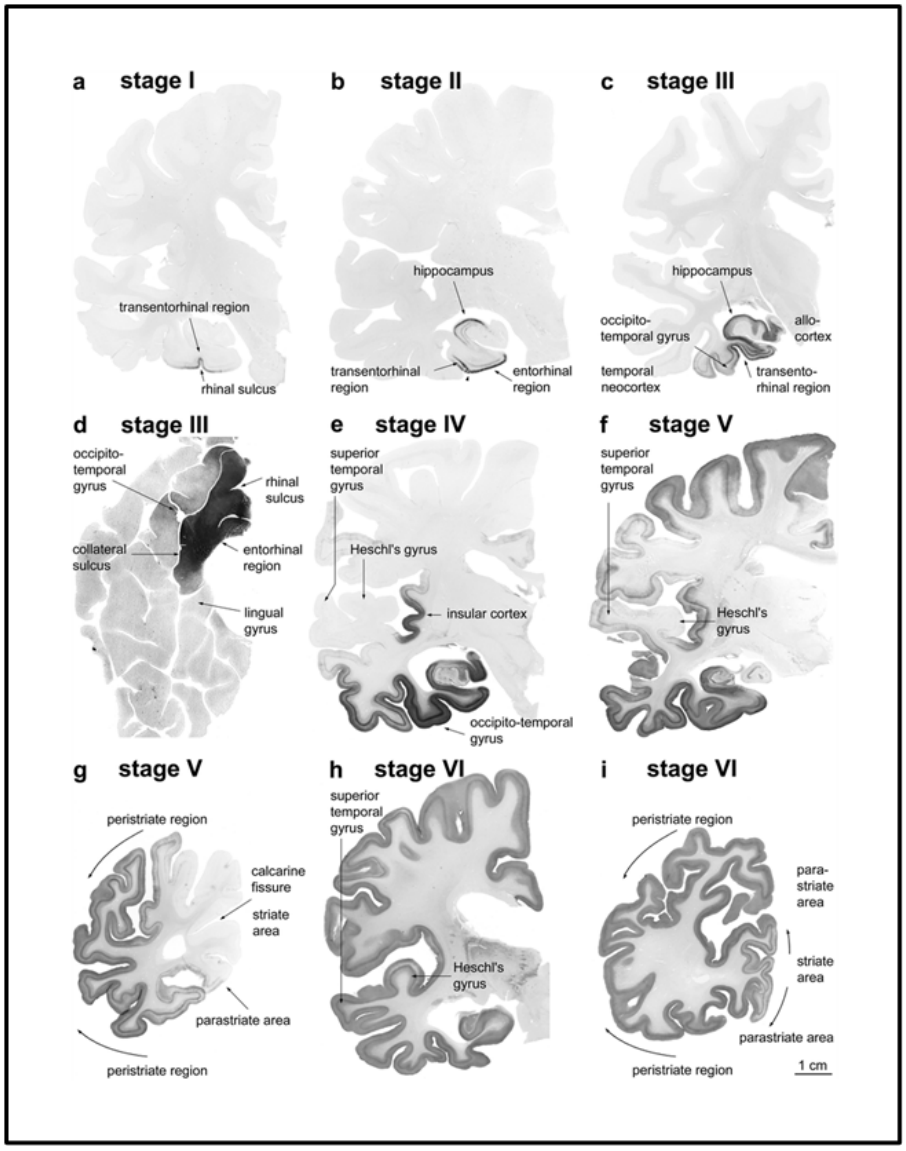

Figure 4.2: Stages IVI of cortical neurofibrillary pathology in 100 μm polyethylene glycol-embedded hemisphere sections immunostained for hyperphosphorylated tau (AT8, Innogenetics) (Braak et al. 2006)

Other studies have also used the hyperphosphorylated Tau as a marker for the disease tracking. The transentorhinal region (TEntR) of the brain is primarily the site of Tau phosphorylation during the early Braak stages (III). In the TEntR at Braak stage III/IV, phosphorylation at certain sites like as Tyr18 and Thr231 has already grown dramatically in comparison to earlier stages (Neddens et al. 2018).In the isocortex, Tau phosphorylation at most sites (e.g. Ser199, Ser396, Ser422) starts increasing significantly only at late Braak stages (V-VI). At Braak stage V/VI, phosphorylation at these sites is 50- to 1300-fold higher compared to healthy controls, with the highest levels in the temporal and frontal cortex (Therriault et al. 2022; Neddens et al. 2018). Phosphorylation of tau at Ser199 and Tyr18 shows a similar progression pattern, with a significant increase in the TEntR at Braak stage III/IV and much higher levels in the TEntR compared to isocortical regions at late stages. Tau phosphorylation at Thr231 is an exception, as it is significantly increased (30- to 160-fold) in both the allo- and isocortex at late Braak stage V/VI. Phosphorylation at Ser262 remains very low and shows almost no progression, except for an 8-fold increase in the TEntR between early and late Braak stages (Neddens et al. 2018).
An example of a protective phosphorylation site is the phosphorylation of Ser262, which is a key target for kinases like PAR-1/MARK that regulate Tau's binding to microtubules. Phosphorylation

at Ser262 reduces Tau's affinity for microtubules, and inhibiting its aggregation (Despres et al. 2017; Haj-Yahya et al. 2020).
Recent studies have developped antibodies targeting phosphorylated Tau proteins, for immunotherapy aims. Active p-Tau immunotherapy involves immunization with a p-Tau peptide to generate antibodies (Figure 4.3, Xia, Prokop, and Giasson 2021).
Antibodies that target phosphorylated Tau (p-Tau) proteins are being explored for immunotherapy applications in tauopathies such as Alzheimer's disease. There are two main approaches: active and passive p-Tau immunotherapy.
Active p-Tau immunotherapy involves immunizing patients with a p-Tau peptide to elicit antibodies against specific phosphorylated epitopes. For instance, the Tau379-408[P-Ser396,404] peptide immunogen targets the phospho-serine 396/404 region and has been shown to reduce tauopathy development in mouse models (Sigurdsson 2018).
In contrast, passive p-Tau immunotherapy entails the direct administration of pre-formed antibodies that target specific p-tau epitopes. Several monoclonal antibodies have been developed and characterized for this purpose. For example, CBTAU-22.1 recognizes the phosphorylated Ser422 epitope and can inhibit the spread of pathological tau aggregates in vitro. An affinity-matured variant, dmCBTAU-22.1, boasts improved binding and a greater ability to interfere with tau aggregation (**vanAmeijdeEnhancementtherapeuticpotential2018**). Additionally, antibodies such as AT8, AT180, PHF-6, TG-3, and PHF-1 exhibit high specificity for their respective p-Tau epitopes, as demonstrated by quantitative specificity assays ("High Specificity of Widely Used Phospho-tau Antibodies Validated Using a Quantitative Whole-cell Based Assay" 2020).
Both active and passive immunotherapy strategies aim to produce antibodies that selectively target and clear pathological p-Tau species, with the goal of potentially slowing or preventing the spread of Tau pathology.

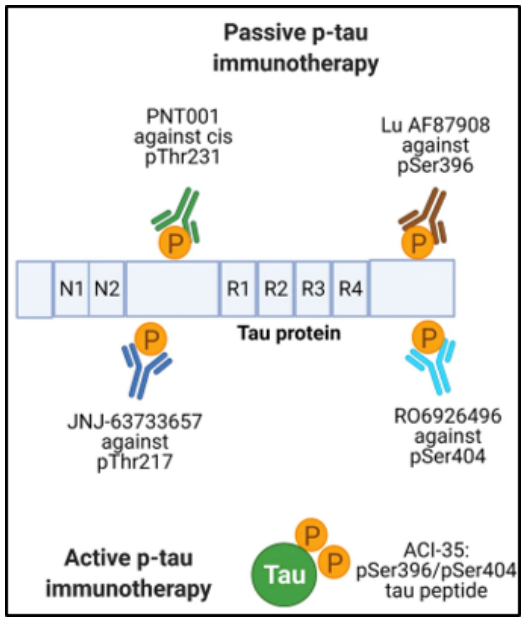

Figure 4.3: Summary of therapies targeting phosphorylated Tau (Xia, Prokop, and Giasson 2021)

Despite hyperphosphorylation being known to induce Tau aggregation, identifying the specific sites that trigger this aggregation is also necessary. In 2018, Despres et al. 2017 identified the phosphorylation site within the AT8 epitope necessary to induce Tau aggregation. After phosphorylating Tau with ERK2 kinase, only two phosphorylation sites were found on the AT8 epitope: Ser202 and Thr205. However, these two phosphorylations were not sufficient to induce Tau aggregation. Subsequently, after phosphorylation by Rat Brain Extract (RBE), an additional phosphorylation on Ser208 was discovered, leading to Tau aggregation (Figure 4.4 A, B). This could be caused by the disruption of the protective turn-like structure of AT8-2P described by Gandhi et al. 2015 (Figure 4.4 C, D).

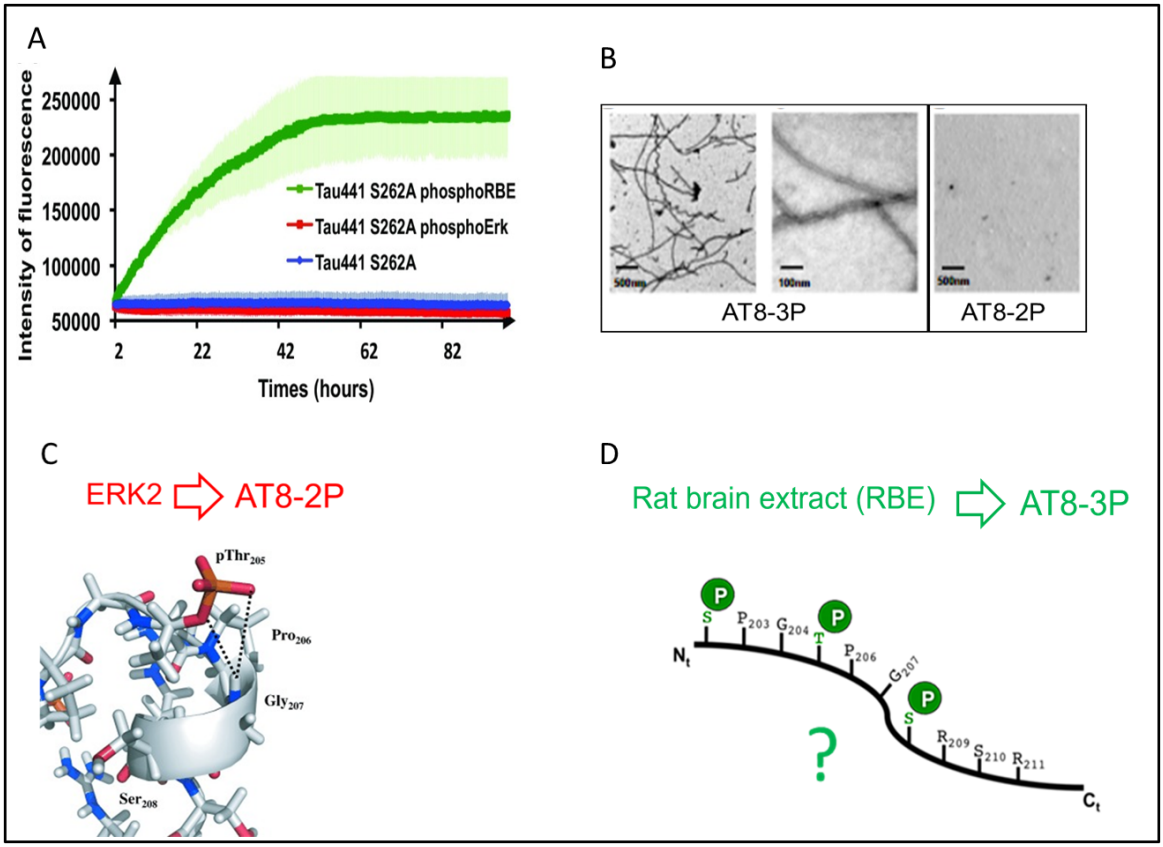

(A) Aggregation of Tau441, phosphorylated by ERK2, and RBE followed by ThT emission at 490 nm, (B) TEM images at the end point of the aggregation assay of Tau441 phosphorylated by RBE or by Erk2 (C) Turn-like structure of AT8-2P (Gandhi et al. 2015) (D) Disruption of turn-like structure of AT8-3P

Figure 4.4: Additional phosphorylation of Ser208 by RBE promotes aggregation of Tau441

3. Tau O-GlcNAcylation and aggregation

Phosphorylation of certain proteins, including Tau, can compete with O-GlcNAc at specific locations as they have similar activity sites. Impaired glucose metabolism is one of the first signs of AD pathogenesis (Heiss et al. 1991). Variations in O-GlcNAc levels in the brains of Alzheimer's disease (AD) patients are a topic of ongoing debate, with studies showing both decreases and increases in O-GlcNAcylation. A general consensus points to a reduction in O-GlcNAcylation in AD brains, often linked to impaired glucose metabolism, a hallmark of AD. This reduction in O-GlcNAc, especially on proteins like Tau and amyloid precursor protein (APP), is thought to contribute to neurodegeneration by diminishing the protective effects of O-GlcNAc against protein toxicity (Zhu et al. 2014). For instance, decreased O-GlcNAcylation has been associated with increased Tau phosphorylation and neurofibrillary tangle formation, exacerbating Tau pathology due to metabolic dysfunction (Liu et al. 2009). Moreover, the glycosylation of Tau, particularly O-GlcNAcylation, seems to inversely affect its phosphorylation, with reduced glycosylation observed in AD-affected brains. However, some studies have reported increased O-GlcNAcylation in specific contexts, such as in detergent-insoluble Tau fractions, indicating a more complex relationship between O-GlcNAcylation and Tau aggregation (Förster et al. 2014). The discrepancies in these findings could be due to factors like age, gender, genetic background, disease progression, and the specific brain regions examined, underscoring the need for standardized approaches in future research (Park et al. 2020).
Other Genome-Wide Association Studies (GWAS) studies have linked the decrease in glucose transporters to Tau pathology (Shulman et al. 2011).
O-GlcNAcylation serves as a nutrient sensor, responding to variations in glucose availability and

other metabolic stresses. It enables cells to adjust their physiology to changes in nutrient intake and to maintain blood glucose levels within a narrow range (Gonzalez-Rellan et al. 2022). Therefore, it represents a crucial post-translational modification (PTM) to investigate regarding the regulation of Tau aggregation. As Tau O-GlcNAcylation occurs on similar sites as Tau phosphorylation, numerous studies have proposed a protective role of O-GlcNAcylation by inhibiting Tau phosphorylation and impeding its aggregation. In 2014, Yuzwa et al. 2014 demonstrated in vitro that the O-GlcNAcylation of Tau can reduce its aggregation.
Using in vitro biochemical assays, they demonstrated that O-GlcNAcylation of Tau directly inhibits its oligomerization and aggregation into higher-order structures like fibrils. High-resolution NMR spectroscopy showed that O-GlcNAcylation at S400 alters the local conformation of Tau, potentially preventing aggregation by interfering with the interactions necessary for Tau self-assembly (Figure 4.5) (Yuzwa et al. 2014).

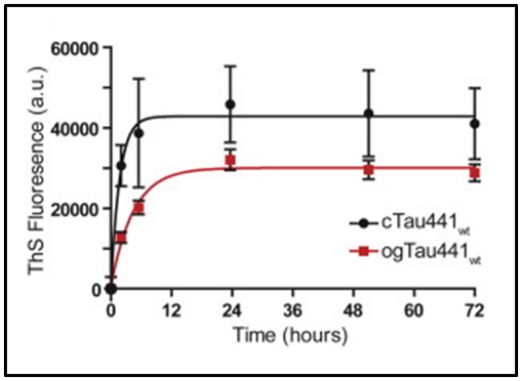

Figure 4.5: O-GlcNAc modification causes slower aggregation of Tau441 in vitro, induced by heparin (Yuzwa et al. 2014)

4. Cross-talk between phosphorylation and O-GlcNAcylation

The crosstalk between phosphorylation and O-GlcNAcylation refers to the intricate interplay between these two PTMs on proteins, occurring through multiple mechanisms. Several types of cross-talks can exist:

- Reciprocal crosstalk involves both modifications competing for the same serine or threonine residue, potentially altering the modification patterns and functions of the protein.
- Proximity crosstalk occurs when modifications influence each other nearby on the protein sequence, allowing O-GlcNAcylation to regulate phosphorylation and vice versa.
- Distal crosstalk involves modifications affecting each other at distant sites on the protein sequence, where O-GlcNAcylation can impact phosphorylation far from the initial modification site. Enzyme crosstalk involves interactions between the enzymes responsible for these modifications, such as kinases and O-GlcNAc transferase, influencing each others activities.
- Substrate crosstalk occurs when the protein substrates of these enzymes interact and affect each others modification patterns.

The interplay between O-GlcNAcylation and phosphorylation reveals a complex regulatory network within cells, where an overall increase in O-GlcNAcylation can lead to changes in the phosphoproteome, with certain phosphorylation sites decreasing while others increase, albeit to a lesser extent. O-GlcNAc and phosphate can compete for the same sites on serine and threonine residues of proteins, or occupy nearby or different sites on the same substrate. A large-scale study demonstrated that

inhibiting GSK-3 with lithium resulted in significant alterations in O-GlcNAcylation across various protein substrates, highlighting a competitive regulation between O-GlcNAc and phosphate. Additionally, treatments that modify the activity of protein kinases A, C, or tyrosine kinases induce reciprocal effects on the O-GlcNAcylation of cytoskeletal proteins, suggesting a broader reciprocal regulation between these two post-translational modifications (Zeidan and Hart 2010; Wang, Pandey, and Hart 2007; Wang, Gucek, and Hart 2008).
This extensive crosstalk between phosphorylation and O-GlcNAcylation plays critical roles in various cellular processes, including signaling, transcription, and the development of chronic diseases (**vanderLaarseCrosstalkphosphorylationOGlcNAcylation2018**; Hart et al. 2011).
On Tau, although phosphorylation is more abundant, these two post-translational modifications coexist. The crosstalk between O-GlcNAcylation and phosphorylation of Tau is relevant to understanding neurodegenerative diseases like Alzheimer's.
It has been shown that when Tau is O-GlcNAcylated, it is less phosphorylated, and vice versa. This underscores the reciprocal relationship and competition between these two modifications.
O-GlcNAcylation and phosphorylation of Tau are dynamically regulated and can have opposing effects. Increased O-GlcNAcylation of Tau generally decreases its phosphorylation, while decreased O-GlcNAcylation leads to hyperphosphorylation of Tau (Cantrelle et al. 2021; Lee, Suh, and Kim 2021; Gatta et al. 2016).
Increases in Tau levels and hyperphosphorylation are caused by directly targeting the ogt gene in mice's neurones; these changes are associated with Tau pathology in Alzheimer's disease (Lefebvre et al. 2003). Conversely, decreasing Tau phosphorylation at specific locations results from increasing Tau O-GlcNAcylation by OGT overexpression. In hemizygous JNPL3 mice harbouring the human Tau-P301L mutant, chronic administration of the OGA inhibitor Thiamet-G dramatically lowers neurofibrillary tangles (NFTs) without changing total Tau phosphorylation at Alzheimer's disease-relevant sites (AT8 and pS422). Additionally, this medication raises O-GlcNAc levels, which specifically lowers tangles' AT8 immunoreactivity. Comparable outcomes were noted in rTg4510 mice, where long-term administration of Thiamet-G elevated Tau O-GlcNAcylation and reduced pathological Tau aggregation while leaving non-pathological Tau phosphorylation unaltered (O'Donnell et al. 2004). Therefore, OGA inhibition can lessen neurodegeneration and NFTs without affecting Tau hyperphosphorylation. On the other hand, in human neuroblastoma cells, causing Tau hyperphosphorylation with the phosphatase inhibitor okadaic acid results in a decrease in Tau O-GlcNAcylation and a reduction in its nuclear transfer (Graham et al. 2014). It's interesting to note that compared to less phosphorylated versions, hyperphosphorylated Tau has less O-GlcNAcylation (Bourré et al. 2018).
Another study revealed that although prolonged Thiamet-G treatment improved survival and motor impairments, it did not alter Tau O-GlcNAcylation or phosphorylation in Tau.P301L transgenic mice. Instead, it enhanced protein O-GlcNAcylation. These results imply that increased O-GlcNAcylation of proteins other than Tau may be the source of the advantages associated with raised O-GlcNAc levels (Borghgraef et al. 2013) (Figure 4.6).

O-GlcNAcylation of Tau reduces Phosphorylation Levels

O-GlcNAcylation of Tau is crucial for regulating its phosphorylation levels (Graham et al. 2014). Research consistently shows that O-GlcNAcylation reduces Tau phosphorylation at various sites associated with AD. This reduction likely occurs through a site-specific mechanism, where O-GlcNAcylation interferes with the sequential phosphorylation of specific residues.
When Tau protein is O-GlcNAcylated, it exhibits lower levels of phosphorylation, and the reverse is also true. This reciprocal relationship reinforces the concept of a competitive and dynamic interplay between these two modifications. O-GlcNAcylation directly affects the cellular localization of Tau. Lefebvre et al. 2003 shows that O-GlcNAcylated Tau, which is less phosphorylated, is preferentially transferred to the nucleus. This localization shift underscores the functional significance of

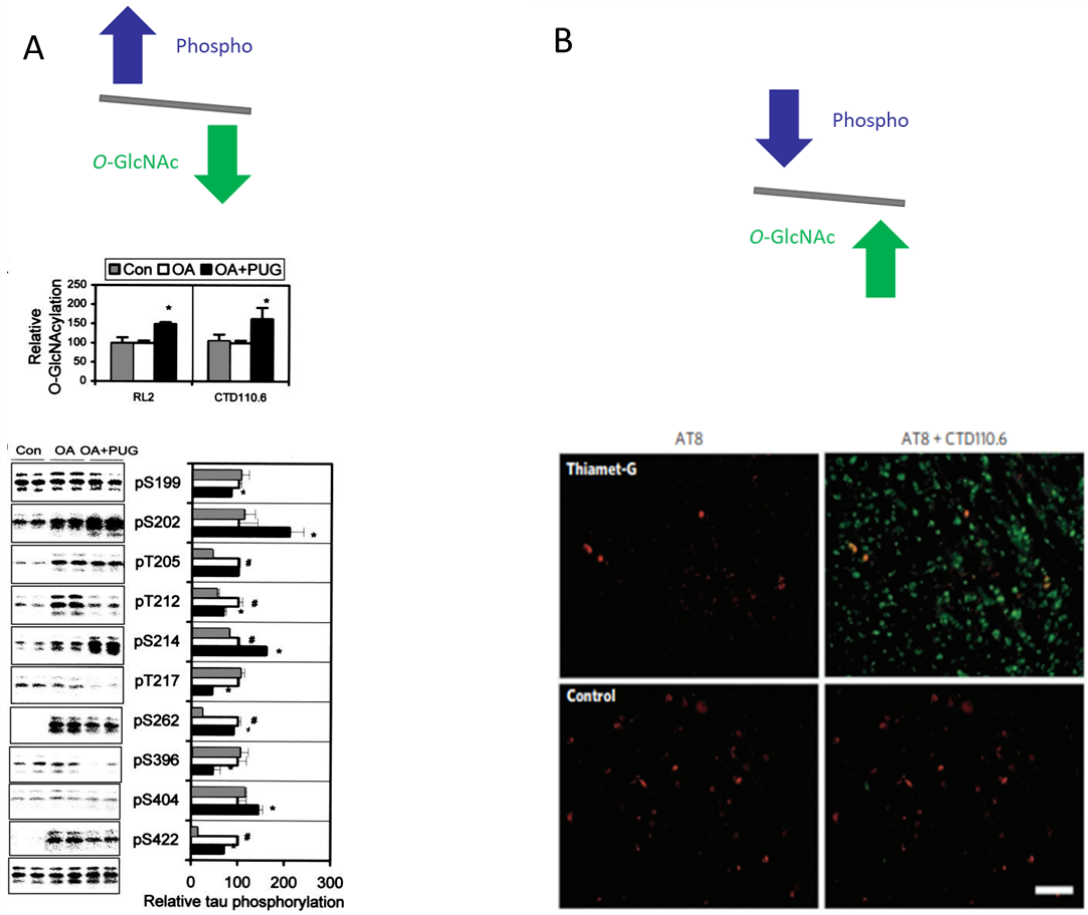

(A) Relative O-GlcNAc levels between control (CON, grey bars) and mice treated with okadaic acid (OA, white bars) or OA and PUGNAc inhibitors (OA+PUG, black bars) that are PP2A and OGA inhibitors, respectively, are determined either by RL-2 or CTD110.6 staining. Site-specific Tau phosphorylations are measured by their respective antibody responses in each conditions (Liu et al. 2004) (B)Representative data from the quantification in a reveals a general reduction in AT8 staining (left panels, in red), whereas the amount of global O-GlcNAc (CTD110.6) is greatly increased in the thiamet-Gtreated group of JNPL3 mice (upper right panel, in green). Scale bar indicates 100 m. (Yuzwa et al. 2012)

Figure 4.6: Effect of O-GlcNAcylation level on phosphorylation level of Tau

O-GlcNAcylation in regulating Tau's cellular dynamics and potential roles in nuclear processes. These O-GlcNAcylated forms of Tau show reduced phosphorylation by GSK3β compared to non-modified Tau (Lee, Suh, and Kim 2021; Cantrelle et al. 2021). Priming of Tau by CDK2 phosphorylation can influence subsequent GSK3β phosphorylation, but O-GlcNAcylation still reduces the overall level of GSK3β phosphorylation on Tau (Cantrelle et al. 2021).

Phosphorylation of Tau reduces O-GlcNAcylation Levels

Phosphorylation of Tau significantly impacts its O-GlcNAcylation levels. Studies consistently demonstrate that phosphorylation of Tau reduces O-GlcNAcylation at several epitopes associated with AD in rodent brains. This reduction likely occurs through a site-specific mechanism, where phosphorylation of Tau disrupts the binding of OGT to Tau, thereby decreasing O-GlcNAcylation levels. This effect is observed even under conditions of low phosphorylation, mimicking physiological states. The reduction in O-GlcNAcylation due to Tau phosphorylation has important implications for understanding Tau function and its role in neurodegenerative diseases like AD. Since O-GlcNAcylation plays a critical role in regulating Tau's aggregation and neurotoxicity, decreased O-GlcNAcylation due to phosphorylation may contribute to the development and progression of these diseases (**CantrellePhosphorylationOGl

Graham et al. 2014; Liu et al. 2004). Phosphorylation of Ser396 and Ser404 reduces O-GlcNAcylation

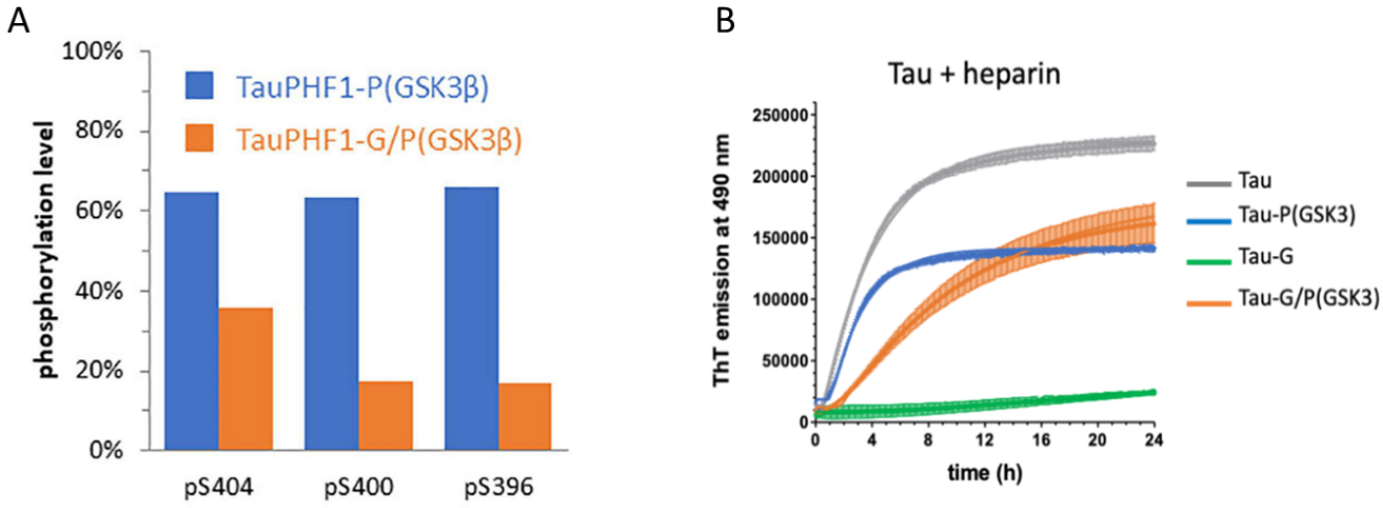

(A) Phosphorylation patterns of PHF1-G by GSK3β (B) Aggregation of PHF1 series induced by heparin

Figure 4.7: Effect of O-GlcNAcylation level on phosphorylation and aggregation of Tau (**CantrellePhosphorylationOGlcNAcylationPHF12021**)

of Ser400, which is notably identified as the principal site on the Tau protein (Morris et al. 2015). Conversely, prior O-GlcNAcylation of Ser400 decreases GSK3 kinase activity at the two adjacent serine residues. This study further highlights the protective role of O-GlcNAcylation, as it inhibits the formation of the PHF-1 phospho-epitope implicated in Alzheimer's disease (Figure 4.7).

Phosphorylation and O-GlcNAcylation Crosstalk in Tau Protein Aggregation

The cross-talk between phosphorylation and O-GlcNAcylation of the Tau protein significantly impacts its aggregation propensity, a critical factor in the pathology of AD.
O-GlcNAcylation plays a role in site-specific regulation of Tau phosphorylation under different experimental conditions, including cultured cells, in vivo models, and metabolically active brain slices. Their study revealed that in a mouse model of starvation, which mimics the disrupted glucose metabolism seen in Alzheimer's disease (AD), there was a significant reduction in Tau O-GlcNAcylation. This reduction was associated with increased Tau phosphorylation at certain sites, although not all phosphorylation sites exhibited elevated levels (Liu et al. 2004; Bourré et al. 2018).
While O-GlcNAcylation decreases Tau phosphorylation, it does not fully prevent Tau aggregation. The PHF1-3P isoform of Tau, which is both phosphorylated and O-GlcNAcylated, still plays an active role in Tau aggregation (Cantrelle et al. 2021).
Disruption of the balance between O-GlcNAcylation and phosphorylation of Tau has been implicated in the development of AD and other neurodegenerative disorders. Maintaining proper O-GlcNAcylation levels may be a potential therapeutic approach. In summary, the search results demonstrate that O-GlcNAcylation and phosphorylation of Tau are closely intertwined, with O-GlcNAcylation generally acting to reduce Tau phosphorylation. This crosstalk plays an important role in regulating Tau function and aggregation, with implications for neurodegenerative diseases (Bourré et al. 2018; Pratt and Vocadlo 2023).
In conclusion, increasing or decreasing O-GlcNAcylation does not always produce an opposing effect on Tau phosphorylation at specific sites, indicating an indirect interaction between these two post-translational modifications (PTMs) that could involve enzymatic crosstalk. Direct assessments (**CantrellePhosphorylationOGlcNAcylationPHF12021**; Bourré et al. 2018) have shown that O-GlcNAcylation of Tau has minimal impact on its phosphorylation by various kinases or the kinase

activity of rat brain extracts. Research further supports that while O-GlcNAcylation may influence certain phosphorylation sites, its overall effect remains modest, particularly in physiological contexts. Moreover, in mice, whether wild-type (WT) or APP mutant, only one O-GlcNAc site (S400) has been identified despite using lectin column enrichment methods (Morris et al. 2015; Wang et al. 2010b), and this without the application of OGA inhibitors. However, more recent studies have identified additional sites using more advanced enrichment techniques (IP-LC-MSMS) (Bijttebier et al. 2023), highlighting the challenges in detecting and identifying GlcNAc residues. Notably, in animal models, a reduction in O-GlcNAcylation has been associated with Tau hyperphosphorylation, which may contribute to neurodegenerative pathology, emphasizing the importance of a balanced interaction between these modifications to maintain normal Tau function and prevent its aggregation.

Chapter 5: Tau and LLPS

Recent research has uncovered that Tau protein has the capacity to undergo a phenomenon known as Liquid-Liquid phase separation (LLPS) (Ainani et al. 2023; Li et al. 2023a). Liquid-liquid phase separation (LLPS) is defined as a phenomenon that occurs when a homogeneous mixture containing multiple components spontaneously separates into two distinct liquid phases, each with varying concentrations of components. In living cells, LLPS is a spontaneous process wherein proteins or nucleic acids segregate from the solution into a dense phase in thermodynamic equilibrium with a dilute phase. They form condensed liquid-like droplets or coacervates, which can play a role of membraneless compartments/ organelles (Ainani et al. 2023).

1. Liquid-Liquid Phase Separation

Liquid-liquid phase separation (LLPS) is a fundamental biophysical process that enables the formation of membrane-less biomolecular condensates within cells (Li et al. 2023a). This phenomenon is propelled by multivalent interactions among proteins and/or nucleic acids, often found in proteins containing intrinsically disordered regions (IDRs) or modular domains capable of transient, weak interactions. As the concentration of these biomolecules surpasses a certain threshold, their interactions intensify, surpassing those with the surrounding solvent, leading to phase separation into a protein-rich condensed liquid phase and a protein-depleted dilute phase (Figure 5.1).

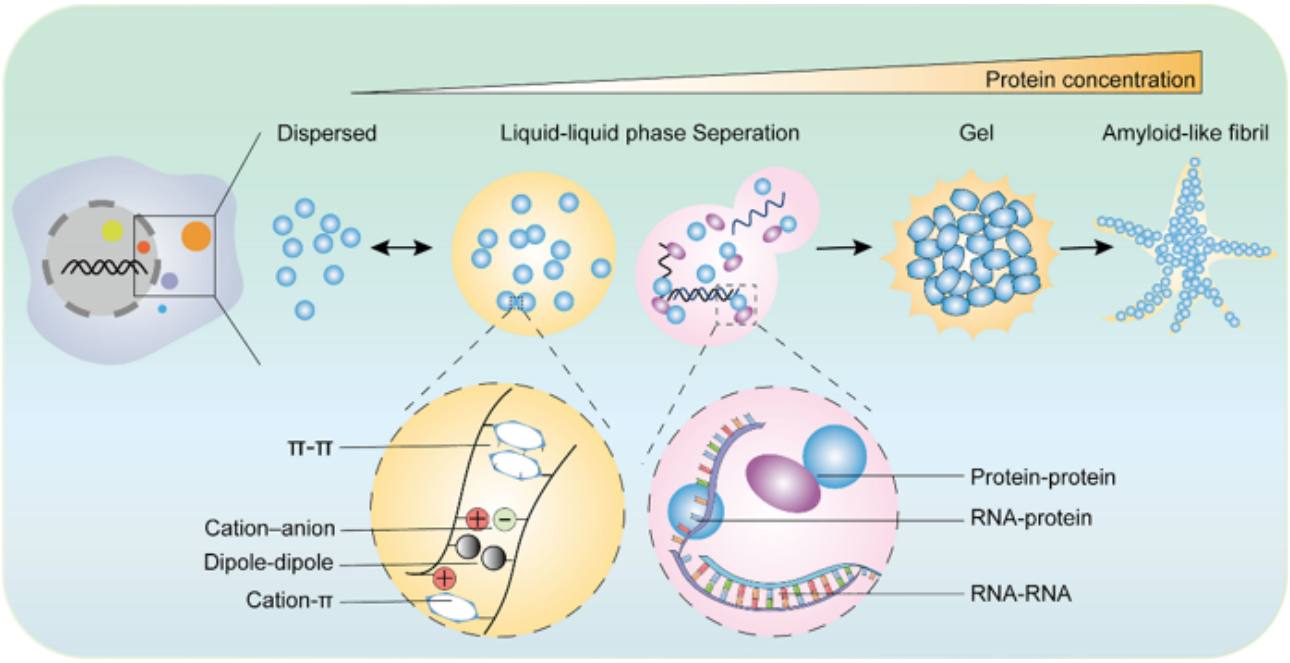

Figure 5.1: Formation mechanism of LLPS (Yang et al. 2023)

We can use LLPS diagram, also known as a phase diagram, that is a graphical representation that illustrates the conditions under which a protein solution undergoes phase separation into a dense

protein-rich phase and a dilute protein-poor phase (Figure 5.2).

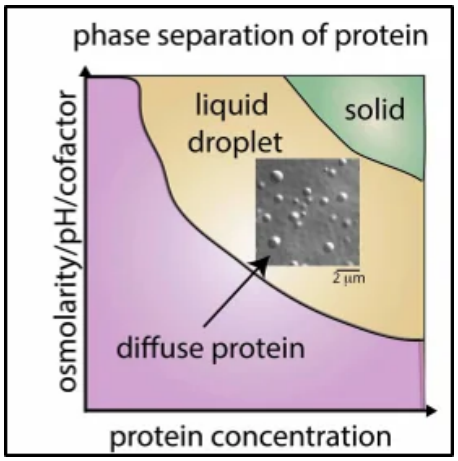

Figure 5.2: Phase diagram of LLPS (*The McGurk Lab* 2018)

Proteins involved in LLPS are typically categorized as "scaffolds," essential for initiating LLPS through their multivalent nature, and "clients," which are drawn into the condensates by the scaffolds. LLPS facilitates the concentration of specific proteins and nucleic acids into discrete cellular locations, thereby enabling various biological functions such as gene expression regulation, stress response, and the formation of membrane-less organelles like nucleoli and stress granules.

2. Molecular interactions underlying LLPS

LLPS is a process in which macromolecules, such as proteins and nucleic acids, assemble into liquid droplets or condensates. This process is driven by various molecular interactions, each playing a crucial role in the formation and stability of these condensates.

2.1. Hydrophobic Interactions

Hydrophobic interactions are essential for stabilizing liquid condensates. Proteins with hydrophobic residues tend to aggregate to minimize their exposure to water, promoting the formation of droplets. This behavior is particularly pronounced in intrinsically disordered proteins, which often contain a high proportion of hydrophobic residues. These interactions are pivotal in the assembly and maintenance of the condensates (Murthy et al. 2019).

2.2. Electrostatic Interactions

Electrostatic interactions between charged side chains of amino acids are also fundamental in LLPS. These interactions encourage protein self-association, especially in low ionic strength environments. The presence of salts like NaCl can disrupt these interactions, thereby influencing the formation and stability of the condensates (Poudyal et al. 2023).

2.3. Dipolar and Cation-π Interactions

Dipolar interactions and cation-π interactions further contribute to the stability of condensates. Proteins containing aromatic residues often engage in cation-π interactions, which help stabilize the liquid-liquid phase-separated structures. These interactions are important in maintaining the integrity of the condensates (Dignon, Best, and Mittal 2020).

2.4. Fraction and Modelling of Residues

The fraction, pattern, and identity of charged and hydrophobic residues within proteins are crucial in inducing LLPS. For example, a high concentration of charged residues and low solvation energy in the aqueous phase are key characteristics for proteins that act as clients in the phase separation process (Dignon, Best, and Mittal 2020).

2.5. Properties of Scaffold Proteins

Scaffold proteins play a crucial role in liquid-liquid phase separation (LLPS) due to their unique structural properties, particularly the presence of intrinsically disordered regions (IDRs) and low-complexity sequences. These regions enable scaffold proteins to form multivalent interaction networks, increasing the likelihood of condensation into liquid droplets, while their flexible nature allows them to adapt to environmental changes and interact with other proteins. Specific amino acid ratios, such as phenylalanine (Phe), glycine (Gly), and arginine (Arg), are also important for LLPS, as aromatic residues like Phe promote hydrophobic interactions and charged residues like Arg facilitate electrostatic interactions, both of which are crucial for stabilizing condensates. Additionally, a low solvation energy associated with a high concentration of charged residues in the aqueous phase supports the formation of these condensates, highlighting the dynamic role scaffold proteins play in driving LLPS (Ozawa et al. 2022). LLPS predictors were built based on studies of sequence properties of scaffold proteins (Vernon and Forman-Kay 2019). General characteristics of a scaffold include intrinsically disordered and low-complexity regions (Elbaum-Garfinkle et al. 2015; Molliex et al. 2015; Nott et al. 2015), RNA binding, and Phe, Gly, Arg ratios.
Thermodynamic conditions, including protein concentration, salt concentration, temperature, and post-translational modifications, play crucial roles in modulating the formation and properties of these condensates (Peng, Hsu, and Wu 2021; Tong et al. 2022). Several databases, including PhaSePro, catalog experimentally verified instances of proteins undergoing LLPS, providing valuable insights into their biophysical driving forces, biological functions, and regulatory mechanisms.Additionally, predictive tools such as FuzDrop, IUPred2A, PLAAC, PScore, catGRANULE, and PSPredictor offer computational resources for studying LLPS-related phenomena (Figure 5.3).

3. Tau's phase separation

In recent years, there has been a growing body of research suggesting the potential involvement of liquid-liquid phase separation in neurodegenerative processes. A significant proportion of proteins undergoing LLPS are either intrinsically disordered or contain intrinsically disordered regions (IDRs) (Martin and Holehouse 2020), this characteristic is why Tau has been particularly intriguing and prone to study its LLPS.
Bioinformatic analysis indicates that the amino acid sequence of Tau harbors a high propensity for granule formation.

3.1. Physiological roles of Tau LLPS

The formation of Tau-enriched condensates through LLPS holds the potential to locally concentrate Tau, thereby regulating its capacity to bind and stabilize microtubules within specific subcellular regions. This concentration mechanism may facilitate the spatial organization of Tau-mediated microtubule dynamics, influencing various cellular processes such as cytoskeletal organization, intracellular transport, and neuronal signaling (Liu et al. 2023). To establish their microtubule arrays, neurons encounter several challenges. Initially, they need to initiate microtubule nucleation in a manner independent of the centrosome. Additionally, they must arrange microtubules into bundles that can extend

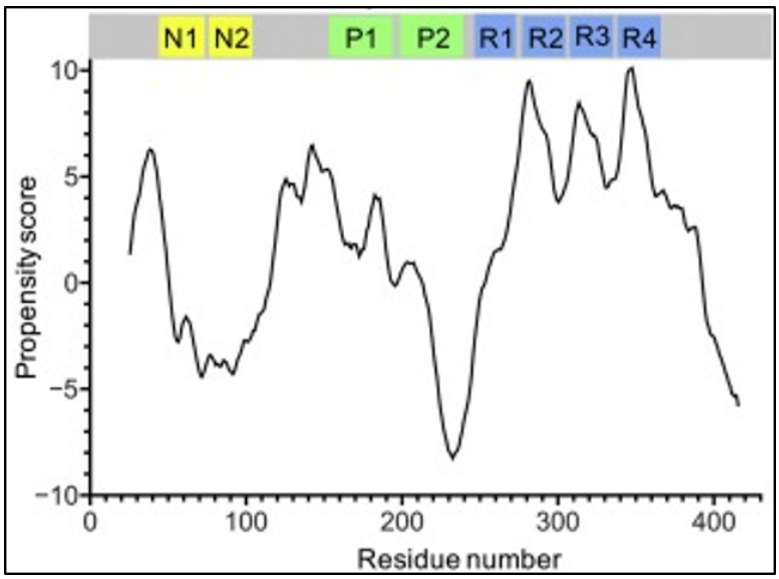

Figure 5.3: Residue-specific propensity scores for granule formation of Tau2N4R calculated by the software catGRANULE

for millimeters in length particularly within the long axons of neurons where these structures are crucial for maintaining cell shape and facilitating intracellular transport (Hernández-Vega et al. 2017). In 2017, Hernández-Vega et al. 2017 demonstrated that under conditions of molecular crowding, Tau forms liquid-like drops. Tubulin partitions into these drops, where it nucleates and drives the formation of microtubule bundles. These bundles deform the drops and remain enclosed by diffusible tau molecules, exhibiting a liquid-like behavior. They suggest that Tau drops can drive the formation of microtubule bundles in neurons by acting as non-centrosomal microtubule nucleation centers and that a liquid-like encapsulation by tau could provide both stability and plasticity to long axonal microtubule bundles (Figure 5.4).

3.2. Pathological role of Tau LLPS

Pathological role of Tau LLPS remains primarily with its relation to Tau aggregation. Insights into the relationship between LLPS and amyloid fibrils were first derived from studying FUS and TDP-43, two RNA-binding proteins that form inclusions in FTD and ALS (Patel et al. 2015; Mann et al. 2019). It has been suggested that phaseseparated tau droplets from soluble tau species, which undergo LLPS under cellular conditions, can serve as an intermediate toward tau aggregate formation (Wegmann et al EMBO J 2018).Both proteins have an IDR responsible for oligomerization, phase separation, hydrogel formation (via cross-β structures), and fibrillar aggregation (Loughlin and Wilce 2019). However, for tau protein, the relationship between LLPS and fibril formation remains less well understood.
The hypothesis of the mechanism of Tau aggregation involving LLPS, is that Tau forms liquid condensates that can accelerate Tau amyloid aggregation (Figure 5.5) (Wen et al. 2021). The connection between Tau LLPS and amyloid aggregation is complex, with studies suggesting that Tau LLPS may not always lead to amyloid aggregation (Loughlin and Wilce 2019). It has been suggested that phaseseparated Tau droplets from soluble tau species, which undergo LLPS under cellular conditions, can serve as an intermediate toward tau aggregate formation (Wegmann et al. 2018).

3.3. LLPS regulation by PTMs

Post-translational modifications (PTMs) play a crucial role in regulating the liquid-liquid phase separation (LLPS) behavior of Tau.

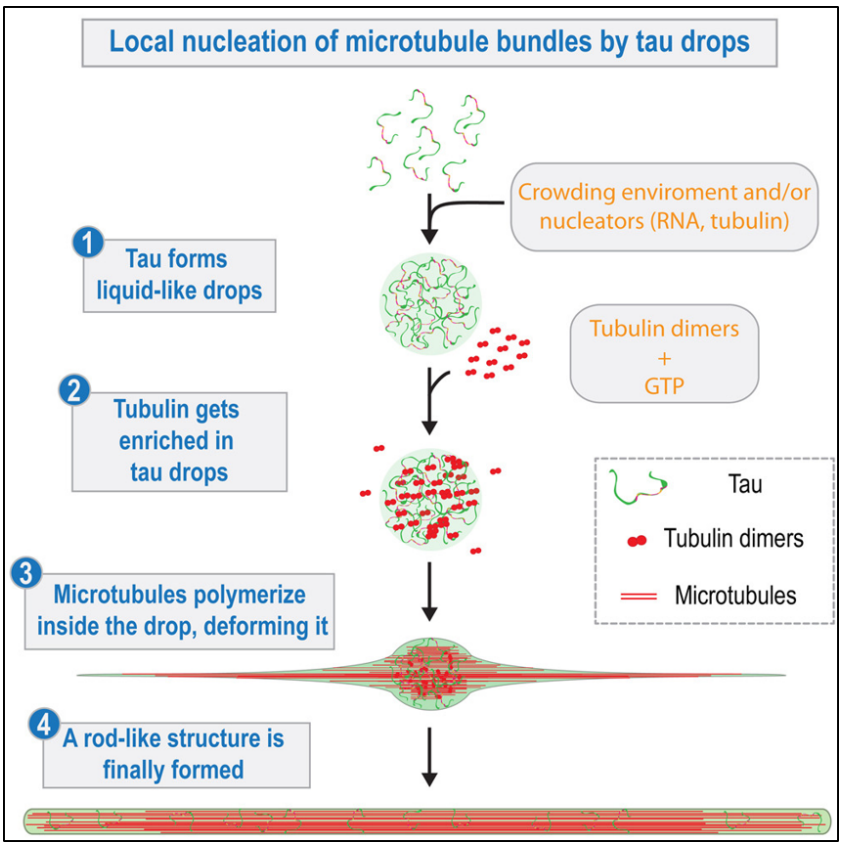

Figure 5.4: Regulation of microtubule dynamics by Tau LLPS

Phosphorylation

Phosphorylation by kinases such as MARK2, GSK3β, and PKA promotes Tau LLPS by adding negative charges and decreasing the overall positive charge, which facilitates hydrophobic interactions and compaction. Specific phosphorylation sites like T181, T212, S214, S404, S202/T205, and S396/S404, linked to Alzheimer's disease, increase the propensity for Tau LLPS. Consequently, hyperphosphorylated Tau shows greater LLPS than minimally phosphorylated forms. Notably, phosphorylation of Tau by GSK3β drives the maturation of liquid droplets into gel-like aggregated structures over time, highlighting the critical role of phosphorylation in Tau's pathological aggregation (Kanaan et al. 2020; Abasi et al. 2024).

Acetylation

Acetylation of lysine residues by acetyltransferases such as p300 neutralizes the positive charges on Tau and increases its hydrophobicity. Unlike phosphorylation, acetylation significantly attenuates or blocks Tau LLPS by disrupting electrostatic interactions and hydrogen bonding with RNA (Kanaan et al. 2020; Powell et al. 2024).

Other PTMs

Ubiquitination and glycation can influence Tau LLPS behavior, but their specific effects remain poorly understood (Abasi et al. 2024).

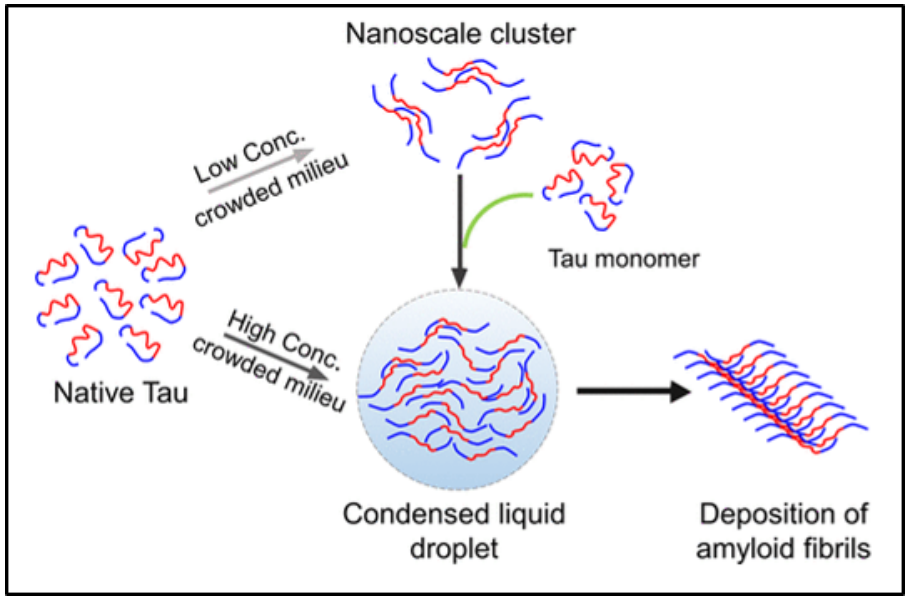

Figure 5.5: Schematic linking Tau LLPS and it's aggregation (Wen et al. 2021)

Chapter 6: GSK3β and Alzheimer's disease

1. Generalities about GSK3β

Glycogen synthase kinase 3 (GSK3) is a kinase that have more than 100 substrates (Linding et al. 2008). GSK3 refers to two paralogs that are commonly referred to as isoforms, GSK3α and GSK3β that share 97% identity in their catalytic cores but have different N- and C-terminal extensions.
GSK3β is a serine/threonine kinase that plays crucial roles in various cellular processes by regulating multiple signaling pathways. Its involvement in pathways like Wnt/β-catenin and receptor tyrosine kinase (RTK)/PI3K highlights its significance in fundamental cellular functions such as proliferation, differentiation, and cell survival (Hetman et al. 2000; Morgan-Smith et al. 2014). One of the intriguing aspects of GSK3β is its constitutive activity, meaning it is active under basal conditions in the absence of upstream signaling inputs. This constitutive activity allows GSK3β to continuously phosphorylate its substrates, exerting its regulatory effects on various cellular processes. Hence, GSK3 activity is inhibited rather than activated upon signaling pathways, notably phosphorylation by Akt/PKB at the GSK3 N-terminal residue (S9/21, depending on the GSK3 isoform) was described as an inhibitory process of GSK3 activity. Another way of regulation of GSK3 activity is based on substrate priming (Fang et al. 2000). GSK3β typically requires priming phosphorylation on its substrates, but not mandatory for some of them, for efficient phosphorylation to occur. This priming phosphorylation creates a recognition site for GSK3β, facilitating its subsequent phosphorylation of nearby residues. This requirement for priming phosphorylation adds an additional layer of regulation to the specificity and activity of GSK3β in signaling pathways (Beurel, Grieco, and Jope 2015).

2. Structure of GSK3β

The overall structure of the GSK3β catalytic domain resembles that of other protein kinases, featuring an N-terminal lobe primarily composed of β-strands and a C-terminal lobe predominantly consisting of α-helices (Figure 6.1). The N-terminal lobe serves functions such as binding to ATP, the phosphate donor molecule, and positioning the substrate for phosphorylation (Stamos et al. 2014). Conversely, the C-terminal lobe harbors the catalytic residues essential for transferring the phosphate group from ATP to the substrate. This structural arrangement is conserved among protein kinases and is crucial for their catalytic activity and substrate recognition.
In June 2001, Dajani et al. 2001 resolved the crystallographic structure of GSK3β using Human GSK3β expressed in the baculovirus expression system. Crystals were grown from full-length human GSK3β (420 residue-cleavable His-tag) but clear electron density is only evident for the 351 residues from Lys 35 to Ser 386. The N-terminal region of GSK3β (residues 35-134) is characterized by a structural motif composed of seven β strands arranged in a curved fashion, ultimately forming a closed orthogonal β barrel. The connection between the N-terminal domain and the rest of the protein is facilitated by an α helix (residues 138149) extending from the end of the 7^{th} beta strand. The core of the α-helical domain (residues 152342) exhibits a topology resembling that of the corresponding region found in mitogen-activated protein (MAP) kinases such as ERK2 and p38. Beyond residue 342, GSK3β diverges significantly from the typical MAPK (mitogen-activated protein kinase) fold.

Residues 342-386 constitute a series of short helices and loops tightly packed against the long C-terminal alpha-helical domain of the kinase. These findings suggest that the C-terminal region of GSK3β, post the 342nd residue, exhibits a unique structural arrangement compared to its N-terminal kinase domain. Contrary to the standard MAPK fold, this C-terminal region adopts a distinctive configuration consisting of short helices and loops, which intricately interact with the alpha-helical domain of the kinase.

(A) Stereo pair secondary structure cartoon of human glycogen synthase kinase 3β colored blue-red from the visible N terminus at residue 35 to the visible C terminus at residue 384. The orthogonal β barrel formed by the N-terminal domain is on the left (B) As (A), but with the view rotated by 90ř around the horizontal

Figure 6.1: Structure of Human GSK3β

3. Primed phosphorylation mechanism

GSK3β exhibits a distinctive substrate preference compared to other kinases, as it is one of the few kinases that require prior phosphorylation of its substrate before further phosphorylation can occur (**terHaarStructureGSK3vreveals2001**; Stamos et al. 2014).
GSK3β phosphorylates various substrates, yet its phosphorylation of different targets varies in terms of manner and efficiency. The recognized canonical phosphorylation motif for GSK3β, [S/T]XXX[S/T](P), features two serine residues separated by three intervening residues. In general, substrates of GSK3β are initially phosphorylated by another kinase, at the P + 4 position which is a proline-directed phosphorylation site. This feature is explained by the 3D structure of the GSK3 catalytic site, where the primed substrate binds a pocket close to the active site in which Arg96 plays a critical role. A GSK3-Arg96 mutated form is not able to phosphorylate primed substrates anymore or bind its own N-terminal phospho-Ser9 (pSer9) regulatory site, resulting in a loss of phosphorylation-mediated control of GSK3 activity (Frame, Cohen, and Biondi 2001). In addition, in consecutive [S/T]XXX[S/T] phosphorylation motifs, GSK3 can sequentially phosphorylate several S/T site in a stepwise manner.

4. Regulation of GSK3β

The regulation of GSK3β by PTMs plays a crucial role in modulating its activity and cellular functions. GSK3β undergoes diverse PTMs, including phosphorylation, acetylation, ubiquitination, and others, which finely tune its enzymatic activity, subcellular localization, and substrate specificity (Woodgett 2001; Eom and Jope 2009; Ko et al. 2015).
Phosphorylation is perhaps the most extensively studied PTM regulating GSK3β, with phosphorylation at specific serine or tyrosine residues affecting its catalytic activity and interactions with binding partners. Inhibitory serine 9-phosphorylation stands out as the most extensively studied mechanism regulating the activity of GSK3β. This phosphorylation leads the N-terminal tail of GSK3β to act as an prephosphorylated inhibitory peptide by occupying the priming site binding pocket (Frame, Cohen, and Biondi 2001).

One of the most studied GSK-3β upstream kinases is Akt/PKB (Stambolic and Woodgett 1994; Cross et al. 1995–0028). One major way that growth factor signalling, such as that which occurs through the PI3 kinase pathway, might increase neuronal survival and prevent death is through the inhibition of GSK3β activity by Akt activation (Figure 6.2).

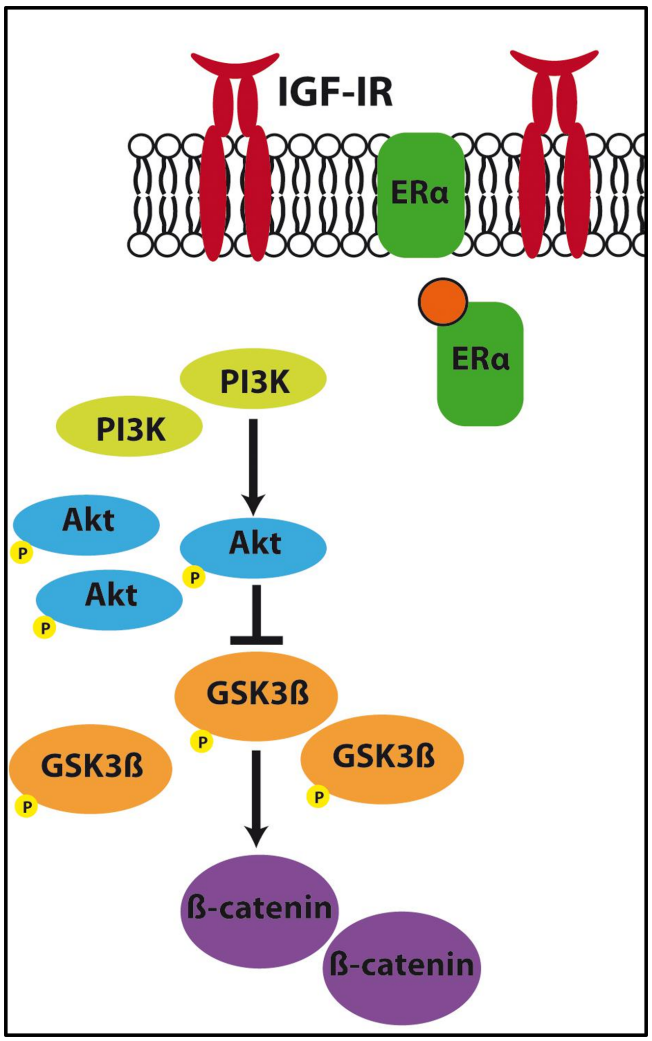

Figure 6.2: The signalling pathway by which insulin inhibits GSK3 (Figure adapted from Saraceno et al. 2018

5. GSK3β in AD pathology

GSK3β emerges as a pivotal player in the intricate pathogenesis of Alzheimer's disease (AD), orchestrating various mechanisms that contribute to its progression. Foremost among these is GSK3β's involvement in the hyperphosphorylation of Tau protein, a hallmark event leading to the formation of neurofibrillary tangles, a defining pathological feature of AD (Hooper, Killick, and Lovestone 2008; Toral-Rios et al. 2020). GSK3β is a key kinase that phosphorylates Tau at multiple sites, particularly in the proline-rich and C-terminal regions of the Tau protein. It most efficiently phosphorylates the PHF-1 epitope (pS396 and pS404) in the C-terminus of Tau, which is a hallmark of Alzheimer's disease pathology (Avila et al. 2012; Zhou et al. 2022). GSK3β phosphorylates S396, S400, and S404 in the C-terminal domain of Tau, with phosphorylation levels of 56%, 59%, and 81% respectively (Chakraborty et al. 2023). In the study by Cantrelle et al. 2021, the phosphorylation levels of Tau at sites S396, S400, and S404 were reported to be similar, each around 60%, even in the absence of priming. This suggests that GSK3β can effectively phosphorylate these sites without the need for

prior phosphorylation events, which aligns with the mechanism of sequential phosphorylation. Sequential phosphorylation involves the phosphorylation of one site facilitating the phosphorylation of adjacent sites, and the similar levels observed for S396, S400, and S404 support this concept.
Moreover, heightened GSK3β activity exacerbates the production of amyloid-β (Aβ) peptides, the primary constituents of amyloid plaques, further driving neurotoxicity and neuronal demise (Hooper, Killick, and Lovestone 2008; Lauretti, Dincer, and Praticò 2020).
Beyond these hallmarks, dysregulated GSK3β signaling disrupts synaptic plasticity, neurogenesis, and memory formation, thereby exacerbating cognitive deficits observed in AD. Additionally, GSK3β's pro-inflammatory actions fuel neuroinflammation, exacerbating neuronal damage. Consequently, targeting GSK3β has emerged as a promising therapeutic avenue for AD (Hooper, Killick, and Lovestone 2008; Toral-Rios et al. 2020).
While preclinical studies have shown the neuroprotective potential of GSK3 inhibitors in animal models, clinical efficacy in AD patients remains to be established definitively (Griebel et al. 2019; Sayas and Ávila 2021). Nevertheless, ongoing research endeavors continue to explore the therapeutic potential of GSK3 inhibition in mitigating AD pathology and associated cognitive decline (Griebel et al. 2019).

Chapter 7: Studying Tau Aggregation

Understanding Tau protein aggregation involves various methodologies that span *in vitro*, cell-based, and *in vivo* approaches. This chapter details the key methods employed to study tau protein aggregation, elucidating their principles, applications, and significance.

1. Inducing Tau Aggregation

Tau is a highly soluble protein, making its spontaneous aggregation in vitro challenging, which necessitates the use of specific aggregation-inducing agents (Crespo, Koudstaal, and Apetri 2018). Heparin, arachidonic acid (ARA), and RNA are commonly used to promote Tau polymerization, as their negative charges facilitate this process (Zheng et al. 2024; Rankin, Sun, and Gamblin 2007; Crespo, Koudstaal, and Apetri 2018). Additionally, phosphorylation of Tau, particularly by glycogen synthase kinase 3 beta (GSK3β), is crucial in driving the formation of stable, dense aggregates, including paired helical filaments (PHFs) similar to those found in Alzheimer's disease. These phosphorylated aggregates migrate in a manner akin to neurofibrillary tangles (NFTs) isolated from the brains of Alzheimer's patients during sucrose gradient centrifugation (Rankin, Sun, and Gamblin 2007).

1.1. In vitro

Seeding Experiments

In vitro Tau seeding assays involve adding pre-formed Tau aggregates, or "seeds," to solutions of monomeric recombinant Tau protein to study their ability to induce further Tau aggregation. Seeds can be sourced from sarkosyl-insoluble Tau extracts from diseased brains, such as those affected by Alzheimer's or other tauopathies, or from synthetic Tau fibrils formed from recombinant Tau. The kinetics of Tau fibril formation upon seeding are monitored using thioflavin-T fluorescence, which tracks fibril formation over time, as well as light scattering or turbidity measurements to report on aggregation kinetics. Electron microscopy is utilized to visualize the resulting fibrillar Tau aggregates. The seeding potency of different Tau strains is assessed by comparing their ability to accelerate Tau aggregation against unseeded controls, with more potent seeds leading to faster nucleation and elongation kinetics. These experiments provide mechanistic insights into the nucleation-polymerization process of Tau aggregation and allow for the study of how factors such as mutations, cofactors, and inhibitors modulate the distinct nucleation and elongation phases. However, the in vitro conditions do not fully replicate the complex intracellular environment, and typically only a single recombinant Tau isoform is used, unlike the isoform mixture found in vivo (Lathuiliere and Hyman 2021; Xu, Martini-Stoica, and Zheng 2016; Nam and Choi 2018).

Effects of Cofactors

Cofactors such as polyanions (heparin, RNA), fatty acids, and other molecules play crucial roles in inducing and modulating the kinetics of Tau protein aggregation in vitro.
Heparin:

Heparin, a highly sulfated glycosaminoglycan, has played a crucial role in advancing our understanding of Tau aggregation, a key process in Alzheimer's disease pathology. As early as 1996, pioneering work by Goedert and colleagues demonstrated that heparin acts as a polyanionic cofactor that promotes the assembly of Tau into fibrillar structures by neutralizing the positive charges on lysine residues. This interaction facilitates Tau-Tau binding, stabilizing aggregation-prone conformations and accelerating the formation of Tau filaments similar to the paired helical filaments (PHFs) found in Alzheimer's disease brains (Goedert et al. 1996a; Townsend et al. 2020). Subsequent research has shown that the sulfation pattern of heparin significantly affects the kinetics and morphology of Tau fibrils, with specific modifications, such as the removal of 2-O-sulfates, leading to a marked slowdown in aggregation kinetics.

Recent studies using proteomics and cryo-electron microscopy have revealed that Tau fibers induced by heparin exhibit structural and biochemical differences compared to those purified from the brains of Alzheimer's patients. Specifically, heparin-induced fibers are more heterogeneous and have a slightly different conformation than the disease-associated fibers. These findings raise concerns about the pathological relevance of heparin-induced fibers as models for Tau pathology in vitro. Heparin, while a powerful inducer, might obscure the effects of other natural cofactors and post-translational modifications of Tau. Additionally, since heparin is an artificial compound, it may not accurately represent the endogenous cofactors responsible for Tau aggregation in vivo, which are yet to be identified. Therefore, while heparin has been a valuable tool for studying Tau aggregation in vitro, it is now evident that the fibers it induces do not fully reflect the in vivo pathology of Tau, highlighting the need for new approaches to better replicate Tau aggregation under more physiological conditions (Chakraborty et al. 2021; Limorenko and Lashuel 2021).

Heparin's ability to promote Tau aggregation has been further complemented by the discovery that other molecules, such as RNA and fatty acids, also act as cofactors, with RNA inducing seeding-competent amyloid fibrils and fatty acids like arachidonic acid accelerating aggregation through conformational changes in Tau.

RNA:

RNA's role in the aggregation of Tau protein into paired helical filaments (PHF) has become a significant focus in neurodegenerative disease research, particularly in Alzheimer's disease (AD). Initial studies highlighted that RNA, especially poly(A) RNA, serves as a potent driver of Tau aggregation, facilitating the formation of Tau oligomers that are pivotal in the early stages of pathological aggregation. It was found that Tau binds to RNA with high affinity, forming Tau-RNA complexes that inhibit Tau's interaction with microtubules, thereby modulating its aggregation. Subsequent research revealed that Tau aggregates in both cellular and animal models are enriched with RNA, particularly small nuclear RNAs (snRNAs) and small nucleolar RNAs (snoRNAs), which suggests RNA's involvement in altering nuclear speckle dynamics and pre-mRNA splicing. Moreover, RNA has been shown to induce the formation of distinct Tau strains, contributing to the diversity of tauopathies, with different RNA sequences influencing the structural characteristics of Tau aggregates. Intriguingly, Tau can also aggregate into seeding-competent fibrils without traditional co-factors, with these fibrils sequestering RNA, indicating that RNA interactions are crucial for the stability and propagation of Tau aggregates, potentially guiding them toward disease-specific structures (Maziuk et al. 2018; McMillan et al. 2023a).

Other polyanions, such as RNA oligonucleotides and polyglutamic acid, can similarly induce Tau aggregation (Montgomery et al. 2023), while small molecules like phenothiazines can selectively inhibit heparin-induced Tau aggregation (Limorenko and A. Lashuel 2022).

The use of aggregation inducers, such as polyanions, presents several disadvantages, including the risk of false positives, as these inducers can interact with non-target molecules, leading to results that do not accurately reflect the true aggregation of Tau. This complicates the interpretation of experimental data and may skew conclusions about the mechanisms of aggregation. Additionally, PTMs like phosphorylation and acetylation significantly influence Tau's interactions with other proteins and

its aggregation behavior; phosphorylation introduces negative charges that can disrupt aggregation interactions, while acetylation neutralizes positive charges, also affecting aggregation potential. These modifications can obscure the actual role of PTMs in Tau aggregation, making it challenging to assess their specific contributions. Moreover, the complex interactions between inducers and PTMs may lead to misinterpretations, where PTMs are incorrectly assumed to be responsible for observed aggregation in the presence of inducers, even though they might merely alter Taus response without directly causing aggregation (Kamah et al. 2014).
In summary, various cofactor molecules, especially polyanions like heparin and RNA, are extensively used in vitro to induce, accelerate, and modulate the kinetics and structural properties of Tau aggregates, providing valuable insights into the mechanisms of pathological Tau aggregation.
Research has shown that certain fragments of Tau, particularly those that include the core-forming region of the fibers, can spontaneously aggregate to form structures resembling paired helical filaments (PHFs) or the protofilaments of PHFs/straight filaments (SFs) under very specific conditions, without the need for external inducers. For instance, Tau fragments containing the repeat domains can assemble into fibrillar structures under controlled conditions, providing insight into the mechanisms of aggregation. The study by Lövestam et al. 2022 demonstrated that Tau fragments, such as those spanning amino acids 266 to 391, can be assembled in vitro into filaments identical to those isolated from the brains of Alzheimer's disease patients.

Studying Tau Fragments/Mutations

Studying Tau fragments and mutations has provided valuable insights into how they influence the key nucleation and elongation steps of Tau aggregation. Truncated Tau fragments containing just the repeat domain, such as K18 and K19, are widely used in vitro since these repeats form the core of Tau fibrils. Specific fragments like F2 (Tau274-305) and F3 (Tau306-336), generated by proteolysis, readily aggregate and act as seeds to accelerate the aggregation of full-length Tau (Chen et al. 2019; Wang et al. 2009; Wang et al. 2007).
Additionally, fragments like Tau151-391 exhibit a higher propensity for self-aggregation compared to full-length Tau when expressed in cells. N-terminal and C-terminal truncations modulate Tau aggregation differently, with C-terminal truncations generally promoting aggregation more robustly (Boyarko and Hook 2021).
Mutations also play a significant role in Tau aggregation. For instance, the P301L mutation in the repeat domain enhances aggregation kinetics by destabilizing structures around the amyloidogenic 306VQIVYK311 motif. Molecular dynamics simulations have shown that P301L increases the exposure of this motif, driving nucleation and self-assembly. Similarly, the S320F mutation stabilizes the local Tau structure but allosterically increases the exposure of the 306VQIVYK311 motif, promoting aggregation (Chen et al. 2019). Mutations like ΔK280 in the repeat domain facilitate the formation of proteolytic fragments such as F2 and F3, which further seed aggregation. In terms of nucleation and elongation, fragments like F2 and F3 act as potent nucleation seeds, accelerating the elongation of full-length Tau into fibrils. Mutations such as P301L and S320F enhance the initial nucleation phase by increasing the exposure of aggregation-prone motifs, while C-terminal truncations generally increase elongation rates once nuclei are formed (Wang et al. 2009; Wang et al. 2007). Other mutations in the Tau protein are known to enhance its aggregation and are associated with various tauopathies. For instance, the R406W mutation is linked to Frontotemporal Dementia with Parkinsonism linked to chromosome 17 (FTDP-17) and is characterized by increased Tau aggregation and reduced binding to microtubules. Similarly, the P301S, G272V, V337M, ΔK280, G335V, and N279K mutations, all associated with FTDP-17, also promote Tau aggregation and impair its ability to bind to microtubules, with N279K specifically affecting 4-repeat Tau. Additionally, the G303V and R406W mutations are associated with PSP and lead to increased Tau aggregation. These pro-aggregation mutations contribute to the pathogenesis of tauopathies by disrupting Taus normal function and promoting the

formation of neurofibrillary tangles, a hallmark of these diseases (Fontaine et al. 2015).

1.2. In vivo

Injection of Preformed Tau Fibrils

The provided research articles illustrate the technique of injecting preformed Tau fibrils or pathological Tau aggregates from diseased brains into animal models to seed the aggregation of endogenous Tau and study the prion-like spreading of Tau pathology. Clavaguera et al. 2009 injected Tau filament-containing brain homogenates from transgenic mice expressing mutant human Tau into the brains of transgenic mice overexpressing wild-type human Tau, which induced the formation of neurofibrillary tangle-like Tau inclusions that spread to anatomically connected brain regions over time. Ahmed et al. 2014 injected brain extracts from aged P301S Tau transgenic mice into younger P301S mice, resulting in rapid induction and propagation of Tau pathology along neuroanatomical connections.Guo et al. 2016 injected distinct pathological Tau strains isolated from Alzheimer's disease (AD), progressive supranuclear palsy (PSP), and corticobasal degeneration (CBD) patient brains into non-transgenic wild-type mice. These different Tau strains induced distinct patterns of neuronal Tau pathology that spread over time, recapitulating aspects of the respective human tauopathies. Narasimhan et al. 2017 injected pathological Tau isolated from AD patient brains into triple-transgenic AD mice, inducing time-dependent Tau aggregation that propagated from the injection site to connected brain regions. Lasagna-Reeves et al. 2012 showed that the injection of oligomeric Tau species derived from AD brain extracts into wild-type mice induced widespread templated misfolding of endogenous mouse Tau into filamentous aggregates over time. These studies collectively demonstrate how pathological Tau seeds can induce and propagate Tau pathology in various animal models, mirroring the progressive nature of human tauopathies.

Inducible Expression Systems

Inducible expression systems are widely used to study intracellular Tau aggregation mechanisms by allowing precise control over the expression of wild-type or mutant Tau proteins. These models offer valuable insights into the dynamics and regulation of Tau aggregation. Developed conditional expression systems in human neuroglioma H4 cells for 4-repeat wild-type (WT) Tau and the FTDP-17 mutants V337M and R406W were done . Upon induction, Tau expression increased over 5-7 days, leading to the formation of Tau filaments detectable by thioflavin-S binding and electron microscopy. The R406W mutant exhibited the highest proportion of sarkosyl-insoluble, aggregated Tau compared to WT and V337M (DeTure et al. 2002). Similarly, Lim et al. 2014 and Khlistunova et al. 2006 used doxycycline-inducible systems to express Tau in N2a neuroblastoma cells, resulting in robust intracellular Tau aggregation detected by thioflavin-S staining. These studies compared different Tau constructs, such as the repeat domain (K18), the δK280 mutant, and aggregation-inhibiting mutants. Inducible expression systems enabled researchers to investigate the effects of various mutations, such as P301L, V337M, and R406W, on Tau aggregation propensity, and to explore the role of cofactors like heparin or small molecules in modulating aggregation. They also allowed for the study of correlations between Tau phosphorylation, fragmentation, and aggregation, as well as the reversibility of aggregation upon silencing Tau expression. The benefits of these systems include the ability to control Tau levels, compare mutations and isoforms in identical genetic backgrounds, and study the temporal dynamics of aggregation. However, they also have limitations, such as potentially not fully recapitulating physiological conditions due to overexpression and the need for additional cellular factors for later stages like tangle formation.

2. Monitoring and Visualizing Tau Aggregates

2.1. In Vitro Methods

In vitro methods allow for controlled, reproducible studies of Tau aggregation under defined conditions, providing detailed insights into the mechanisms and kinetics of the process.

Thioflavin T Fluorescence Assays

The thioflavin T (ThT) fluorescence assay is a widely used method to study Tau protein aggregation in vitro. ThT is a benzothiazole dye that exhibits enhanced fluorescence upon binding to cross-β sheet structures present in amyloid fibrils and aggregates (Harada et al. 1994).

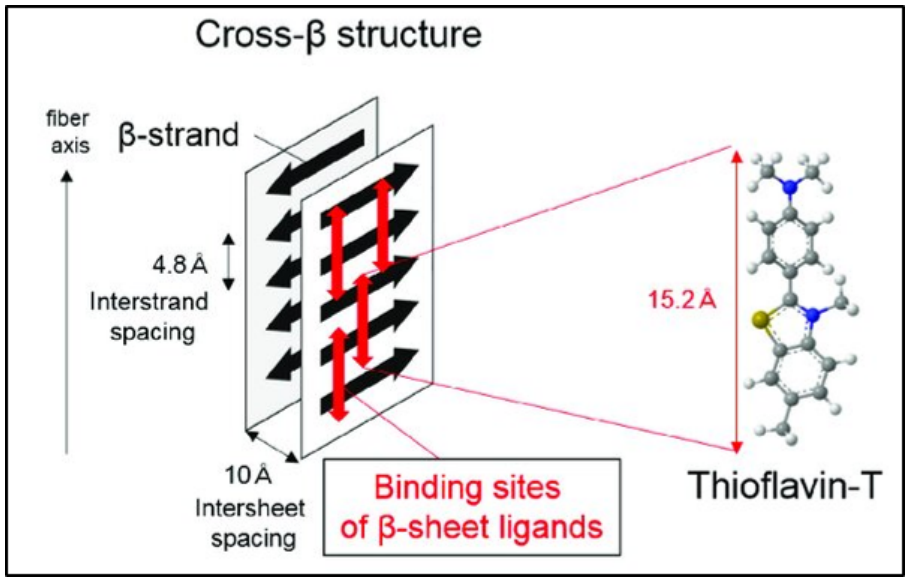

Figure 7.1: Illustration of cross-β structure in protein aggregates and proposed binding mechanism of β-sheet ligands such as thioflavin-T

As Tau aggregation proceeds, the formation of β-sheet rich Tau fibrils allows ThT binding, resulting in an increase in ThT fluorescence signal over time (Lim et al. 2014). In the experimental setup, recombinant Tau protein (often the 4R2N isoform or mutants like P301L) is incubated under conditions that promote its aggregation into fibrils. ThT is added to the aggregation reaction mixture at a low micromolar concentration, and fluorescence readings (ex/em 440/490nm) are taken at different time points to monitor the kinetics of Tau aggregation. This method is widely used to quantify the extent of Tau aggregation by measuring the endpoint ThT fluorescence signal (Sui, Liu, and Kuo 2015), allowing comparisons of the effects of mutations, cofactors, and inhibitors on the rate and extent of Tau fibril formation. It can provide insights into aggregation mechanisms by analyzing kinetic profiles and is used for screening and identifying potential Tau aggregation inhibitors in drug discovery efforts.
The assay is simple, cost-effective, and amenable to high-throughput screening formats, providing real-time monitoring of the aggregation process. However, it detects only β-sheet rich fibrillar aggregates, not oligomeric or disordered aggregates, and potential interference from test compounds binding to ThT may occur (Figure 7.1). Additionally, it requires purified recombinant Tau, which does not fully recapitulate intracellular conditions.

Transmission Electron Microscopy (TEM)

Transmission electron microscopy (TEM) is a microscopy technique where an electron beam is transmitted through a specimen to form an image, offering significantly higher resolution than light microscopes, capable of capturing details as small as a single column of atoms.
TEM is widely applied in fields such as cancer research, virology, materials science, nanotechnology, semiconductor research, pollution, paleontology, and palynology (*Transmission Electron Microscopy | Nanoscience Instruments* 2024).
In Tau aggregation research, TEM is crucial for directly visualizing Tau fibril morphologies formed during in vitro aggregation studies. Samples from these experiments, involving recombinant Tau protein, are deposited onto TEM grids and negatively stained before imaging.
TEM can distinguish between different Tau aggregates, such as oligomers, protofibrils, and mature fibrils, based on their distinct morphologies. Mature tau fibrils typically appear as long, unbranched filaments with a characteristic cross-over repeat distance of approximately 80 nm. TEM enables the monitoring of the effects of mutations (e.g., P301L), cofactors (heparin, RNA), inhibitors, and other variables on Tau fibril formation by imaging at different time points. It provides detailed ultrastructural characterization, including filament widths, twists, and polymorphic variations, which are essential for understanding the assembly mechanisms of Tau fibrils. Techniques like electron tomography can reconstruct the 3D structures of Tau fibrils from 2D TEM projection images, while immuno-gold labeling combined with TEM can map specific Tau epitopes within the fibril structures (Ksiezak-Reding and Wall 2005; Lim et al. 2014).
In summary, TEM is an indispensable technique in Tau aggregation research, offering direct visualization and characterization of Tau oligomers and fibrils, complementing other biophysical methods to provide comprehensive structural insights into Tau aggregation mechanisms and fibril assembly pathways.

2.2. Cell-Based Models

Cell-based models provide a more physiologically relevant environment to study tau aggregation, allowing for the investigation of intracellular processes and interactions.
Techniques based on the fusion of Tau with fluorescent probes, such as "turn-on" or "turn-off" fluorescence approaches, have significant limitations, particularly in accurately describing the form in which Tau aggregates within the cell. One study showed that the presence of fluorescent probes can create steric hindrance that is incompatible with the structure of filaments observed in Alzheimer's disease, casting doubt on the reliability of these methods for analyzing Tau aggregation (Kaniyappan et al. 2020).

Bimolecular Fluorescence Complementation (BiFC) Assays

The bimolecular fluorescence complementation (BiFC) assay is a powerful cell-based technique that enables the visualization of Tau protein aggregation in live cells. In this assay, a fluorescent protein such as Venus or YFP is split into two non-fluorescent fragments (e.g., VN and VC). These fragments are genetically fused to Tau molecules, creating Tau-VN and Tau-VC fusion constructs. In their monomeric state, the VN and VC fragments remain apart, resulting in no fluorescence. However, when Tau molecules interact and aggregate, the VN and VC fragments are brought into close proximity, allowing them to complement and reconstitute the fluorescent protein. Experimentally, cells are co-transfected with Tau-VN and Tau-VC constructs. Under normal conditions with monomeric Tau, there is little to no fluorescence. Upon induction of Tau aggregation through mutations, hyperphosphorylation, or seeding, fluorescent puncta appear in the cells, indicating sites of Tau-Tau interactions and aggregates (Wang et al. 2009; Wang et al. 2007; Tak et al. 2013).
This technique offers several advantages, including the direct visualization and monitoring of Tau ag-

gregation in live cells over time, providing spatial information on the localization of Tau aggregates, and detecting a range of Tau species from dimers/oligomers to larger insoluble aggregates. It eliminates the need for exogenous dyes or staining procedures. BiFC assays are useful for studying the effects of Tau mutations, modifications, and cofactors on aggregation propensity, screening potential inhibitors of Tau aggregation, and investigating the dynamics and cellular trafficking of Tau aggregates. Additionally, it can be combined with other fluorescent sensors to correlate Tau aggregation with various cellular processes.

Förster Resonance Energy Transfer (FRET) Sensors

Fluorescence Resonance Energy Transfer (FRET) sensors are powerful tools used to study Tau protein aggregation and conformational changes in live cells. In these assays, Tau is genetically fused to a FRET pair of fluorescent proteins, such as CFP (donor) and YFP (acceptor). In the monomeric state, the FRET pair is positioned at a specific orientation and distance that allows energy transfer from CFP to YFP upon excitation. During Tau aggregation or conformational changes, the relative orientation and distance between the FRET pair change, thereby altering the FRET efficiency. Experimentally, cells are transfected with the FRET Tau fusion construct. FRET efficiency is measured by exciting CFP and monitoring the emission ratios of YFP/CFP, which indicate changes in FRET. This can be achieved using techniques such as fluorescence lifetime imaging (FLIM) or ratiometric imaging. These sensors are used to monitor intracellular Tau aggregation by detecting FRET changes corresponding to oligomer and fibril formation. They also allow the study of the effects of mutations, post-translational modifications, and inhibitors on Tau conformational dynamics and aggregation propensity. Additionally, FRET sensors can investigate the seeding and propagation of different Tau strains by adding preformed seeds and tracking subsequent FRET changes (Lim et al. 2014; Tak et al. 2013; Lo 2021b).
The advantages of FRET sensors include the ability to study Tau aggregation in live cells in real-time, providing detailed information on conformational changes during different stages of aggregation. They can also be combined with other fluorescent biosensors to correlate Tau aggregation with various cellular processes. However, there are limitations, such as the potential impact of fusing large fluorescent proteins on Tau behavior, limited sensitivity for detecting the earliest oligomeric species, and issues with photobleaching and phototoxicity from prolonged excitation.

2.3. In Vivo Models

In vivo models are crucial for studying the pathological consequences of tau aggregation and the mechanisms of disease progression in a whole-organism context.

Transgenic Animal Models

To study the in vivo propagation of Tau protein, researchers have developed various animal models and experimental methods. Transgenic mouse models are widely used, including P301S mice, which express the human mutated tau protein (4R0N) and develop neurofibrillary lesions, and ALZ17 mice, which express the longest non-mutated human tau isoform (4R2N) but do not form aggregates (Pádua et al. 2024; Wenger et al. 2023). Invertebrate models like Drosophila, with transgenic flies expressing human Tau, allow for rapid examination of Tau toxicity and aggregation mechanisms, while *C. elegans*, a nematode, can be genetically modified to express different Tau forms to study their effects on neurons. Non-mammalian vertebrate models such as zebrafish, with their rapid development and transparency, are advantageous for in vivo imaging of Tau pathology. Among other mammalian models, transgenic rats offer benefits over mice due to their larger brain size, which facilitates certain studies, and their well-characterized behavior. Additionally, non-human primates, though less commonly used due to ethical and practical reasons, provide insights into Tau pathology in a brain

structure closer to that of humans (Langui, Lachapelle, and Duyckaerts 2007; Dujardin, Colin, and Buée 2015). Models using neuropsin promoters enable the expression of mutated Tau specifically in the entorhinal cortex to study its propagation to the hippocampus. Experimental methods include intracerebral injections of Tau aggregates to observe their spread, grafting Tau-expressing neurons into mouse brains to track propagation, in vivo imaging techniques like positron emission tomography (PET) to monitor labeled Tau, and biochemical and histological analyses to study Tau phosphorylation and aggregation over time (Krishnaswamy et al. 2018; Tagai et al. 2021; Calvo-Rodriguez et al. 2019). While these models help elucidate tau propagation mechanisms, they have limitations, such as non-physiological Tau overexpression in some cases and challenges in distinguishing active Tau propagation from simple diffusion post-injection. Nevertheless, the combined use of these approaches enhances our understanding of Tau propagation in vivo within the context of tauopathies like Alzheimer's disease.

Part V

Objectives

As discussed, Tau protein, a vital component of neuronal homeostasis, is implicated in various neurodegenerative diseases when it malfunctions. Currently, there are two predominant theories regarding the role of post-translational modifications (PTMs) in the pathological aggregation of the Tau protein. Some scientists argue that these processes are independent (Lai, Harrington, and Wischik 2016; Wischik et al. 1988), while others propose a connection and emphasize the necessity of studying PTMs to understand the mechanism of paired helical filament (PHF) formation, which remains unclear (Brion et al. 1985; Grundke-Iqbal et al. 1986). We have chosen to investigate this second hypothesis. Consequently, the objectives of this thesis are based on exploring the link between the deregulation of the PTM process of the Tau protein and its aggregation.
Several studies have been conducted to understand the structure of Tau aggregates, the dynamics of aggregation, Tau misfolding, and its pathological toxicity in the body. However, the precise mechanism of Tau aggregation remains unknown. Additionally, the role of PTMs in the aggregation process has yet to be fully elucidated. Although many structures of Tau amyloid fibers obtained through cryo-electron microscopy (cryo-EM) are highly informative, they do not provide clear insights into the mechanism or the role of PTMs in the fibrillation process. Among the PTMs, phosphorylation is the most extensively studied, but regulation through O-GlcNAcylation offers alternative therapeutic avenues. An O-GlcNAcase (OGA) inhibitor, ASN120290 (also known as ASN-561, developed by Asceneuron), is currently in Phase 1 clinical trials as a potential treatment for progressive supranuclear palsy (PSP) and other Tau-related dementias. By increasing the glycosylation of Tau protein, OGA inhibitors appear to stabilize Tau in a non-pathogenic soluble form, and improve tau pathology and neurodegeneration in rodent models of tauopathies.
However, data previously collected on Tau O-GlcNAcylation in the team indicate that there are three major O-GlcNAc sites in Tau, all located in the C-terminal domain: S400, S412, and S413. Other minor sites, representing less than 5% of occupancy, were also found within the PRD (S185, S191, S208, S238) (Smet-Nocca et al. 2011; Bourré et al. 2018). Enrichment of O-GlcNAc proteoforms allowed the study of the O-GlcNAc impact on Tau phosphorylation by diverse kinases or the kinase activity of a whole rat brain extract (**CantrellePhosphorylationOGlcNAcylationPHF12021**; Bourré et al. 2018), and its effect on Tau aggregation induced by heparin or the aggregation of phosphorylated proteoforms of Tau induced by unmodified Tau seeds. A reciprocal regulation has been demonstrated between O-GlcNAcylation and phosphorylation restricted to the single pathological epitope PHF-1 (pS396/pS400/pS404). In particular, O-GlcNAcylation of residue S400 decreases phosphorylation of S404 by the kinase CDK2 and blocks sequential phosphorylation of the epitope by the kinase GSK3β. In addition, phosphorylation at S404 induces a local conformational change that is enhanced either by multiple phosphorylations of the PHF-1 epitope or O-GlcNAcylation at S400. Furthermore, O-GlcNAcylation reduces the rate of Tau aggregation, whether phosphorylated or not, but has a limited impact on the fibril formation. In contrast, GSK3β phosphorylation were shown to stimulate the aggregation of monomeric Tau induced by non-phosphorylated tau seeds. The study of the interplay between phosphorylation and O-GlcNAcylation of Tau does not indicate a significant direct regulation, except for the PHF-1 epitope, suggesting rather an indirect effect via the O-GlcNAc regulation of enzymes involved in the dynamics of phosphorylation. Hence, our study focuses on the regulation of Tau phosphorylation and its role in the function and fibrillar assembly of Tau protein. More especially, we have focused on:

1. The regulation of GSK3β kinase activity by O-GlcNAcylation as an alternative mechanism to regulate tau hyperphosphorylation (El Hajjar et al. 2024)

2. The role of phosphorylation of the PHF-1 epitope in the regulation of Tau (dys)functions. In this context, we have used two strategies:
   a. To study the seeding activity of C-terminal tau fragments in the aggregation of tau and the role of PHF-1 phosphorylation in this process (El Hajjar et al, submitted)
   b. To discriminate between different phosphorylation states of the PHF-1 epitope on Tau func-

tion in microtubule assembly and aggregation using the native chemical ligation approach to provide homogenously phosphorylated Tau.

The advantages of our approach are multiple. First, the quantitative characterization of PTM profiles at a per-residue resolution using Nuclear Magnetic Resonance (NMR) spectroscopy allows us to identify the modification sites of Tau, determine the relative levels of modification at each individual site, and highlight interactions between different PTMs (**CantrellePhosphorylationOGlcNAcylationPHF12021**; Bourré et al. 2018; Theillet et al. 2012; Lippens et al. 2016). Modified Tau samples characterized by NMR - which is a non-destructive analytical method- can then be used to evaluate the aggregation capacity with or without heparin in vitro, and the function in tubulin polymerization. NMR also allows us to identify conformational changes induced by PTMs. Then, our approach is based on the manipulation of enzymatic activities in solution or semi-synthetic proteins. It provides molecular details to study the effect of site-specific phosphorylation on Tau (dys)function, or the direct crosstalk between phosphorylation and O-GlcNAcylation on the regulation of GSK3β kinase activity and its impact on Tau phosphorylation, which are more intricate to capture in a complex cellular environment. Our experimental setup is adapted to address this concern not only through a reduction of the number of interacting partners to a strict minimum (recombinant kinases and/or OGT), but it also provides a snapshot of these dynamic regulatory systems by preventing PTM removal by antagonist enzymes.

Project Objectives

This project is directed along two main axes:

Axis 1: Studying the Role of Phosphorylation in Tau Aggregation

The primary challenge in studying the mechanisms of Tau aggregation is to avoid using the use of external inducers of aggregation, such as polyanions like heparin. The aggregation of full-length phosphorylated Tau proteins without heparin remains difficult to achieve and is not reproducible. Heparin is very effective in triggering rapid and massive aggregation of recombinant Tau proteins, both full-length and truncated forms. However, the presence of multiple negative charges interferes with the binding of (highly) phosphorylated forms, preventing the use of heparin in aggregation reactions involving phosphorylated Tau. Moreover, heparin does not play a physiological role in Tau aggregation within neurons, even though synthetic fibers obtained have a morphology similar to Alzheimer's disease PHFs under electron microscopy. However, heparin-induced synthetic fibers have a very different ultrastructure from PHFs in cryo-EM. For these reasons, our objective is to determine the factors influencing the aggregation of phosphorylated Tau.
In this first project, aggregation reactions of Tau fragments are initially carried out with heparin. These fragments are then used as *seeds*, which correspond to fibrillar and/or oligomeric forms, to initiate aggregation of full-length Tau. The fragments are phosphorylated with GSK3β kinase and their aggregation is induced with heparin, then they are used as *seeds* to induce aggregation of the full-length 2N4R Tau isoform, both phosphorylated Tau through a semi-synthetic approach involving expressed protein ligation (EPL) , and non-phosphorylated Tau, carrying the aggregation-prone P301L mutation or not.

Axis 2: Studying the Role of O-GlcNAc-mediated regulation of GSK3β, a kinase involved in Tau pathology

Within the laboratory, it has been shown that the phosphorylation profile of Tau is minimally affected by O-GlcNAcylation, suggesting an indirect regulation between phosphorylation and O-GlcNAcylation. The objective of this project is to evaluate the effect of O-GlcNAcylation on the phosphorylation and

physiological function of Tau through the O-GlcNAc-mediated regulation of kinases. We have thus addressed the question of GSK3β kinase regulation because it is one of the major kinases involved in the pathological phosphorylation of Tau associated to AD and it is modified by O-GlcNAcylation. We have investigated whether O-GlcNAcylation regulates the activity of GSK3β, which could ultimately lead to changes in the phosphorylation profile and consequently, in Taus ability to polymerize microtubules or form fibrillar aggregates. It has been proposed that in vivo, O-GlcNAcylation of the N-terminal domain of GSK3β modulates phosphorylation of Ser9 residue by Akt/PKB, which plays an inhibitory role in the kinase activity. The objective of this second project is to characterize the O-GlcNAcylation profile of GSK3β and modulation of its kinase activity by this PTM.

Part VI

Results and discussion

Chapter 8: GSK3β kinase activity regulation

1. Different GSK3β constructs

Based on a recent study conducted by Li et al. 2023b in 2023, a new vector design was presented to enable the co-expression of Tau and OGT. In this model, the Tau gene sequence is fused with an OGT-binding peptide (OBP) to enhance Tau O-GlcNAcylation by OGT. This peptide is separated from the Tau sequence by a linker composed of five amino acids repeated twice: $(GGGGS)_2$. The fusion of this peptide, whether at the N-terminal or C-terminal of Tau, increases OBP-tagged protein O-GlcNAcylation level in E. coli and, more especially, had a significant impact on the levels and homogeneity of Tau O-GlcNAcylation had little significant impact on the results obtained (Figure 8.1) (Li et al. 2023b).

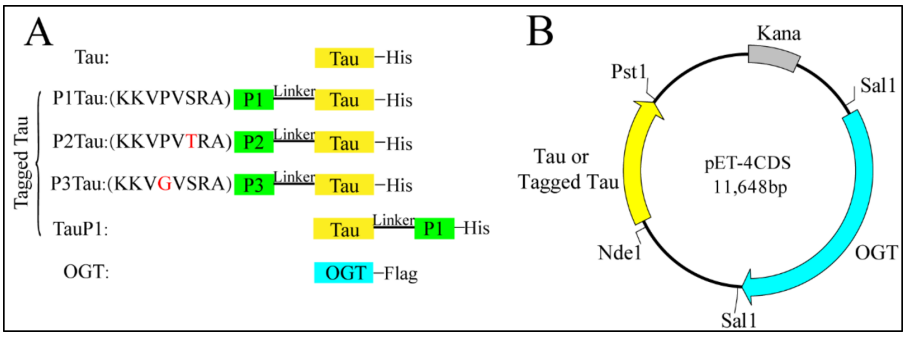

Figure 8.1: Linear representation of target gene and tag fusion genes and overview of the OGT binding peptides (OBP)-tagged strategy (Li et al. 2023b)

Based on these findings, we adopted this approach and adapted it to our project by modifying the expression vectors for GSK3β-His_6 and the GSK3β-OGT co-expression system. The objective was to promote the interaction between GSK3β and OGT, either during the incubation of the two enzymes or within the cell for co-expression. For the existing vectors, the polyhistidine tags are located at the C-terminal for the GSK3β-His_6 vector and at the N-terminal for the GSK3β-OGT co-expression vector.
Our approach involved integrating the OBP peptide sequence at the N-terminus or C-terminus of GSK3β-His6. Unlike the study by (Yang et al. 2023), we added a TEV protease recognition sequence (GGGGS-TEV) to our linker to enable tag removal if required. We generated synthetic genes with these constructs. In this chapter, different peptides will be used and are described in table 8.1.

2. Protein purification

Purification of OBP-tagged GSK3β

With the OBP tag at either the C-terminus (marked Go) or N-terminus (marked oG) of GSK3β, we produced OBP-GSK3β fusion proteins. These fusion proteins were expressed as C-terminal

Peptide Name	Sequence	Molecular Weight (Da)
Tau-pS404	Ac-IVYKSPVVSGDTpSPRHLSNV-NH2	2276.43
pSer9-GSK3β	Ac-SGRPRTTpSFAES-NH2	1416.37
LRP6a-2P	Ac-NPPPpSPApTERSH-NH2	1490.37
GSK3β N-ter [218]	Ac-SGRPRTTSFAESCKPVQ-NH2	1892.1
GSK3β C-ter [385420]	Ac-QAAASTPTNATAASDANTGDRGQTNNAASASASNST-NH2	3395.35

Table 8.1: List of peptides with their sequences and molecular weights used for chapter 11

polyhistidine-tagged proteins in *E. coli*, together with non-OBP tagged GSK3β, and refined using the identical procedure (Figure 8.2). We verified that the OBP tag had no discernible impact on GSK3β kinase activity in kinase tests (Figure 8.2 D).

3. Kinase activity of GSK3β constructs

The kinase activity of the different constructs of GSK3β was studied by phosphorylation assays of full-length ^{15}NTau or primed peptide Tau-pS404 by GSK3β analyzed using MALDI-TOF MS. Recombinant Tau protein was incubated with active GSK3β decorated by different PTMs (phosphorylation at S9, O-GlcNAcylation or both PTMs introduced sequentially with O-GlcNAc first, then phosphorylation or the other way around) and ATP, followed by MALDI-TOF MS analysis to detect phosphorylated proteins. The mass spectra revealed a shift corresponding to phosphorylated Tau, indicating successful phosphorylation by GSK3β. Control samples lacking ATP showed significantly no phosphorylated Tau proteins, confirming the specificity of GSK3β-mediated phosphorylation (Figure 8.3).
It is important to distinguish between the phosphorylation of the primed peptide Tau-pS404, which allows for quantification of the relative proportions of product (3P form) and substrate (1P form), and the phosphorylation of full-length Tau, where a global phosphorylation level is measured specifically at the PHF-1 epitope. Notably, the quantification of kinase activity on peptides is relative rather than absolute, due to differences in ionization efficiencies between the 1P and 3P forms of the peptides.

4. Phosphorylation and kinase activity of GSK3β

Using recombinant GSK3β and active Akt-1 proteins, we have characterised the effect of Akt-mediated phosphorylation of GSK3β on its kinase activity towards a primed Tau peptide substrate (Tau-pS404) prior to studying the O-GlcNAcylation of GSK3β and its possible regulatory role and interplay with phosphorylation.

4.1. Phosphorylation of GSK3β by Akt-1

When GSK3β was preincubated with active Akt-1 and ATP for two hours at 30 °C, the phospho-Ser9-GSK3β antibody response significantly increased (by approximately two times) when compared to recombinant GSK3β or GSK3β incubated with Akt without ATP as a control. This indicates that Akt effectively phosphorylated GSK3β Ser9 (Figure 8.4 B).

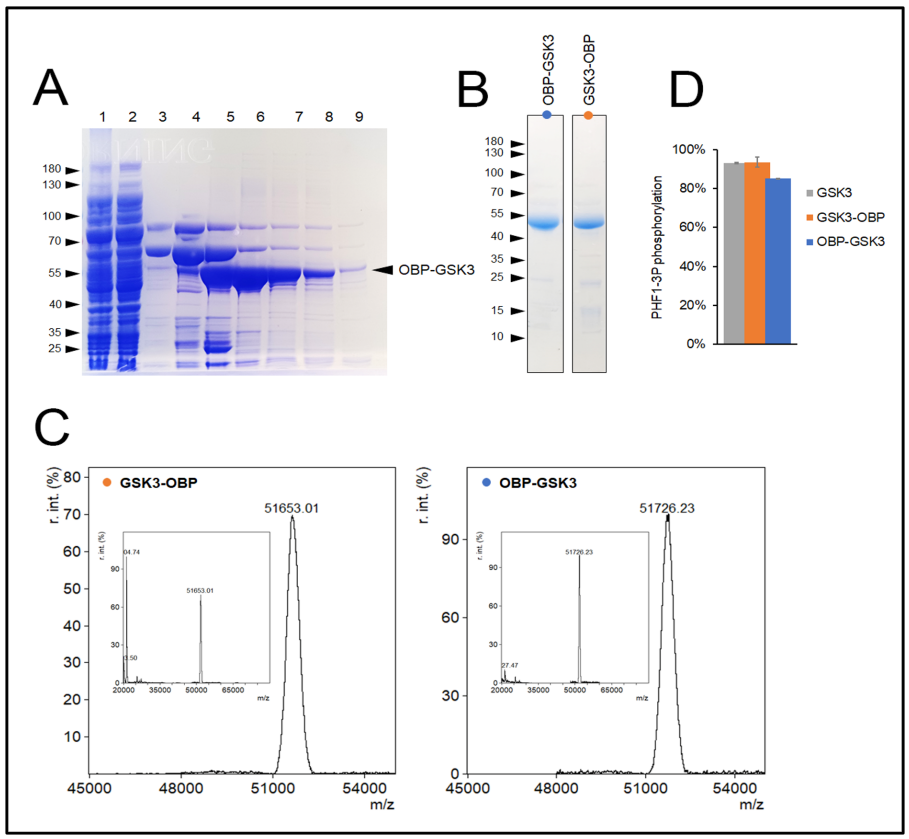

(A) SDS-PAGE analysis of the purification of OBP-GSK3β from the soluble extract of *E. coli BL21*(DE3), displaying the elution fractions (lanes 3 to 9) from the linear gradient of increasing imidazole concentration and the column flow through (lane 2) (B) SDS-PAGE control of the combined homogeneous fractions following dialysis (lanes 5 to 9 in panel A) Panel B displays the results of the MALDI-TOF mass spectrometry analysis of the OBP GSK3β fusion proteins MALDI-TOF mass spectrometry analyses of OBP GSK3β fusion proteins shown in panel B. (D) Kinase activity of N-(blue) and C-terminal (orange) OBP GSK3β fusion proteins compared to GSK3β (grey)

Figure 8.2: Ni-NTA purification of OBP GSK3β fusion proteins with a C-terminal polyhistidine tag

4.2. Effect of Akt on GSK3β Kinase Activity

Based on these observations of Akt-mediated phosphorylation of GSK3β, we next investigated how this phosphorylation event influences the kinase activity of GSK3β. We observed only a slight inhibition of GSK3β activity on the primed Tau-pS404 peptide following Akt phosphorylation (Akt/+) compared to nonphosphorylated GSK3β (absence of Akt). However, our control experiment with GSK3β and Akt without ATP (Akt/-) revealed a more pronounced, phosphorylation-independent inhibition of GSK3β kinase activity probably through the binding of phosphorylated Akt to the GSK3b catalytic domain (Figures **??** A, B). Although it is possible that GSK3β could be phosphorylated by Akt during the GSK3β kinase assay, which requires ATP to phosphorylate the Tau-pS404 peptide, this is unlikely due to the dilution of both kinases by a factor of ten in the assay compared to the conditions used for initial GSK3β phosphorylation.
Interestingly, in a similar kinase assay using unprimed full-length Tau protein as the substrate, Akt-mediated Ser9 phosphorylation of GSK3β did not reverse the inhibitory effect of Akt binding (Figure refakt-gsk32 B). These findings reveal an unexpected inhibitory effect of Akt on GSK3β kinase activity that is mitigated only by Akt-mediated Ser9 phosphorylation on the primed Tau-pS404 substrate. Remarkably, Ser9 phosphorylation of GSK3β's N-terminal domain significantly reduces the inhibitory impact, most likely via competing with Akt binding. The competing process between the phosphate from primed substrates and GSK3 Ser9 itself is reinforced by the finding that Akt-mediated phos-

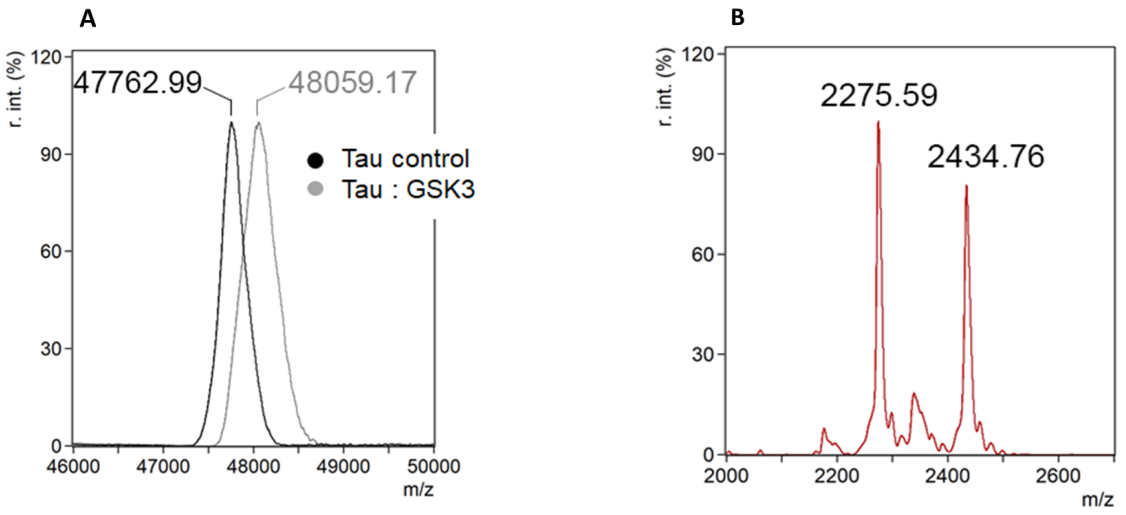

(A) MALDI-TOF MS characterization of GSK3β-mediated phosphorylation of protein in the absence (black) and the presence (grey) of ATP (B) MALDI-TOF MS characterization of OBP-GSK3β-mediated phosphorylation of Tau-pS404 peptide in the presence of ATP. m/z signals at 2275 correspond to the unreacted Tau-pS404 peptide while signals at 2435 (increment of +160) correspond to the product of the enzymatic reaction

Figure 8.3: Characterization of GSK3β-mediated phosphorylation

phorylation does not restore GSK3β kinase activity on unprimed Tau protein. Moreover, it has been suggested that the concentration of primed substrates may differ in their capacity to oppose GSK3's Ser9 phosphorylation. Though it is frequently overlooked, Ser9 phosphorylation does not always result in a clear suppression of GSK3 activity. It has been proposed that detecting Ser9 phosphorylation is a helpful indicator of the conditions under which GSK3 activity is regulated (Beurel, Grieco, and Jope 2015). GSK3 activity in some protein complexes is not susceptible to the inhibitory mechanism controlled by Ser9, as was previously described for Wnt signalling.

Our results thus imply that GSK3β's action towards a subset of certain substrates, or Tau epitopes, that are prephosphorylated by other kinases, may be regulated by Akt-mediated phosphorylation of GSK3β. It has been demonstrated before that GSK3β promotes the aggregation of Tau protein into filaments in vitro and raises the phosphorylation of primed Tau at the pathogenic AT8 and PHF-1 epitopes. The hyperphosphorylation of the PHF-1 epitope, linked to Tau pathology, and the distinct Tau epitope that doesn't require priming was impacted by Akt-mediated regulation of GSK3β kinase activity. When considered collectively, our findings point to a distinct phospho-dependent control of GSK3β function and emphasize the role that priming plays in the process of Tau hyperphosphorylation that involves GSK3β. Consequently, if Ser9 phosphorylation is inhibited, GSK3β becomes inactive, which lowers Tau hyperphosphorylation.

Conversely, Ser9 phosphorylation by Akt does not restore GSK3β kinase activity to the same degree on unprimed Tau (Figures **??** A and **??** (B)). This suggests that there is competition between active phosphorylated Akt, the primed substrate, and the N-terminal pSer9 of GSK3β itself for the phosphate binding pocket, influencing the regulation of GSK3β kinase activity.

5. O-GlcNAcylation and Kinase Activity of GSK3β

Apart from the regulation depending on phosphorylation, the possible function of O-GlcNAcylation in modifying GSK3β activities is yet mysterious. The relationship between phosphorylation and O-GlcNAcylation in cellular regulatory processes has been proposed, and while O-GlcNAcylation

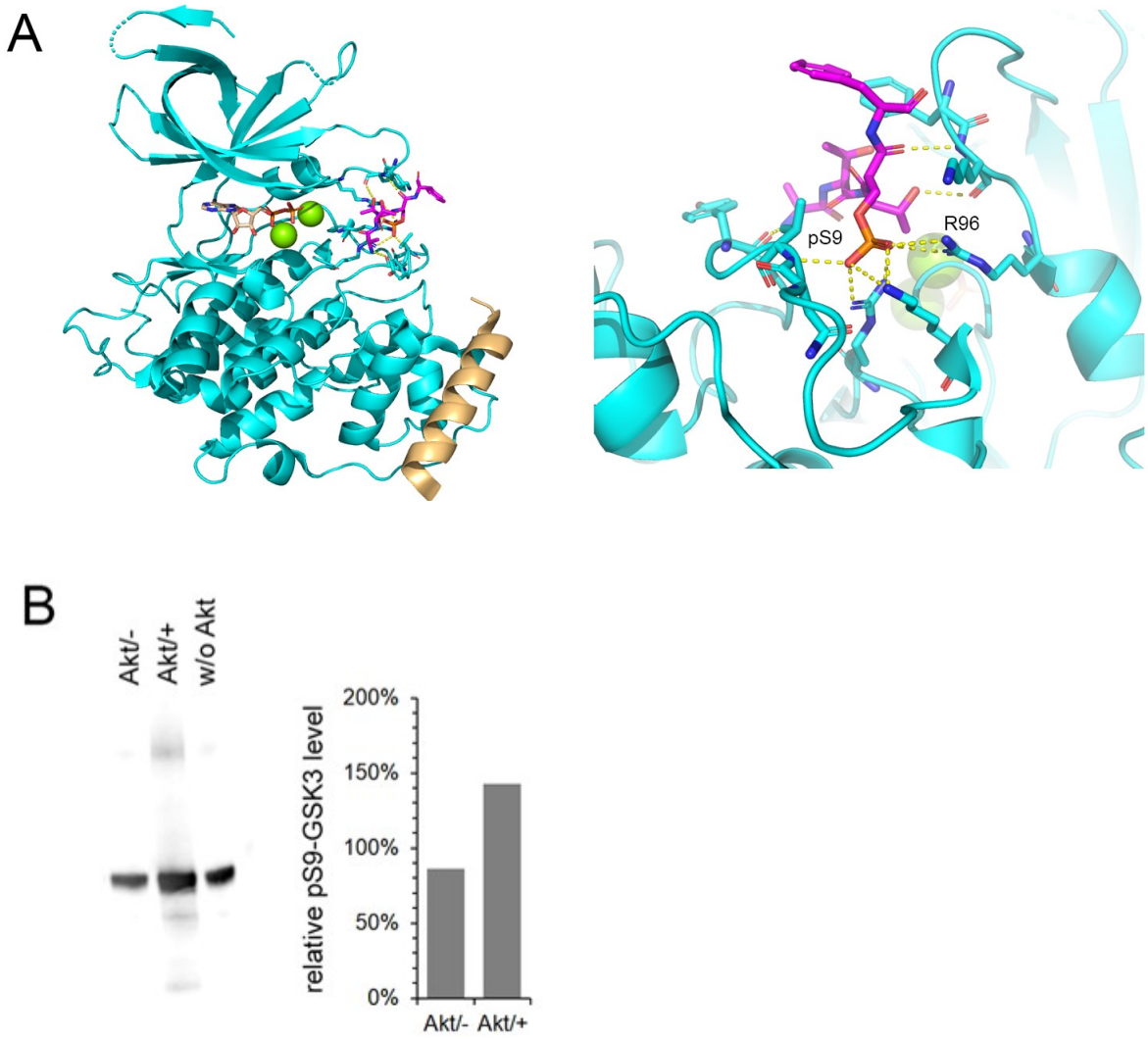

(A) Crystal structure of the GSK3β/Axin complex bound to the phosphorylated N-terminal autoinhibitory pSer9 peptide (PDB ID: 4NM3) is shown. GSK3β and Axin are depicted in cyan and beige ribbons, respectively, with the pSer9-GSK3 peptide in purple. ATP and the pSer9 peptide are shown as sticks. The close-up view highlights the polar interactions (dotted yellow lines) between pSer9 and arginine/lysine residues, including Arg96 of the priming site binding pocket (B) Western blot analysis of GSK3β phosphorylation by Akt-1 in the absence (Akt/-) or presence (Akt/+) of ATP, with a control lacking Akt-1 (w/o Akt). Densitometric quantification shows relative pSer9-GSK3β phosphorylation compared to the control (w/o Akt)

Figure 8.4: Akt binding and autoinhibitory Ser9 phosphorylation control the activity of GSK3β

of GSK3β has been identified, its precise role within GSK3β activities remains unclear, and only a handful of O-GlcNAc sites has been identified so far. Changes in the AD brain have been linked to variations in O-GlcNAc levels, yet these findings are still up for debate. While dysregulation of protein levels involved in O-GlcNAc dynamics may result in an overall increase in O-GlcNAc levels in the AD brain, a decrease in glucose uptake/metabolism, a substantial metabolic shift in the ageing brain, may equally diminish protein O-GlcNAcylation in AD.
Previous research has shown that using the Thiamet-G OGA inhibitor to raise O-GlcNAc levels can interfere with Tau pathology associated with Alzheimer's disease (AD) and other neurodegenerative illnesses. This is accomplished by alleviating cognitive deficits in AD mice models, lowering neurodegeneration, and reducing the buildup of neurofibrillary tangles. O-GlcNAcylation of Tau protein prevents the development of filaments generated by heparin in vitro. It is yet unknown, neverthe-

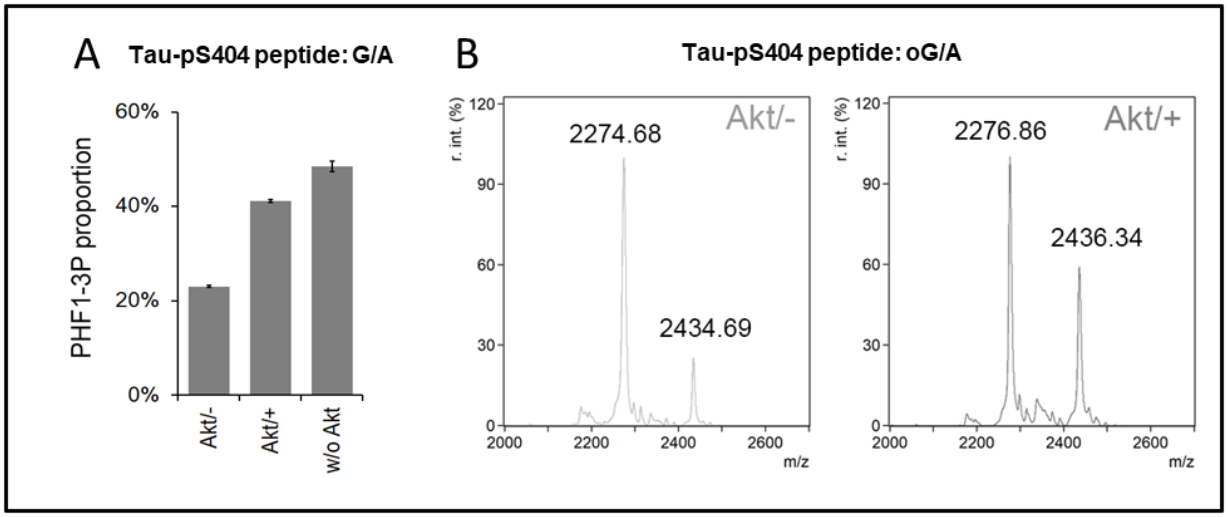

(A) Kinase activity of GSK3β from the Akt-mediated phosphorylation reaction, with and without ATP, or without Akt as a control, on a primed Tau-pS404 peptide. The percentage of triple PHF-1 phosphorylation (PHF1-3P) is presented as the mean ś SD of three replicates. (B) Phosphorylation of a primed Tau-pS404 peptide by OBP-GSK3β in the presence of active, phosphorylated Akt-1 (B) with (Akt/+) or without (Akt/-) ATP

Figure 8.5: Effect of Akt mediated phosphorylation on GSK3β activity

less, how Tau O-GlcNAcylation and phosphorylation at particular locations are related. According to past research, O-GlcNAcylation of Tau protein only affects the phosphorylation of the PHF-1 epitope and has no effect on the pathological formation of amyloid-like fibrils by phosphorylated Tau. This provides credence to the theory that O-GlcNAc regulation of other variables implicated in Tau disease, such as kinases that produce Tau hyperphosphorylation, is the source of O-GlcNAc-mediated regulation of Tau pathology in neurodegeneration, such as with OGA inhibitors.

5.1. O-GlcNAcylation Characterization of different GSK3β constructs

We initially attempted to O-GlcNAcylate GSK3β using recombinant OGT. Subsequently, we adopted a strategy to enhance O-GlcNAc modification by fusing an OGT-binding peptide (OBP) to either the N- or C-terminus of GSK3β. This approach allowed us to investigate the impact of the OBP tag on O-GlcNAc transferase activity both in solution with purified OGT and through coexpression in *E. coli*.

GSK3β and OBP-tagged GSK3β O-GlcNAcylation

We used different techniques to increase the overall O-GlcNAcylation level and uniformity in order to better understand the O-GlcNAc glycosylation pattern of GSK3β and its functional impact on kinase activity and Akt regulation. We investigated the effects of fusing an OGT-binding peptide (OBP; KKVPVSRA sequence) to GSK3β and the activity of recombinant OGT on GSK3β. It has previously been demonstrated that using this strategy will increase the homogeneity of O-GlcNAc modifications for additional functional analysis by encouraging the O-GlcNAcylation of Tau and other target proteins coexpressed with OGT in *E. coli* (**LiOGTBindingPeptideTagged2023**).
Recombinant OGT was incubated with untagged or OBP-tagged GSK3β for 6 hours at 31 řC, either with (OGT/+) or without UDP-GlcNAc (OGT/-) as a negative control. Extended incubation periods dramatically reduce kinase activity but do not appreciably raise O-GlcNAc levels (data not shown). The crude O-GlcNAcylation processes were then exposed to chemo-enzymatic labeling reactions in order to selectively detect O-GlcNAc modified proteins (TAMRA labeling) and better characterize

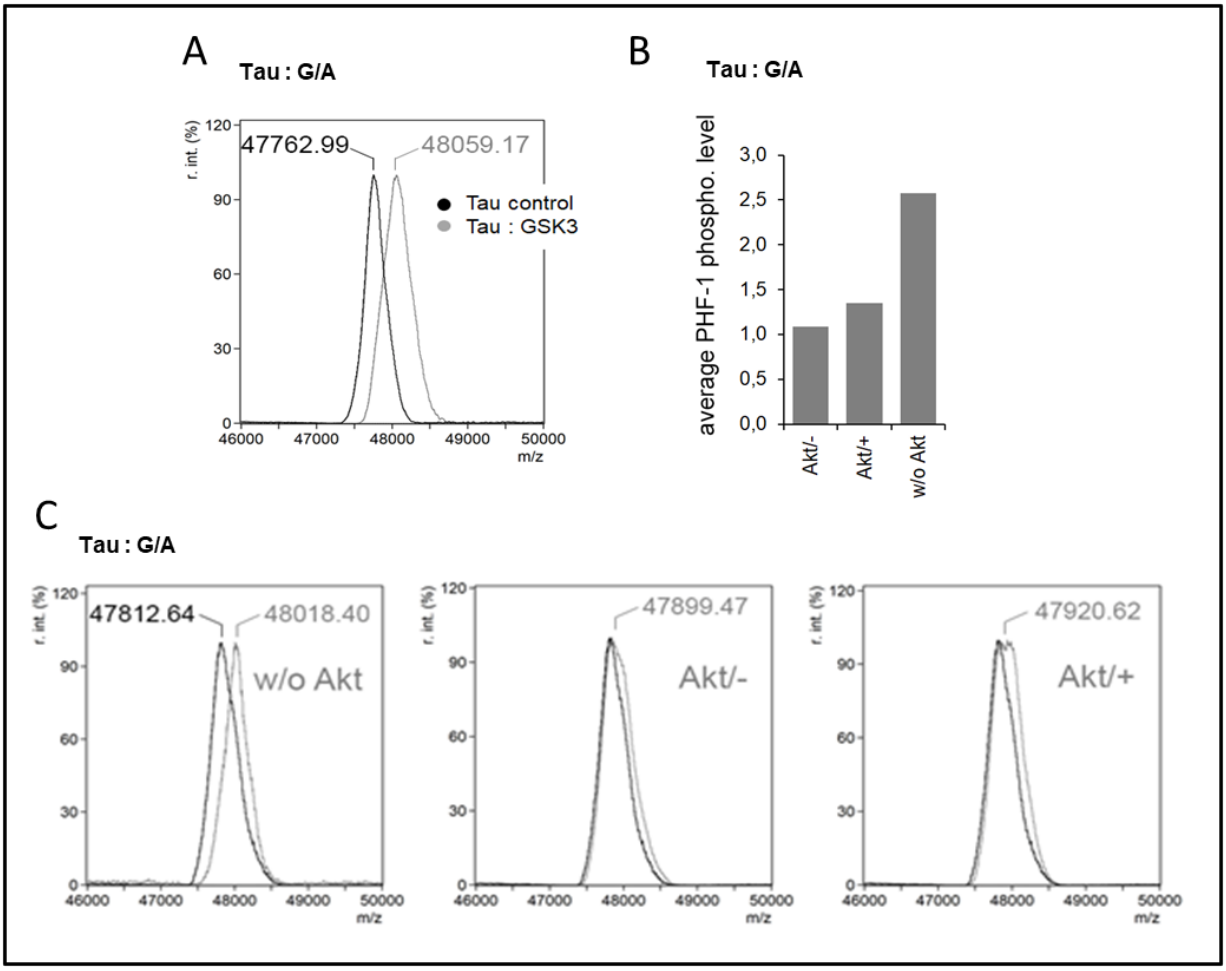

(A) Phosphorylation of full-length ^{15}NTau 2N4R isoform by unmodified GSK3β (grey). Non-phosphorylated Tau (black) is shown as a reference for determination of the m/zdifference of 296.18corresponding to 3.7 phosphate per Tau molecule (considering a mass increment of +80 Da per phosphorylation)(B) Kinase activity of GSK3β from the Akt-mediated phosphorylation reaction with and without ATP or without Akt as a control on unprimed, full-length Tau protein. The phosphorylation level is monitored by mass spectrometry (as shown in C), and the level of PHF-1 phosphorylation (number of phosphates per tau) is determined by the overall m/z difference of phosphorylated to the nonphosphorylated Tau (C) Regulation of GSK3β kinase activity on unprimed tau by Akt-1 in the absence or presence of ATP or without Akt as a control, monitored by or mass spectrometry

Figure 8.6: Phosphorylation pattern of full-length ^{15}NTau 2N4R isoform by unmodified GSK3β

the distribution of O-GlcNAc proteoforms (mass tag labeling with mPEG5K).
All OBP-tagged or untagged constructs exhibited effective O-GlcNAcylation of GSK3β, as demonstrated by the selective TAMRA labeling of O-GlcNAc transferase reactions with recombinant OGT in the presence of UDP-GlcNAc (Figure 8.7 A,B). This was further verified using RL-2 (antibody, which specifically recognizes O-GlcNAcylation) to serine or threonine residues of proteins) selective staining of O-GlcNAc transferase processes in the presence of UDP-GlcNAc (Figure 8.7 C).
Additionally, mass tag labeling showed a decrease in the non-O-GlcNAc proteoform in favor of the mono-, di-, and tri-O-GlcNAc proteoforms, with the majority of mono-O-GlcNAc species (Figure 8.7 D). Further glycosylation changes (+4 or +5 GlcNAc) resulted in faint bands whose intensities were just over the detection limit, but they were still discernible.
The addition of the OBP tag to either the N- or C-terminus of GSK3β had a limited effect on the overall level of O-GlcNAcylation compared to untagged GSK3β, and no significant difference was observed between the N- and C-terminal positions.

O-GlcNAcylation of GSK3β and OBP-tagged GSK3β coexpressed with OGT

Next, we examined the O-GlcNAcylation of GSK3β proteins with and without the OBP tag by co-expressing them with OGT in *E. coli*. With this thorough approach, we were able to evaluate the functional implications of the O-GlcNAc modification patterns on GSK3β activity and regulation. However, in the coexpression system, where the non-O-GlcNAc form barely shows up (representing less than 5% of all proteoforms), the O-GlcNAcylation level is significantly higher (Figure 8.8). According to these findings, GSK3β O-GlcNAcylation is significantly more effective in bacteria that co-express OGT than it is in solutions containing purified OGT.
Thus, by attracting regulatory proteins, it is anticipated that the OBP tag will facilitate the formation of O-GlcNAcylation complexes with OGT and target proteins.

5.2. Identification of O-GlcNAcylation Sites on GSK3β by MS analysis

To map the O-GlcNAcylation sites on GSK3β, mass spectrometry analysis was employed on both untagged and OBP-tagged GSK3β constructs. Using a bottom-up MS strategy with digestion by trypsin and chymotrypsin, we achieved over 98% sequence coverage for all constructs under each condition (Table 8.2).

Construct/O-GlcNAcylation Condition	**O-GlcNAc Sites**	**Number of Sites**
OBP-GSK3β/OGT/+	T7/T8/S9, S13, S21, T38, T43, S368, T392	8
GSK3β-OBP/OGT/+	T7, S9, S13, S21, T38, T39, T43, S55, T364, S368/S369, S389, T392, S398, T408, S415, S417	16
GSK3β/OGT/+	T7, S9, S13, S6, T43, T364, S389/T390, S389, T390, T392, S398	11
OBP-GSK3β/OGT coexpression	T7/T8, S9, S21, T43, S55, S389, T392, T395, S398, T408, S413, S419	12
GSK3β-OBP/OGT coexpression	T43, T408, S415	3
GSK3β/OGT coexpression	T7/T8, S9, S389, T390, T392, S398	6

Table 8.2: O-GlcNAcylation Conditions and Sites for GSK3β Constructs

Mass spectrometry analysis identified between 3 and 27 O-GlcNAc modification sites through higher-energy collisional dissociation (HCD)-based LC MS/MS across different O-GlcNAcylated peptides. These sites predominantly reside within the disordered N- and C-terminal domains of GSK3β (Figure 8.9).
The identification of O-GlcNAc (N-acetylglucosamine) modifications using Higher-energy Collision-induced Dissociation (HCD) is challenged by the complexity of peptides containing multiple serine (Ser) or threonine (Thr) residues, making it difficult to pinpoint specific modification sites. The main issue with HCD fragmentation lies in the lability of the glycosidic bond between GlcNAc and Ser/Thr residues (Nagel et al. 2013; Ma and Hart 2017). During HCD fragmentation, GlcNAc often detaches before the peptide backbone is fragmented, leading to a critical loss of information about the modification site. This complicates the identification of O-GlcNAcylated peptides, as database search algorithms may fail to detect modifications when GlcNAc is lost prior to peptide fragmentation. Additionally, when multiple Ser/Thr residues are present within a peptide, HCD fragmentation

can produce fragment ions that do not clearly indicate which residue is modified (Burt et al. 2022; Xu et al. 2021). This problem is exacerbated in longer peptides or those with similar sequences, where distinguishing between modification sites becomes challenging. In contrast, other fragmentation methods, such as Electron Transfer Dissociation (ETD), preserve the O-GlcNAc bond, allowing for direct detection of modified peptides and more confident assignment of modification sites. Therefore, ETD is often preferred for analyses requiring precise localization of O-GlcNAc modifications (Nagel et al. 2013; Ma and Hart 2017).

Based on analyses of 7002 human O-GlcNAc site surrounding sequences, the majority of identified O-GlcNAc sites fulfil the semi consensus sequences described for Ser/Thr-O-GlcNAcglycosylated residues, indicating a highprevalence of Ser, Thr, Pro, Ala, Val, and Gln residues from the -5 to +5 positions relative to the glycosylation site (Wulff-Fuentes et al. 2021).

Further validation of O-GlcNAcylation in these regions was performed using peptides encompassing the entire N- and C-terminal domains of GSK3β. These peptides were subjected to O-GlcNAcylation with recombinant OGT, followed by reverse-phase HPLC isolation of O-GlcNAc-enriched fractions, and subsequent electron transfer dissociation (ETD)-based MS/MS to identify O-GlcNAc sites.

The presence and diversity of O-GlcNAc sites varied depending on the position of the OBP tag and the conditions used for O-GlcNAcylation, whether in solution or by co-expression of GSK3β and OGT. Within the conserved N-terminal regulatory domain, O-GlcNAc sites were identified among the three consecutive residues Thr7, Thr8, and Ser9 in both untagged and OBP-tagged GSK3β constructs, from GSK3β either incubated with OGT in vitro or co-expressed with OGT in *E. coli* (Figure 8.10). ETD MS/MS analysis of isolated GSK3β N-terminal peptides confirmed the O-GlcNAcylation at Thr8 and Ser9, including the di-O-GlcNAcylated form at Thr8/Ser9.

O-GlcNAc modifications were also detected on Ser13 and Ser21 in the N-terminal disordered domain, and on at least five distinct sitesSer389 and/or Thr390, Thr392, Thr395, Ser398, Thr408in the C-terminal domain. The number and exact location of these O-GlcNAc sites varied depending on the OBP tag positioning and O-GlcNAcylation conditions. Notably, Thr392 was consistently O-GlcNAcylated across all constructs (Figure 8.11).

In addition to the disordered regions, at least six O-GlcNAc sites were identified within the kinase domain of GSK3β. Thr43 was consistently found to be O-GlcNAcylated under all conditions. Other notable sites within the kinase domain included Thr38/Thr39, Ser55, Thr363/Thr364, and Ser368/Ser369. These sites are located either within the β2 and β3 strands of the N-terminal β-barrel (residues 35-134) or in a flexible loop of the C-terminal domain (Figure 8.9 B), contributing to the solvent-accessible surface area opposite the phosphate and Axin binding pockets.

Resuming, we found multiple O-GlcNAc sites in the C-terminal disordered domain and within the kinase domain in a solvent-accessible area across from the active site and phosphate binding pocket. We also identified O-GlcNAc sites within the disordered, regulatory N-terminal domain on Thr7, Thr8, Ser9, Ser13, and Ser21 residues. GSK3β has just a small number of O-GlcNAc sites that have been previously discovered, all of which were found in the kinase domain. Thr38, Thr39, and Thr43which we have also identifiedare among the known O-GlcNAc sites (https://www.oglcnac.mcw.edu/). These sites were previously discovered from human embryonic stem cells using multiple reaction monitoring mass spectrometry (Maury et al. 2014).

The results suggest a high degree of heterogeneity in O-GlcNAc modifications within the disordered regions of GSK3β, while the kinase domain exhibits a lesser extent of modification. The presence of the OBP tag influenced the diversity of O-GlcNAc sites, particularly when positioned at the N-terminus, and to a greater extent at the C-terminus in solution conditions. However, the C-terminal OBP tag reduced the diversity of O-GlcNAc modifications in the co-expression system, unlike the N-terminal OBP tag. The co-expression of GSK3β with OGT improved overall O-GlcNAcylation levels, indicating an increased homogeneity of O-GlcNAc modifications in C-terminal OBP-tagged GSK3β constructs. Thus, the OBP tag modulates O-GlcNAcylation levels and impacts site diversity based on its position relative to the GSK3β protein and the conditions used for O-GlcNAcylation.

5.3. O-GlcNAcylation Marginally Improves GSK3β Kinase Activity

We next investigated the kinase activity of GSK3β after O-GlcNAcylation reactions with OGT and UDP-GlcNAc (OGT/+) or control reactions without UDP-GlcNAc (OGT/-) for untagged and each OBP-tagged construct. Our findings showed a slight improvement in GSK3β kinase activity upon O-GlcNAcylation, as measured by the phosphorylation level of a primed Tau-pS404 substrate. The proportion of PHF1-3P was marginally higher in OGT/+ reactions compared to OGT/- reactions (Figure 8.12). For the unprimed Tau protein, a characteristic phosphorylation-dependent electrophoretic mobility shift on SDS-PAGE was observed under both OGT/+ and OGT/- conditions (Figure 8.12 B), while a complete triple phosphorylation of the PHF-1 epitope was achieved, as monitored by MALDI-TOF MS and NMR spectroscopy (Figure 8.12 C and D).
These results demonstrate that both O-GlcNAc-modified and nonmodified GSK3β exhibit similar kinase activity on primed and unprimed Tau substrates.
We further analyzed the effect of O-GlcNAcylation on the inhibition of GSK3β kinase activity using the autoinhibitory pSer9-GSK3 peptide and the diphosphorylated LRP6a-2P (fragment of the Wnt co-receptor LRP6a that contains two phosphate groups on specific amino acid residues. This modification mimics the activated state of LRP6a, which is crucial for propagating signals in the Wnt signaling pathway) (Table 8.1). Consistent with previous findings, the pSer9-GSK3 peptide showed significantly lower inhibition capacity (IC_{50} in the 500 μM1 mM range) compared to LRP6a-2P on the phosphorylation of the primed Tau-pS404 substrate.
The LRP6a-2P peptide was tested, as a GSK3β inhibitor, against the primed Tau-pS404 substrate at 20 μM, which was phosphorylated by OBP-tagged GSK3β from OGT/+ and OGT/- reactions. The IC_{50} values (concentration for 50% inhibition) were measured. When comparing OGT/+ to OGT/- GSK3β, the IC_{50} values were somewhat lower for both N- and C-terminal OBP-tagged proteins for OGT/+ (77 μM and 51 μM, respectively) than for OGT/- GSK3β (124 μM and 64 μM, respectively). This impact was more noticeable for the N-terminally OBP-tagged GSK3β. This implies a higher efficiency of inhibition for the glycosylated O-GlcNAc form of GSK3β (Figure 8.13).
A significant variety of O-GlcNAc proteoforms is suggested by the total O-GlcNAcylation level, the number of O-GlcNAc sites, and their position, of which only a tiny fraction may have an up- or down-regulatory activity.

6. O-GlcNAcylation and Phosphorylation interplay

O-GlcNAcylation of various residues within the N-terminal domain of GSK3β may directly compete with Ser9 phosphorylation by either occupying the same site or adjacent sites, hence controlling GSK3β kinase action.
We investigated the potential role of O-GlcNAcylation in modulating Akt-mediated phosphorylation and/or non-phosphorylation-dependent GSK3β inhibition.
The phospho-Ser9-GSK3β antibody responded similarly for GSK3β from both OGT/+ and OGT/- circumstances when GSK3β was incubated with Akt and ATP (Akt/+). Comparing it to matching nonphosphorylated GSK3β (Akt/- or without Akt), it rose by approximately 1.7 times, suggesting that the phosphorylation levels of O-GlcNAc and non-O-GlcNAc glycosylated GSK3β are similar (Figure 8.14 A).
Furthermore, OGT binding does not obstruct Akt-mediated control of GSK3β kinase activity in the absence of O-GlcNAcylation (without UDP-GlcNAc), indicating different interfaces for Akt and OGT interactions inside GSK3β. This theory is supported by the fact that phosphorylated Akt, which most likely occupies the phosphate-binding site, inhibits GSK3β kinase activity, and that OGT glycosylates Ser/Thr sites on the kinase domains opposing side (Figure 8.9 B).
When OBP-GSK3β without GlcNAcylation (oG/O-) and Akt were incubated together without OGT (oG/O), the GSK3β kinase activity on a primed Tau-pS404 substrate remained similar to conditions

without OGT. GSK3β is inhibited when Akt is present but devoid of kinase activity (Akt/-), and partially restored when Akt phosphorylates Ser9 (Akt/+). This pattern holds true even in the presence of O-GlcNAcylation (oG/O+), indicating that GSK3β O-GlcNAcylation and interactions with OGT do not obstruct Akt's phosphorylation-independent inhibition of GSK3β kinase activity. Instead, Akt-dependent phosphorylation restores the activity of O-GlcNAcylated GSK3β, suggesting O-GlcNAcylation plays a minor role in enhancing GSK3β kinase activity (Figure 8.14).
On the other hand, we demonstrated that coexpression of GSK3β (with an N-terminal OBP-tag) with OGT in bacteria significantly downregulates the Akt-mediated phosphorylation of Ser9 (Figure 8.14 B). This coexpression led to a significant increase in O-GlcNAc levels and a redistribution of the O-GlcNAc proteoforms (Figure 8.8). These findings suggest that, depending on the O-GlcNAcylation profile, O-GlcNAcylation can modify the Akt-mediated phosphorylation of Ser9 and suggest that Ser9 phosphorylation-mediated Akt-mediated control of GSK3β function may face competition from elevated O-GlcNAc levels. The coexpression of OBP-GSK3β and OGT in bacteria likely results in an increase in Ser9 O-GlcNAcylation or proximal sites within the GSK3β N-terminus, which substantially inhibits the subsequent Akt-mediated Ser9 phosphorylation.
Elevated O-GlcNAc levels, resulting from GSK3β and OGT coexpression through the downregulation of Ser9 phosphorylation, mildly alter the Akt-mediated regulation of GSK3β activity. According to our findings, Akt can still phosphorylation-independently block the kinase activity of O-GlcNAcylated GSK3β, although the residual Ser9-phosphorylated version of GSK3β most likely helps to mitigate some of Akt's inhibitory effects (Figure 8.14C).
Then, we investigated the effect of Akt phosphorylation prior O-GlcNAcylation of GSK3β. When GSK3β is phosphorylated (oG/A+) as opposed to nonphosphorylated (oG/A−) or control (oG) GSK3β, the total O-GlcNAc level of GSK3β (as measured by RL-2) is significantly reduced by 2.4 times. This is accompanied by a slight redistribution of O-GlcNAc proteoforms, which shows an increased proportion of the non-O-GlcNAc form along with a decreased proportion of the di- and tri-O-GlcNAc forms. The kinase activity of GSK3β on a primed Tau-pS404 peptide is inhibited by Akt in the absence of phosphorylation (oG/A−), regardless of subsequent O-GlcNAcylation or not, whereas the kinase activity of phosphorylated GSK3β (oG/A+) is restored. As a result, the subsequent O-GlcNAcylation has no effect on the phosphorylation-dependent and independent control of GSK3β kinase activity by Akt (Figures 8.14 F).

7. Conclusion

Our study highlights the intricate regulation of GSK3β activity through the interplay of phosphorylation and O-GlcNAcylation. O-GlcNAcylation, particularly of Ser9 or nearby residues, can modulate GSK3β activity in a cell type- or stimulus-specific manner, potentially counteracting the effects of Akt hyperactivation seen in cancer. Elevated O-GlcNAc levels, achieved through Thiamet-G treatment, for instance, affect site-specific Tau phosphorylation by modulating GSK3β activity via Akt regulation.
Our findings show that active Akt can inhibit GSK3β without direct phosphorylation, and Akt-mediated phosphorylation can restore GSK3β activity on primed Tau substrates. This suggests a dynamic conformational switch in GSK3β, where O-GlcNAcylation favors an active conformation, preventing Ser9 phosphorylation from binding and thereby regulating GSK3β function.
This study provides molecular insights into the regulation of GSK3β in a controlled environment, reducing the complexity found in cellular contexts. Our results indicate that conditions promoting N-terminal O-GlcNAcylation of GSK3β, without directly inhibiting its kinase activity, could work with active Akt to inhibit GSK3 activity by preventing pSer9-induced reactivation toward primed Tau epitopes.
These regulatory mechanisms have significant implications for Tau hyperphosphorylation, potentially

impacting the understanding and treatment of Alzheimer's disease and other Tau-related neurodegenerative disorders. A schematic conclusion is shown in Figure 8.15.

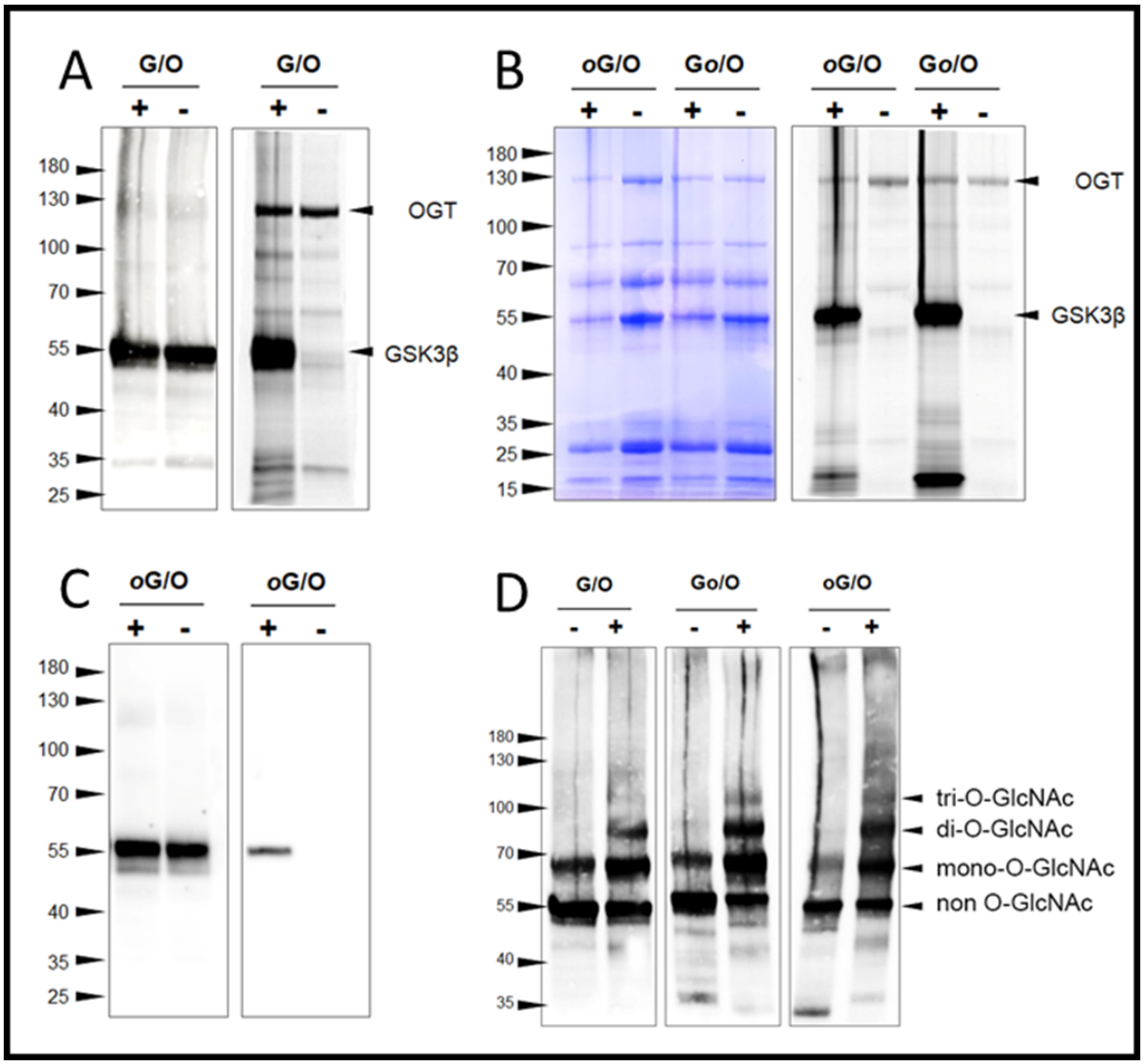

(A) TAMRA labeling of GSK3β O-GlcNAcylation reactions with OGT (G/O) (right panel) and control of protein loading by Western blotting with GSK3 antibody (left panel) (B) TAMRA labeling of OBP-GSK3β (oG/O) or GSK3β-OBP (Go/O) O-GlcNAcylation reactions (right panel) and control of protein loading by Coomassie staining (left panel) (C) Western blot of OBP-GSK3β O-GlcNAcylation reactions with OGT (oG/O) with RL-2 (right panel) and GSK3 antibodies (left panel) (D) Mass-tag labelling of GSK3β proteins in O-GlcNAc transferase reactions with UDPGlcNAc (+) or control reactions without (-) UDP-GlcNAc

Figure 8.7: In vitro GSK3β and OBP-Tagged GSK3β O-GlcNAcylation with recombinant OGT

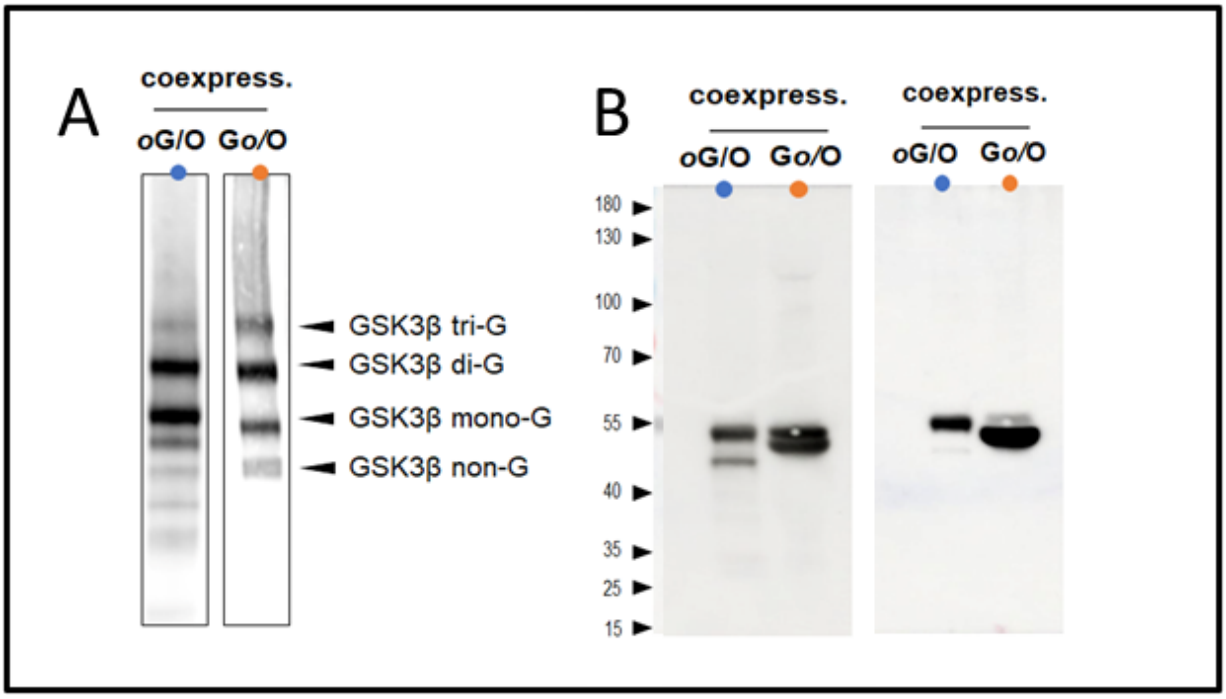

(A) Mass-tag labelling of OBP-GSK3β or GSK3β-OBP coexpressed with OGT in bacteria (B) Western blot of OBP-GSK3β or GSK3β-OBP coexpressed with OGT in bacteria with RL-2 (right panel) and GSK3 antibodies (left panel)

Figure 8.8: Characterization of O-GlcNAcylated GSK3β proteins coexpressed with OGT in *E.coli*

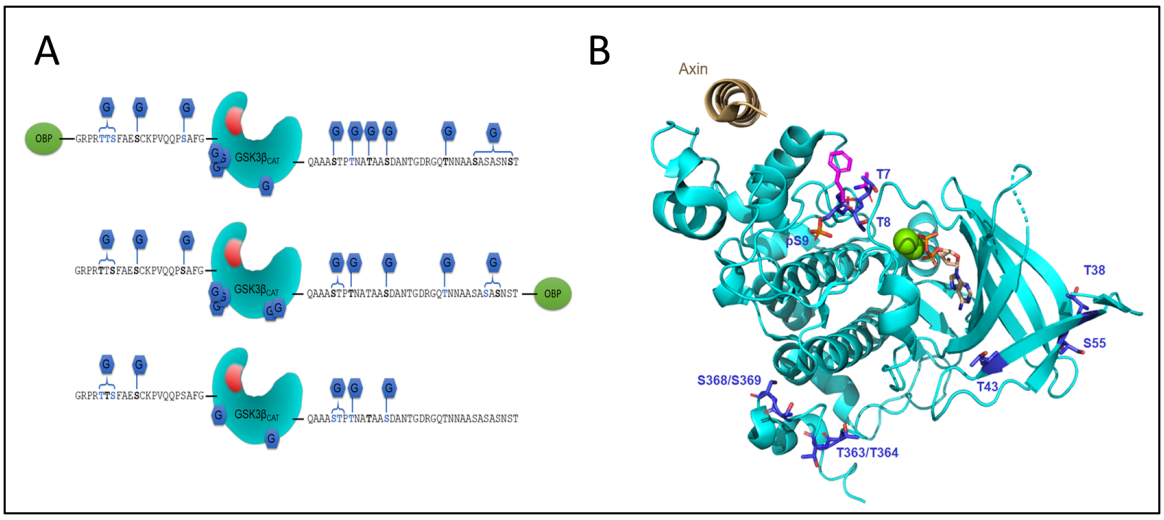

(A) Schematic representation of identified O-GlcNAc sites (blue hexagons) on the GSK3β sequence within the N- and C-terminal OBP-tagged and untagged constructs (B) GSK3β kinase domain O-GlcNAc sites (blue) in the 3D structure of the complex GSK3β: pSer9-GSK3 peptide (sticks): Axin (PDB ID: 4NM3), ATP as beige sticks, and Mg^{2+} ions as green balls

Figure 8.9: Mapping of GSK3β O-GlcNAc sites by bottom-up LC MS/MS identification

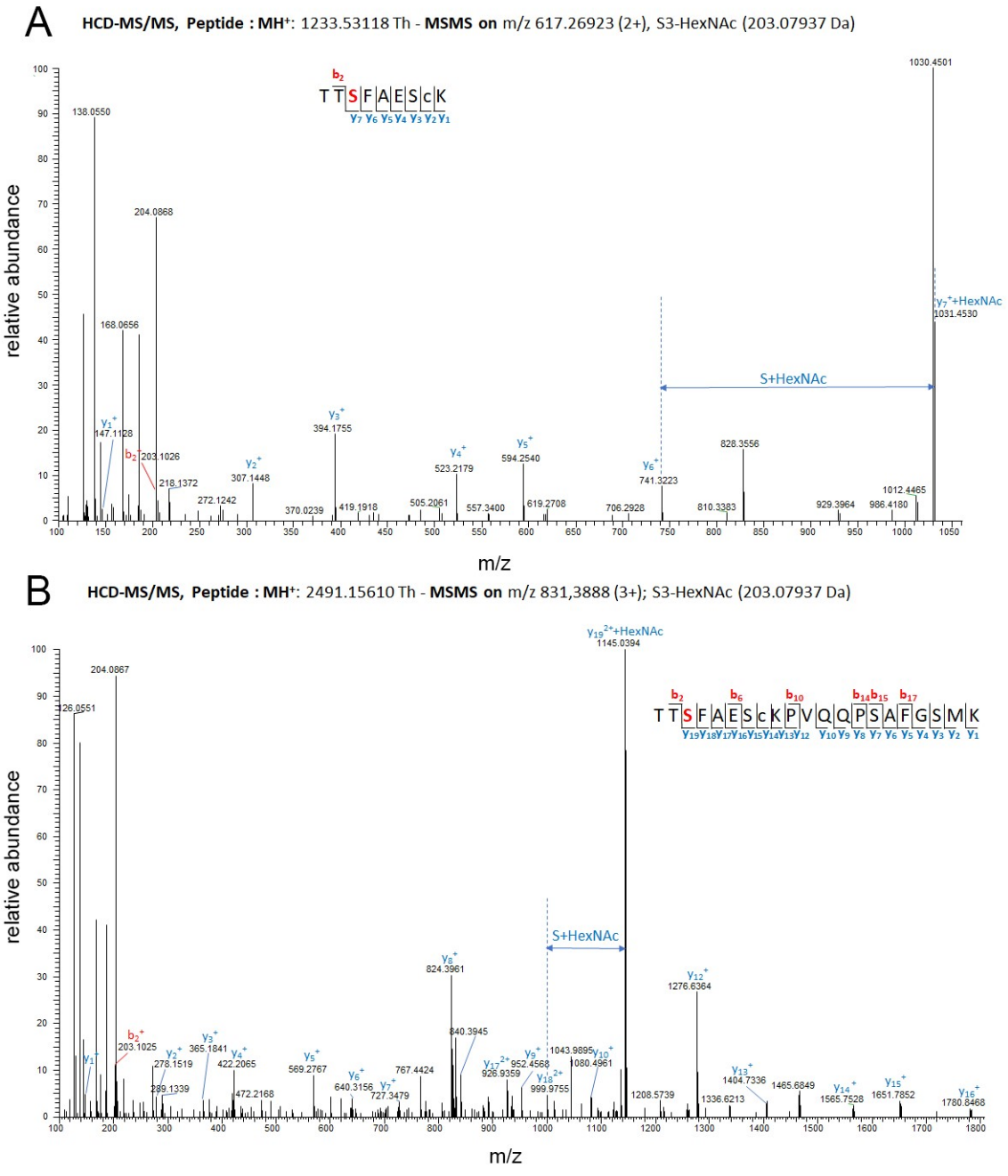

Figure 8.10: MS fragmentation spectra of OBP-GSK3β from LC-MS/MS analyses using HCD-based fragmentation, identifying Ser9 as O-GlcNAc site from two different peptides (A) and (B). b-ions and y-ions are annotated in red and blue, respectively

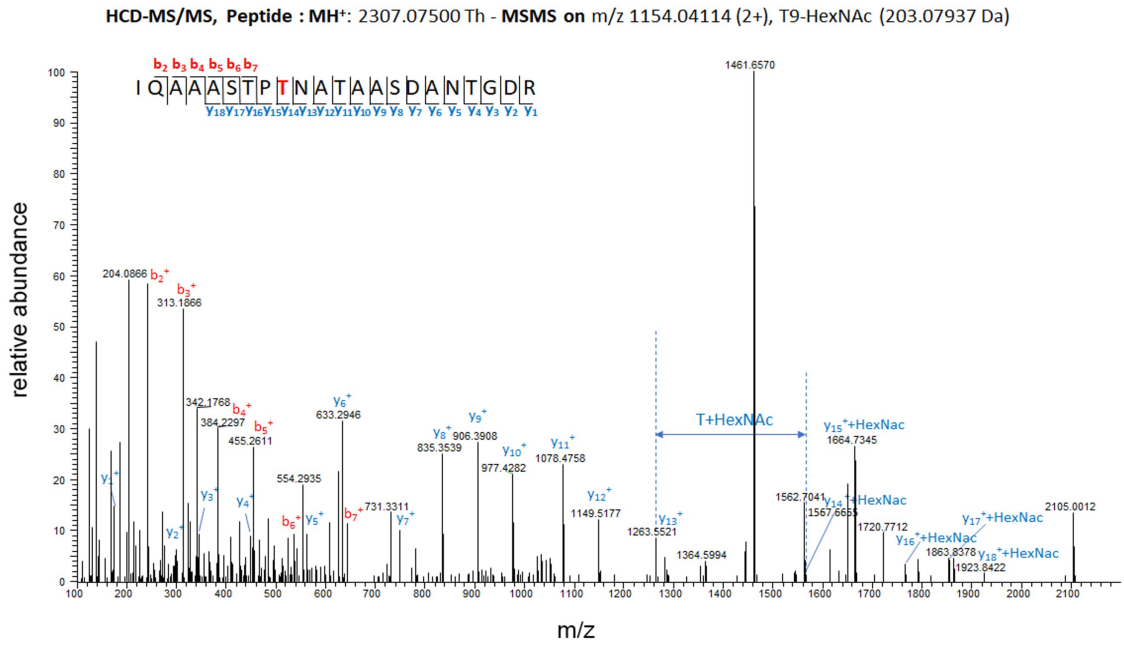

Figure 8.11: MS fragmentation spectra from HCD-based LCMS/MS analyses for identification of Thr392 O-GlcNAc site of the C-terminal domains of GSK3β

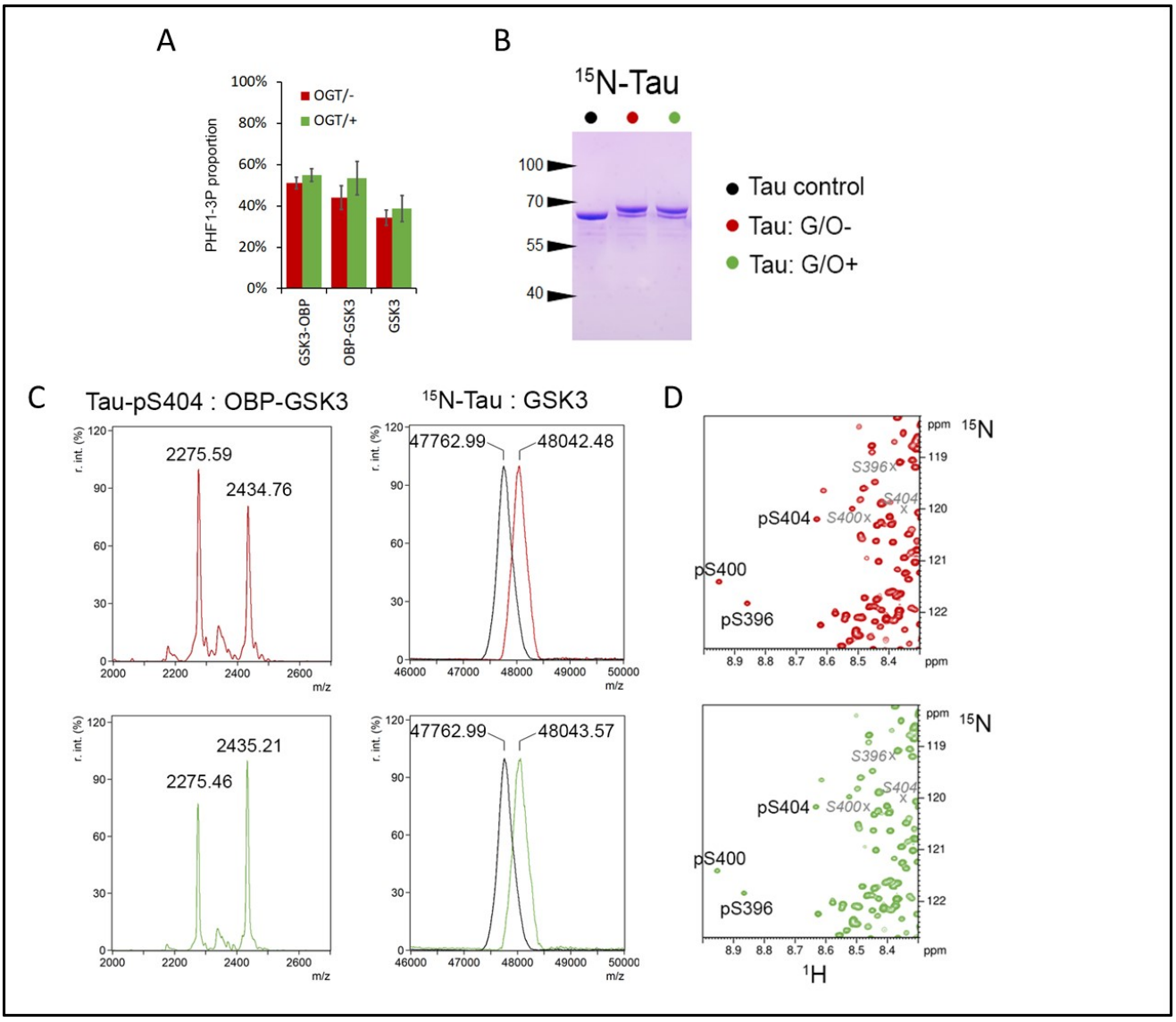

(A) Kinase activity of GSK3β, OBP-GSK3β, and GSK3β-OBP on a primed Tau-pS404 peptide monitored by mass spectrometry as shown in (B) SDS-PAGE analysis of phosphorylation reactions of full-length, unprimed ^{15}N-labeled Tau protein with GSK3β preincubated with OGT with (G/O+) or without (G/O-) UDP-GlcNAc (C)MALDI-TOF MS analysis of phosphorylation of a primed Tau-pS404 peptide with OBP-GSK3β (left panels) or full-length, unprimed ^{15}N Tau with GSK3β (right panel) preincubated with OGT and UDP-GlcNAc or in the absence of UDP-GlcNAc (D) NMR analysis of ^{15}N-labeled phosphorylated Tau protein

Figure 8.12: Kinase activity of O-GlcNAc glycosylated GSK3β on primed Tau-pS404 and unprimed Tau. GSK3β O-GlcNAc reactions with recombinant OGT with (OGT/+, green) or without (OGT/-, red) UDP-GlcNAc as a control

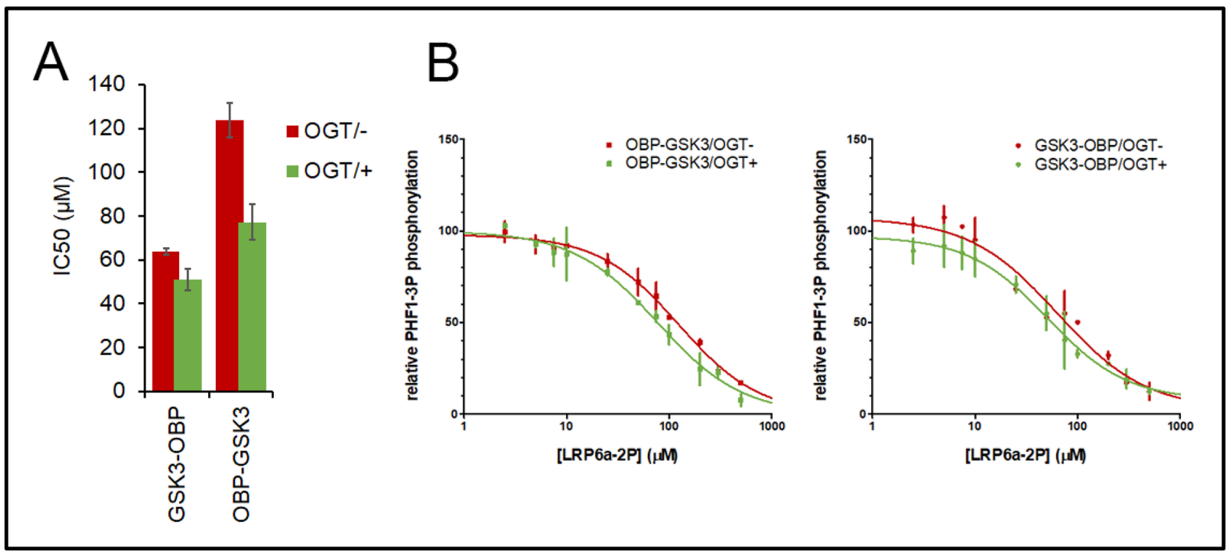

GSK3β kinase activity was measured in the presence of the diphosphorylated peptide LRP6a-2P, derived from the Wnt LRP6 receptor. OBP-GSK3β fusion proteins were incubated with OGT, either with (OGT/+, green) or without (OGT/-, red) UDP-GlcNAc. (A) IC_{50} values of the LRP6a-2P peptide were determined by testing increasing concentrations of the inhibitor (from 2.5 to 500 μM) on the kinase activity of OBP-GSK3 (B, left panel) and GSK3-OBP (B, right panel) using a primed Tau-pS404 substrate at 20 μM. The percentage of PHF1-3P was determined as the mean $\pm$ SD of two replicates

Figure 8.13: Regulation of GSK3β kinase inhibition by O-GlcNAcylation

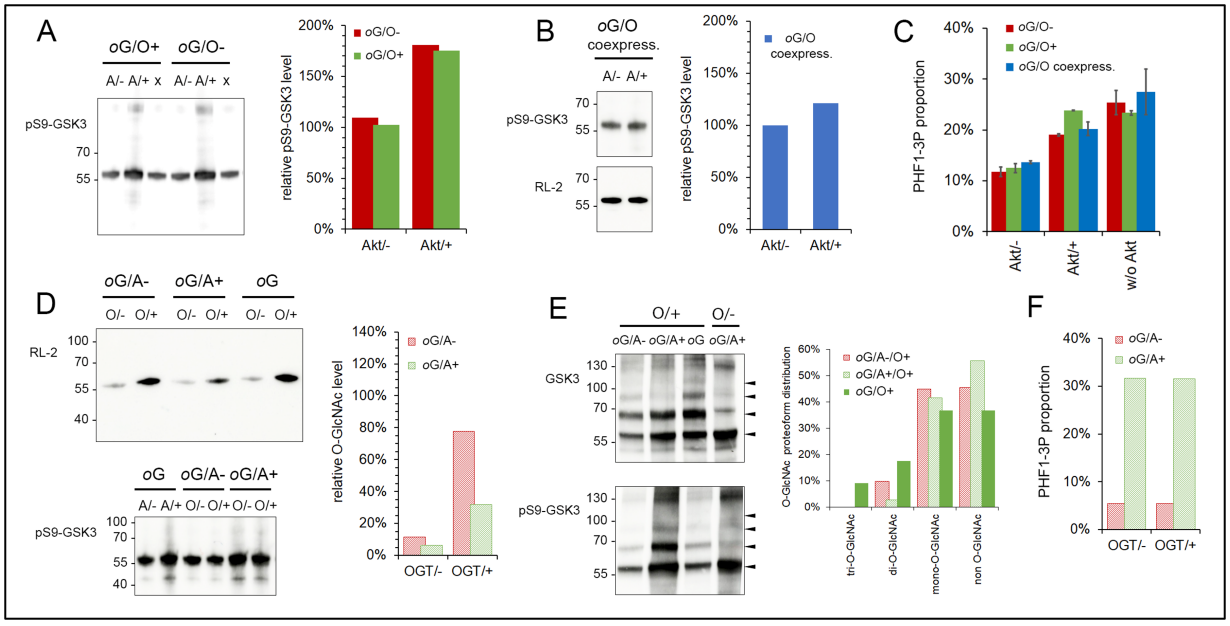

(AC) Effect of O-GlcNAcylation on GSK3β phosphorylation by Akt-1. OBP-GSK3β (oG) is obtained from O-GlcNAc reactions with OGT and UDP-GlcNAc (oG/O+, green), without UDP-GlcNAc (oG/O, red), or through OGT coexpression (blue), and phosphorylated by Akt-1 with ATP (A/+) or without ATP (A/-). Controls are oG/O+ and oG/O samples without Akt-1 (x) (A) Western blot showing pSer9-GSK3 phosphorylation levels (B) Western blot showing reduced Ser9 phosphorylation in OBP-GSK3β coexpressed with OGT (C) Kinase activity of GSK3β variants on primed Tau-pS404 peptide (D-F) Effect of Akt-1 phosphorylation on GSK3β O-GlcNAcylation. OBP-GSK3β is phosphorylated by Akt-1 with ATP (oG/A+, green) or without ATP (oG/A-, red) and O-GlcNAcylated by OGT with UDP-GlcNAc (O/+) or without (O/-). Controls include OBP-GSK3β without Akt-1, with OGT and UDP-GlcNAc (green) or without (red) (D) Western blot showing OGT-mediated O-GlcNAcylation levels (E) mPEG5K-labeling analysis of O-GlcNAc proteoforms (F) Kinase activity of phosphorylated and nonphosphorylated GSK3β on primed Tau-pS404 peptide

Figure 8.14: Cross-talk between phosphorylation and O-GlcNAcylation of GSK3β, and regulation of GSK3β kinase activity on a primed Tau-pS404 peptide

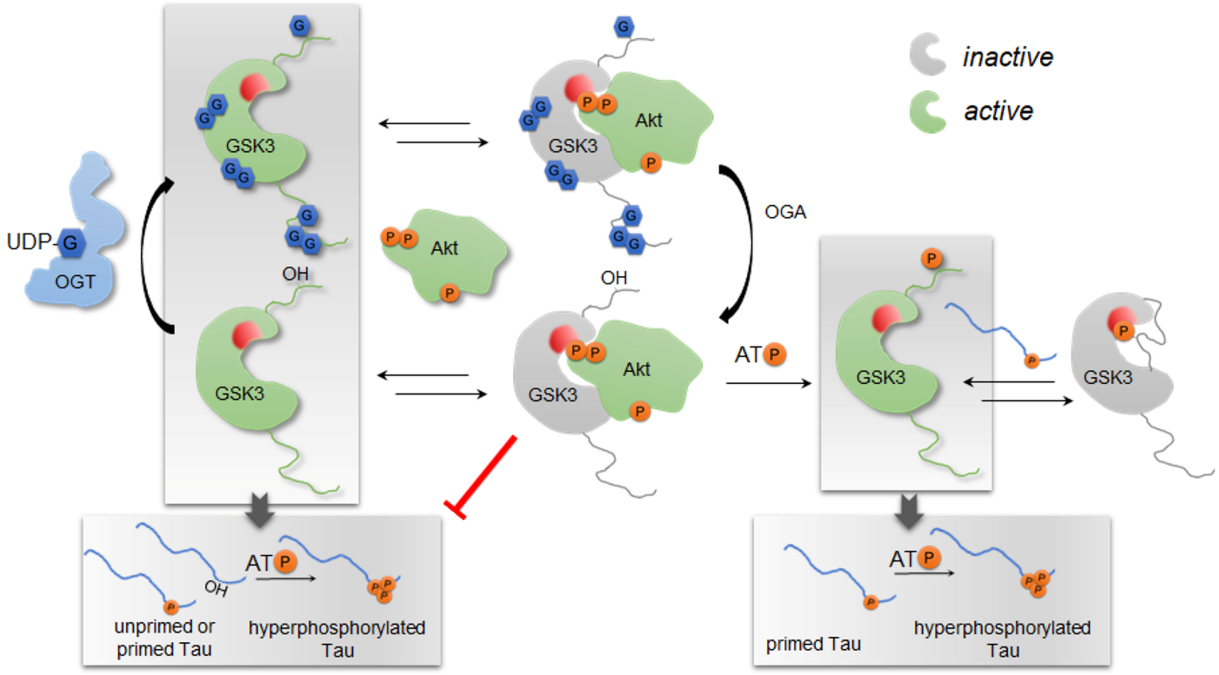

Figure 8.15: Schematic conclusion for the regulation of GSK3β by phosphorylation and O-GlcNAcylation

Chapter 9: Phosphorylation and aggregation

Phosphorylation of Tau plays a crucial role in both normal physiological processes and neurodegenerative diseases like Alzheimers disease (AD). Tau hyperphosphorylation reduces its ability to bind to microtubules, leading to microtubule destabilization, accumulation of free Tau in the cytosol and promoting Tau aggregation into paired helical filaments (PHFs) and NFTs. The phosphorylation of the PHF-1 (paired helical filament-1) epitope of Tau, specifically at serine residues S396 and S404, is significant in the context of Alzheimers disease (AD). Hyperphosphorylation of the PHF-1 epitope, which may also include the additional S400 site, is a hallmark of AD and is associated with the formation of neurofibrillary tangles (NFTs), a characteristic feature of AD pathology.
The filament core in AD demonstrates structural conservation among patients and primarily consists of the R3 and R4 microtubule-binding repeats of Tau. The core composition includes these microtubule-binding repeats together with variable flanking regions pertaining to part of the C-terminal domain including the R pseudo-repeat, and the N-terminal region of R3 repeat, which could be part of the R2 or R1 repeat depending on the 4R or 3R isoform, respectively. Cryo-EM studies have revealed that the core structure of paired helical filaments (PHFs) is conserved across different AD patients, indicating a common pathological mechanism of Tau aggregation in AD. The core forms a distinctive β-arch structure that turns at residues 322CGS324, located within the R3 repeat region, and this structural feature is consistent across AD Tau filaments. Two protofilaments stack together to form the filament, with an interface extending from residue G323 to I354, encompassing parts of both R3 and R4 repeats (Duan et al. 2023; Falcon et al. 2018b).
In this chapter, we studied the physiological and pathological roles of Tau R2Ct and R3Ct, two aggregation-prone Tau fragments. These fragments were designed as they span the entire C-terminal domain to include the PHF-1 epitope. They also include the core of Tau filaments starting either at the R2 repeat for the R2Ct fragment or R3 repeat for the R3Ct fragment. Thus, R3Ct could originate from both 3R and 4R isoforms while R2Ct from 4R isoforms only. We also looked at the function of GSK3β phosphorylation, which results in a triple phosphorylation of the PHF-1 epitope (S396, S400, and S404).
First, we will present the phosphorylation pattern and its impact on microtubule binding and heparin-induced aggregation of these fragments (section 1). Following this, we will examine the *seeding* activity of these fragments on themselves (section 2), on full-length Tau (section 3), and on full-length semi-synthetic Tau bearing diverse patterns of homogenous phosphorylation at the PHF-1 epitope (section 4).

1. Characterization of Tau fragments

1.1. Phosphorylation of R2Ct and R3Ct

The full-length Tau protein has already been assigned by our team. In this study, we aimed to assign the NMR spectra of R2Ct and R3Ct, as well as their phosphorylated proteoforms, to investigate conformational effects of phosphorylation using high-resolution NMR spectroscopy and further functional implications.

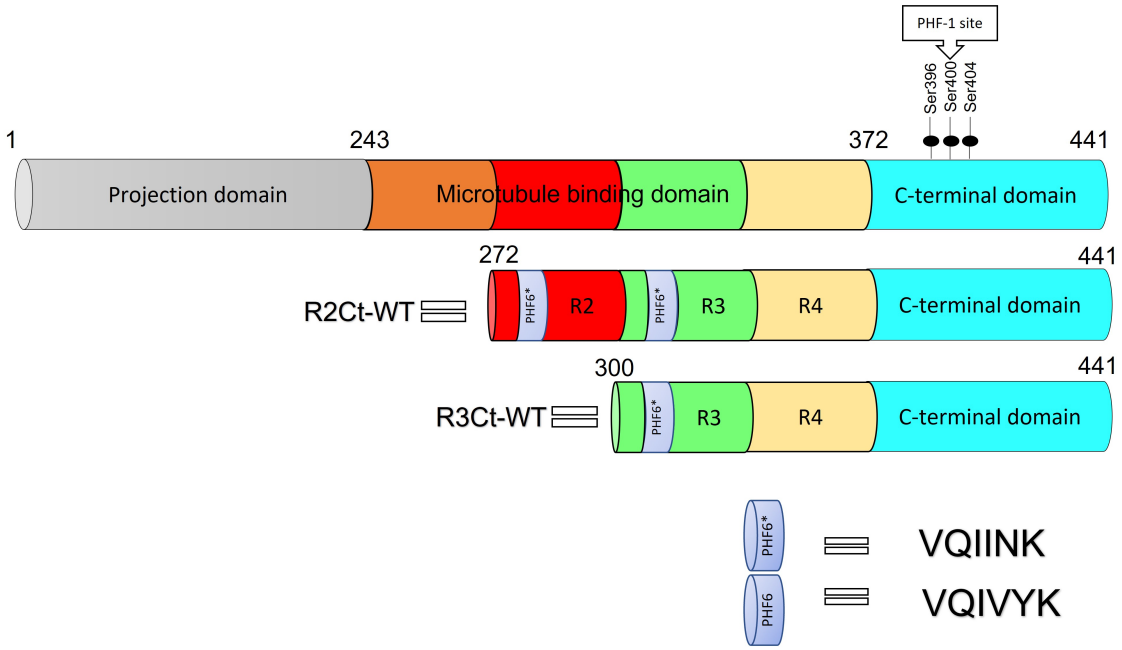

(A) Full-length Tau, (B) R2Ct fragment, (C) R3Ct fragment indicating the different domains encompassed in each protein. PHF6 and PHF6* correspond to hexapeptide sequences that have been described as nuclei of Tau fibrillar aggregation. PHF-1 indicated by black dots is a phospho-epitope of the Cterminal domain (S396/S400/S404) found in Tau inclusions from AD brains which is generated by the kinase activity either of GSK3β alone or combination of CDK2/cyclin A and GSK3β (D) Recombinant fragment encompassing the 297-391 residues as the minimal fragment able to fold into PHFs in solution (E) Core of PHF-Tau filaments from AD brains (inset, PDB ID: 5O3L) is shown for comparison

Figure 9.1: Representation showing the R2Ct and R3Ct segments used in this study, as well as the domains of Tau protein

As demonstrated in ^{1}H-^{15}N HSQC spectra (Figure 9.2), GSK3β produced a homogeneous triple phosphorylation of the C-terminal PHF-1 epitope at S396, S400, and S404 in both R2Ct and R3Ct segments, in accordance with a prior characterization in full-length Tau protein. While sequential phosphorylation by CDK2/cyclin A and GSK3β resulted in the same phosphorylation pattern of the PHF-1 epitope as GSK3β alone. As previously described for full-length Tau, CDK2/cyclin A phosphorylation of R2Ct and R3Ct fragments produced a heterogeneous phosphorylation at PHF-1 epitope with a near homogenous phosphorylation of S404 but partial phosphorylation of S396.
Using consistent ^{15}N,^{13}C isotope labelling for NMR triple resonance backbone assignment, we produced R2Ct and R3Ct fragments in both their non-phosphorylated and GSK3β-phosphorylated forms in order to determine their conformational propensity.

We have studied the conformational propensity of the different variants based on the chemical shifts of HN, N, CO, Cα, Hα, and Cβ nuclei. This has allowed us to examine the conformational propensity of the R2Ct and R3Ct fragments, as well as a potential differential effect of PHF-1 triple phosphorylation on the fragment conformation that would explain their distinct behaviors in MT polymerization activity. The ^{13}C secondary chemical shifts of Cα and Cβ show that all variations of Tau fragments have a random coil shape. The non-phosphorylated R2Ct and R3Ct Tau fragments both take on the identical structural propensity profile, as demonstrated by the neighbor-corrected Structural Propensity (ncSP) score (Figure 9.5 A).
Each repeat domain in Tau protein exhibits a tendency to adopt an extended β-structure, including the R' pseudo-repeat, in line with earlier findings (Mukrasch et al. 2009). Additionally, a helical propensity is demonstrated by a 10-residue stretch of the extreme C-terminus, namely residues 427437.

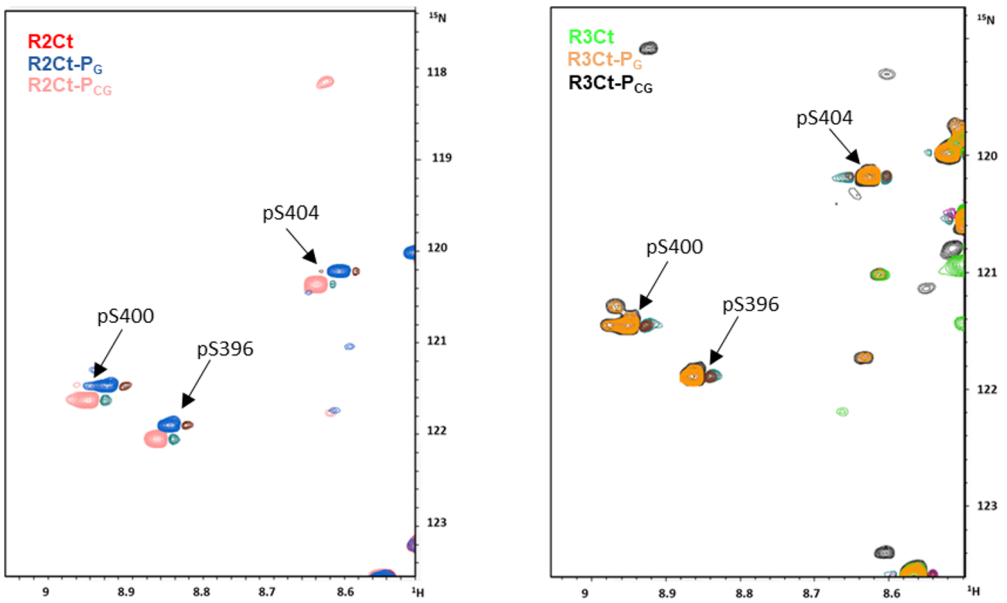

^{1}H-^{15}N HSQC NMR spectra of T au fragments in their nonphosphorylated and GSK3β phosphorylated form for R2Ct (red), R2Ct-P (blue), R3Ct (green) and R3Ct-P (orange) highlighting the homogenous triple phosphorylation of the PHF-1 epitope

Figure 9.2: Comparision of the PHF-1 phosphorylation of R2Ct and R3Ct fragments by GSK3β with or without priming by CDK2/Cycline A

As demonstrated by ncSP scores (Figure 9.5), secondary structure propensity (SSP) based on ^{1}Hα, ^{13}Cα, and ^{13}Cβ, and backbone torsion angles prediction from TALOS-N (Figure 9.6), the PHF-1 phosphorylation induces an additional extended conformation within the N-terminal region of the phosphorylation sites (residues 392-402) in both GSK3-phosphorylated fragments.
Furthermore, at a brief stretch C-terminal to PHF-1, the phosphorylated portions of PHF-1 have a modest tendency to adopt a turn conformation (pS404-L408). It has been previously demonstrated that pS404 induces this tendency to adopt a turn conformation, which is further aggravated when additional PTMs are present at S396 and/or S400 in 20-mer peptides containing the (392-411) region.
Phosphorylation of T231/S235 in the AT180 epitope has been demonstrated to trigger an N-cap stabilising an α-helix in the C-terminal region of phosphorylation sites, which is consistent with our data. Moreover, it has been suggested that the peptide is locked in a poly-proline II (PPII) conformation by an intramolecular salt bridge between the phosphate and the arginine or lysine side chain. An intermolecular salt bridge with tubulin is in competition with a salt bridge interaction between R230 and pT231 in the Tau RT231PP sequence. Similar to this, pS396 may lock K395 in a salt bridge, inhibiting interactions of these residues with binding partners, as demonstrated by significant perturbations of K395 NH resonance upon phosphorylation of PHF-1 epitope. This would account for the loss of function in tubulin polymerisation.
Nonetheless, no discernible variations in the structural alterations generated by phosphorylation have been seen between the R2Ct and R3Ct segments. When considered collectively, these findings indicate that extra N- and C-terminal sequences in fragments have no effect on the conformational changes brought about by repeated phosphorylation, which do not spread outward.

1.2. Tubulin polymerization assay

Each fragment was incubated at a concentration of 20 μM with 20 μM tubulin at 37°C in polymerization buffer. The non-phosphorylated R2Ct fragment promotes tubulin polymerization, although to a lesser extent than the full-length 2N4R Tau. This ability is entirely lost when the fragment undergoes phosphorylation by GSK3. In contrast, the R3Ct fragment, whether phosphorylated or not, does not

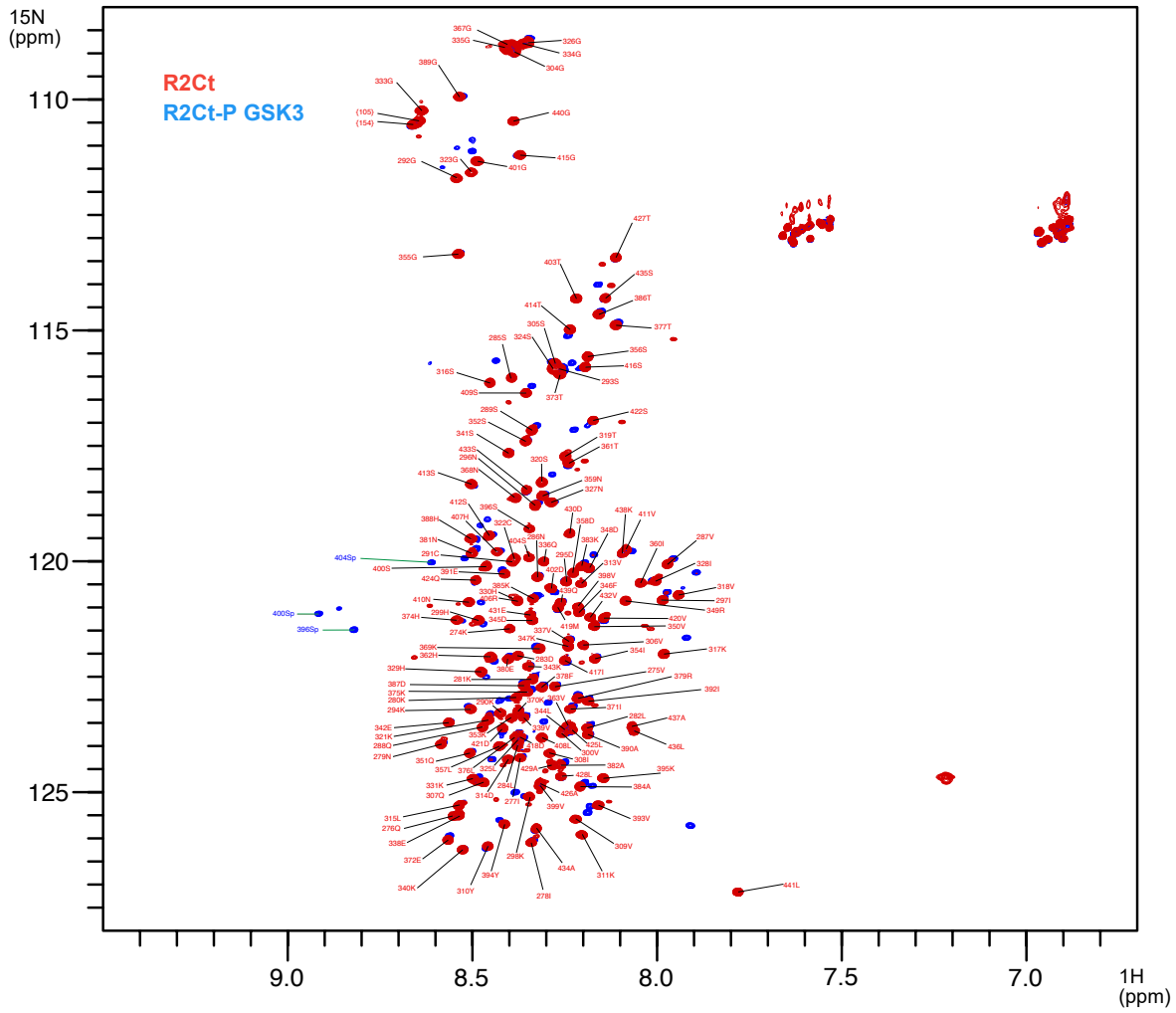

Figure 9.3: $^{15}N^{13}C$-HSQC spectra of R2Ct (red) and R2Ct-P (phosphorylated by GSK3β, blue)

support tubulin polymerization. The complete loss of polymerization activity observed in both phosphorylated R2Ct and R3Ct Tau fragments containing the PHF1-3P phosphorylation sites suggests that a minimum number of microtubule-binding repeats, potentially in combination with the adjacent proline-rich regulatory region, is necessary to mitigate the reduction in tubulin polymerization activity caused by PHF-1 phosphorylation (Figure 9.7).

1.3. Heparin aggregation

We have seen that Tau is present in the NFTs in an aggregated form of highly ordered fibrillar material known as PHF (Brion et al. 1985). This protein is also found phosphorylated in those PHFs (Grundke-Iqbal et al. 1986). The mechanisms of Tau aggregation are still poorly understood, but it is now known that the regions of the MTBD that make up the majority of PHFs are repeat regions, and the structural organisation of PHFs varies depending on the type of isoform and tauopathy from which they originate (Fitzpatrick et al. 2017). Furthermore, a number of researchers now propose that Tau may also exhibit prion-like behaviour, spreading among nerve cells and attracting endogenous normal Tau to trigger its aggregation, leading to the production of new NFTs (Mudher et al. 2017).

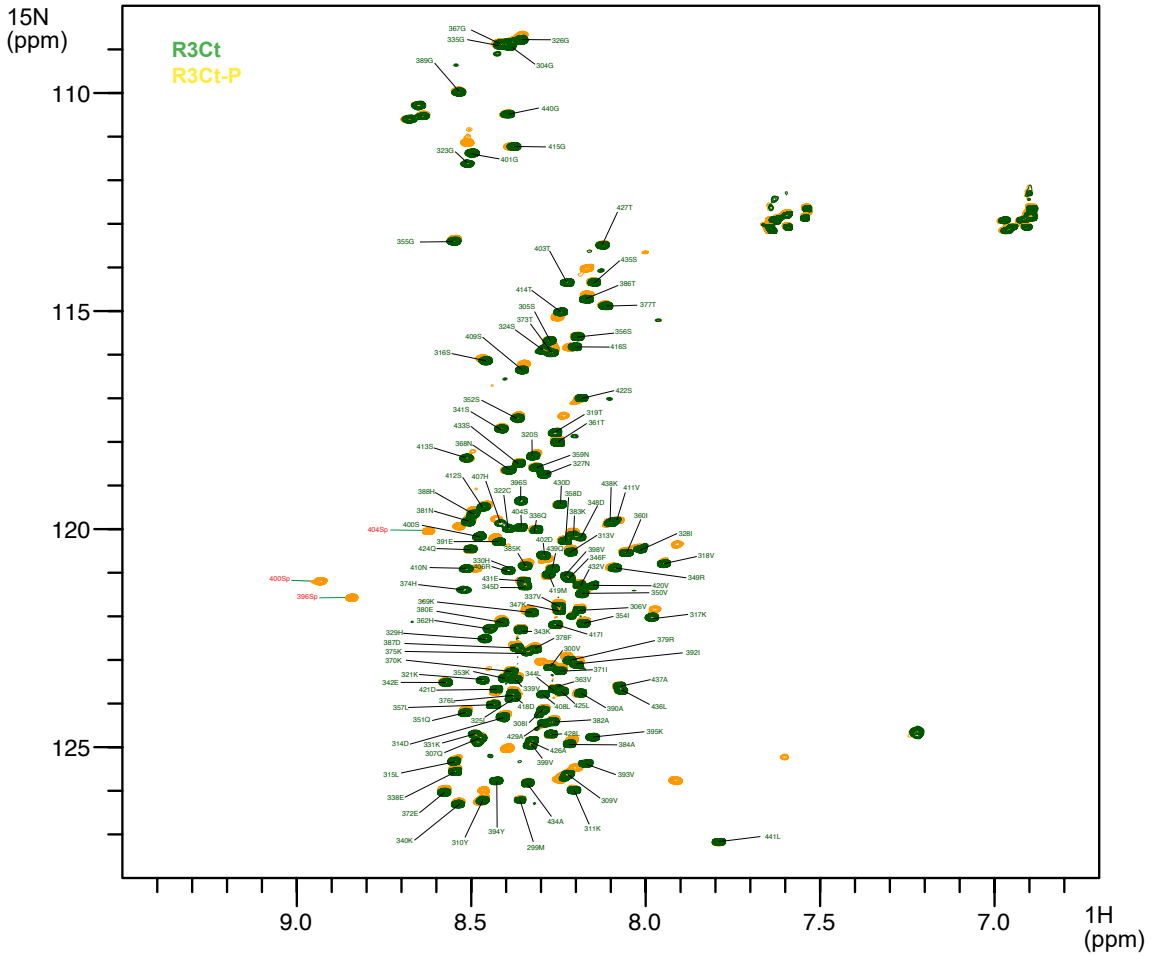

Figure 9.4: $^{15}N^{13}C$-HSQC spectra of R3Ct (green) and R3Ct-P (phosphorylated by GSK3β, orange)

Full length Tau heparin-induced aggregation

First, we conducted a test to determine the minimum concentration of heparin necessary for Tau aggregation. Aggregation reactions were screened at different heparin concentrations ranging from 0 to 5 μM. This study will allow us to select an optimal concentration for the *seeding* reactions.
The aggregation conditions remain constant, using the same buffer. For a 100 μL aggregation reaction, a concentration of 10 μM TauS262A is incubated with increasing concentrations of heparin: 0, 0.05, 0.1, 0.15, 0.2, 0.25, 0.3, 0.4, or 0.5 μM. By adding 50 μM ThT and 0.33 mM DTT, the reaction is incubated for several days at 37 °C.
After several experiments, we saw that Tau begins to aggregate at a heparin concentration of 0.15 μM. Therefore, for our seeding experiments, we should use a concentration below 0.15 μM. A concentration of 0.05 or 0.1 μM would be appropriate for this experiment.

Seeds preparation from non- and phosphorylated Tau fragments

Heparin-induced self-assembly of R2Ct and R3Ct fragments and their GSK3β-phosphorylated proteoforms, R2Ct-P and R3Ct-P, was seen for 48 hours at 37řC using TEM and ThT fluorescence. Heparin-induced Tau filaments differ structurally from those taken from AD brains (Fichou et al. 2018b; Zhang et al. 2019), but when Tau proteins or fragments were incubated without heparin, as was demonstrated for comparable non-phosphorylated fragments (Lövestam et al. 2022), no aggregation was found. All segments show a time-dependent increase in ThT fluorescence in the presence of

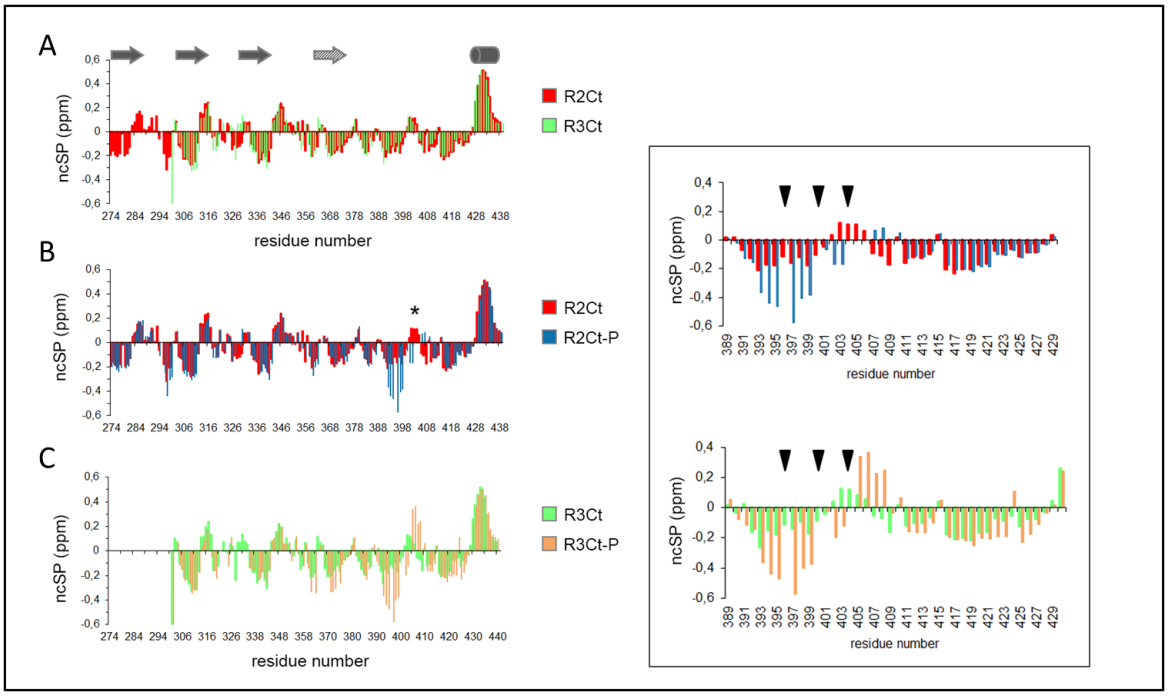

(A-C) R2Ct's non-phosphorylated (red) or phosphorylated (blue) forms, or R3Ct's non-phosphorylated (green) or phosphorylated (orange), were assigned neighbor-corrected secondary structure propensity (ncSP) scores. Phosphorylation-induced conformational alterations are mostly localised in the PHF-1 site (phosphorylation sites are marked by triangles) and its C-terminal region at residues [405-427] (inset). These changes are highlighted by comparisons of R2Ct and R3Ct (A), R2Ct and R2Ct-P (B), and R3Ct and R3Ct-P (C)

Figure 9.5: GSK3β phosphorylation-induced conformational alterations in R2Ct and R3Ct fragments

heparin (at a Tau:heparin ratio of 4:1), indicating the creation of amyloid-like structures (Figure 9.8 A, B).
According to negative-staining TEM, all Tau self-associates to form filamentous aggregates of varying lengths, with total amounts consistent with the relative ThT signals at the end point. While R2Ct-P and R3Ct-P produce small aggregates in which the PHF-like structure is not discernible, R2Ct exhibits longer PHF-like fibrils than R3Ct, albeit with a heterogeneous length distribution (Figure 9.8 C).
Using a Tau:heparin ratio of 10:1, *seeds* were generated for both segments in their non-phosphorylated and GSK3β-phosphorylated forms for 7 days at 37řC. The 10-fold dilution of seeds in subsequent *seeding* reactions with soluble monomers results in a heparin concentration of 0.1 μM, which is below the critical concentration for Tau fragment self-association, based on the heparin concentration used here to create *seeds*. Those aggregates are then used as *seeds* for the *seeding* reactions in the following sections. To assess the impact of intermediate phosphorylation state further, *seeds* containing CDK2-phosphorylated fragments were generated.

2. R2Ct and R3Ct *seeding* and cross-*seeding* by R2Ct and R3Ct seeds

Using a final monomer concentration of 25 μM for 1 μM of *seeds*, we assessed the *seeding* and cross-*seeding* characteristics of R2Ct and R3Ct *seeds*, whether or not they were phosphorylated by GSK3β, on the aggregation of the non-phosphorylated or GSK3β-phosphorylated monomeric fragments.

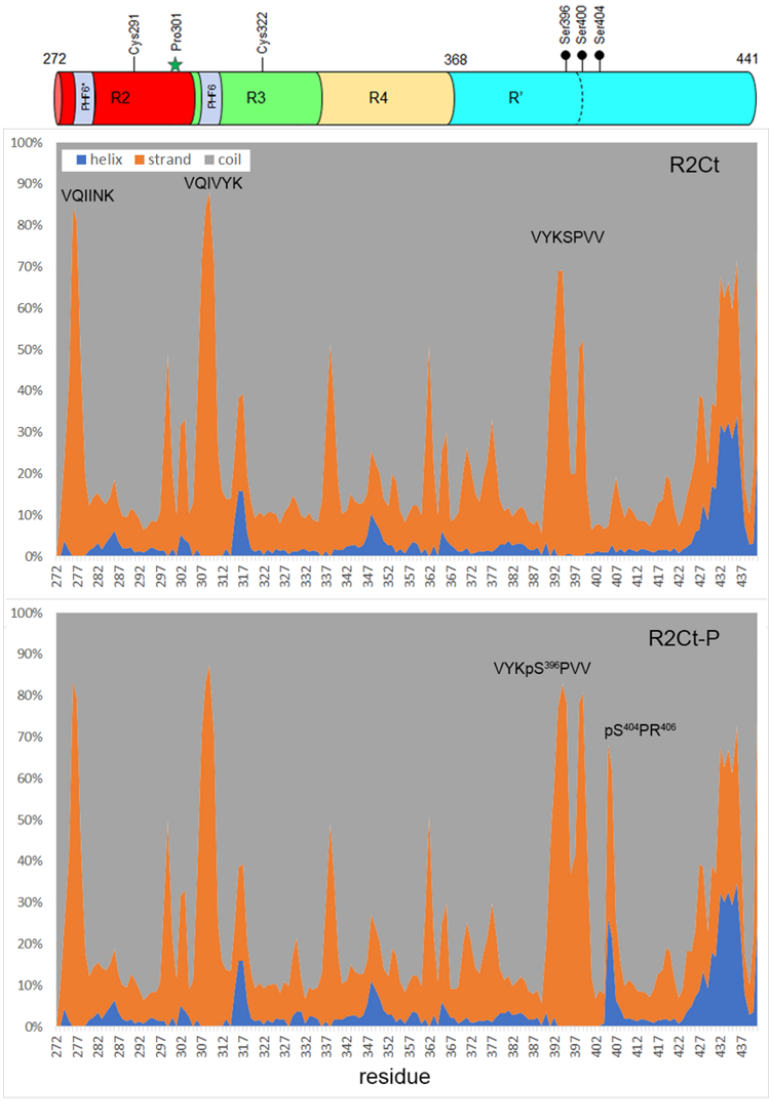

Figure 9.6: Protein backbone torsion angles for the R2Ct and R2Ct-P segments, which illustrate the cumulative proportions of helical (blue), extended strand (orange), and coil (grey) conformations, are predicted from NMR chemical shifts using Talos-N

2.1. *Seeding* and Cross-*seeding* behavior by unphosphorylated *seeds* fragments

R2Ct and R3Ct seeds have different *seeding* effects on the aggregation behaviour of the soluble version of those fragments in their non-phosphorylated state. Differential seeding activity on both protein variants is suggested by the fact that R2Ct *seeds* increased aggregation of R2Ct fragment as indicated by a larger rise of ThT signal while having a limited impact on aggregation of R3Ct. On the other hand, R3Ct *seeds* showed comparable *Seeding* effects on the R2Ct and R3Ct fragment aggregation (Figure 9.9).

These results highlight how well R2Ct and R3Ct *seeds* encourage the aggregation of their own soluble species. Furthermore, whereas R2Ct *seeds* do not encourage R3Ct aggregation, R3Ct *seeds* allow R2Ct aggregation to cross-*seed* (Figure 9.9). This pattern was noted for the K18 and K19 fragments, which correspond to the isolated MTBR domain of the 4R and 3R isoforms, respectively. K19 *seeds*, on the other hand, encourage K18 aggregation, whereas K18 *seeds* do not. It has been proposed that the catalytic centres for conformational selection in K18 and K19 fibril development are the R2 and R3 repetitions, which are the most stable repeats in K18 and K19, respectively. Because R2 is absent from K19, R3 in K19 *seeds* can thus recruit identical R3 in K18, but K19 must overcome a

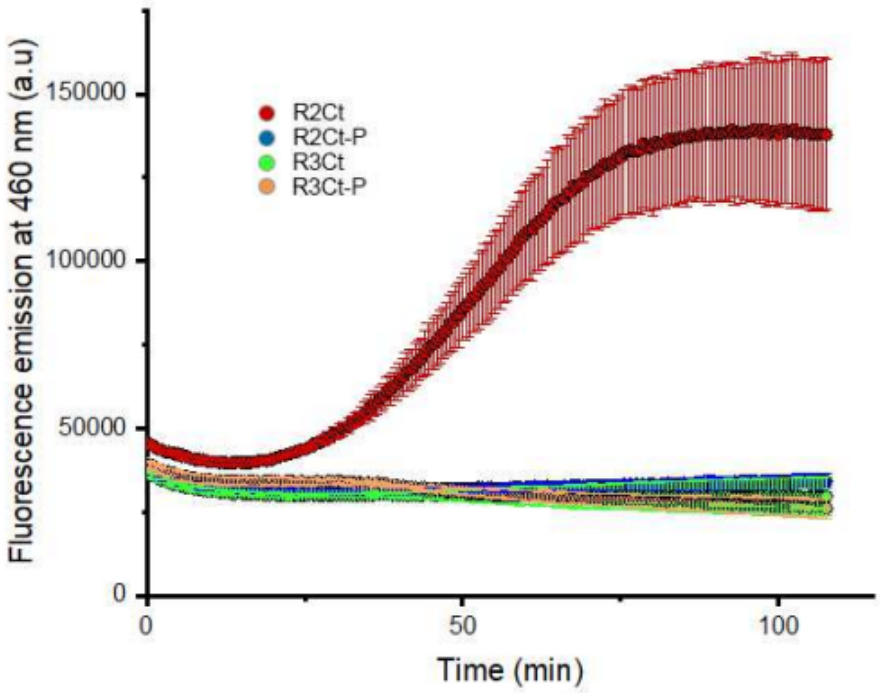

Figure 9.7: Kinetics of tubulin polymerization in the presence of Tau fragments R2Ct (red), R3Ct (green), and their GSK3β-phosphorylated proteoforms, R2Ct-P (blue) and R3Ct-P (orange). Polymerization activity is represented as mean ś standard error of the mean (SEM) from three experimental replicates (n = 3)

seeding barrier when fibril development is driven by K18 *seeds* (Siddiqua et al. 2012). Furthermore, it has been demonstrated that in Tau fibrils, R2 demonstrates greater structural plasticity than R3, and that this conformational adaption controls R2/R2 dimerisation (El Mammeri et al. 2023). Our results indicate that, if R3 is the catalytic centre of R3Ct fibrillization, it can template R3 conformational selection in both R2Ct and R3Ct monomers. In contrast, when R2Ct *seed* template protein misfolding with R2 acting as the driver of conformational selection, R3Ct aggregation has to overcome a cross-*seeding* barrier.

2.2. Effect of the PHF-1 phosphorylation on the *seeding* reaction

Overall, the aggregation of phosphorylated fragments is more efficiently seeded when non-phosphorylated monomers are used as *seeds* (9.10 A-C) or when the monomers themselves are phosphorylated (Figure 9.10 G-I), using R2Ct and R3Ct *seeds*. Compared to R3Ct-P, R2Ct-P *seeds* appear to more effectively induce the aggregation of all monomers, resulting in a high number of short fibrils and the appearance of amorphous aggregates/oligomers (Figures 9.10). Conversely, R3Ct-P *seeds* promote the formation of a few long PHF-like fibrils from both non-phosphorylated R2Ct and R3Ct monomers. The same pattern was observed when R2Ct-P monomers were seeded with R3Ct-P *seeds*. According to these findings, phosphorylated fragments aggregate less efficiently under *seeding* conditions compared to their non-phosphorylated counterparts, and R3Ct aggregates less efficiently than R2Ct. This observation aligns with previous findings regarding heparin-induced aggregation. The behavior of *seeding* under phosphorylated conditions (phosphorylated monomers/*seeds*) differs notably from what is observed under non-phosphorylated conditions. Cross-*seeding* of aggregation, such as R3Ct-P by R2Ct-P *seeds* or R2Ct-P by R3Ct-P *seeds*, appears more effective than homologous *seeding* (using the same *seed*/monomer combination). Specifically, homologous seeding of R2Ct-P results in fewer long fibrils, whereas cross-*seeding* generates a greater number of short fibrils and amorphous aggregates. These findings suggest that PHF-1 hyperphosphorylation of *seeds* may lower the cross-*seeding*

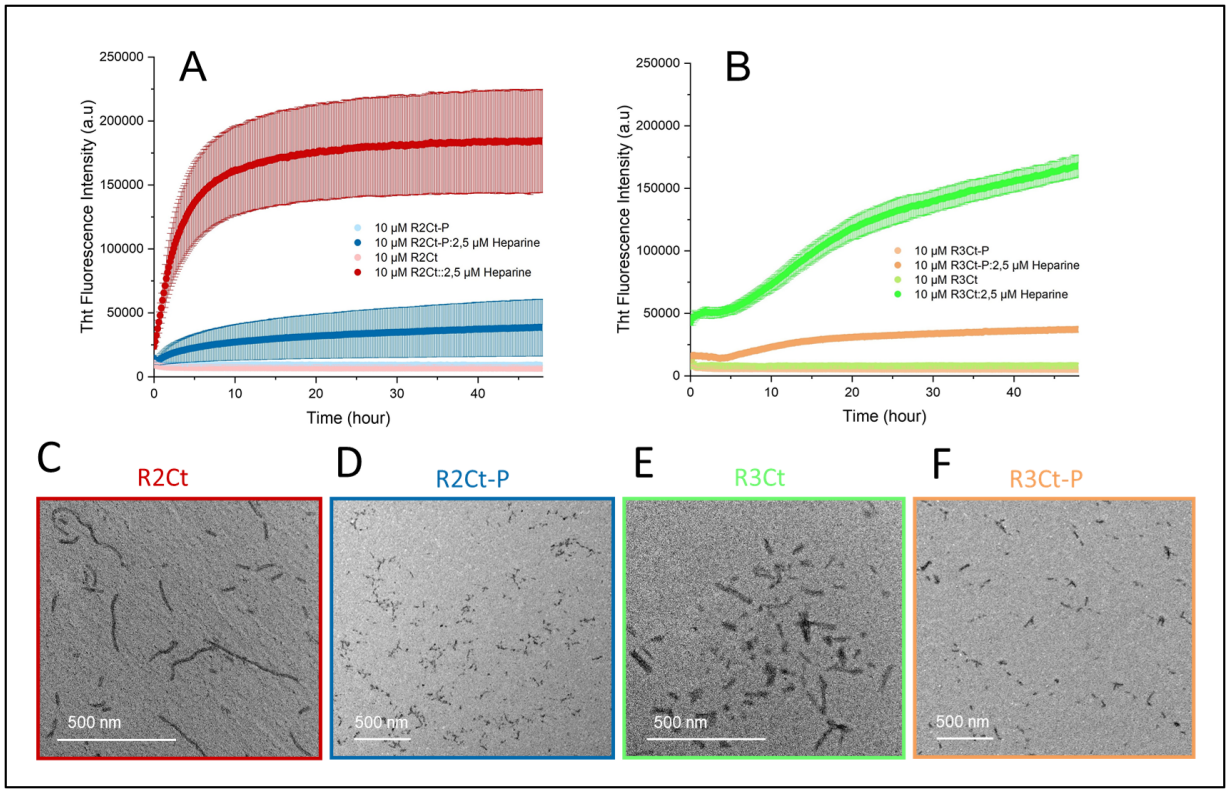

Thioflavin T emission at 490 nm of (A) aggregation of R2Ct (red) and R2Ct-P (blue, phosphorylated by GSK3β) fragments (B) and aggregation of R2Ct (red) and R2Ct-P (blue, phosphorylated by GSK3β) fragments(C-F) Observations under TEM of the aggregation reaction of (C) R2Ct, (D) R2Ct-P, (E) R3Ct and (F) R3Ct-P after 48 h of incubation

Figure 9.8: In vitro heparin-aggregation of Tau fragments and it's phosphorylated proteoforms

barrier and/or indicate that R2 or R3 may no longer serve as the catalytic center for conformational selection.

3. Full-lenght *seeding* by R2Ct and R3Ct seeds

Next, we looked into the ability of phosphorylated and non-phosphorylated fragments to seed full-length Tau that either included or did not possess the aggregation-prone P301L mutation. First, the two isoforms of Tau, non-mutant and mutant (P301L), were aggregated in the presence of heparin to ensure their ability to self-assemble. The results showed that while Tau and the Tau-P301L mutant had similar kinetics and an identical elongation rate constant, Tau-P301L reached a plateau twice as high as Tau and both produced fibrils that resembled PHFs of different lengths (Figure 9.11).
This will be followed by *seeding* reactions in the absence of heparin for comparison.

3.1. *Seeding* by non-phosphorylated *seeds*

In our experiments, we investigated the aggregation of 2N4R Tau proteins upon *seeding* with non-phosphorylated R2Ct and R3Ct *seeds*, as well as in the absence of *seeds* as controls. The kinetics of aggregation were monitored by measuring changes in ThT fluorescence. The initial nucleation and elongation steps were challenging to observe under certain conditions, as the ThT signal started at a high intensity without significant changes over time, indicating that the presence of *seeds* significantly accelerates nucleation. To further analyze *seeding*, we utilized sedimentation assays and negative-staining TEM at the end-point (200 hours) (Figure 9.12), taking advantage of the difference

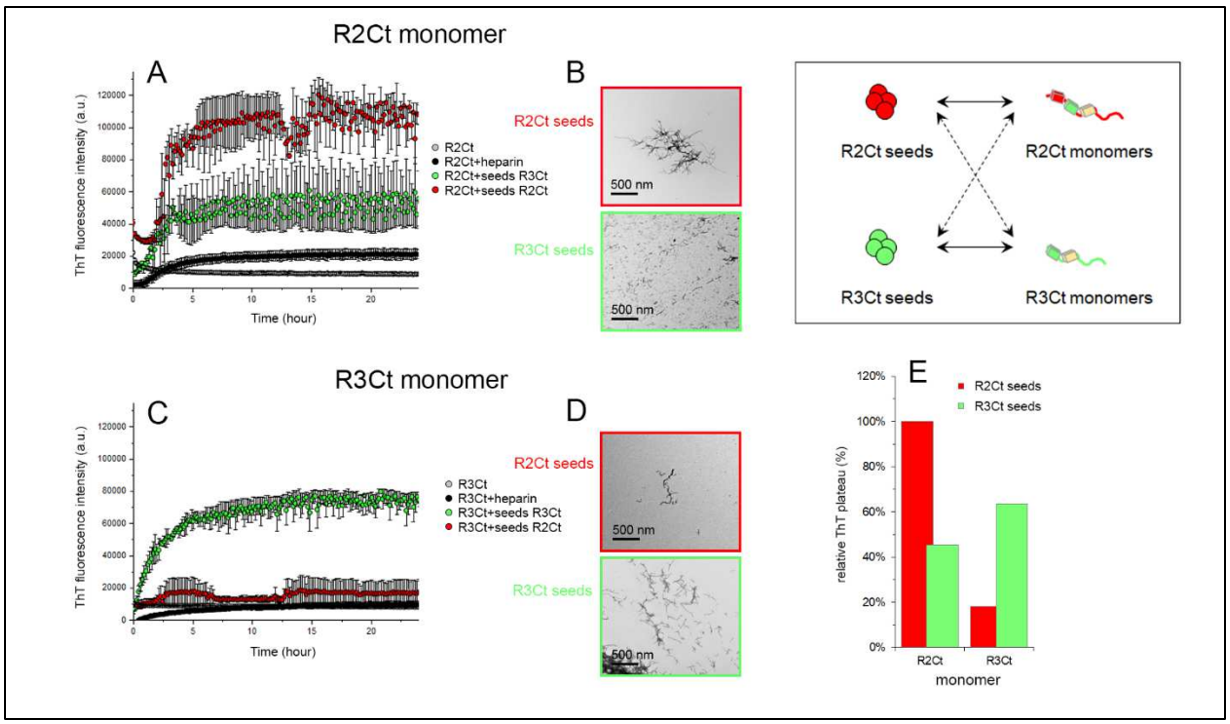

(A, C) Changes in ThT fluorescence (n=3, displayed as the mean ś SEM) demonstrate the time-dependent seeding activity at 37řC by 1 μM of either R2Ct (red) or R3Ct (green) *seeds* on 25 μM monomeric R2Ct (A) or R3Ct (C). The R2Ct or R3Ct fragment control with no heparin (grey) and at a high Tau:heparin ratio (100:1) that resembles the heparin concentration made possible by *seed* dilution (black) are shown. (A, D) Fibrillar aggregates caused by R2Ct (red) or R3Ct (green) *seeds* on monomeric R2Ct (B) and R3Ct (D) are depicted in negative staining TEM images. The relative plateau of ThT signals normalised on R2Ct aggregation caused by R2Ct *seeds* is shown graphically in (E)

Figure 9.9: *Seeding* and cross-*Seeding* activity of non-phosphorylated R2Ct and R3Ct *seeds* on non-phosphorylated R2Ct and R3Ct soluble monomers (inset)

in molecular weight between the seed fragments and 2N4R Tau monomers. The loss of soluble Tau or Tau-P301L monomers over time in the sedimentation assay could indicate the formation of various insoluble species, including oligomers or amorphous aggregates, in addition to the *bona fide* fibrils observed by TEM.

3.2. *Seeding* by phosphorylated *seeds*

In parallel, we examined the aggregation of 2N4R Tau proteins using CDK2/GSK3β-phosphorylated R2Ct and R3Ct *seeds* (namely, R2Ct-PP and R3Ct-PP), as well as CDK2-phosphorylated fragments, which mimic an intermediate phosphorylation state closer to physiological conditions. It was observed that the Tau-P301L mutant is more prone to aggregation when seeded with preformed R2Ct or R3Ct *seeds* compared to wild-type Tau, with R3Ct being particularly effective, irrespective of its phosphorylation state. However, the *seeding* of Tau-P301L aggregation was more dependent on the phosphorylation state, with PHF-1 phosphorylated R2Ct-PP and R3Ct-PP *seeds* showing greater *seeding* activity than CDK2-phosphorylated or non-phosphorylated *seeds* (Figure 9.12 A-C). TEM analysis revealed the formation of PHF-like filaments that were longer than the initial fibrils or aggregates used as *seeds* (Figures 9.8 and 9.12). The sedimentation assays also indicated that *seed* phosphorylation facilitates the aggregation process, potentially by reducing the cross-*seeding* barrier and promoting conformational changes that favor aggregation, particularly involving the PHF-1 sequence, which tends to adopt a β-sheet conformation.
This finding was further supported by immunoelectron microscopy, which confirmed the incorpo-

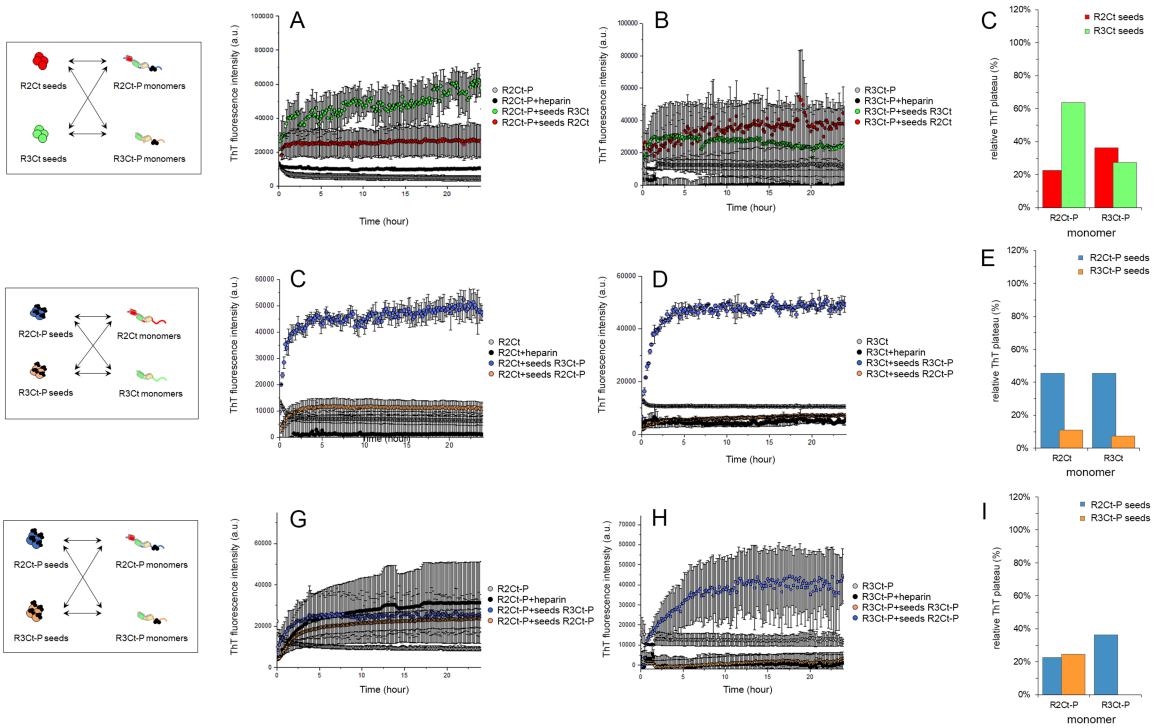

Monomers at 25 μM with 1 μM of *seeds*, or non-phosphorylated R2Ct (C) and R3Ct (D) and R3Ct-P (A, G). The control groups consist of aggregation of 25 μM Tau fragments without heparin (grey) or 0.1 μM heparin (black). Figure 4 displays the relative plateau of ThT signals that have been normalised on R2Ct aggregation induced by R2Ct seeds. This occurs for non-phosphorylated seeds on R2Ct-P and R3Ct-P (C), phosphorylated seeds on R2Ct and R3Ct (E), and phosphorylated seeds on R2Ct-P and R3Ct-P (I).

Figure 9.10: Cross-*seeding* of different fragments proteoforms

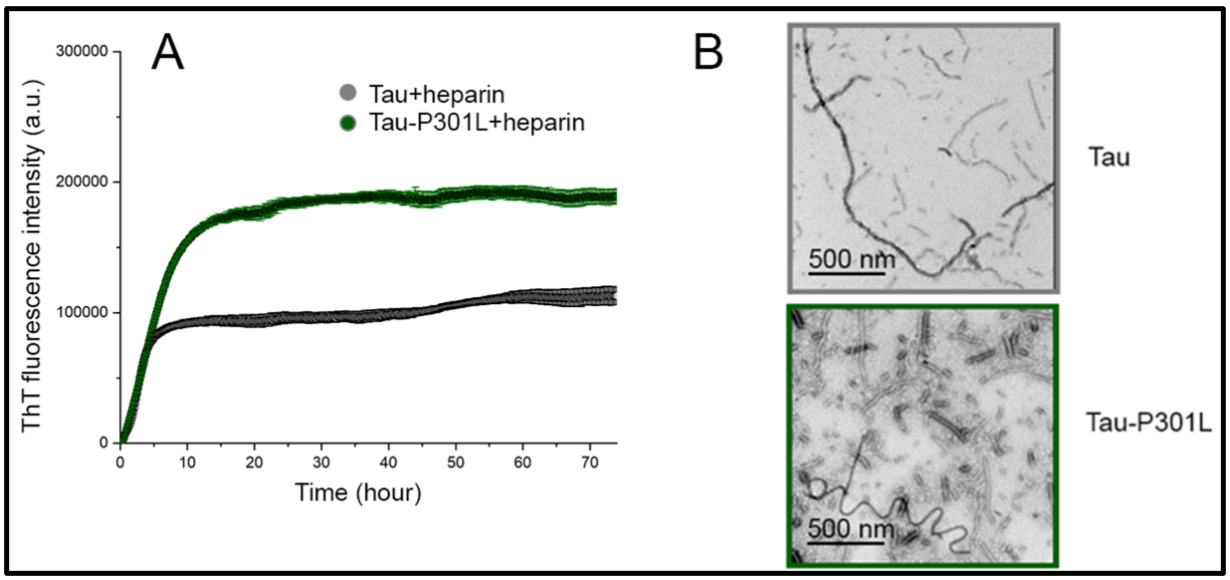

(A) Aggregation kinetics of Tau (grey) and Tau (dark green), monitored by Thioflavin T emission at 490 nm
(B) Observations under TEM of the aggregation reaction after 75h of incubation

Figure 9.11: In vitro heparin-aggregation of Tau and Tau-P301L

ration of full-length Tau monomers into the fibrils. The P301L mutation, localized near the R2-R3 junction, likely reduces the *seeding* barrier for both R2Ct and R3Ct, making them equally effective in promoting the aggregation of Tau-P301L, independent of the phosphorylation state of the *seeds*.

3.3. Conclusion

Tau aggregation originates from protein misfolding, where misfolded Tau can aggregate into fibrils that act as templates, facilitating the misfolding and incorporation of adjacent Tau monomers during fibril elongation or driving surface-catalyzed secondary nucleation to generate new fibrils. This process, known as "*seeding*," is a critical mechanism in the propagation of Tau pathology (Mroczko, Groblewska, and Litman-Zawadzka 2019; Ashraf et al. 2014). *Seeding* is thus considered a key mechanism in the formation and spread of Tau pathology, where *seeds* act as templates to drive new fibril formation (Mudher et al. 2017). These *seed*-competent species can range from single misfolded monomers to various oligomer assemblies or aggregates, comprising a wide array of Tau proteoforms with diverse PTMs, not limited to phosphorylation, and truncated variants (Mirbaha et al. 2018; Mirbaha et al. 2015; Mair et al. 2016). Despite these advances, the exact molecular mechanisms underlying Tau aggregation, propagation, and the specific species involved in seeding remain unresolved.
Our study focused on the R2Ct and R3Ct Tau fragments, which include the entire C-terminal domain starting from either the R2 or R3 repeats. These fragments can arise from both 4R and 3R isoforms for R3Ct, or exclusively from 4R isoforms for R2Ct. We found that R2Ct and R3Ct exhibit reduced or completely absent tubulin polymerization activity, respectively. Phosphorylation by GSK3β, which induces triple phosphorylation at the PHF-1 epitope, inhibits tubulin polymerization and causes a local conformational change that increases the likelihood of folding into an extended β-sheet conformation, particularly over the sequence containing the PHF-1 motif (residues 392-402) in both fragments.
Given the observed loss of microtubule (MT) polymerization function, we investigated the potential toxic roles of these fragments, both phosphorylated and unphosphorylated, in aggregation *seeding*. Heparin-induced *seeds* from these fragments demonstrated the ability to promote aggregation of the soluble versions of the fragments, depending on the monomer/*seed* combinations and their phosphorylation states. We observed that R3Ct *seeds* can induce *seeding* of both R2Ct and R3Ct monomers,

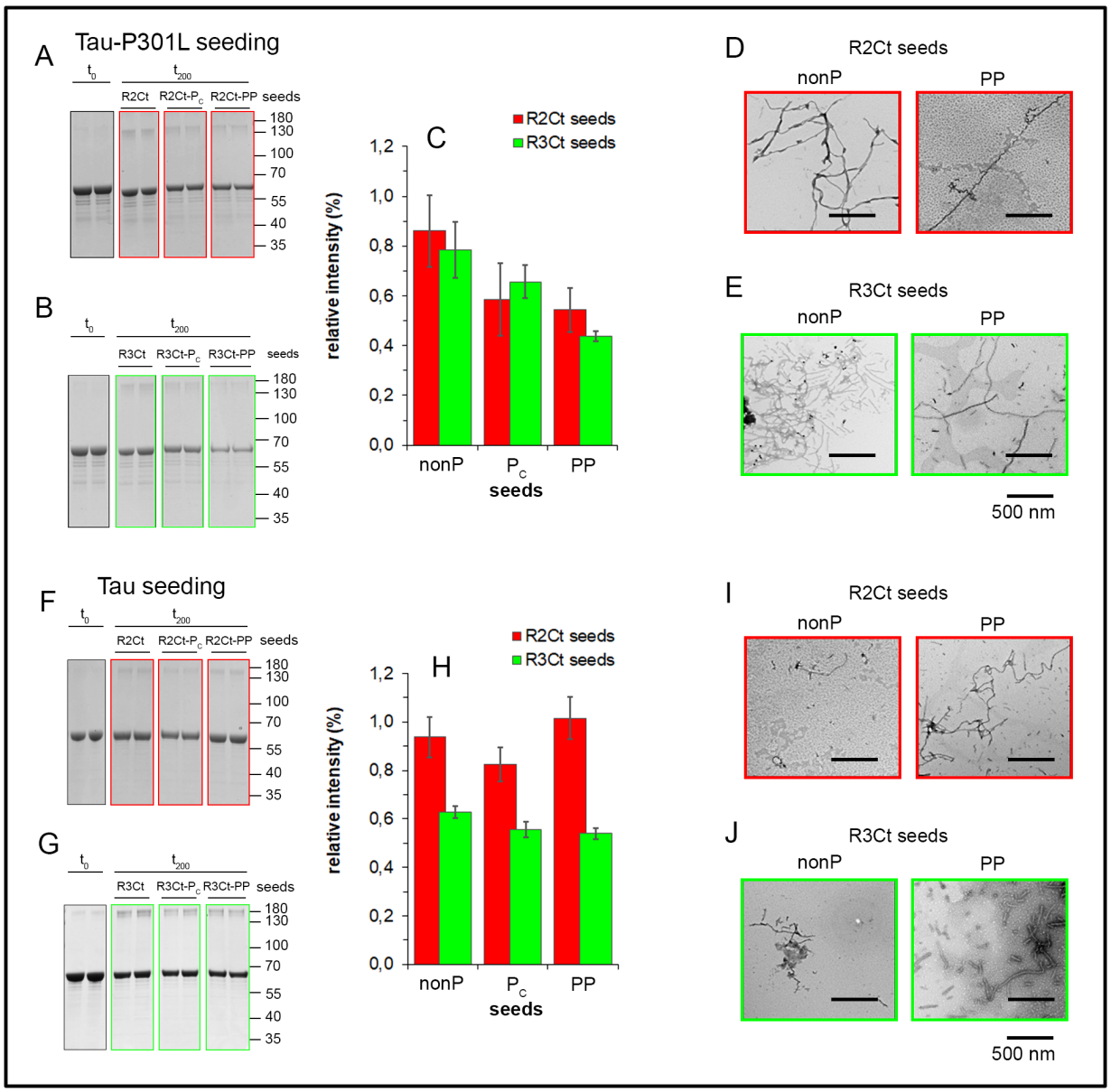

(AE) or Tau (FJ) devoid of the aggregation-prone mutation. *Seeds* are made from R2Ct or R3Ct segments that have not been phosphorylated (nonP), have been phosphorylated by CDK2 (R2Ct-PC or R3Ct-PC), or have been phosphorylated sequentially by CDK2 and GSK3β (R2Ct-PP or R3Ct-PP). When R2Ct (A, F) or R3Ct *seeds* (B, G) are applied, the sedimentation experiment is used to examine how full-length Tau aggregates. Measured as the ratio of the amount of protein in the soluble fraction after 200 hours at 37řC (t_{200}) with R2Ct (red) or R3Ct (green) *seeds* on the initial protein concentration prior to incubation (t_0) (n=2), the extent of Tau-P301L (C) or tau (H) aggregation is expressed as the mean ś SEM. fibrillar aggregates produced by R2Ct (red) or R3Ct (green) seed, as seen in negative staining TEM images.The ratio of the quantity of protein in the soluble fraction after 200 hours at 37řC (t_{200}) with R2Ct (red) or R3Ct (green) *seeds* on the initial protein concentration before incubation (t_0) (n=2), expressed as the mean ś SEM, indicates the degree of Tau-P301L (C) or Tau (H) aggregation. Images obtained by negative staining TEM demonstrating fibrillar aggregates generated on Tau-P301L (D, E) or tau (I, J) by *seeds* of R2Ct (red) or R3Ct (green), either non-phosphorylated (nonP) or phosphorylated by CDK2/GSK3β (PP)

Figure 9.12: Cross-*seeding* activity of full-length Tau 2N4R soluble monomers, either Tau-P301L mutant, with non-phosphorylated and phosphorylated R2Ct (red) or R3Ct (green) *seeds*

while R2Ct *seeds* only facilitate homologous *seeding*, indicating a cross-*seeding* barrier that restricts R2Ct *seeds* from promoting R3Ct aggregation, possibly due to the presence or absence of the R2 repeat. Our findings reveal that GSK3β phosphorylation of *seeds* can reduce the *seeding*/cross-

seeding barrier and/or modify conformational selection, enhancing the recruitment of monomers into *seeds*. Additionally, the efficiency of aggregation *seeding* appears to be a complex cooperative process involving interactions between the ability of *seeds* to template conformational changes and the monomers aggregation capacity. This study sheds light on the mechanisms of Tau aggregation *seeding* and the factors influencing Tau aggregation and pathology.

4. Application on Semi-Synthetic Tau

4.1. Generalities about Semi-Synthetic Proteins

Semi-synthetic proteins represent an advanced approach that integrates chemical synthesis techniques with recombinant protein expression methods. This hybrid strategy provides several distinct advantages over natural proteins, enhancing the ability to study and manipulate protein structures and functions. One of the primary benefits of using semi-synthetic proteins is the ability to introduce specific modifications at exact positions within the protein sequence. This precise control is often unattainable with natural proteins, where modifications are typically constrained to what is naturally encoded by the organism. Semi-synthetic methods also facilitate the incorporation of non-natural elements, such as synthetic amino acids, post-translational modifications, or spectroscopic probes, which are challenging or impossible to integrate using biological systems alone. This capability opens up new avenues for investigating novel protein functions and mechanisms.
Moreover, semi-synthesis addresses the limitations of size that are inherent in purely chemical synthesis approaches. By combining synthetic peptide segments with recombinant protein components, researchers can produce larger and more complex proteins that would be difficult to synthesize entirely through chemical methods. One of the key techniques enabling this capability is native chemical ligation (NCL) , developed by Stephen Kent and his student Philip Dawson, which allows the chemoselective condensation of unprotected peptide segments in aqueous solution. NCL specifically facilitates the ligation of a peptide with a C-terminal thioester to another peptide with an N-terminal cysteine residue, forming a native peptide bond at the ligation site. This method has revolutionized the field of chemical protein synthesis by allowing the total chemical synthesis of proteins over 30 kDa, thus overcoming the size limitations of traditional chemical synthesis methods (Dawson and Kent 2000).
This approach also ensures a high level of purity and homogeneity in the produced proteins, overcoming the biological variability often encountered with natural proteins. Semi-synthesis refers to methods that combine synthetic and recombinant techniques to produce proteins, allowing for greater control over the structure of the protein and the incorporation of specific modifications that may not be achievable through traditional recombinant methods. For instance, semi-synthetic strategies have been employed to produce acetylated forms of Tau, which can exhibit different aggregation properties compared to unmodified Tau (Haj-Yahya and Lashuel 2018). The flexibility offered by semi-synthetic methods allows researchers to design proteins with specific modifications tailored to particular applications, particularly in chemical biology and biophysical studies. This ability is crucial for understanding the impact of post-translational modifications on protein structure and function, offering insights into biological mechanisms that are not easily studied with natural proteins alone. Additionally, semi-synthetic proteins are particularly useful in spectroscopy. By preparing proteins with incorporated spectroscopic probes, researchers can conduct detailed studies on protein dynamics and interactions, gaining valuable information about protein behavior that might otherwise be inaccessible. Overall, semi-synthetic proteins provide a powerful tool for advancing protein science, enabling more precise and controlled studies of protein structure and function, and facilitating the exploration of complex biological systems (De Rosa et al. 2013).

4.2. Semi-Synthetic Tau Protein

Semi-synthetic Tau proteins are produced through a combination of chemical synthesis techniques and recombinant expression methods, allowing for the precise introduction of specific post-translational modifications (PTMs) at designated locations within the Tau protein sequence. This precision is particularly essential for studying the role of Tau in neurodegenerative diseases, such as Alzheimer's disease, where PTMs like phosphorylation play a critical role.

Advantages of Semi-Synthetic Tau Proteins

The semi-synthetic approach offers numerous advantages for studying Tau proteins, including precise control of modifications, which allows for the introduction of specific PTMs at defined positions in the Tau proteinsomething unattainable with purely biological methods. This approach also provides access to disease-associated modifications observed in tauopathies, aiding in the understanding of their impact on Tau aggregation and toxicity. Additionally, semi-synthetic methods enable researchers to study protein dynamics by analyzing how specific modifications affect Taus structural dynamics and interactions with microtubules and other cellular components. The production of semi-synthetic proteins with high purity and homogeneity overcomes the biological variability often seen with natural proteins. This approach also offers flexibility in research, allowing for the systematic introduction of multiple modifications to explore the complex interactions and functions of Tau in cellular environments. Furthermore, the knowledge gained from studying semi-synthetic Tau proteins can inform the development of targeted therapies aimed at preventing or reversing Tau-related pathologies.

Applications

Semi-synthetic Tau proteins have diverse applications in research, including the study of aggregation, where they are used to investigate the mechanisms of Tau aggregation and the formation of neurofibrillary tangles (NFTs), a key marker of neurodegenerative diseases. They also facilitate a deeper understanding of post-translational modifications (PTMs), allowing researchers to produce Tau proteins with specific modifications to directly examine the impact of these PTMs on Tau structure and function. Additionally, the ability to produce diverse Tau proteoforms with high purity offers unique opportunities for biomarker development, enabling the discovery of new biomarkers and the creation of more precise assays to quantify total Tau and specific PTMs in tauopathies.
Given that Tau phosphorylation is one of the most extensively studied PTMs, we have specifically focused on the phosphorylation of the PHF1 epitope in this project. In collaboration with Prof. Christian Hackenberger's team at FMP-Berlin, Germany, and through the various stays of his post-doc in our laboratory, we used the semi-synthetic proteins they developed, carrying either two phosphorylations (Ser396, Ser404 as ss2P) or three phosphorylations (Ser396, Ser400, Ser404 as ss3P). This was achieved by leveraging the C-terminal position of the PHF-1 epitope in the Tau sequence, allowing a single ligation step with the recombinant (1-389) domain to complete the semi-synthesis of the full-length protein (Figure 9.13).
The objective of achieving proteins via semi-synthetic methods is to overcome the issue of heterogeneity. This approach allows for the site-specific installation of any desired modification, such as phosphorylation. Typically, they first prepared the phospho-Ser building block and then incorporate it into the peptide via solid-phase peptide synthesis. For wild-type Tau, there are no differences between recombinant and semi-synthetic methods (ssWT). However, using the semi-synthetic approach to achieve proteins bearing PTMs or even different PTMs offers significant advantages for subsequent cross-talk analysis. This innovative approach to semi-synthetic Tau proteins opens new perspectives for fundamental and applied research on neurodegenerative diseases, providing valuable tools to better understand and potentially treat these conditions (Lim and Li 2022).

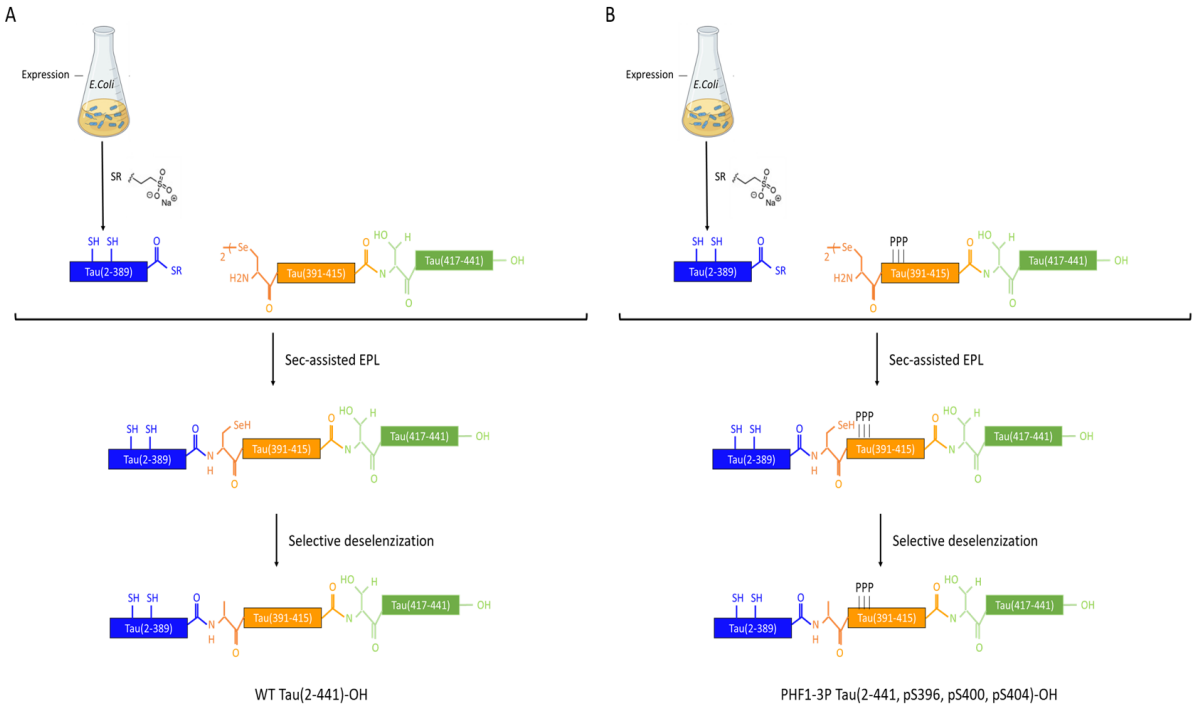

(A) ssWT Semi-Synthesis: Expression of Tau(2-389) in E. coli and subsequent ligation with synthetic Tau(391-415) containing N-terminal selenocysteine and Tau(417-441) via Sec-assisted EPL, followed by selective deselenization to produce WT Tau(2-441)-OH. (B) ss3P Semi-Synthesis: Expression of Tau(2-389) in E. coli and ligation with modified Tau(391-415) containing N-terminal selenocysteine and multiple phosphorylation sites (pS396, pS400, pS404), and Tau(417-441) through Sec-assisted EPL, followed by selective deselenization to generate PHF1-3P Tau(2-441, pS396, pS400, pS404)-OH.

Figure 9.13: Semi-synthesis of (A) ssWT and (B) ss3P Tau(2-441) using Sec-assisted Expressed Protein Ligation (EPL) and selective deselenization.

4.3. PHF-1 Phosphorylation impact on Semi-Synthetic Tau-Induced Tubulin Polymerization

Using *in vitro* tubulin polymerisation assays, all three semi-synthetic Tau proteins were incubated at 37 řC in tubulin polymerisation buffer (80 mM PIPES, pH 6.9, 0.5 mM EGTA, 2 mM $MgCl_2$) containing 20 μM of α,β-tubulin dimer and a fluorescent reporter in order to assess the role of Tau proteins in controlling the stability and assembly of MT. The fluorescence at 460 nm was recorded for one hour in order to track the MT assembly. As seen in Figure 9.14, tubulin assembly was induced more quickly in case of ssWT; fluorescence peaked after 30 minutes, whereas the plateau was achieved by both ss2P and ss3P after 40 minutes. As anticipated, the PHF-1 proteoforms of ss2P and ss3P significantly hindered Tau-mediated MT assembly, resulting in a 20% reduction in total fluorescence intensity in comparison to ssWT. Those results are compatible with what is described in the literature (Gong and Iqbal 2008; Alonso et al. 2018).

Negative charge can inhibit Tau-tubulin polymerization. Tau's interaction with tubulin and microtubules is influenced by electrical properties, as Tau normally has a positive charge that allows it to bind to the negatively charged microtubules. More especially, it is thought that Tau interacts with the acidic tubulin C-terminal tails (CTTs), which are disordered segments extended from each tubulin monomer of α β tubulin heterodimers. The tubulin CTTs contribute to the regulation of MT interaction with other proteins and control MT polymerization dynamics impacting the intracellular transport of organelles and vesicles through protein motors. Factors that neutralize or modulate tau's electrical properties can facilitate conformational changes and expose aggregation-prone motifs (Hu et al. 2023). RNA, a negatively charged molecule, inhibits Tau-mediated microtubule assembly; for exam-

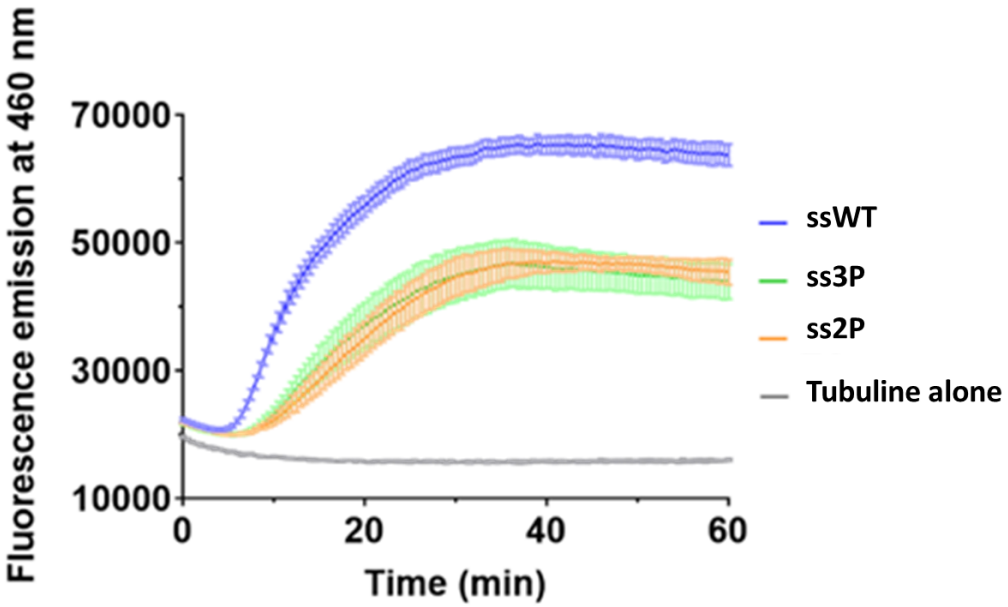

Figure 9.14: In vitro tubulin polymerization assay (2 μM) in the presence of 20 μM of WT Tau (blue), homogeneous and site-specific PHF1-2P Tau (green), PHF1-3P Tau (orange) and Tubulin alone (grey)

ple, poly(A) RNA blocks Tau's ability to stimulate microtubule polymerization in a dose-dependent manner. Tau has a higher affinity for linear homopolymeric RNA (like poly(A)) compared to tubulin, with about a five-fold greater affinity (McMillan et al. 2023b). Phosphorylation, which adds negative charges to Tau, affects its interaction with microtubules, as hyperphosphorylation of Tau reduces its ability to bind to microtubules. Phosphorylation may neutralize the positive charges in Tau, limiting its intermolecular interactions with tubulin. Here, the phosphorylation restricted to the single PHF-1 epitope only moderately affects MT assembly in a way that is dependent of the phosphorylation state.

4.4. Heparin induced self-assembly into PHF-like filaments of semi-synthetic Tau

We first conducted a *in vitro* aggregation assay to examine the effects of phosphorylation on the kinetics of Tau fibril formation. We did this by incubating the semi-synthetic Tau proteins (10 μM for ssWT, ss2P, and ss3P) in aggregation buffer (50 mM MES, pH 6.9, 2.5 mM EDTA, 30 mM NaCl, 0.33 mM DTT) for approximately two days without shaking. Thioflavin T (ThT) fluorescence was used as a reporter to track the development of fibril formation. None of the three semi-synthetic Tau proteins (ssWT, ss2P, and ss3P) could form fibrils in the absence of heparin (negative control) (Figure 9.15 A).

Heparin-induced aggregation was shown to begin slower in the PHF-1 proteoforms of ss2P and ss3P than for the non-phosphorylated ssWT, with ss3P aggregating even more slowly than ss2P.

Fitting the kinetic data with AmyloFit, a model system implemented for Aβ42 aggregation as described by Knowles and coworkers (Meisl et al. 2016) suggests a mechanism involving both primary and secondary nucleation pathways in which the primary fibril surface act as a catalyst to promote the growth of new fibrils in a second step of nucleation. For both ss3P and ss2P, AmyloFit indicates an aggregation process dominated by the secondary nucleation pathway in contrast to ssWT where the primary nucleation pathway dominates. We also observed an increased lag phase in both ss3P and ss2P as compared to ssWT. Collectively, for the above-mentioned reasons, both ss2P and ss3P demonstrate a slower onset of heparin-induced aggregation with the primary formed fibrils contributing to the acceleration of the aggregation process thanks to a secondary nucleation pathway.

All three semi-synthetic Tau proteins, ssWT, ss2P, and ss3P, were able to form PHF-like fibrils in a

ssTau proteoform	non-P	PHF1-2P	PHF1-3P
k_+k_n $[\text{Tau monomer}]^{-2} \cdot \text{h}^{-2}$	$1,57 \times 10^8$	$3,13 \times 10^7$	$1,93 \times 10^7$
k_+k_2 $[\text{Tau monomer}]^{-3} \cdot \text{h}^{-2}$	$1,58 \times 10^4$	$2,11 \times 10^{13}$	$1,05 \times 10^{13}$
n_c	2	2	2
n_2	2	2	2

Table 9.1: Kinetics parameters of aggregation of ssWT, ss2P and ss3P incorporating both primary and secondary pathways where kn is the rate constant of primary nucleation, k2 the rate constant of secondary nucleation, k_+ the rate constant of elongation, n_c and n_2 the reaction orders describing the dependencies of primary and secondary pathways, respectively, on the monomer concentration. Kinetics were fitted with AmyloFit

heparin-induced aggregation assay, according to a transmission electron microscopy (TEM) analysis of the fibril morphologies at the end of the *in vitro* aggregation reactions (Figure 9.15 C). To be more precise, ssWT produced a large number of flexible fibrils, while ss2P and ss3P produced fewer, longer, curly fibrils, with a lower quantity of fibrils in both samples than in ssWT.
A different series of studies was carried out to evaluate the distribution of Tau species in order to further quantify heparin-induced aggregation of semi-synthetic Tau proteins. We used a filter-trap test, in which aggregation reactions were stained with either Ht-7 (epitope defined as residues 159-163) or PHF-1 (epitope usually defined as pS396/pS404) antibody, to quantify insoluble/aggregated proteins, and a sedimentation assay to assess loss of soluble protein monomers. All of the heparin-induced aggregation samples were put onto SDS-PAGE at t_0 and t_{48}, the times after which they were incubated at 37řC with heparin.
After 48 hours of incubation, the sedimentation assay results showed a considerable loss of soluble Tau for all three semi-synthetic proteins. In the filter-trap assay, Tau sample ssWT consistently accumulated in the insoluble fraction (Figure 9.15 E). On the other hand, even while the soluble fraction in the sedimentation experiment decreased similarly to that of the phosphorylated Tau aggregates ss2P and ss3P, their abundance in the insoluble fraction was lower than that of ssWT.
When considered collectively, these data imply that site-specific hyperphosphorylation of the PHF-1 epitope may lessen the *in vitro* heparin-induced aggregation of Tau by encouraging the creation of soluble oligomers or tiny aggregates that are not caught in the filter-trap experiment.
Those results contradict the hypothesis that Tau phosphorylation accelerates or induces Tau aggregation and that C-terminal serine PHF-1 residues (S396, S400, S404) phosphorylated by GSK3β are abnormally hyperphosphorylated in AD brains (Chakraborty et al. 2023). However, we continued to see longer PHF-like fibrillar aggregates and increased ThT fluorescence intensity with ss2P and ss3P (Figure 9.15 B and C). When considered collectively, these data suggest that homogenous site-specific PHF-1 hyperphosphorylation of Tau protein merely lowers the elongation rate in the heparin-induced aggregation model.
A previous finding reported that the PHF-1 hyperphosphorylation mediated by GSK3β kinase activity promotes fibril formation with kinetics comparable to non-phosphorylated Tau as induced by heparin (Chakraborty et al. 2023). The heterogeneity of the enzymatic phosphorylation pattern may therefore retain sufficient amounts of non- or less phosphorylated species to promote aggregation to some extent in a primary nucleation step. The non- or less-phosphorylated aggregates may then act as seeds for the aggregation of highly phosphorylated species, which can be efficiently incorporated during the elongation step. In contrast, the secondary nucleation mechanism observed in our study would likely be caused by the homogeneous phosphorylation where repulsion between phosphate groups and heparin further interferes with heparin binding to the microtubule binding domain in the primary nucleation pathway of the aggregation process. The homogeneous phosphorylation obtained by the expressed protein ligation thus provided mechanistic details of the aggregation process of phos-

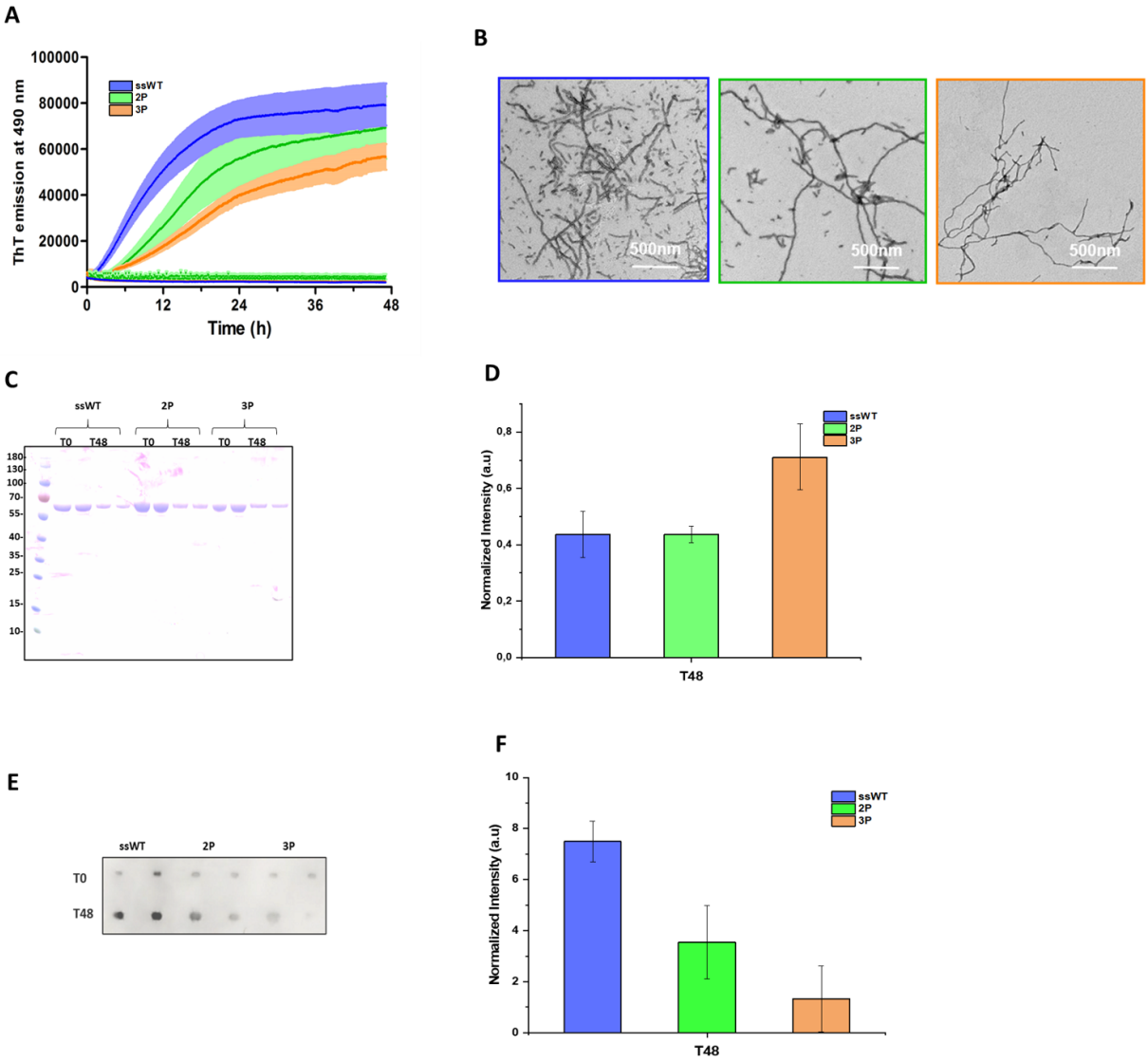

(A) Time-dependent aggregation induced by heparin monitored by changes of ThT fluorescence intensity for ssWT (Blue), 2P (Green), and 3P (orange). (B) TEM images of fibrils from the three semi-synthetic Tau proteins induced by heparin. (C-D) Sedimentation assay: (C) SDS-PAGE showing proteins in the aggregation reaction and (D) quantitative analysis normalized to the initial time point (t0). (E-F) Filter trap assay: (E) Dot blot stained with HT-7 monoclonal antibody and (F) quantitative analysis normalized to t0. Data shown correspond to the total aggregation reaction

Figure 9.15: In vitro heparin (2.5 μM)-induced aggregation assay (10 μM) in the presence of semi-synthetic Tau

phorylated Tau protein induced by heparin, suggesting that phosphorylation reduces the efficiency of primary nucleation and makes better use of the secondary nucleation pathway.

4.5. Seeding and Cross-seeding of semi-synthethic Tau

In order to mitigate potential issues arising from Tau protein phosphorylation-induced interference with heparin binding (ss2P, ss3P), we opted to assess Tau aggregation capabilities through a cross-seeding approach that better simulated disease.
Based on the following factors, we chose and used the Tau(300-441) fragment (R3Ct), previously characterized as *seeds*: It has two microtubule binding repeats (R3 and R4) that make up the core of the PHFs from AD brain, it has the C-terminus so that we can use known kinases, like GSK3β

or CDK2/cyclin A, to recapitulate the various phosphorylation patterns of the PHF-1 epitope (Figure 9.1 C). Additionally, in our previous study (described in Paragraph 3 of this Chapter), we have shown that the R3Ct seeds are more efficient than R2Ct seeds to promote seeding of full-length tau 2N4R isoform.
As a recombinant protein, unmodified R3Ct was produced and purified with ease. Two additional phosphorylated proteoforms were subsequently generated by either sequentially incubating CDK2 and GSK3β to produce a comparatively homogenous (> 95 %) tri-phosphorylated PHF-1 epitope (PP-R3Ct, pS396, pS400, and pS404, Figure 9.16) or by incubating unmodified R3Ct with CDK2 to yield primarily a mono-phosphorylated fragment on S404 and a lesser degree of phosphorylation on pS396 (P-R3Ct, Figure9.16).

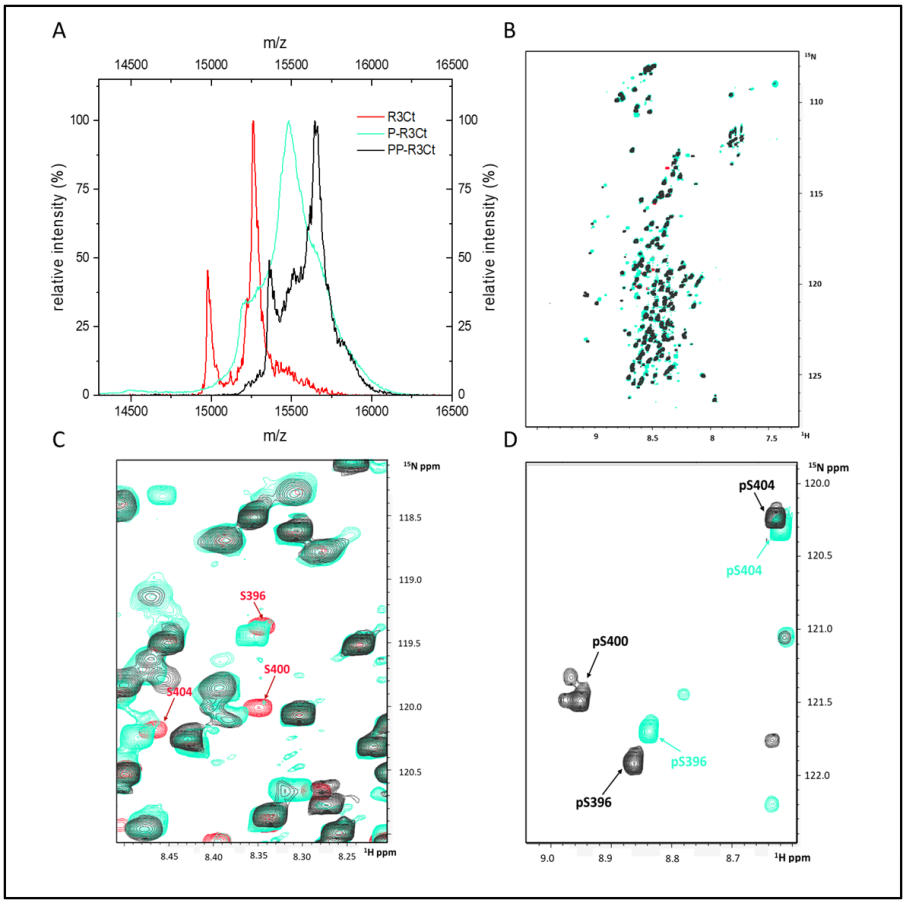

(A) Mass spectrometry analyses of R3Ct before (red) and after after CDK2 (Cyan) or CDK2/ GSK3β (black) phosphorylation (B) ^{15N}HSQC spectra of R3Ct before (red) and after after CDK2 (Cyan) or CDK2/ GSK3β (black) phosphorylation (C-D) Zoom of the ^{15N}HSQC on PHF-1 region where we can see the unphosphorylated (C) and phopshorylated sites

Figure 9.16: Phosphorylation of R3Ct

Having obtained the fragment proteoforms (R3Ct, R3Ct-P, and R3Ct-PP), we proceeded to create the *seeds* by starting the fragment aggregation process (10 μM) with 1 μM heparin at 37 řC for a duration of 7 days. After that, 1 μM of every *seed* was incubated for an additional 8 days at 37 řC without shaking with 10 μM of each of the three semi-synthetic Tau proteins for ssWT, 2P, and 3P.
To produce the *seeds*, we reduced the protein to heparin ratio (to 1:10). We then diluted the Tau seeds (R3Ct, R3Ct-P, and R3Ct-PP) to 1 μM in order to rule out the possibility that the heparin was causing the newly added monomeric semi-synthetic Tau proteins to aggregate.
The cross-*seeding* procedure was observed using ThT. However, the ThT fluorescence intensity rose very slowly, which made it challenging to compare the relative kinetic parameters of aggregation and interpret future data.

Following the cross-*seeding* reactions, TEM was used to examine the fibril structures in each instance. The three variants R3Ct, R3Ct-P and R3Ct-PP, which were generated as *seeds*, primarily aggregated into individual short-length fibrils. However, we saw mostly clusters of short-length fibrils in every instance when we incubated unmodified R3Ct *seeds* with each of the three semi-synthetic Tau proteins (ssWT, ss2P and ss3P) (Figure 9.17).

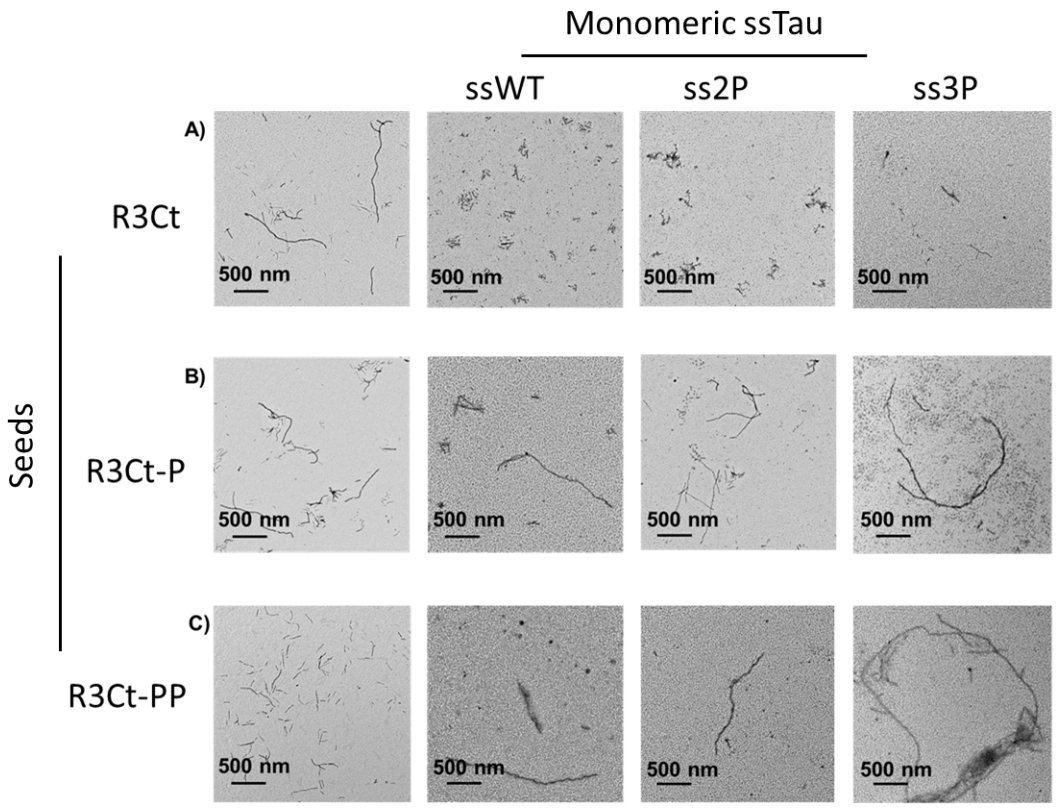

Negative staining TEM images showing fibrillar aggregates of the semi-synthethic *seeding* assay by (A) R3Ct, (B) R3Ct-P and (C) R3Ct-PP

Figure 9.17: Negative staining TEM images showing fibrillar aggregates of the semi-synthethic *seeding* assay

When monomeric semi-synthetic Tau proteins (ssWT, ss2P, and ss3P) were present during the cross-*seeding* experiment using either R3Ct-P or R3Ct-PP *seeds*, the TEM images that were gathered demonstrated a noticeable increase in fibril length, indicating the development of PHF-like fibrils. We observed that cross-*seeding* with R3Ct primarily resulted in the formation of short-length fibrillar clusters. In contrast, in other cases, we mainly saw the presence of PHF-like filaments, with particularly large elongated fibrillar clusters forming when cross-*seeding* R3Ct-PP with ss3P (Figure 9.17 C).

These observations were consistent with the data collected from sedimentation and filter-trap assays when we quantified the Tau cross-*seeding* aggregates, which are described for heparin-induced aggregation experiments, in accordance with the unique fibril labelling seen by TEM. For the sedimentation experiment, 0.5 μg of each cross-*seeding* reaction was loaded onto SDS-PAGE before (t_0) and after 200 hours of incubation at 37 řC (t_{200}) and 10 ng were dotted onto the membrane for the filter-trap assay (Figure 9.18). According to our findings, using R3Ct *seeds* significantly reduces the amount of soluble protein while simultaneously causing the greatest degree of insoluble protein/aggregates out of all ssWT seedings. When phosphorylated semi-synthetic Tau ss2P and ss3P are seeded with R3Ct-P as opposed to ssWT, there is a notable rise in the quantity of insoluble protein/aggregates seen. Additionally, the filter-trap and sedimentation experiments demonstrate that the maximum level of soluble protein loss and insoluble protein accumulation for phosphorylated semi-synthetic Tau ss3P

occurs during *seeding* procedures utilising R3Ct-PP *seeds*. Interestingly, these findings highlight how crucial triple phosphorylation of the PHF-1 epitope is for effective 2N4R Tau fibril production and *seeding*. Consequently, it seems that phosphorylated *seeds* preferentially promote templated aggregation of phosphorylated 2N4R Tau with the highest efficiency for the identical triple phosphorylation of PHF-1 in both *seeds* and monomers, whereas non-phosphorylated R3Ct *seeds* were able to template the aggregation of 2N4R Tau regardless of their phosphorylation state with the highest efficiency for non-phosphorylated Tau. When considered collectively, these findings show that hyperphosphorylated Tau at the PHF-1 epitope can stimulate the aggregation within a modelled diseased setting.

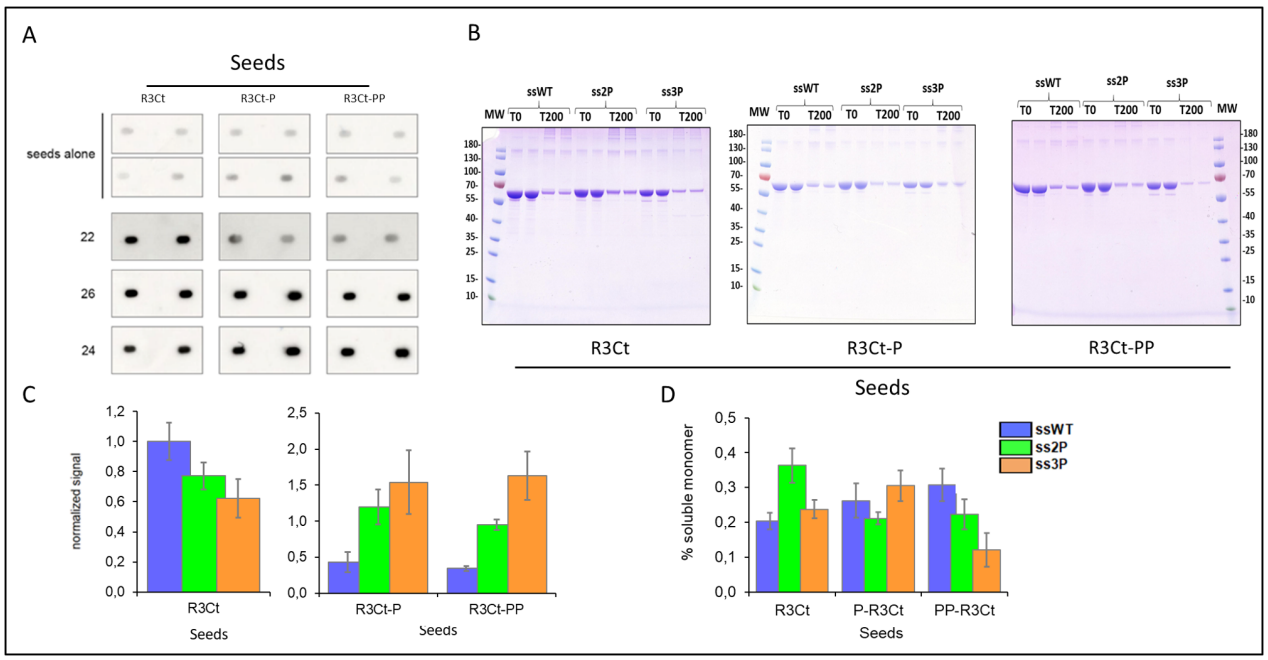

Cross-*seeding* experiment using 1 μM of R3Ct, R3Ct-P, and R3Ct-PP Tau *seeds* with semi-synthetic 2N4R ssWT (blue), homogenous and site-specific 2N4R ss2P Tau (green), and ss3P Tau (orange). The aggregation responses at T0 and T200 were assessed using the following methods: (A) filter-trap assay; and (C) quantitative analysis for normalization of ssTau monomer seeding with R3Ct seeds. In the first graph, all ssTau protein monomers are normalized using R3Ct seeds. In the second graph, each ssTau monomer seeding with R3Ct-P or R3Ct-PP seeds is normalized against R3Ct seeds (B) SDS-PAGE of the sedimentation test and (D) quantitative analysis. T0 was used for normalisation in the sedimentation test

Figure 9.18: Cross-*seeding* experiment of semi-synthetic Tau proteins using *seeds* of R3Ct and phosphorylated proteoforms

To ascertain if the fibrils shown in TEM were caused by the aggregation of monomeric semi-synthetic Tau proteins integrated into the seeds, we carried out an immuno-gold labelling of fibrils. Except for the cross-seeding of ssWT with R3Ct-P and R3Ct-PP, all of our cross-seeding processes produced fibrils containing the semi-synthetic Tau proteins. Only the non-phosphorylated seeds (R3Ct) exhibit the seeding of non-phosphorylated Tau ssWT aggregation (Figure 9.19). This implies that the semi-synthetic Tau (ss2P, ss3P) must be phosphorylated in order for phosphorylated *seeds* to initiate aggregation.

The cryo-EM structures of filament cores from different tauopathies do not contain PHF-1 or other phospho-epitopes, despite the fact that hyperphosphorylation is a common characteristic of fibrillar Tau from patient brains. Phosphorylation sites, which are often located in the regions flanking the repeat domains or in the C-terminal domain, are not part of the ordered core structure visible in these cryo-EM studies (Figure 3.2). For phosphorylation sites that potentially occupy residues within the fibril core, it could be difficult to see phosphorylation sites inside the fibril structure due to the heterogeneity of phosphorylation. Because of the homogeneity of PHF-1 phosphorylation that our method provides, cryo-EM may be able to shed more light on atomic interactions, particularly the structural

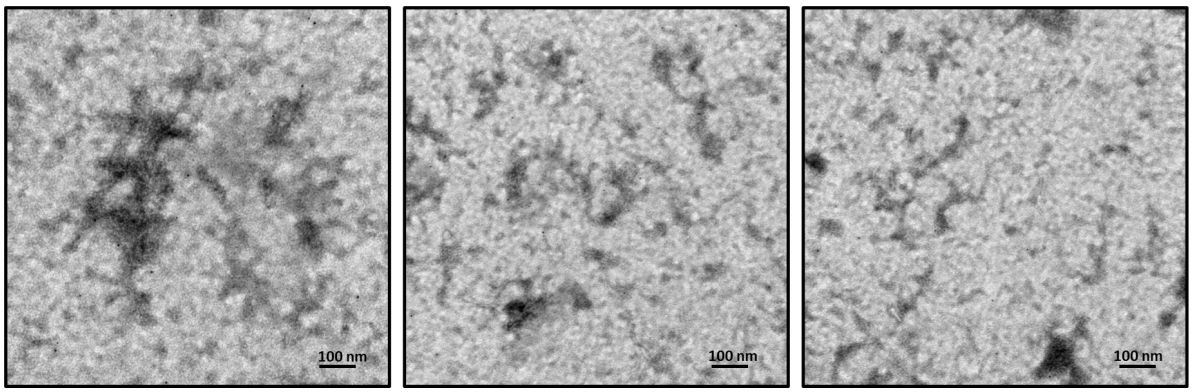

Figure 9.19: Immuno-gold labeling assay on ssWT Tau with R3Ct *seeds*

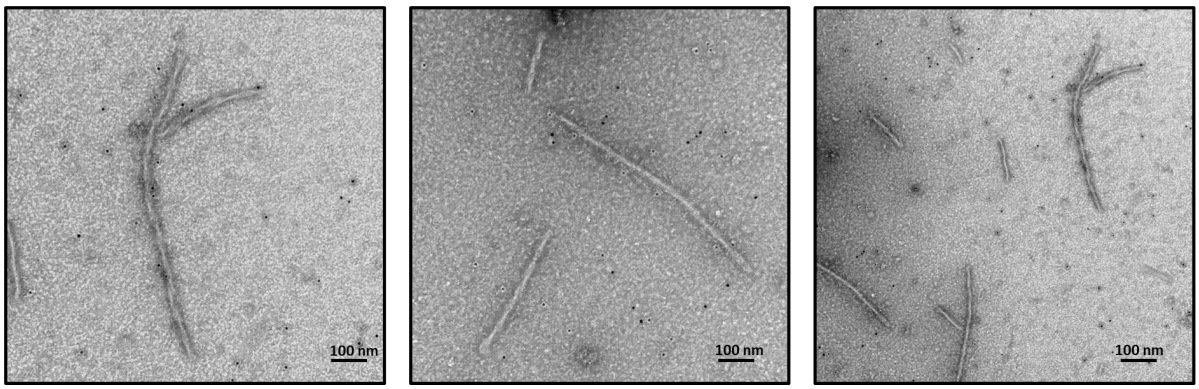

Figure 9.20: Immuno-gold labeling assay on ss3P Tau with R3Ct-PP *seeds*

ones. This could lead to new discoveries regarding the aggregation mechanisms that underlie neurodegenerative diseases and the identification of possible therapeutic targets.

4.6. Conclusion

Tau is subjected to numerous PTMs, particularly phosphorylation, which impacts its interactions with microtubules (MTs), fibril aggregation, and *seeding* activity. The PHF-1 epitopewhich includes pS396/pS404 or pS396/pS400/pS404is relevant to pathogenesis. The primary challenge in studying Tau phosphorylation is the lack of specific tools for accurately identifying and quantifying phosphorylated Tau at various sites. Research indicates that Tau is hyperphosphorylated in the brains of tauopathy patients, a factor crucial to disease progression. This limitation has led to reliance on generalized assays that may not fully capture Tau's phosphorylation profile. In contrast, significant progress has been made in understanding α-synuclein, particularly concerning its phosphorylation and O-GlcNAcylation. Recent advancements involve using semi-synthetic α-synuclein proteins to create fibrils that can be precisely modified and analyzed, revealing how phosphorylation and O-GlcNAcylation affect α-synuclein's aggregation and toxicity (Hu et al. 2024). These findings suggest that adopting similar semi-synthetic approaches for Tau could enhance site-specific phosphorylation analysis, offering deeper insights into Tau's role in neurodegeneration and potentially uncovering new therapeutic targets.

PHF1-3P Tau can be prepared to a high standard using our semi-synthetic approach, which maintains the native sequence and important cysteine residues. Using this technique, it was found that hyperphosphorylated Tau proteins (ss2P and ss3P) impede MT binding and decrease aggregation kinetics in comparison to Tau protein ssWT. This is probably because heparin's activity is inhibited by the repulsion of negative charges.

PHF-1 proteoforms with triple phosphorylation are important in pathological aggregation, as evidenced by cross-*seeding* tests that revealed phosphorylated seeds preferentially enhance phosphory-

lated Tau aggregation while non-phosphorylated *seeds* effect all proteins similarly.
The significance of homogenous site-specific Tau proteins for comprehending PTM codes and their influence on Tau-MT interactions and aggregation is emphasised by this study. Research on tauopathy and Alzheimer's is aided by the semi-synthetic approach, which offers a fresh paradigm for examining PTMs and related cross-talk pathways.

Chapter 10: Nanobody Inhibition of Aggregation

Alzheimer's and related conditions known as tauopathies cause Tau proteins to clump into filaments in brain cells. Here, we employed single domain antibody fragments or camelid heavy-chain-only antibody fragments (VHHs) that target Tau as immuno-modulators of its pathologic seeding.
The results presented in this section are part of a laboratory project in which I participated during a one-month internship in Lisbon, conducted in collaboration with Professor Cláudio Gomes's team. Some of the obtained results were included in an article: *A selection and optimization strategy for single-domain antibodies targeting the PHF6 linear peptide within the tau intrinsically disordered protein*.

1. General introduction about nanobodies

Nanobodies, also known as single-domain antibodies, are emerging as powerful tools for targeting Tau protein in the context of tauopathies such as Alzheimer's disease (AD).
Derived from the variable domains of heavy chain-only antibodies found in camelids (e.g., alpacas, llamas), nanobodies are small ($\approx$ 15 kDa) and consist of a single variable domain, enabling specific antigen binding. They can be generated through immunization followed by phage display library screening or direct panning of synthetic phage libraries, often requiring extensive secondary screening for high specificity and affinity.
Recent advancements include using quantitative flow cytometric sorting of yeast-displayed libraries to directly select nanobodies that bind selectively to Tau fibrils, bypassing secondary screening (Zupancic et al. 2023). The goal is to develop nanobodies with high sequence specificity, conformational specificity, and low off-target binding to effectively target pathological Tau. Nanobodies can detect Tau aggregates in biological samples and tissues, valuable for research and diagnostics, and hold therapeutic potential by inhibiting the seeding of Tau fibrils and oligomers, potentially preventing Tau pathology spread in neurodegenerative diseases. Their small size allows better tissue penetration and potential blood-brain barrier crossing, making them attractive candidates for in vivo applications and therapies for tauopathies (Abskharon et al. 2023).
The penetration of the blood-brain barrier (BBB) by single-domain antibodies (VHHs) is not consistent, and several mechanisms influence this process. Receptor-mediated transcytosis is a key mechanism through which certain molecules, including antibodies, can cross the BBB. This process involves specific receptors, such as the transferrin receptor (TfR), which facilitate the transport of molecules across the endothelial cells of the BBB. VHHs that target these receptors can be internalized and transported into the brain (Wouters et al. 2022). Adsorptive transcytosis is another mechanism by which positively charged molecules can cross the BBB. VHHs with a high isoelectric point (pI), often above 7, enhance this passage due to their positive charge, which facilitates interaction with cell membranes (Pothin, Lesuisse, and Lafaye 2020). Although passive diffusion is less common for antibodies due to their size, certain VHHs, especially those with specific characteristics like increased hydrophilicity, can cross the BBB via passive diffusion (Tsitokana et al. 2023). To enhance BBB crossing, several strategies can be employed. Adding positive charges to the surface of VHHs has been shown to improve their ability to cross the BBB; for instance, cationized VHHs have demonstrated better brain

penetration due to their enhanced interaction with endothelial membranes. Encapsulating VHHs in nanoparticles, such as liposomes, can improve their bioavailability and ability to cross the BBB, as this method allows targeting of specific receptors on the BBB, thereby increasing transport efficiency (Pothin, Lesuisse, and Lafaye 2020). Optimizing the affinity of VHHs for specific BBB receptors, such as TfR, can also enhance their penetration. Studies have shown that VHHs with higher affinity for these receptors are more effective at crossing the BBB (Wouters et al. 2022). Finally, developing in vitro models of the BBB allows for testing and optimizing VHHs for their ability to cross the barrier, helping to evaluate the impact of various modifications on brain penetration (Tsitokana et al. 2023).

1.1. Structure and properties of nanobodies

Structurally, VHHs have a compact, globular form characterized by three complementarity-determining regions (CDRs) that form the antigen-binding site. Their small size, around 2-3 nm in diameter, enables them to access epitopes that are often unreachable for conventional antibodies. VHHs exhibit remarkable stability, maintaining functionality under extreme pH and temperature conditions, and they generally have higher solubility compared to conventional antibody fragments. Their small size also facilitates better tissue penetration and, in some cases, the ability to cross the blood-brain barrier more effectively than full antibodies. Furthermore, VHHs can be engineered to target intracellular proteins, demonstrating high specificity and affinity towards their targets while maintaining low immunogenicity due to their similarity to human VH domains. Additionally, VHHs are easily produced in microbial expression systems and can be readily engineered into multivalent or bispecific formats. These properties render VHHs valuable tools across various applications, including research for protein detection and imaging, therapeutic interventions targeting intracellular proteins, diagnostic assays, and as potential delivery vehicles for drugs or other therapeutic agents (Mortelecque et al. 2024).

1.2. Mechanism of Tau aggregation inhibition

The mechanism of Tau aggregation inhibition by VHHs (nanobodies) involves several key aspects. Primarily, VHHs such as E4-1 and Z70 target the PHF6 sequence (VQIVYK) within the Tau protein (Danis et al. 2022; Mortelecque et al. 2024). This sequence is critical for Tau aggregation as it nucleates the aggregation process and forms part of the core of Tau fibrils. By specifically binding to the PHF6 sequence, these VHHs interfere with the assembly of Tau into fibrils, as evidenced by reduced formation of Tau fibrils in in vitro aggregation assays in their presence. The presence of VHHs, like E4-1, slows down the kinetics of Tau aggregation, demonstrated by a longer time to reach 50% of the maximal aggregation signal compared to controls. Additionally, at equimolar concentrations of Tau and VHH, the total amount of aggregation, measured by thioflavin T fluorescence, is significantly reduced. VHH Z70, for instance, shows almost complete inhibition of fibril formation at equimolar concentrations.

VHHs can be engineered to penetrate cells and act intracellularly, targeting Tau aggregation directly within neurons where most pathological Tau resides. By binding to the PHF6 region, VHHs may also compete with aggregation-promoting factors like heparin in in vitro assays. Although not explicitly stated in the results, the binding of VHHs to the PHF6 sequence may stabilize the monomeric form of tau, preventing its conversion into aggregation-prone conformations. Moreover, the inhibition of Tau aggregation by VHHs appears to be dose-dependent, with higher concentrations of VHHs leading to greater inhibition of aggregation. These properties collectively highlight the potential of VHHs as therapeutic agents in mitigating tauopathies by inhibiting Tau aggregation through multiple mechanisms (Danis et al. 2022; Mortelecque et al. 2024).

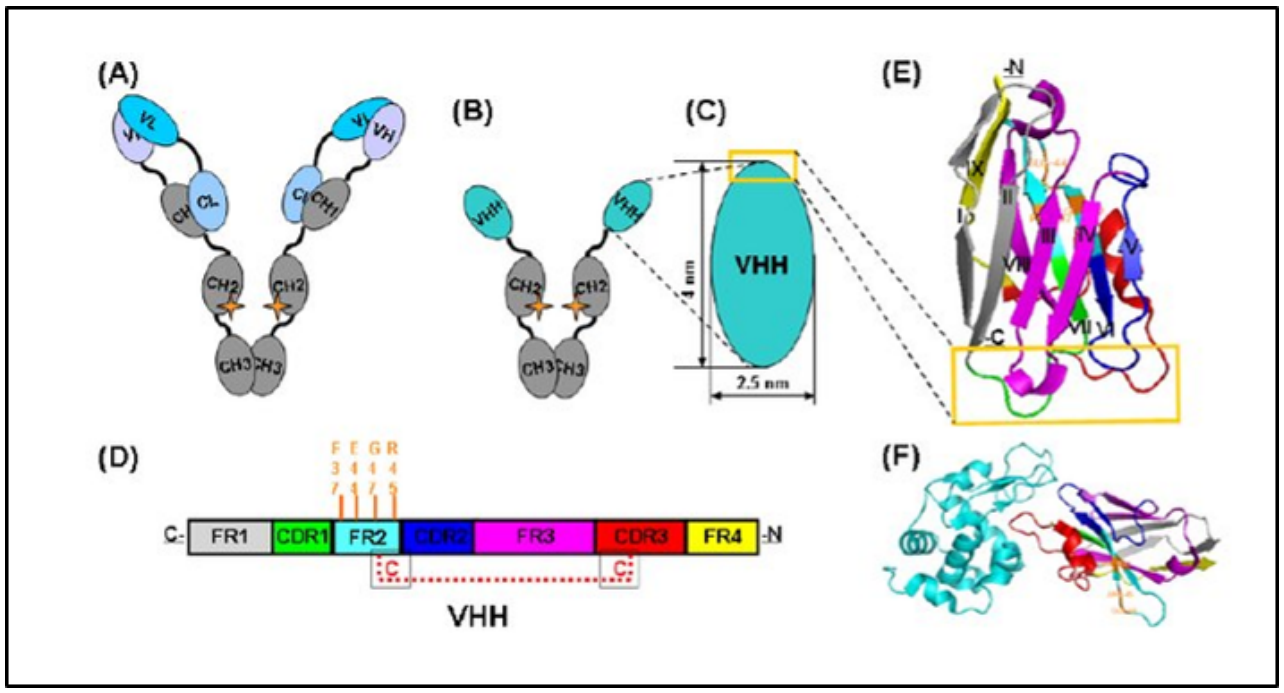

(A) A typical IgG antibody is a dimer with two heavy and two light chains. The heavy chain includes variable (VH) and constant (CH1, CH2, CH3) domains, while the light chain has one variable (VL) and one constant (CL) domain. Glycosylation sites in CH2 (orange stars) contribute to flexibility and effector functions (B) HCAbs have a single variable domain (VHH) as the paratope (yellow box) and lack the light chain and CH1 (C) VHHs are soluble, 15 kDa molecules with an antigen-binding site (yellow box) (D) VHHs contain three CDRs (green, blue, red) and four FRs (grey, cyan, magenta, yellow). FR2 has key hydrophobic residues (orange). A disulphide bond (dotted red) stabilizes FR2 and CDR3 (E) The anti-lysozyme VHH structure shows Ig folding with β sheets. The antigen-binding site (yellow box) is formed by CDRs (F) VHH binds lysozyme (light blue), with CDR3 (red) recognizing and inhibiting its catalytic cleft (Cardoso et al. 2012).

Figure 10.1: Diagrams showing an HCAb, a VHH, and a typical antibody

1.3. Study of the effect of H3-2 and Z-70 nanobodies on the inhibition of Tau aggregation

Seeding Inhibition by Z-70

We investigated the impact of the nanobody Z-70 on the aggregation of the Tau protein fragment K18 under two distinct conditions: one without *seeds* and one with 10 μM of seeds. For each condition, we tested three different ratios of K18 to Z-70: 1:0, 1:0.1, and 1:0.25.

Initially, we analyzed the aggregation curves of K18 in the presence of different concentrations of Z-70, without the presence of K18 *seeds*. The aggregation curves are displayed in Figure 10.3. In these experiments, aggregation was induced by the addition of 5 μM heparin. The curves represent four replicates per condition.

From these curves, we extracted the half-reaction times for each aggregation reaction. It was observed that the half-reaction times were consistent within the same conditions. Based on these data, we plotted a histogram of the averaged half-reaction times, as shown in Figure 10.3 B. The data indicate that the half-reaction time increases with the increasing concentration of Z-70, suggesting that Z-70 slows down the aggregation process. This indicates that Z-70 likely inhibits the primary nucleation phase of K18 aggregation.

Next, we examined the aggregation of K18 in the presence of varying concentrations of Z-70 and 10 μM of K18 *seeds*. This setup allowed us to evaluate the effect of Z-70 on the elongation phase of K18 aggregation. The aggregation results are presented in Figure 10.4.

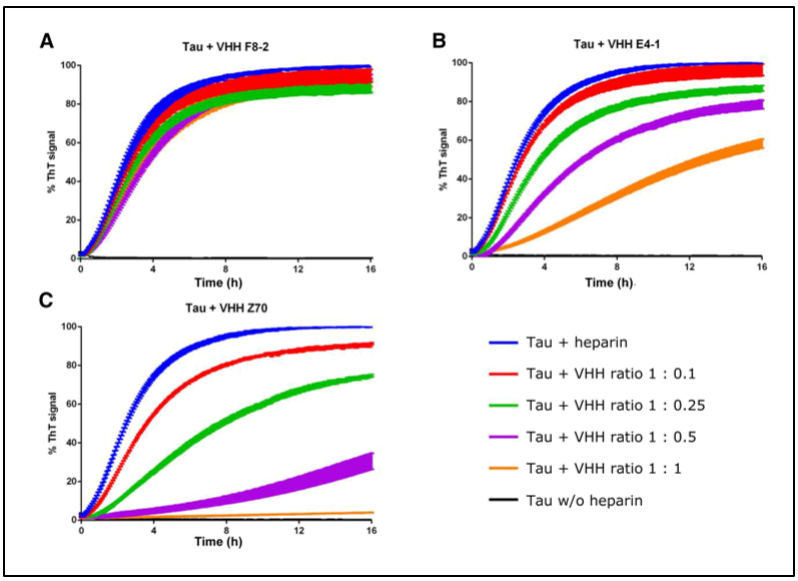

Aggregation of Tau (10 μM) in the absence of heparin (black curve), in the presence of heparin and of increasing concentration of (A) VHH F8-2, (B) VHH E4-1, and (C) VHH Z70 (0, 1, 2.5, 5, and 10 μM) monitored by Thioflavin T fluorescence at 490 nm (n = 3). Error bars: SEM

Figure 10.2: VHH E4-1 and VHH Z70 inhibit in vitro Tau aggregation (Danis et al. 2022)

The slopes of the aggregation curves, obtained through analysis using the software Origin, were found to be similar across the different conditions. The most relevant parameter derived from these analyses is the slope, which represents the elongation rate constant (k+) of the aggregation reaction. The consistent slopes across varying Z-70 concentrations suggest that Z-70 does not significantly affect the elongation of K18 aggregation.
The normalized elongation rate constants (k+) are provided in Table 6. Comparison of these constants indicates that they do not vary significantly with increasing concentrations of Z-70, further suggesting that Z-70 has little effect on the elongation phase of K18 aggregation.
By inputting these constants into the Amylofit software, we obtained the primary and secondary nucleation constants (Table 10.1).

Dataset	**kn (s^{-1})**	**k2 ($M^{-1}s^{-1}$)**	**k+ ($M^{-1}s^{-1}$)**
K18	13.13746	1.31E+07	1.00E+08
K18:0.1 Z70	3.590436	1.17E+07	9.42E+07
K18:0.25 Z70	1.195843	7.58E+06	9.94E+07
K18:0.4 Z70	1.64	6.27E+06	3.99E+07

Table 10.1: Aggregation rate constants for different concentrations of Z70 in the K18 aggregation reaction. Units: k_n (s^{-1}), k_2 ($M^{-1}s^{-1}$), k_+ ($M^{-1}s^{-1}$).

The most significant variation was observed in the primary nucleation constant (kn), indicating that Z-70 primarily inhibits the primary nucleation process. An inhibition strength histogram of Z-70 on various stages of K18 aggregation (Figure 4) shows that Z-70 exhibits a strong inhibitory effect on primary nucleation but only minimal effects on elongation and secondary nucleation at a concentration of 2.5 μM.
These results suggest that Z-70 specifically targets and inhibits the primary nucleation phase of K18 aggregation, which is a critical step in the formation of pathological Tau aggregates.

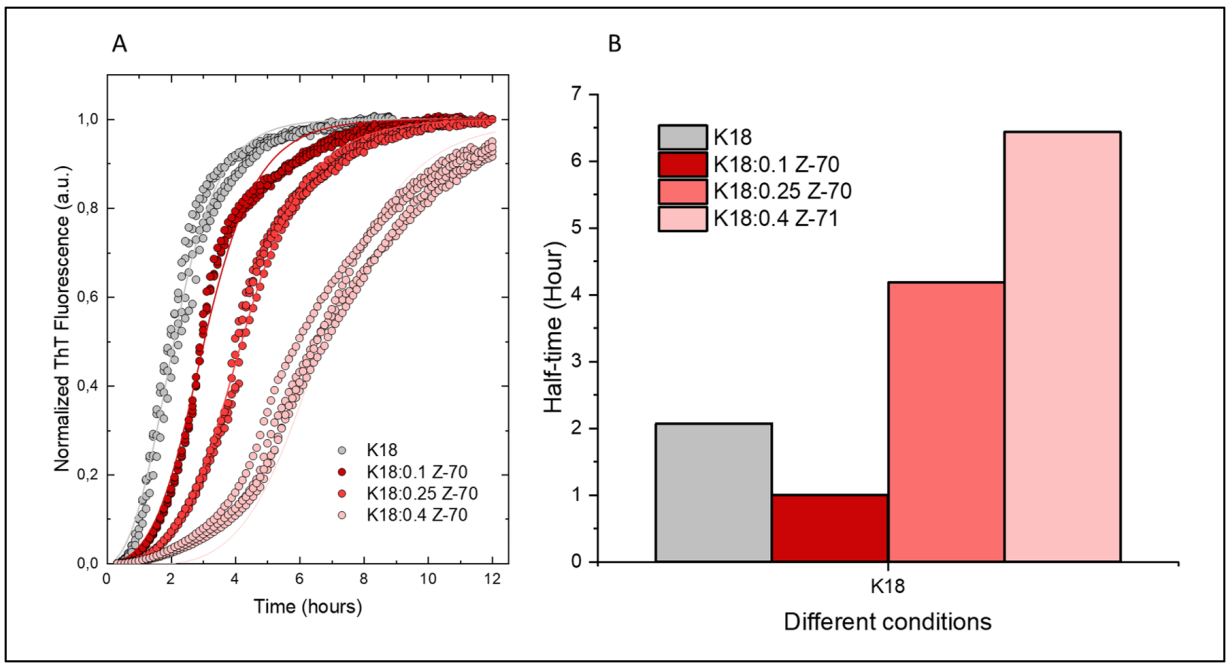

(A) inhibition of Tau-K18 aggregation by Z70 at VHH:Tau-K18 ratios between 0.1 and 0.4, n = 4

Figure 10.3: In vitro inhibition of Tau aggregation by the VHHs

Seeding Inhibition by H3-2

Initially, this experiment was designed to serve as a negative control, as H3-2 was not expected to have a recognition site on K18 (a surprising finding will be discussed later). Consequently, high concentrations of H3-2 were used directly, at a 1:1 ratio. The same protocol used with Z-70 was followed with H3-2.
The results of the initial experiments are shown in figure 10.6 A. It can be observed that the presence of H3-2 leads to a longer aggregation time. From this curve, we extracted the half-reaction times for each aggregation reaction (Figure 10.6 B).
In this set of experiments, 10 μM of seeds were added to each condition. The aggregation results are displayed in Figure 10.7.
We then extracted the various aggregation rate constants, which are provided in Table 10.2.

Dataset	k_n **(s^{-1})**	k_2 **(M^{-1}s^{-1})**	k_+ **(M^{-1}s^{-1})**
K18	13.77201	1.22E+07	1.00E+08
K18:H3-2	0.136884	7.38E+06	2.89E+07

Table 10.2: Aggregation rate constants for K18 in the presence and absence of H3-2. Units: k_n (s^{-1}), k_2 (M^{-1}s^{-1}), k_+ (M^{-1}s^{-1}). The dataset K18 represents aggregation in the absence of H3-2, while K18:H3-2 reflects aggregation in its presence.

To assess the inhibitory strength of H3-2 on different stages of aggregation, we calculated the ratios of the rate constants and plotted an inhibition strength histogram (Figure 10.8 A). The data indicate that H3-2 significantly inhibits the primary nucleation step.
Subsequently, we studied the formation of oligomers in the absence and presence of 10 ţM H3-2, as shown in Figure 10.8 B.
The number of K18 oligomers formed under these conditions was calculated and presented in Table 16

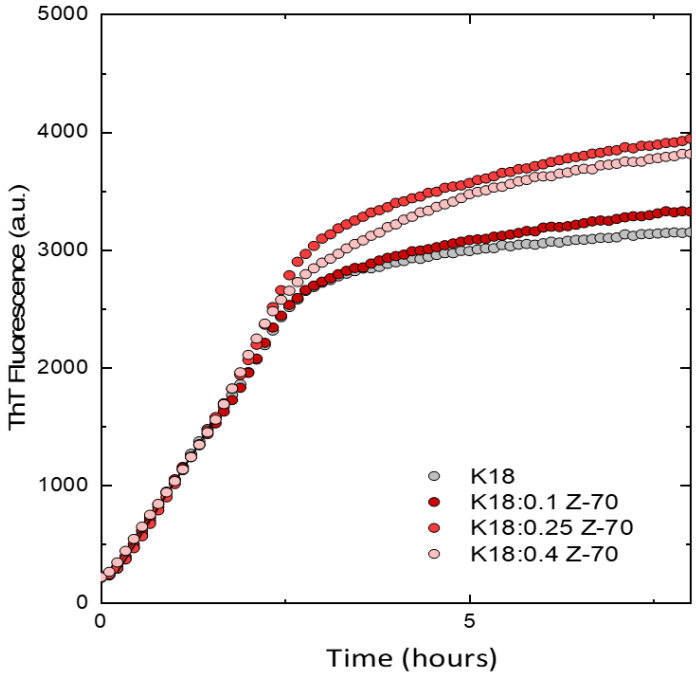

Figure 10.4: Seeded fibril formation of 10μM K18, in the absence (Grey) or the presence of 4 μM (pink) of Z-70 at 37°C. Aggregation is induced by 10 μM of K18 seeds. 4 replicates are present for each condition

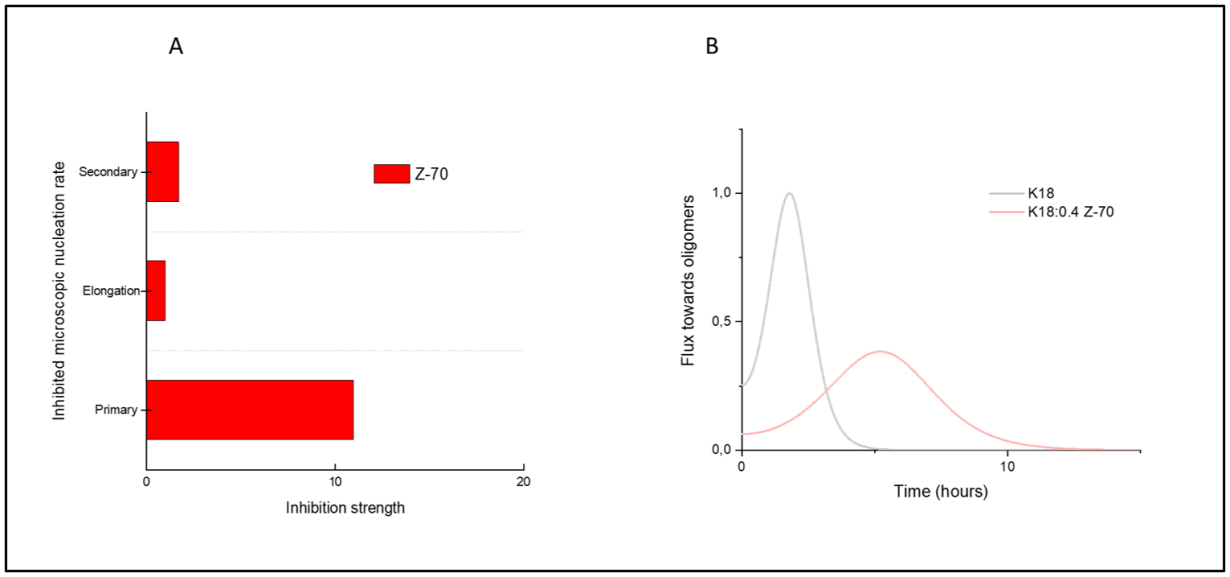

(A) Inhibition strength of Z-70 on each aggregation step (B) Number of oligomers formed and the relative percentage in the absence and the presence of 4 μM of Z-70

Figure 10.5: Effect of Z-70 on K18 *seeding*

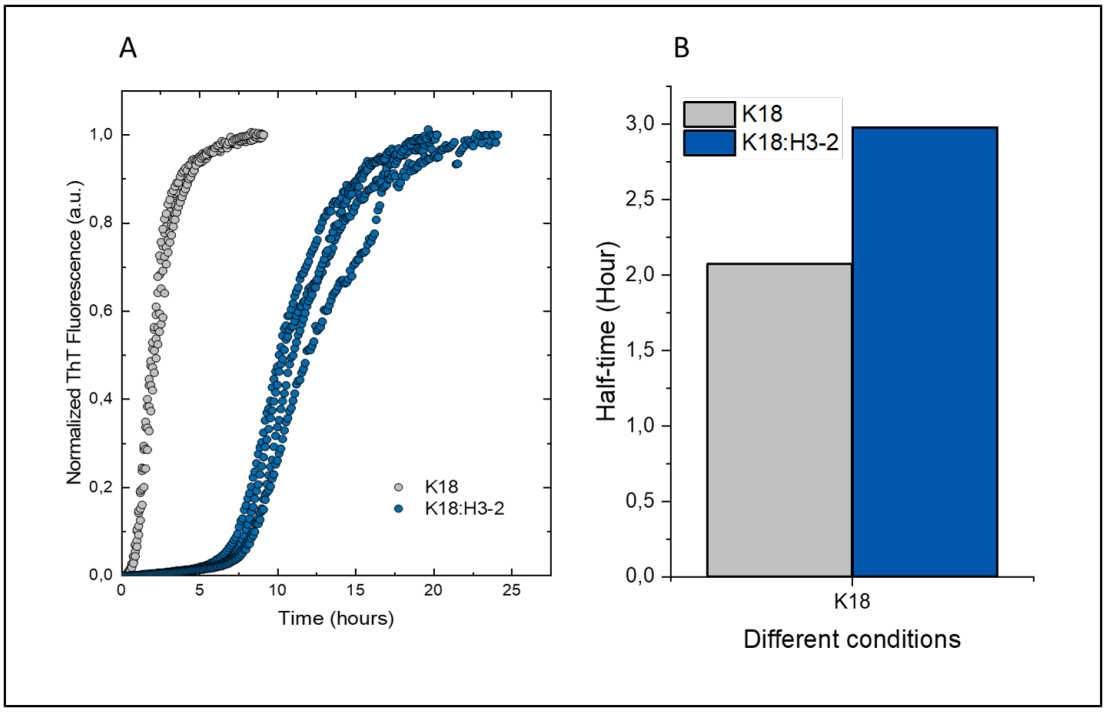

(A) inhibition of Tau-K18 aggregation by H3-2 at H3-2:Tau-K18 ratio of 1:1, n = 4, (B) Average of the extracted Half-times of K18 aggregation reaction in the absence (grey) or the presence of 10 μM (blue) of H3-2

Figure 10.6: In vitro inhibition of Tau aggregation by H3-2

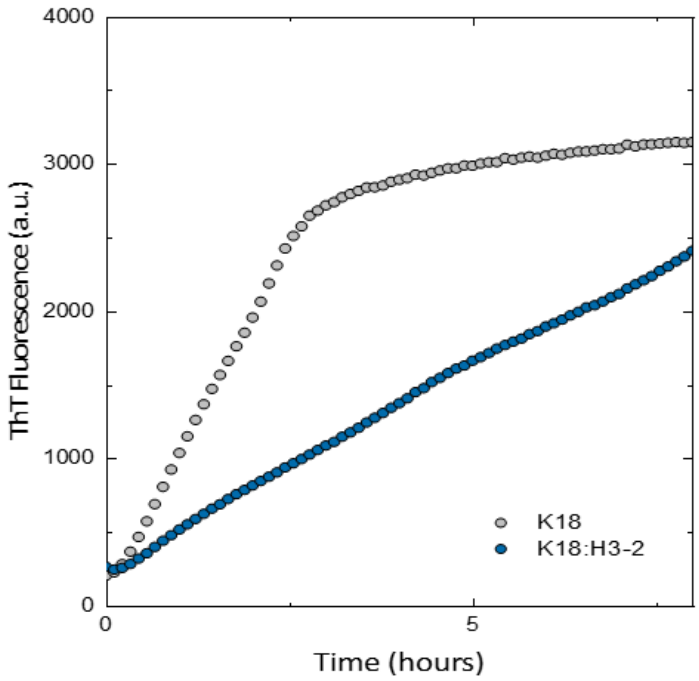

Figure 10.7: Seeded fibril formation of 10μM K18, in the absence (Grey) or the presence of 4 μM (Blue) of H3-2 at 37°C. Aggregation is induced by 10 μM of K18 seeds. 4 replicates are present for each condition

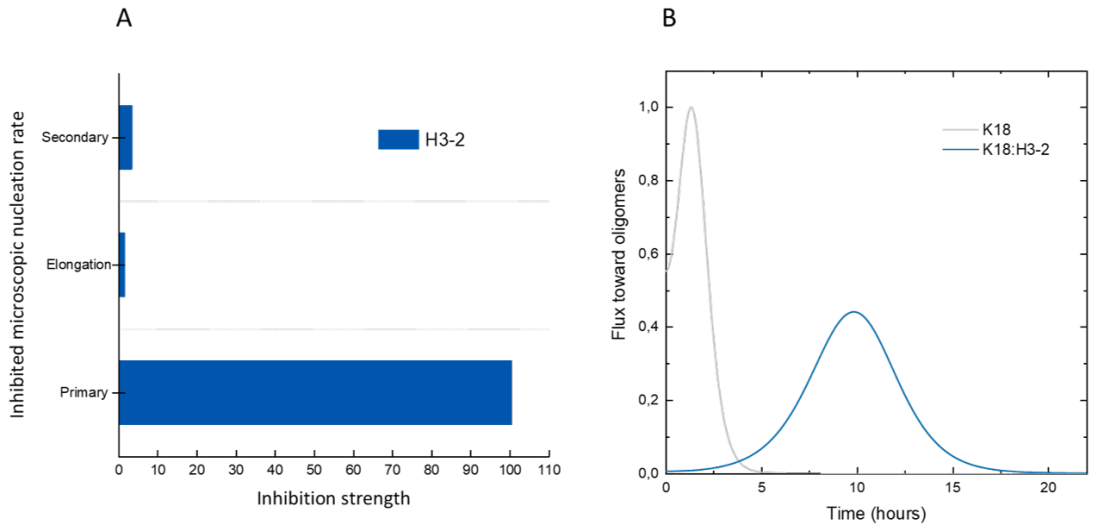

(A) Inhibition strength of H3-2 on each aggregation step (B) Number of oligomers formed and the relative percentage in the absence and the presence of 10 μM of H3-2

Figure 10.8: Effect of H3-2 on K18 *seeding*

Part VII

Material and methods

Chapter 11: Protein expression and production

1. Expression and production of Tau mutants

In this work, we used TauS262A wich is a full-lenght Tau comprising one mutation (a Serine replaced by an Alanin on position 262) wich have no effect on our work. Another full-lenght Tau used also is the TauP301L where a mutation occurs at position 301 in the Tau protein sequence. This mutant of Tau have normally a higher level of aggregation.
In our study, we evaluated also the physiopathological function of two distinct Tau fragments that encompass the full C-terminal region starting either at the R2 or R3 repeat (272-441 or 300-441, respectively), namely Tau R2Ct and R3Ct, corresponding to fragments of the 4R or 3R isoforms, respectively.

The characteristics of the studied Tau mutants and fragments are given in table 11.1.

Protein	**Molecular Weight (MM)**	**Molar Extinction Coefficient (ϵ) (L mol^{-1} cm^{-1})**
Tau S262A	46410.5078 g/mol	7575 L mol^{-1} cm^{-1}
R2Ct-WT	17933.33 g/mol	3105 L mol^{-1} cm^{-1}
R3Ct-WT	15841.59 g/mol	1490 L mol^{-1} cm^{-1}

Table 11.1: Characteristics of Studied Proteins

Tau mutants constructs in pET15b

Before my arrival at the laboratory, various non-tagged Tau constructs cloned into the pET15b vector were generated: pET15b-TauS262A, pET15b-TauR2Ct, and pET15b-TauR3Ct. pET15b is an expression vector that overexpresses proteins under the control of a T7 promoter. The pET15b vector contains an ampicillin resistance gene.

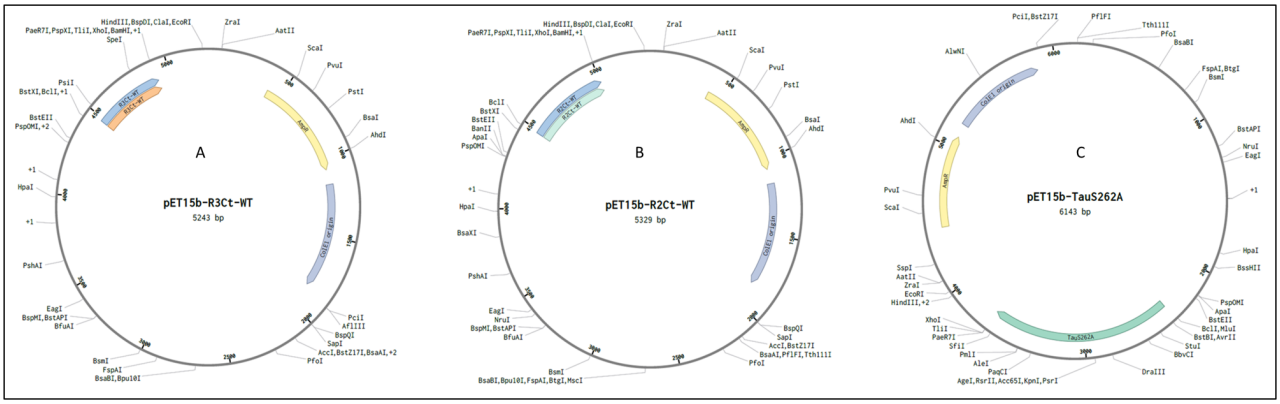

Figure 11.1: Gene Plasmid Map of (A) pET15b-TauS262A, (B) pET15b-R2Ct, pET15b-R3Ct

Figure 11.2: Different constructions generated

Full-length TauS262A include all the known domains such as the N-terminal region, proline-rich region, microtubule-binding repeats (R1-R4), and the C-terminal region, with only one Serine (262) replaced by Alanine.
The R2Ct fragment starts at residue 272 and ends at residue 441. It includes the PHF6* and PHF6 hexapeptide sequences, which are a nucleus for Tau fibrillar aggregation. The fragment encompasses the second repeat (R2), the third repeat (R3), and the fourth repeat (R4). The R3Ct fragment starts at residue 300 and ends at residue 441. It includes the PHF6 hexapeptide sequence in the third repeat (R3) and the fourth repeat (R4) (Figure 9.1).

Transformation into Expression Bacteria

The plasmid constructs are inserted into the E. coli bacteria for protein expression (BL21(DE3) strains, Invitrogen). 1 ţL (10 ng/ţL) of vector is added to 45 μL of competent BL21(DE3) bacteria. An electric shock is applied using an electroporator to permeabilize the bacterial membrane and facilitate the entry of the vector into the cell. Subsequently, 1 mL of LB medium is added and incubated at 37řC, 150 rpm for 1 hour, and then plated on an LB-Agar plate containing the corresponding antibiotic: ampicillin for Tau constructs. The plate is incubated at 37řC overnight.

Overproduction of Proteins

IPTG Induction Principle: IPTG (Isopropyl β-D-1-thiogalactopyranoside) is used to induce protein expression in bacteria containing the vectors. These genes are placed under the control of a T7 promoter and a lacO operator. Without IPTG, the LacI repressor is synthesized and binds to the operator, inhibiting transcription. In the presence of IPTG, LacI is sequestered and dissociates from the lacO operator, allowing transcription and translation to occur.
Production of TauS262A / TauR2Ct / TauR3Ct
A colony is picked and placed in a 50 mL LB-Antibiotic pre-culture, and incubated at 37řC until an $OD_{600} > 2$ is reached. The pre-culture is then centrifuged for 20 minutes at 6000 g.
In the case where we want ^{15}N or ^{15}N,^{13}C labelled protein, the pellet is resuspended in 20 mL of M9 medium enriched with ^{15}N [6 g/L Na_2HPO_4; 3 g/L KH_2PO_4; 0.5 g/L NaCl; supplemented with 1 g/L $^{15}NH_4Cl$; 4 g/L Glucose; 0.5 g/L ^{15}N-Isogro; 10 mL of MEM vitamin cocktail (filtered through 0.22 μm filters, Sigma); 100 μg/mL ampicillin; 1 mM $MgSO_4$ and 100 μM $CaCl_2$] and then filtered through 0.22 μm into 2 L of M9-ampicillin medium (ampicillin at a concentration of 100 mg/L culture).

Composition	Quantity
M9	1L
20% Glucose	20 ml
1M $MgSO_4$	1 ml
100 mM $CaCl_2$	1 ml
$^{15}NH_4Cl$	1 g
Isogro ^{15}N (CORTEXCNET)	0.5 g
100x Vitamins (SIGMA)	10 ml

Table 11.2: Composition of M9 medium for ^{15}N isotopic labeling.

In the case we don't want labelled protein, the pellet is resuspended in 20 mL of LB medium and then filtered through 2 L of LB-ampicillin medium.
The culture is incubated for 11 hours overnight at 9řC and then for 5 hours at 37řC until an OD_{600} = 0.8-1 is reached. Once the OD_{600} is reached, protein expression is induced with 1 mM IPTG (Euromedex) for 3 hours at 37řC. After induction, the culture is centrifuged for 20 minutes at 6000 g, 4řC, then the pellet is resuspended in 40 mL lysis buffer and frozen at -80řC. DNase (1 ţg/mL)

	Non Labled	^{15}N labled	^{15}N ^{13}C labeled
LB	Yes	No	No
M9	No	Yes	Yes
Glucose $C_6H_{12}O_6$	No	Yes	Yes
Glucose $C_6H_{12}O_6$	No	No	Yes
Chlorure d'ammonium $^{15}NH_4Cl$	No	Yes	Yes
Isogro ^{15}N	No	Yes	No
Isogro ^{15}N,^{13}C	No	No	Yes
$MgSO_4$	No	Yes	Yes
Vitamines	No	Yes	Yes
$CaCl_2$	No	Yes	Yes
Ampicilline	Yes	Yes	Yes

Table 11.3: Conditions for different labeling types

is added to the resuspended pellets which are then thawed at room temperature. The cells are lysed using a high-pressure homogenizer (Emulsiflex, Avestin). The cell extract is then centrifuged for 30 minutes at 30000 g, 4řC. The supernatant is heated for 15 minutes at 80řC, centrifuged for 30 minutes at 30000 g, then loaded onto a column for cation exchange chromatography for purification.
TauS262A, TauR2Ct, and TauR3Ct are purified by cation exchange chromatography, then the fractions corresponding to the proteins of interest are pooled. The protein is then purified by HPLC to increase the purification level and to perform an initial desalting step. Finally, a desalting step is performed to remove as much salt as possible. The proteins are then lyophilized and stored at -20řC.

Tau Purification

Purification of TauS262A / TauR2Ct / TauR3Ct

Purification of Tau by Cation Exchange Chromatography: Ion exchange chromatography is based on ionic interaction between the protein and the column. For positively charged proteins (Tau-S262A pI 8.25; Tau-R2Ct pI 9.36; Tau-R3Ct pI 8.95), a HiTrap SP HP cation exchange column (5 mL) is used in phosphate buffer at pH 6.5. The negative ions of the stationary phase retain Tau through interactions with its positive charge. Elution is performed with a salt gradient from 0 to 25% over 15 minutes at a flow rate of 1 mL/min; Na+ ions interact with the column's negative charges and compete with Tau, allowing protein elution. The samples are analyzed by mass spectrometry and electrophoresis.
Purification of Tau by High-Performance Liquid Chromatography (HPLC): The C8 column (Zorbax Agilent 300SB-CB, semi-preparative) is used for various HPLC purifications of the proteins of interest. Fractions from ion exchange chromatography and mass spectrometry analysis are injected onto the column after equilibration in buffer A (5% ACN; 0.1% TFA). Once the entire sample is injected onto the column and the 280 nm curve stabilizes, a buffer B gradient (80% ACN; 0.1% TFA) is initiated in two steps. First, an increase to 25% in 0 minutes is performed, followed by a linear gradient from 25% to 60% in 40 minutes (the theoretical elution point of the proteins of interest is around 40% buffer B), and finally a gradient to 100% buffer B in 10 minutes to regenerate the column. Collected fractions are analyzed by mass spectrometry. The fractions containing
Buffer Exchange and Desalting: Tau samples are desalted using HiTrap Desalting columns (GE Healthcare) to remove salts from cation exchange and HPLC buffers. Purified Tau is frozen in liquid nitrogen and lyophilized overnight.

2. Expression and production of enzymes

Enzymes constructs

GSK3β and OGT constructs

A construct of kinase cloned into the pET-21a vector is generated: the pET21-GSK3β construct allows for a protein with a polyhistidine tag at the C-terminal end. pET-21a vector contain an ampicillin resistance gene. pET24-OGT construct allows for a protein with a polyhistidine tag at its C-terminal end. The pET24 vectors contain a kanamycin resistance gene.

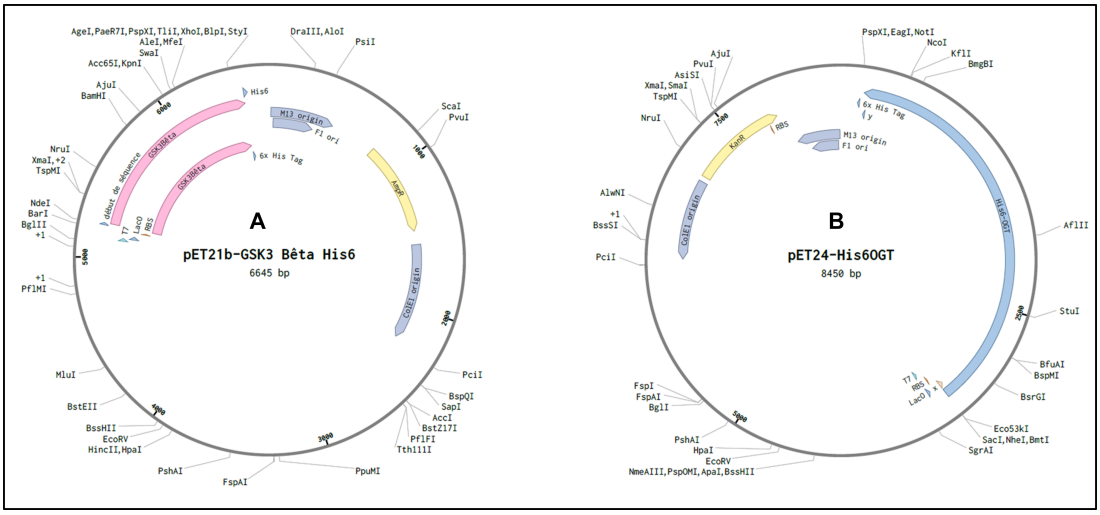

Figure 11.3: Plasmid constructs of (A) GSK3β in pET21a and (B) OGT in pET24

OBP-tagged GSK3β constructs

Two construct of OBP-tagged GSK3β cloned into the pET-21a vector are generated where one have it on the N- and the other on the C-terminal 11.4.

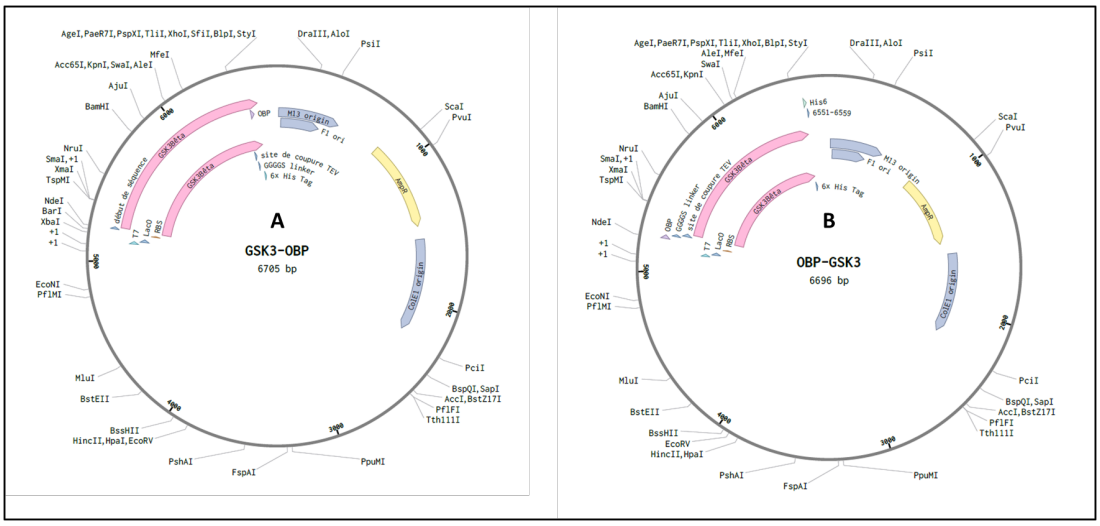

Figure 11.4: Plasmid constructs of (A) GSK3β-OBP and (B) OBP-GSK3β in pET21a

CDK2 and CyclinA constructs

The recombinant pGEX co-expression plasmid GST-CDK2/CIV1 is inserted into competent BL21(DE3) bacterial cells via chemical transformation. Similarly, the recombinant CyclinA expression plasmid (without a tag) is inserted into competent BL21(DE3) bacterial cells via chemical transformation.

Transformation into Expression Bacteria

The plasmid constructs are inserted into the E. coli bacteria for protein expression (BL21(DE3) strains, Invitrogen). 1 ţL (10 ng/ţL) of vector is added to 45 μL of competent BL21(DE3) bacteria. An electric shock is applied using an electroporator to permeabilize the bacterial membrane and facilitate the entry of the vector into the cell. Subsequently, 1 mL of LB medium is added and incubated at 37řC, 150 rpm for 1 hour, and then plated on an LB-Agar plate containing the corresponding antibiotic: ampicillin for GSK3β, CDK2 and CyclinA, and kanamycin for OGT. The plate is incubated at 37řC overnight.

Production of GSK3β and nc-OGT

A colony is picked and placed in a 25 mL LB-kanamycin pre-culture (20 mg/L culture) and incubated overnight at 37řC until an OD > 4 is reached. Once the OD is reached, the pre-culture is placed in 2 L of LB-kanamycin medium (20 mg/L culture). The culture is incubated for 11 hours overnight at 9řC and then for 5 hours at 37řC until an OD = 0.8-1 is reached. Once the OD is reached, protein expression is induced with 1 mM IPTG at 16řC for 20 hours. The culture is then centrifuged for 20 minutes at 6000 g, 4řC. The cells are lysed using a high-pressure homogenizer (Emulsiflex, Avestin) and the cell extract is then centrifuged for 30 minutes at 30000 g, 4řC, then loaded onto a NiNTA affinity chromatography column.

Production of CDK2 and CyclinA

The bacterial pellets of each protein are thawed at room temperature and 150 μL of DNase I are added to each pellet before lysis.

Enzymes purification

Purification of nc-OGT and GSK3β

Nickel Affinity Chromatography (NiNTA) Affinity chromatography is based on the affinity between the protein tag and the column. For poly-histidine tagged proteins, a His-trap HP column (1 mL, Cytiva) containing Nickel ions (Ni $^{2+}$) is used. Ni^{2+} ions retain the proteins through interactions with the histidines of the tag. Elution is performed with an imidazole gradient from 50 mM to 500 mM; imidazole interacts with nickel and competes with histidine, allowing elution. A TEV cleavage (for nc-OGT) or SENP-3 (for GSK3β) (1 mg for 20 mg of protein) is performed for 16 hours at 4řC to remove the histidine tag.
To remove the cleavage enzyme and cleaved tags, the cleaved protein is loaded back onto the NiNTA column. The cleaved protein, without its tag, is eluted in the flow-through.
Protein Concentration: The protein is concentrated using Amicon concentrators (Millipore, 10 kDa cutoff) and filtered through 0.22 μm filters before being stored in aliquots at -80řC.

Purification of CDK2/CyclinA

After lysis, a 30-minute centrifugation at 30,000 g is performed to collect the supernatant, and the soluble bacterial lysates containing the recombinant GST-CDK2 and CyclinA are mixed. The mixture

is loaded onto a washed and equilibrated glutathione Sepharose resin in a wash buffer. Incubation is carried out for 3 hours at 4řC with agitation. The supernatant is removed and the CDK2/CyclinA complex is eluted by incubating the resin in 100% elution buffer at 4řC overnight. The supernatant containing our CDK2/CyclinA protein is collected. To remove the GST tag, enzymatic cleavage with PreScission Protease is performed. The PreScission Protease itself has a GST tag and thus binds to the glutathione Sepharose; it will not co-elute and contaminate the cleaved target protein. The CDK2/CyclinA protein is mixed with the protease and then passed over the resin. The GST tag is cleaved, and the protein passes through the resin while the protease remains on the resin.
MALDI-TOF MS and NMR are also techniques used for the analysis of the proteins purified (specially Tau protein constructs) but they will be detailed in

3. Protein analysis techniques

3.1. SDS-PAGE (Polyacrylamide Gel Electrophoresis in the presence of Sodium Dodecyl Sulfate)

To analyze and interpret the various experiments conducted, methods were used to identify proteins of interest. SDS-PAGE (Polyacrylamide Gel Electrophoresis in the presence of Sodium Dodecyl Sulfate) was performed at each step to monitor purification steps and verify the presence and purity of the proteins. SDS-PAGE is based on the principle of protein migration according to their size and charge under the influence of an electric field on a polyacrylamide gel prepared under denaturing conditions (presence of SDS). SDS binds to the proteins, making them all negatively charged regardless of their pI, and denatures them, facilitating their migration. The gels are prepared at different acrylamide concentrations (ranging from 8 to 20%) depending on the size of the proteins studied.
The samples are prepared in 4X Laemmli buffer (250 mM Tris pH 6.8, 20% (V/V) Glycerol, 3% (M/V) SDS, 0.1% (V/V) Bromophenol Blue, 0.7 M β-Mercaptoethanol). 30 μL of sample is added to 10 μL of 4X buffer (final concentration 1X), then heated for 5 min at 100řC and finally loaded onto the gel. The gel with the samples to be migrated is placed in running buffer (25 mM Tris pH 8, 192 mM Glycine, 1% SDS) with a current of 150V. To reveal the presence of proteins, the gel is placed in Coomassie Blue staining solution (0.1% M/V Coomassie Blue, 40% V/V Ethanol, 10% V/V Acetic Acid) for 30 min, then incubated in destaining solution (15% (V/V) Acetic Acid, 5% (V/V) Ethanol).

3.2. Calculation of Protein Mass

The mass of the different proteins studied is obtained by calculating the area of the peak corresponding to the protein at UV = 280 nm on the various chromatograms.

3.3. Calculation of Protein Concentration

Protein concentration in solution is measured on a Nanodrop where a drop of 1-2 ţL placed on a UV detector allows the measurement of optical density at 280 nm related to protein concentration according to Beer-Lambert law DO = ϵlC.

Chapter 12: Biophysical assays

1. Tubulin Polymerization Assay

The tubulin polymerization assay was conducted using the fluorescence-based tubulin polymerization assay kit (Cytoskeleton, Inc. Cat. # BK011P). Each fragment, phosphorylated or not, was prepared at a 10× concentration (200 μM) in a solution containing 80 mM PIPES pH 6.9, 0.5 mM EGTA, and 2.0 mM $MgCl_2$.
To reconstitute the tubulin polymerization assay, 1 mM GTP, 2 mg/mL of tubulin (porcine tubulin, prepared according to the kit recommendations), and 20 μM of tau fragments were dissolved in 1.5 mL of polymerization buffer. Subsequently, 55 μL of the reaction mixture was dispensed into a 96-well plate (Corning Costar, Cat. # 3686).
Polymerization kinetics were monitored by following the increase in fluorescence emission at 460 nm over a 60-minute period at 37°C on a plate reader (PHERAStar, BMG LABTECH GmbH, Ortenberg, Germany). Three replicates were performed for each condition.

2. Aggregation assays

2.1. Generation of Fibrils and production of seeds

To generate fibrils of R2Ct and R3Ct fragments, as well as their phosphorylated variants, 10 μM of each fragment were incubated in an aggregation buffer. The buffer composition included 50 mM MES (pH 6.9), 2.5 mM EDTA, 30 mM NaCl, and 0.33 mM DTT, and was supplemented with 2.5 μM heparin to reach a final volume of 1 mL. Fibril formation was monitored by adding 50 μM Thioflavin T (ThT) fluorescent probe to 100 μL of the same reaction mixture. This allowed for tracking the aggregation kinetics using a PHERAStar fluorescence plate reader (BMG LABTECH GmbH, Ortenberg, Germany). The aggregation reactions were incubated for 3 to 5 days at 37°C. After incubation, seeds were collected for subsequent seeding experiments. Negative-staining transmission electron microscopy (TEM) was performed using a JEOL JEM-2100 microscope at 200 kV to analyze the fibrils.

2.2. Seeding and Cross-seeding Assays

Seeds were prepared in the same aggregation buffer containing 10 μM of tau fragments (R2Ct, R2Ct-P, R3Ct, or R3Ct-P) in the presence of 1 μM of heparin for 7 days at 37°C. Seeding and cross-seeding assays closely mirrored the aggregation reaction used to produce *Seeds*, except that heparin was substituted with the *Seeds*.
Seeds from aggregation reactions were diluted to a final concentration of 1 μM in the seeding reactions, in the presence of 10 μM of soluble, monomeric Tau protein or Tau fragments. Consequently, the heparin included within the *seeds* was also diluted, ultimately yielding a final concentration of 0.1 μM. A negative control conducted without *seeds*, but in the presence of 0.1 μM heparin, showed that

this concentration of heparin alone is insufficient to stimulate fibril formation in the absence of *Seeds*.

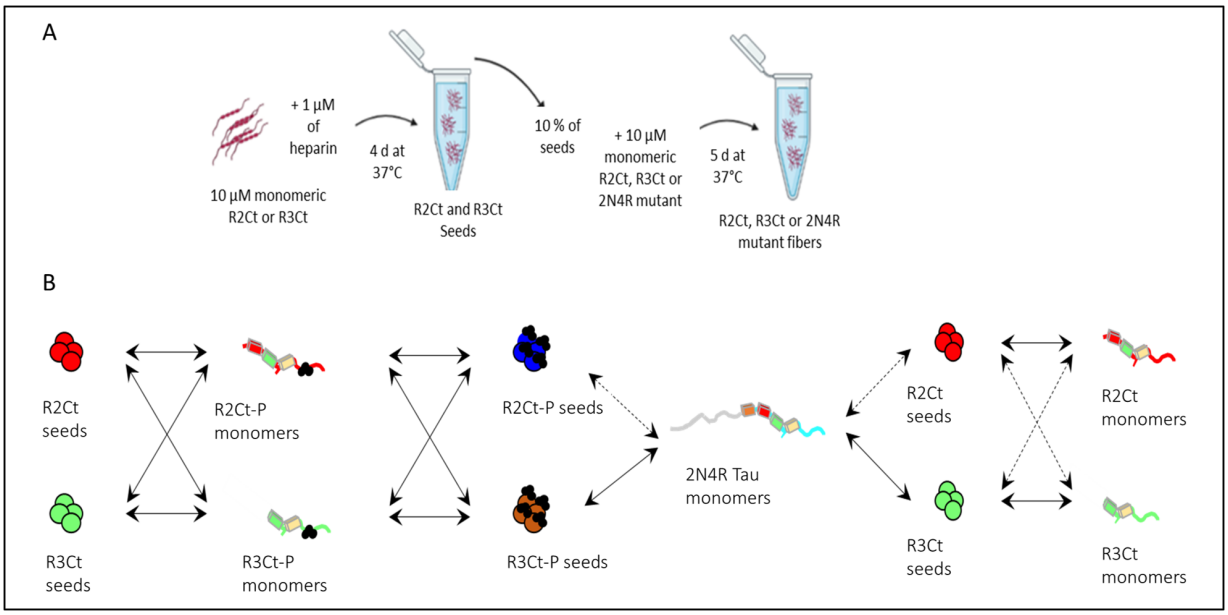

(A) Seeding experimental protocol representation and (B) Seeding combinations done in this thesis

Figure 12.1: *Seeding* mechanism followed in this work

2.3. Aggregation and *seeding* characterization

Sedimentation assay

Sedimentation analysis of Tau protein aggregation involved loading 0.5 μg of the aggregation reactions onto an SDS/PAGE gel at two time points: before incubation (t_0) and after incubation at 37 °C for 48 hours (t_{48}) for heparin-induced aggregation, or a certain number of hours (t_{end}) for seeding reactions. Each sample was loaded in duplicate to ensure even distribution across the gel. Following electrophoresis, the gel was stained with Coomassie Blue to visualize the protein bands. The amounts of soluble protein were measured colorimetrically using the Amersham ImageQuant™ 800 imaging system (Cytiva) and quantified via densitometry using ImageJ-Win64 or ImageQuant TL 10.0.261 (Cytiva) software. The comparison between t_0 and the post-incubation samples provided insights into the extent of protein aggregation.

Filter-trap assay

The nitrocellulose membrane (0.45 μm pore size, Protran™, Cytiva) used for the filter-trap assay was initially hydrated with PBS buffer. Tau fibrillization reaction products (5 μL) were diluted up to 40 times in 2% SDS-PBS buffer and then added to the wells of a 96-well dot blot apparatus (Schleicher & Schuell Minifold Spot Blotting Unit system). Each well was subsequently washed twice with 2% SDS-PBS buffer under vacuum. The membrane was then removed from the filtration apparatus, washed twice more with 2% SDS-PBS, and blocked with 5% non-fat dry milk in PBS buffer. After blocking, the membrane was washed with PBS-T and incubated with the mouse primary antibody HT-7 (targeting antigen 159-163, diluted 1:1000 in PBS-T) for 16 hours at 4 °C. Following three PBS-T washes, the membrane was incubated with the secondary HRP-conjugated anti-mouse antibody (diluted 1:10000) for 45 minutes and washed again with PBS-T. Protein detection was performed using the chemiluminescent reagent (Cytiva Amersham™ ECL™ Prime Western Blotting Detection

Reagent). Chemiluminescent signals were captured with the Amersham ImageQuant™ 800 imaging system (Cytiva) and quantified by densitometry using ImageQuant TL 10.0.261 software (Cytiva).

2.4. Fiber collection and analysis

Negative-staining transmission electron microscopy

Transmission Electron Microscopy (TEM) is a powerful imaging technique that uses a beam of electrons to create highly detailed images of thinly sliced samples. The basic principle of TEM involves transmitting a high-energy electron beam through a very thin specimen. As the electrons interact with the sample, they are scattered depending on the density and composition of the material. These interactions produce an image that is magnified and focused onto an imaging device, such as a fluorescent screen or a digital camera.
Observation of heparin-induced aggregation and seeding reactions was performed by negative staining transmission electron microscopy (HITACHI H7500 microscope at 80 kV). A volume of 3 μL from the aggregation reactions was applied to 400-mesh hexagonal nickel grids (Euromedex) for 30 seconds. The solution was then carefully removed with a filter paper, then the grids were washed three times with ultrapure water. For negative staining, 10 ţL of 2 $\%$ uranyl acetate was applied for 10 seconds, after which the solution was removed with filter paper. The grids were re-stained for 60 seconds with 2 $\%$ uranyl acetate and the solution was removed.

Fibril Immunogold Labelling

5 μL of the aggregation sample were put on 400-mesh hexagonal nickel grids (Euromedex) for one minute in order to immunogold label the fibrils. The EM grids were placed three times over fresh drops of PBS buffer without drying in order to remove excess fibrils. After that, the grids were incubated for 30 minutes with 5$\%$ (wt/vol) BSA in PBS as the blocking step.
The grids were then incubated for 30 minutes with a 1:100 dilution of the main anti-Tau antibody (Ht-7 or PHF-1) in 1$\%$ BSA. The grids were first subjected to five PBS washes, and then they were incubated for 30 minutes with the gold-labeled secondary antibody (6 nm-Gold donkey IgG anti-mouse IgG) diluted 1:40 in 1$\%$ BSA.
To avoid uranyl acetate precipitating in PBS, the sample was rinsed 10 times with water before staining. Subsequently, the sample was immersed in a 2$\%$ (wt/vol) uranyl acetate solution in water for one minute, and allowed to dry for fifteen minutes to achieve a negative stain. TEM imaging was carried out at 80 kV with an HITACHI H7500 microscope.

Chapter 13: Post-traductional modifications

1. PTM of Tau

Phosphorylation reaction of Tau

Phosphorylation is carried out using CDK2/CyclinA and GSK3β enzymes.The phosphorylation of Tau by CDK2/cyclinA and GSK3β is not independent but rather interconnected through a priming mechanism. CDK2/cyclinA can prime Tau by phosphorylating it at specific sites, which then allows GSK3β to further phosphorylate Tau at additional sites.
The priming step performed by CDK2/CyclinA adds approximately 12 phosphate groups to the full-length Tau protein and one phosphate group to the R2Ct and R3Ct fragments. This step increases the phosphorylation rate by GSK3β, which adds four phosphorylations to the full-length Tau and 2 phosphorylations to the R2Ct and R3Ct fragments.
The AT180 phospho-epitope (pT231/pS235) and the AT8 epitope in its doubly phosphorylated state (pS202/pT205) are phosphorylated by CDK2/CyclinA. Other phosphorylations have also been found in the PRD (pT153, pT175, pT181, pT212), with pT212 and pS202 acting as priming sites for GSK3 phosphorylation of pS208 and pS198, respectively, resulting in a triple phosphorylated state of AT8 or AT8-3P, pS202/pT205/pS208.
Normally, GSK3β phosphorylates (S/T)-XXX-(pS/pT) motifs (where pS/pT is the priming site), i.e., a Ser/Thr residue located four residues N-terminal to the priming site, and more rarely at a number of residues of five or six (Leroy et al. 2010). Four new phosphorylation sites are identified after GSK3β phosphorylation in TauS262A-PP: S198 and S208 in the PRD following priming at S202 and T212, respectively, and S396 and S400 in the C-terminal end following priming at S404 (**CantrellePhosphorylationOGlcNAcylationPHF12021**; Despres et al. 2017; Smet-Nocca et al. 2011).
The concentration of Tau for phosphorylation reactions is 100 μM. A quantity of protein is solubilized in a 5X phosphorylation buffer (250 mM Hepes, KOH pH=7.8, 62.5 mM MgCl2, 5 mM EDTA), 10% (v/v) enzyme (CDK2/CyclinA or GSK3β) is added, along with 5 mM DTT and 5 mM ATP. A reaction mixture volume (30 μL) is kept without ATP addition as a negative control.
The phosphorylation reaction and the negative control are incubated for 16 hours at 25řC. The phosphorylation reaction is stopped by a 15-minute incubation at 80řC, then cooled on ice. The mixtures are then centrifuged for 15 minutes at 10 000g, and the supernatant is purified by reverse-phase HPLC. The fractions are analyzed by MS and NMR.
A chapter on the phosphorylation of Tau by CDK2/cyclin and GSK3β can be found in the appendix A.

O-GlcNAcylation reaction

O-GlcNAcylation is carried out by the enzyme OGT. During the incubation of Tau (at 800 μM) with recombinant OGT at approximately 0.5 mg/ml (in its nucleocytoplasmic isoform known as nc-OGT) in the presence of UDP-GlcNAc, in the conservation buffer for OGT and GSK3β, three major O-

GlcNAc sites located in the C-terminal end at residues S400, S412, and S413 are identified by NMR. A global O-GlcNAcylation level of 1.8 1.9 GlcNAc per Tau molecule, determined by MALDI-ToF MS, is obtained according to this protocol (Bourré et al. 2018).
The O-GlcNAcylation reaction and the negative control are incubated for 16 hours at 30řC. The O-GlcNAcylation reaction is stopped by a 15-minute incubation at 80řC, then cooled on ice. The mixtures are then centrifuged for 15 minutes at 10,000 g, and the supernatant is purified by reverse-phase HPLC. The fractions are analyzed by MS.

A chapter on the O-GlcNAcylation of Tau by nc-OGT can be found in the appendix A.

2. PTM of GSK3β

Akt-mediated phosphorylation of GSK3β

OBP-GSK3β proteins, either previously O-GlcNAcylated (oG/O$^+$) or not (oG/O$^-$), or coexpressed with OGT, were prepared at a concentration of 25 μM. These proteins were incubated with 2 μM Akt1/PKBα (UniProtKB P31749; active and phosphorylated at Thr308 and Ser473, Merck) and 1 mM ATP, or without ATP as a control. The incubation was carried out in Akt phosphorylation buffer, which contains 50 mM Tris-HCl (pH 7.5), 0.1% 2-mercaptoethanol, and 10 mM $MgCl_2$, at 30 řC for 2 hours. Following incubation, both phosphorylated and control GSK3β proteins were analyzed via Western blotting. The blotting utilized an antiphospho-GSK3 antibody (Phospho-GSK3beta (Ser9) monoclonal antibody clone C.367.3, Invitrogen).

O-GlcNAcylation reaction of GSK3β

GSK3β proteins were incubated at a concentration of 50 μM with 4.5 μM OGT and 2 mM UDP-GlcNAc, or without UDP-GlcNAc as a control, in OGT reaction buffer (50 mM potassium phosphate buffer pH 7.6, 150 mM NaCl, 1 mM EDTA, 0.5 mM THP, 12.5 mM $MgCl_2$) at 31 řC for 6 hours. The O-GlcNAcylated GSK3β proteins were then analyzed by SDS-polyacrylamide gel electrophoresis and Western blotting using the RL-2 antibody (O-linked N-acetylglucosamine monoclonal antibody, Invitrogen) and the anti-GSK3 antibody (GSK3 alpha/beta monoclonal antibody clone 21A, Invitrogen) to ensure equal protein loading.

3. Techniques used for the detection of PTMs

3.1. Western Blot

Equal amounts of protein (20-30 ţg) were mixed with 4x SDS-PAGE loading buffer and boiled at 95řC for 5 minutes, followed by separation on a 10% SDS-PAGE gel and transfer to a PVDF membrane (Millipore) using a semi-dry transfer system (Bio-Rad) at 20 V for 1 hour. The membranes were then blocked with 5% non-fat dry milk in PBS-T for 1 hour at room temperature. Subsequently, the membranes were incubated overnight at 4řC with primary antibodies: anti-phospho-specific antibody and anti-O-GlcNAc antibody, diluted in 5% BSA in PBS-T. The list of primary antibodies used are in table 13.1.
After washing three times with PBS-T for 5 minutes each, the membranes were incubated with HRP-conjugated secondary antibodies (1:5000 dilution in blocking buffer) for 1 hour at room temperature, followed by three additional washes with PBS-T. Protein bands were visualized using enhanced chemiluminescence (ECL) reagents (Pierce ECL Western Blotting Substrate) as per the manufac-

Used Antibodies	Utilization
Anti-Phospho-Tau (PS396/PS404) Antibody	Detecting phosphorylated Tau at PHF-1 site (pS396/pS404)
Anti-Phospho-Tau Monoclonal Antibody AT8	Detecting phosphorylated Tau at AT8 site (pS202/pS205)
Anti-O-GlcNAc RL2 Monoclonal Antibody	Identifying O-GlcNAc modifications in proteins
Anti-phospho GSK3β	Detecting phosphorylated GS3β at Ser9

Table 13.1: Used antibodies and their utilization in PTMs experiments.

turers instructions. The chemiluminescent signal was captured using a Bio-Rad Imaging System and analyzed using Image Lab software (Bio-Rad).

3.2. Mass Spectrometry (MS)

Mass spectrometry is an analytical technique used for determining the molecular masses of analyzed compounds as well as their identification, and more rarely their quantification.

MALDI-ToF MS

Matrix-Assisted Laser Desorption/Ionization Time-of-Flight Mass Spectrometry (MALDI-TOF MS) is a powerful analytical technique used for the identification and characterization of biomolecules. The principle of MALDI-TOF MS involves the following key steps:

- **Sample Preparation:** The analyte is mixed with a matrix compound, which is typically an aromatic organic compound that absorbs UV light. This mixture is then applied to a metallic sample plate and allowed to co-crystallize.
- **Desorption/Ionization:** A pulsed laser beam, usually in the UV range, is directed at the sample, causing the matrix to absorb the laser energy. This absorption leads to the rapid vaporization and ionization of both the matrix and the analyte. The matrix aids in the desorption process by absorbing the energy and transferring it to the analyte, resulting in the formation of analyte ions.
- **Ion Acceleration:** The generated ions are accelerated by an electric field towards a time-of-flight (TOF) analyzer. The ions are accelerated to the same kinetic energy, allowing their velocities to be dependent on their mass-to-charge ratio (m/z).
- **Time-of-Flight Analysis:** The ions travel through a flight tube and their time of flight is measured. Lighter ions travel faster and reach the detector sooner than heavier ions. The time taken for each ion to reach the detector is proportional to the square root of its m/z ratio.
- **Detection and Analysis:** The detector records the arrival time of the ions, generating a mass spectrum. The spectrum displays the m/z ratio of the ions, allowing for the identification and characterization of the analyte based on its mass and charge.

For peptides and proteins, the MALDI-ToF technique (Axima Assurance, Shimadzu) is used in linear and positive ion mode. MALDI is a soft ionization process that does not cause fragmentation of large molecules and produces few multiply charged ions, facilitating spectrum interpretation. This technique allows us to analyze the various chromatogram peak fractions to verify if the mass obtained by MS matches the expected mass, which is the mass of our protein (or protein fragment). This technique is also used as a control technique to verify the realization of various post-translational

modifications of proteins (phosphorylation and O-GlcNAcylation) by an increase in mass of 80 Da (for phosphorylations) and 203 Da (for O-GlcNAcylations).
In MALDI-ToF mass spectrometry (MALDI-ToF MS), the choice of matrix is crucial for obtaining good spectra. The matrix assists in the ionization of the analyte and affects the quality and accuracy of the mass spectra obtained. Two commonly used matrices for different applications are α-Cyano-4-hydroxycinnamic acid (CHCA) and sinapinic acid (SA). Heres a comparison between the two:

Aspect	**α-Cyano-4-hydroxycinnamic Acid (CHCA)**	**Sinapinic Acid (SA)**
Application	Ideal for peptides and small proteins (up to 10 kDa)	Ideal for larger proteins and high-molecular-weight biomolecules
Ionization Efficiency	Produces predominantly singly charged ions	Produces both singly and multiply charged ions
Peak Characteristics	Sharp, high-intensity peaks	Broader peaks
Usage	Commonly used for peptide mass fingerprinting	Often used for intact protein analysis
Absorption	Strong UV absorption at 337 nm	Strong UV absorption at 337 nm

Table 13.2: Comparison between α-Cyano-4-hydroxycinnamic Acid (CHCA) and Sinapinic Acid (SA) for MALDI-TOF MS

Application on Tau proteins

Reactions were desalted before analysis by MALDI-TOF mass spectrometry (using ZipTip®μC18 for peptides and μC4 for proteins) after co-crystallization with α-cyano-4-hydroxycinnamic acid (HCCA) for peptides and sinapinic acid for proteins, to detect the presence of O-GlcNAcylated and phosphorylated species. This step is not necessary after performing HPLC.

LC-MS/MS

LC-MS/MS (Liquid Chromatography-Tandem Mass Spectrometry) is an analytical technique that combines liquid chromatography separation with mass spectrometry detection and fragmentation. In LC-MS/MS, liquid chromatography separates compounds in a mixture based on their chemical properties before they enter the mass spectrometer. The compounds eluting from the LC column are ionized, typically using electrospray ionization (ESI), which produces charged molecules with minimal fragmentation, allowing determination of molecular weight. The ionized molecules are analyzed in the first stage of the mass spectrometer to determine their mass-to-charge (m/z) ratios. Selected ions (precursor ions) are then fragmented using various dissociation techniques. The most common fragmentation methods are: Collision-Induced Dissociation (CID), where ions collide with neutral gas molecules causing fragmentation; Higher-energy Collisional Dissociation (HCD), a type of CID used in Orbitrap instruments that allows detection of low m/z fragment ions (Baars and Perlman 2016); and Electron Transfer Dissociation (ETD) , where electrons are transferred to multiply charged cations, inducing fragmentation. ETD is particularly useful for analyzing peptides and proteins, especially those with post-translational modifications (*(15) Understanding Mass Spec Fragmentation Techniques | LinkedIn* 2024).
The resulting fragment ions are analyzed in the second stage of the mass spectrometer, providing structural information about the precursor ions.
The fragmentation patterns are used to identify and characterize compounds, often with the help of

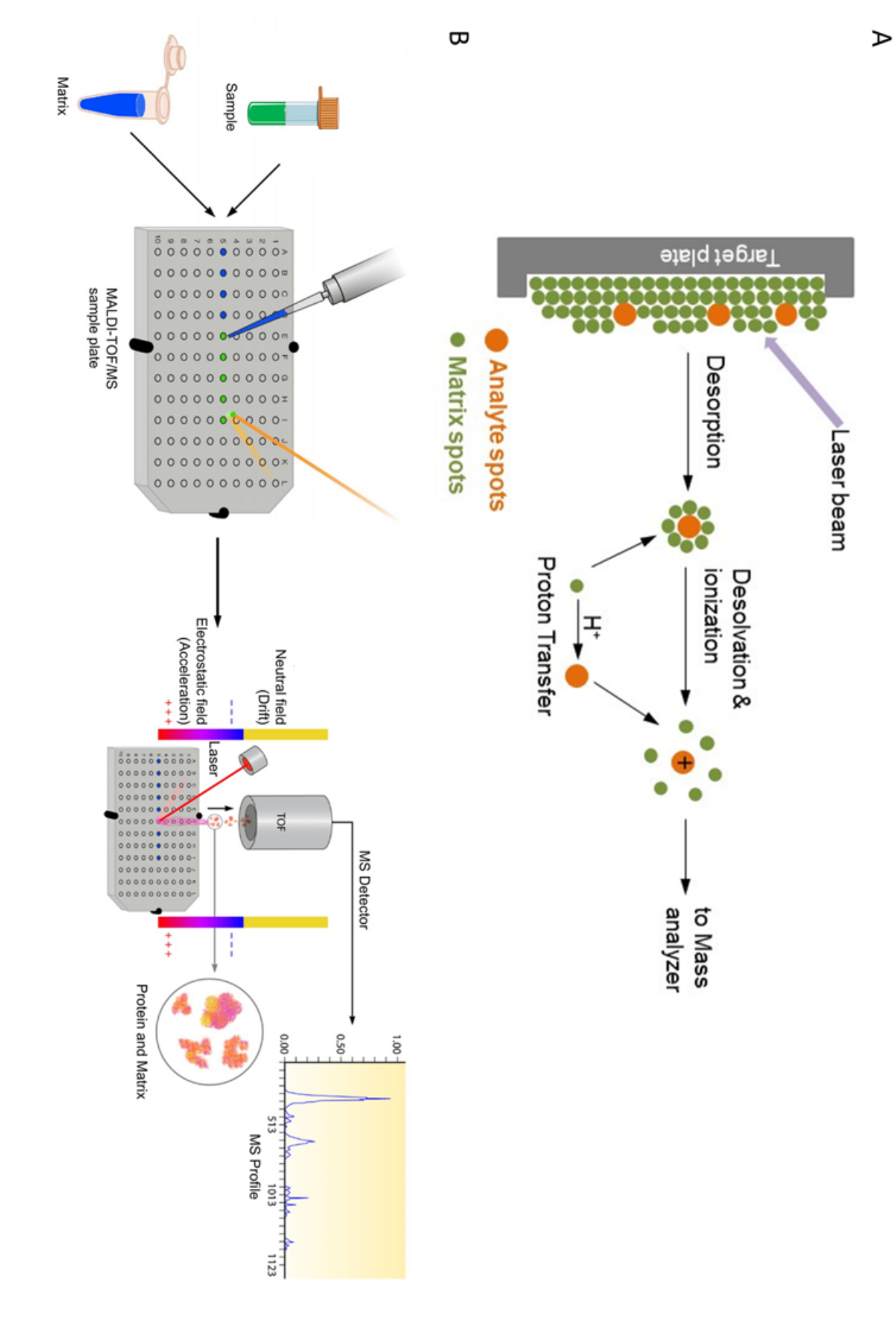

(A) The principle of MALDI-ToF, the analyte is embedded in a very large excess of a matrix compound deposited on a solid surface called a target, usually made of a conducting metal and having spots for several different samples to be applied. After a very brief laser pulse, the irradiated spot is rapidly heated and becomes vibrationally excited. The matrix molecules energetically ablated from the surface of the sample, absorb the ~~laser energy and carry the analyte molecules into the gas phase as well. During the ablation process, the analyte~~ molecules are usually ionized by being protonated or deprotonated with the nearby matrix molecules. The most common MALDI ionization format is for analyte molecules to carry a single positive charge (B) The process of MALDI-TOF mass spectrometry

spectral libraries or database searches. LC-MS/MS offers several advantages, including high sensitivity and selectivity for compound identification and quantification, the ability to analyze complex mixtures, structural elucidation capabilities, and quantification of trace-level compounds. However, there are some limitations, such as the requirement for compounds to be soluble in common LC solvents and ionizable, matrix effects that can influence ionization efficiency, and potentially lower reproducibility compared to UV detection for some analytes. LC-MS/MS is widely used in various fields, including metabolomics, proteomics, pharmaceutical analysis, and environmental testing. The choice of fragmentation technique often depends on the specific application and the type of compounds being analyzed (Baars and Perlman 2016). In this work, LC-MS/MS was used for the identification of O-GlcNACylation of GSK3β, using ETD and HCD fragmentation techniques and the experiments were be done by Collaboration with Adeline PAGE (Protein Science Facility, SFR Biosciences Univ Lyon, ENS de Lyon, CNRS UAR3444, Inserm US8, Université Claude Bernard Lyon 1, 50 Avenue Tony Garnier, Lyon F-69007, France).

ETD-MS fragmentation

ETD is a fragmentation technique used in LC-MS/MS for peptide and protein analysis. ETD induces fragmentation by transferring electrons from singly charged anions to higher charge state cationic molecules like peptides and proteins. This causes fragmentation of the amide bonds along the peptide/protein backbone, generating complementary c- and z-type fragment ions. ETD is particularly useful for analyzing and preserving labile post-translational modifications (PTMs) on peptides and proteins. It is often employed in metabolomics and biopharmaceutical applications (*Dissociation Technique Technology Overview | Thermo Fisher Scientific - FR* 2023).

HCD-Fragmentation

HCD (Higher-energy Collisional Dissociation) is a collision-induced dissociation (CID) technique associated with Orbitrap instruments. It uses voltage offsets to increase the kinetic energy of precursor ions, which then collide with nitrogen molecules in the ion routing multipole cell. HCD can generate and trap fragment ions with low m/z values, making it useful for detecting protein modifications like phosphotyrosine and for tandem mass tag (TMT) experiments. It typically provides a more even distribution of fragment intensities compared to ion trap CID, often resulting in better peptide sequence coverage (*Dissociation Technique Technology Overview | Thermo Fisher Scientific - FR* 2023; *(15) Understanding Mass Spec Fragmentation Techniques | LinkedIn* 2024).
ETD and HCD produce different types of fragment ions (c/z vs b/y), providing complementary sequence information. HCD often provides more consecutive sequence residues ($\geq$7 amino acids) than ETD in de novo sequencing approaches. The m/z ranges where ETD and HCD contribute the most peptide identifications substantially overlap (Shen et al. 2011; *Dissociation Technique Technology Overview | Thermo Fisher Scientific - FR* 2023).

3.3. Nuclear Magnetic Resonance (NMR)

Principle of NMR

NMR allows the study of the folding of the polypeptide chain in space (three-dimensional structure), characterization of protein interactions with their different partners (determination of the dissociation constant of complexes and interaction mapping), characterization of PTMs (site, relative level of modification, crosstalk between PTMs close in sequence, effect on conformation, effect on interactions with partners), and screening of bioactive small molecules, among the main applications.
NMR is based on the phenomenon of resonance that occurs when certain nuclei absorb a specific

amount of energy when placed in a magnetic field and subjected to a radiofrequency. This energy absorption is characteristic of each type of nucleus.

Application on Tau protein

Samples perpataion:
For NMR experiments, we work at concentrations of Tau and its isoforms equal to or greater than 200 μM. 2 mg of lyophilized protein is solubilized in 200 μL of NMR buffer (50 mM phosphate buffer pH 6.6, 50 mM NaCl, 2.5 mM EDTA, 1 mM DTT, 1/10 v/v D_2O, 1/200 v/v TMSP).
To detect the resonances of phosphorylated S and T residues, a 2D ^{15}N HSQC spectrum at 293K on a Bruker 900 MHz Avance NEO NMR spectrometer equipped with a triple resonance cryoprobe is recorded.
Nuclear Magnetic Resonance (NMR) of proteins allows the study of the folding of the polypeptide chain in space (three-dimensional structure), characterization of protein interactions with their various partners (determination of the dissociation constant of complexes and interaction mapping), characterization of PTMs (site, relative level of modification, crosstalk between PTMs close in sequence, effect on conformation, effect on interactions with partners), and screening of bioactive small molecules, among the main applications.
For NMR experiments, we work at concentrations of Tau and its isoforms equal to or greater than 200 μM. 2 mg of lyophilized protein is solubilized in 200 ţL of NMR buffer (50 mM phosphate buffer pH 6.6, 50 mM NaCl, 2.5 mM EDTA, 1 mM DTT, 1/10 v/v D_2O, 1/200 v/v TMSP).
To detect the resonances of phosphorylated S and T residues, a 2D ^{15}N HSQC spectrum at 293K on a Bruker 900 MHz Avance NEO NMR spectrometer equipped with a triple resonance cryoprobe is recorded.

3.4. Detection and analysis of O-GlcNACylated proteins

Click Chemistry Reaction

The Click-iT^{TM} O-GlcNAc Enzymatic Labeling System provides a highly sensitive and efficient method for the in vitro modification of O-GlcNAc modified proteins. Proteins are enzymatically labeled using a permissive mutant β-1,4-galactosyltransferase (Gal-T1 (Y289L)) (Figure 13.2), which transfers azido-modified galactose (GalNAz) from UDP-GalNAz to O-GlcNAc residues on the target proteins. As a second step, target proteins can then be detected using one of the Click-iT^{TM} Pro-

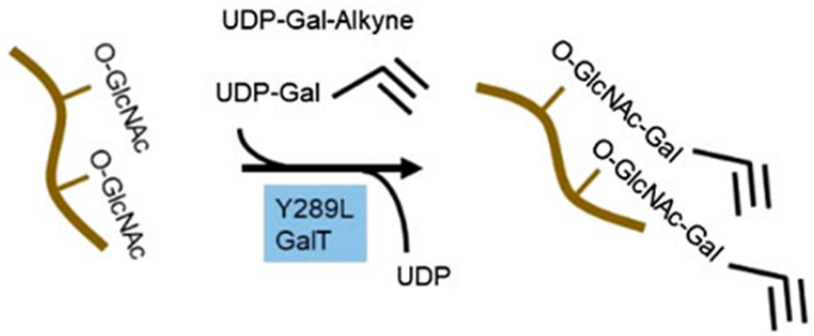

Figure 13.2: Transfer of azido-modified galactose GALNAz from UDP-GalNAz to O-GlcNAc residues

tein Analysis Detection methods (PEG or TAMRA labeling, figure 13.2), which are compatible with downstream mass spectrometry (MS) analyses including LC-MS/MS and MALDI MS, and Invitrogens Multiplexed Proteomics$^{\delta}$ technologies. Labeling and detection can be completed in less than 24

hours, with high sensitivity, detecting as little as 1 picomole of α-crystallin, a protein which is only 210% O-GlcNAc modified.

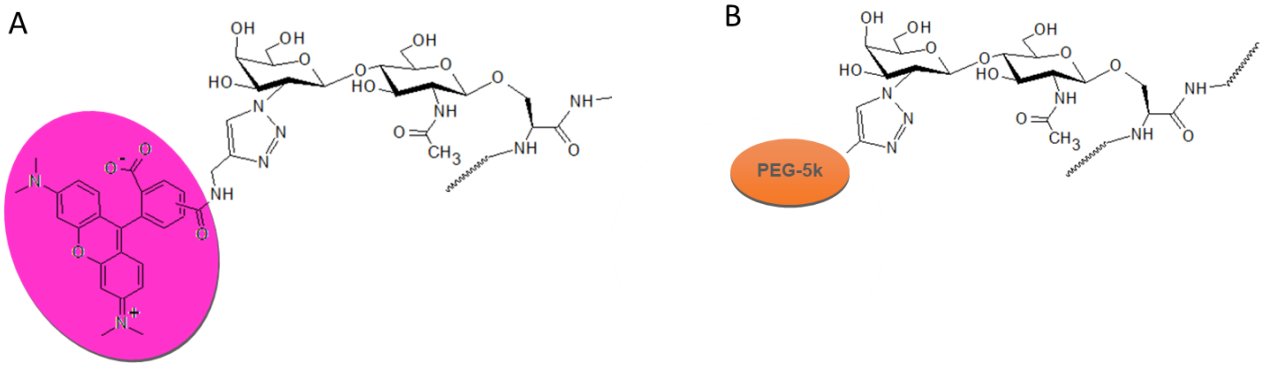

(A) TAMRA and (B) PEG labeling of O-GlcNAc modified protein

Figure 13.3: Click chemistry reaction products

Labeling protocol: This step is similar between the TAMRA and the PEG labeling. The potential O-GlcNAcylated Tau fragments and GSK3β constructs are precipitated using chloroform/ methanol. Two centrifugation steps are performed in the presence of chloroform/ methanol/ water. The upper aqueous phase is removed, while the lower phase and the protein layer are mixed with methanol for a second centrifugation step. The protein pellet is dried and resuspended in a buffer at pH 7.9 containing 20 mM HEPES and 1% SDS, then heated at 80řC for 5 to 10 minutes to resolubilize the proteins. The first step of labeling involves adding GalNAz to the GlcNAc residues using the enzyme Gal-T1, utilizing the Click-iT O-GlcNAc Enzymatic Labeling System (Invitrogen). The sample is incubated with the labeling buffer, 100 mM $MnCl_2$, UDP-GalNAz, and Gal-T1 overnight at 4řC. A negative control is prepared similarly without the enzyme.
Detection protocol: The second labeling step, which allows the click-chemistry reaction, uses the Click-iT TAMRA Protein Analysis Detection Kit (Invitrogenő). For this labeling, the fluorescent TAMRA reagent can be replaced with PEG-alkyne. After a 20-minute incubation with TAMRA or PEG and two additives from the kit, the proteins are precipitated again using chloroform/methanol, and the residual pellet is resuspended in Laemmli buffer and heated at 95řC for 10 minutes. The sample, along with the negative control, is analyzed by SDS-PAGE. Optionally, a Western blot can be performed for increased sensitivity. The click chemistry reactions described are resumed in figure 13.4

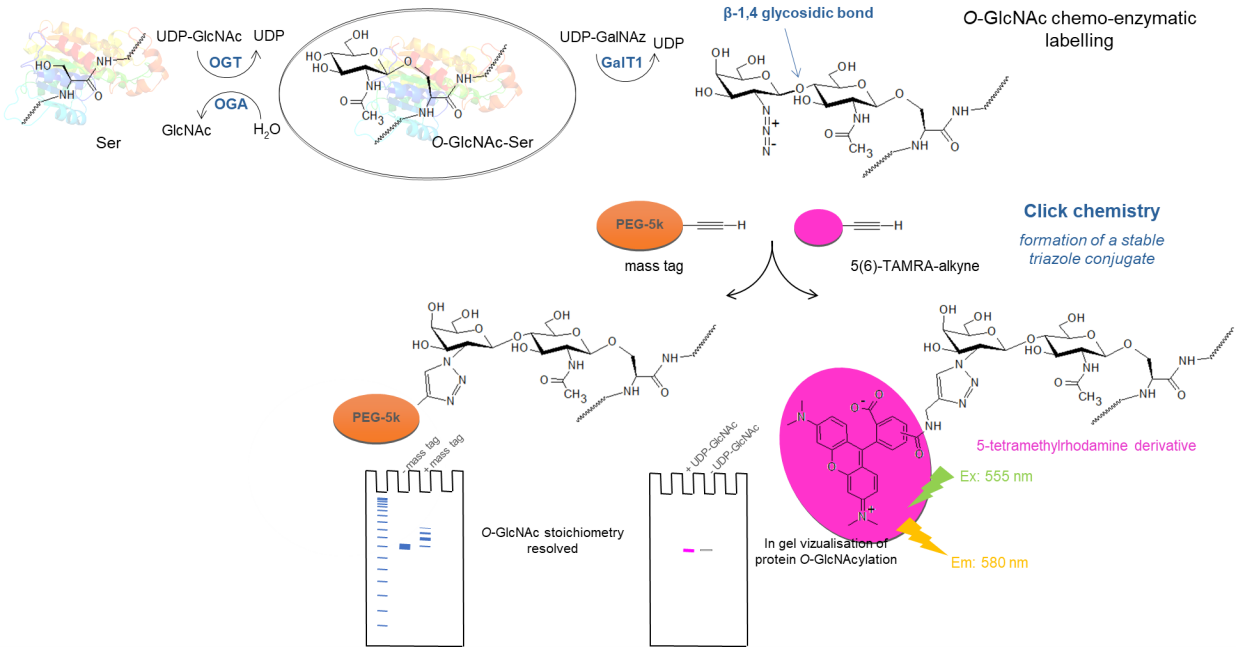

Figure 13.4: General scheme of the protein O-GlcNAcylation reaction using recombinant OGT and the the chemoenzymatic labeling

Chapter 14: Buffers

1. Reagents and Recipes

The compositions of the buffers and media used in the following sections are detailed below. LB media, SDS-PAGE gels, and running buffer were prepared using distilled water, while M9 media and all buffer solutions were prepared using MilliQ grade deionized water.

Bacterial Growth Media

Media	Components
LB Agar	10 g/L peptone 5 g/L yeast extract 10 g/L NaCl 15 g/L agar pH adjusted to 7.5 before sterilization using an autoclave
LB Media	10 g/L peptone 5 g/L yeast extract 10 g/L NaCl pH adjusted to 7.5 before sterilization using an autoclave
M9 Minimal Media	6 g/L Na_2HPO_4 3 g/L KH_2PO_4 0.5 g/L NaCl 0.1 mM $CaCl_2$ 1 mM $MgSO_4$ 100 ţg/mL antibiotics 10 ţg/mL thiamine 1.7 g/L yeast nitrogen base All components pre-sterilized using an autoclave or 0.2 ţm filter, prepared in a laminar flow clean bench

Table 14.1: Bacterial Growth Media and Their Components

2. Buffers and Solutions

Tau purification buffers

GSK3β purification buffer

CDK2/Cycline A purifiation buffer

Buffer	Binding Buffer	Elution Buffer / Buffer Components
CEX Buffer	50 mM phosphate buffer 20 mM NaCl 1 mM EDTA pH adjusted to 6.5, filter-sterilized	50 mM phosphate buffer 1 M NaCl 1 mM EDTA pH adjusted to 6.5, filter-sterilized
HPLC Buffer	5% ACN 0.1% TFA	80% ACN 0.1% TFA
Desalting Buffer	50 mM ammonium bicarbonate	
NMR Buffer	50 mM phosphate buffer 25 mM NaCl 2.5 mM EDTA pH adjusted to 6.6, filter-sterilized	

Table 14.2: Tau Buffers and Their Components

Buffer	Components
Wash Buffer	50 mM sodium phosphate buffer, pH 7.8 300 mM NaCl 10 mM Imidazole Autoclave
Elution Buffer	50 mM sodium phosphate buffer, pH 7.8 300 mM NaCl 250 mM Imidazole
1 M DTT Stock Solution	1 M DTT
HMED 5X Phosphorylation Buffer	250 mM Hepes-KOH, pH 7.8 250 mM NaCl 62.5 mM MgCl2 5 mM EDTA

Table 14.3: GSK3β Buffers and Their Components

Buffer	Components
Wash Buffer	50 mM Tris-HCl pH 7.0 150 mM NaCl 1 mM EDTA Autoclave
Extraction Buffer	50 mM Tris-HCl pH 7.0 150 mM NaCl 1 mM EDTA 1 mM DTT 0.1 % NP40 Protease inhibitor 1X
Elution Buffer	50 mM Tris-HCl pH 7.0 150 mM NaCl 1 mM EDTA 1 mM DTT 0.1 mg/mL GST-tagged PreScis-sion Protease
HMED 5X Phosphorylation Buffer	250 mM Hepes-KOH, pH 7.8 250 mM NaCl 62.5 mM MgCl2 5 mM EDTA

Table 14.4: CDK2/CyclineA Buffers and Their Components

Part VIII

Conclusion

Alzheimers disease and other tauopathies are neurodegenerative disorders characterized by the abnormal accumulation of Tau protein aggregates in the brain (Goedert et al. 1996b). They can be classified based on Tau isoforms, clinical symptoms, and the structural characteristics of Tau aggregates. These conditions include among others Alzheimers disease (AD), fronto-temporal dementia (FTD), Primary agerelated tauopathy (PART), Picks Disease (PiD), progressive supranuclear palsy (PSP), chronic traumatic encephalopathy (CTE), argyrophilic grain disease (AGD) and corticobasal degeneration (CBD), each pre- sening with a variety of clinical manifestations such as cognitive decline, movement disorders, and neuropsychiatric symptoms. The overlap of these features complicates diagnosis and underscores the necessity for a deeper understanding of Taus role in these diseases (Riley, Graner, and Veronesi 2022).

Clinically, tauopathies can be divided into cognitive and behavioral disorders, as seen in Alzheimers and Picks disease, and movement disorders, which are more prominent in PSP and CBD. Structurally, classification based on cryo-electron microscopy reveals filamentous structures of Tau aggregates, distinguishing between left-handed structures typically associated with AD and CTE, and right-handed structures linked to CBD and AGD. This structural classification reflects the cellular localization of Tau lesions and provides insights into the pathogenesis and progression of tauopathies (Shi et al. 2021b).

The balance of 3R to 4R Tau isoforms is crucial for normal Tau function, as imbalance in this ratio are associated with various tauopathies. Classification by Tau isoforms distinguishes between three-repeat (3R) tauopathies, such as PiD, which predominantly feature 3-repeat Tau isoforms, and four-repeat (4R) tauopathies, including PSP, CBD and AGD, characterized by 4-repeat tau isoforms. Addition- ally, mixed 3R and 4R tauopathies, such as AD, PART and CTE, exhibit an approximately equal ratio of both isoforms (Shi et al. 2021b; Chen et al. 2010).

Tau, a crucial microtubule-associated protein, stabilizes microtubules in neurons, which is essential for maintaining cellular structure and function. The microtubule-binding domain facilitates Taus interaction with microtubules and plays a significant role in Tau aggregation into filaments and NFTs, observed in tauopathies (Hu et al. 2023). Within this context, the R2 repeat, only present in 4R isoforms, and R3 repeat, present in 3R and 4R isoforms, each contain a hexapeptide sequencePHF6* (275-VQIINK-280) and PHF6 (306-VQIVYK-311), respectivelythat are critical for fibril formation. Additionally, cysteine residues C291 in R2 and C322 in R3 have been found to accelerate the nucleation phase of the fibrillization process (Savastano et al. 2020; Saito et al. 2021).

Alzheimers disease, as a secondary tauopathy, is notably characterized by the presence of both intraneuronal NFTs and extracellular amyloid plaques in the brain. The extent of NFTs and amyloid plaques correlates with disease severity. It was suggested that amyloid-β, according to the amyloid cascade hypothesis, is the trigger of a cascade of changes, leading to Tau hyperphosphorylation and impairment. From this perspective, Tau is presented as an effector in neurodegeneration, as evidenced by the fact that neuronal loss and cognitive decline better correlates with the progression of Tau inclusions than accumulation of amyloid plaques.

Our study provides significant insights into the complex regulation of Glycogen Synthase Kinase 3β (GSK3β) activity and its implications for Tau pathology. GSK3β, a serine/threonine proline-dependent kinase, is a key player in various cellular processes due to its ability to phosphorylate a broad range of substrates, including transcription factors, microtubule-associated proteins, and components of signaling pathways such as Wnt/β-catenin and PI3K/Akt (Beurel, Grieco, and Jope 2015; Cole and Sutherland 2008; Sutherland 2011). Its activity is modulated by various post-translational modi- fications, particularly phosphorylation. Constitutively active, GSK3β was shown to be inhib-

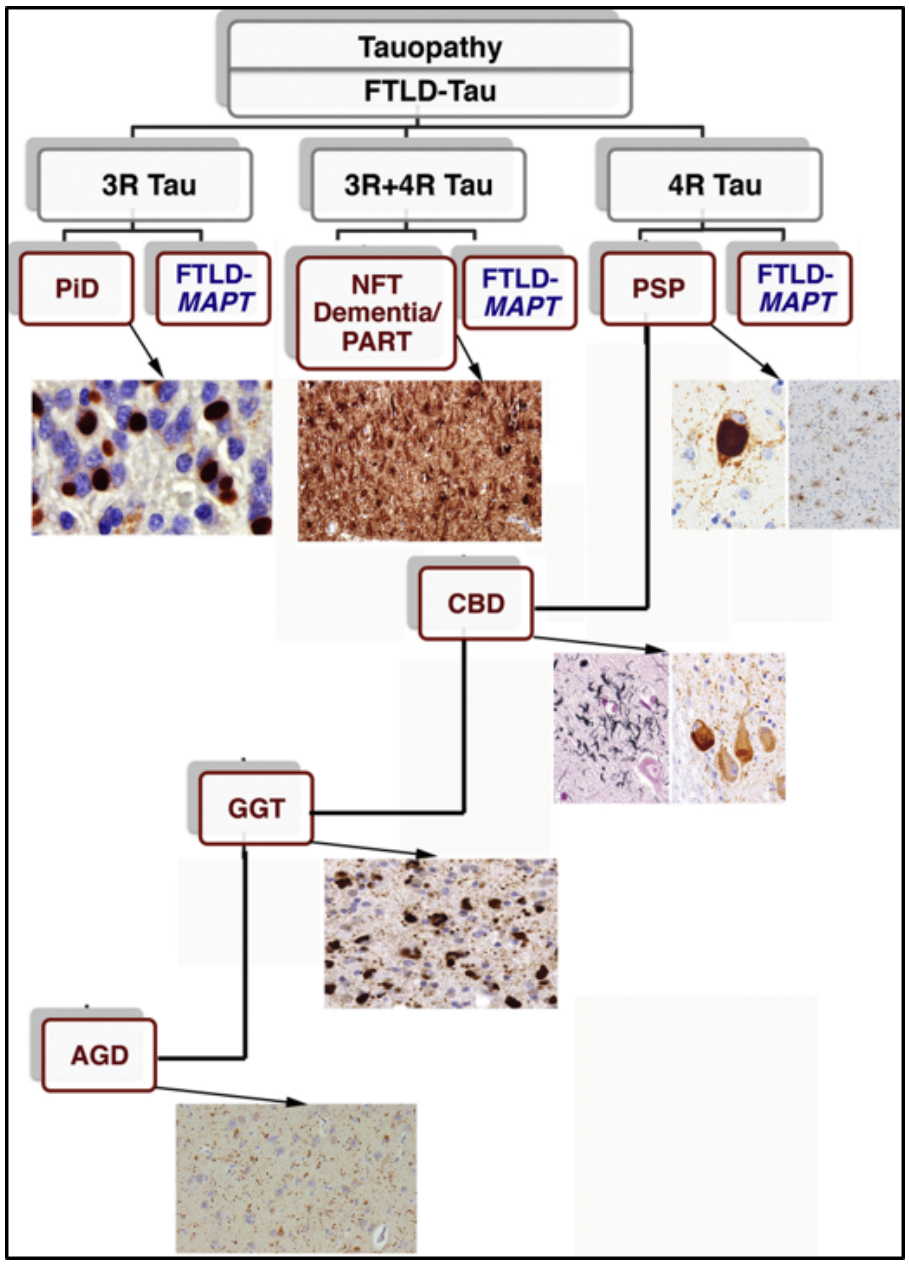

Figure 14.1: Molecular pathological classification of tauopathies (Höglinger, Respondek, and Kovacs 2018)

ited by phosphorylation. Additionally, the O-β-linked N-acetylglucosaminylation, as a dynamic and reversible modification of serine or thre- onine residues, is another PTM of GSK-3β which could play a role in regulating GSK-3β activity, but poorly defined so far. Increased O-GlcNAcylation can stabilize GSK-3β and enhance its activity in certain contexts, such as in cardiac cells under pressure overload conditions, leading to detrimental effects like impaired cardiac hypertrophy and heart failure by inhibiting compensatory signaling pathways such as NFAT (Nuclear Factor of Activated T-cells) (Matsuno et al. 2023). The O-GlcNAcylation of GSK-3β modulates its activity in a cell type- and stimulus-specific manner; for example, in kidney HEK-293FT cells, O-GlcNAcylation positively regulates GSK-3β phosphorylation at Ser9, suggesting a complex interplay that influences insulin signaling and resistance (Shi et al. 2012). Phosphorylation at Ser9 is another key regulatory mechanism for GSK-3β, known to inhibit its kinase activity and thereby promote processes like glycogen synthesis and various signal- ing pathways, often mediated by upstream kinases such as AKT, which is activated in response to insulin signaling (Shi et al. 2012). The relationship between O-GlcNAcylation and phosphorylation is intricate; while O-GlcNAcylation can promote GSK-3β activity, it may also interfere with phosphorylation by reducing AKT activation, creating a feedback loop that affects cel-

lular responses to insulin and other signals (Matsuno et al. 2023; Shi et al. 2012). In addition, a prephosphorylation of substrates (priming) by another kinase is involved in the regulation of GSK3β kinase activity, since it is required for GSK3β activity on most of its substrates. The primed substrate occupies a phosphate-binding pocket close to the active site. Therefore, GSK3β preferred substrates contain the S/T-x-x-x-pS/pT(P) motif (where x is any amino acid) in which pS/pT is the priming site, and GSK3β, eventually sequentially, phosphorylates S/T four residues upstream of the priming site.

GSK3β, the most abundant isoform in the central nervous system, is particularly relevant in neuron physiology, influencing processes such as neuronal morphogenesis, synaptic plasticity, and memory. Notably, GSK3β activity increases with age and is implicated in Alzheimer's disease through its effects on amyloid-beta (Aβ) peptide accumulation and Tau hyperphosphorylation, contributing to neurofibrillary tangle formation and associated neurodegeneration.

Our research shows that active (phosphorylated) Akt inhibits GSK3β in a phosphorylation-independent manner and Akt-mediated phosphorylation on Ser9 selectively restores GSK3β kinase activity on a primed Tau substrate such as Tau PHF-1 epitope (pS396/pS400/pS404). We have previously found that PHF-1 phosphorylation mediated by GSK3 is not dependent on priming, but priming at S404 (e.g. by CDK2/cyclinA) contributes to an increase of PHF-1 phosphorylation level in its triple phosphorylated form. Our results underscore a differential role of GSK3β Ser9 phosphorylation on primed and unprimed PHF-1. GSK3β phosphorylation thus competes with Akt binding on one hand to alleviate its inhibitory effect only on the primed substrate, and on the other, prevent binding of the unprimed substrate. Our findings suggested that Ser9 phosphorylation dynamically regulates interactions of the phosphate-binding pocket towards the N-terminus of GSK3 itself, the primed substrates and Akt. A competition between phosphorylated Akt and GSK3β pSer9 for the phosphate-binding pocket might explain the recovery of kinase activity in which a dynamic conformational exchange between a closed, inactive and an open, active form of pSer9-GSK3β is likely to occur. Such equilibrium could be displaced only by a primed substrate that would compete with GSK3β pSer9 for the phosphate-binding pocket in contrast to an unprimed substrate.

In addition, we have extensively described the O-GlcNAc modification of GSK3β in a site-specific manner highlighting multiple O-GlcNAc occupations in the disordered N- and C-terminal domains, including Ser9 and surrounding Thr7, Thr8 and Ser13 residues, as well as in the kinase domain opposite to the active and phosphate-binding sites. O-GlcNAcylation does not have any effect on GSK3β kinase activity nor on inhibitory Akt binding. Our findings reveal that O-GlcNAcylation may contribute to GSK3β inhibition through Akt binding while Akt-mediated phosphorylation in the absence of O-GlcNAcylation promotes GSK3β activation and subsequent PHF-1 hyperphosphorylation. Therefore, O-GlcNAcylation may counteract Akt hyperactivation, e.g. as seen in various cancers, by stabilizing inhibitory Akt binding to GSK3β and preventing its reactivation mediated by Ser9 phosphorylation with respect to primed substrates. Elevated O-GlcNAc levels, such as those achieved through Thiamet-G treatment, could thus influence Tau hyperphosphorylation by modulating GSK3β activity via the PI3K/Akt pathway, potentially mitigating Tau aggre- gation and seeding behavior (Figure 14.2). This complex interplay between phosphorylation and O-GlcNAcylation underscores the in- tricate regulation of GSK3β and its critical role in Tau pathology, highlighting potential therapeutic targets for tauopathies and other neurodegenerative conditions. By differentially targeting GSK3s regulatory mechanisms, it may be possible to finetune its activity toward specific substrates, providing a strategic approach to modulate the effects of dysregulated GSK3β in neurodegenerative diseases, including Alzheimers, Parkinsons, and Huntingtons diseases, as well as CNS-related disorders like autism and cognitive disabilities.

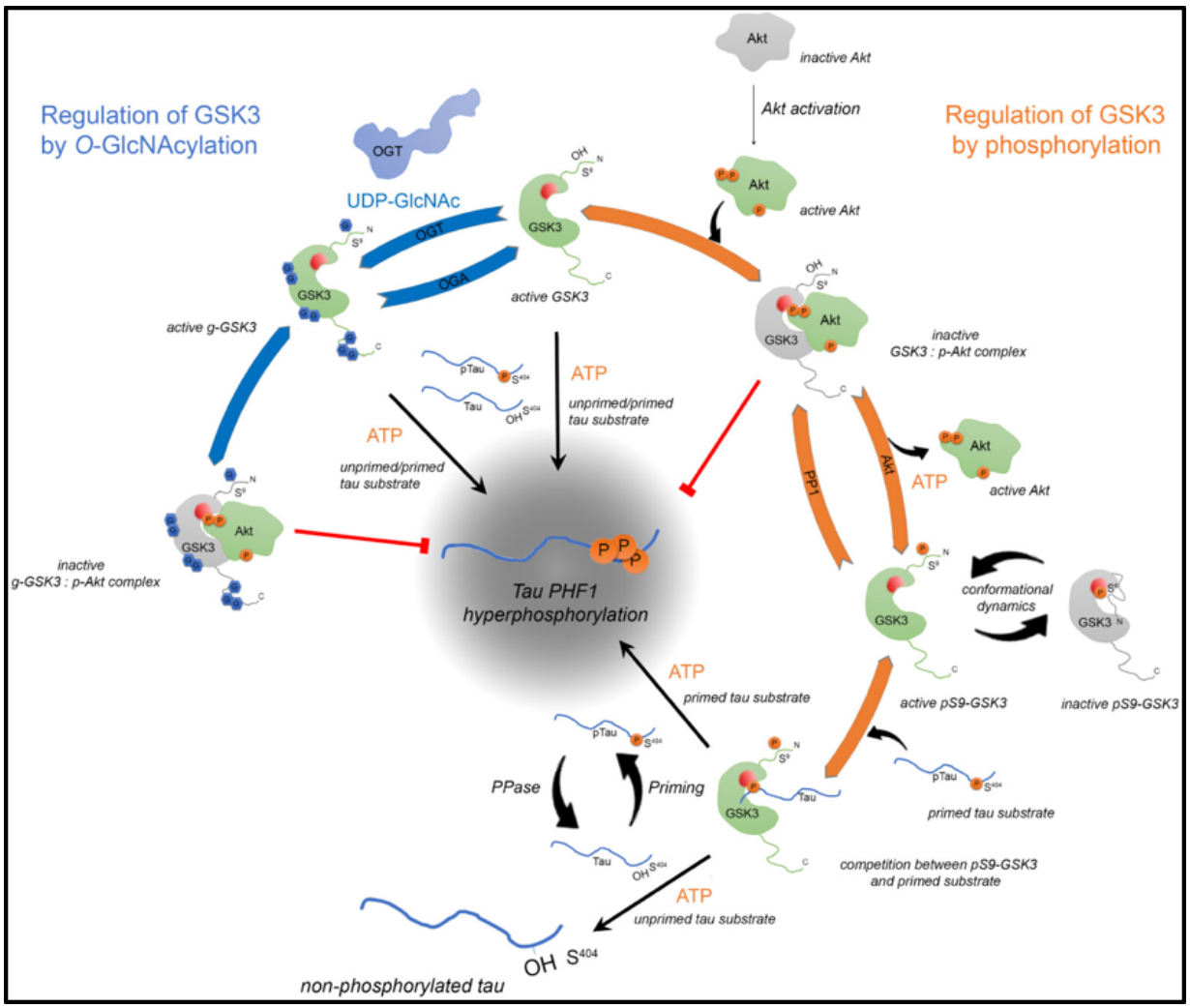

Figure 14.2: Model of GSK3β kinase activity regulation on primed and unprimed Tau substrates by binding to active, phosphorylated Akt and Ser9 phosphorylation (orange) and by OGT-mediated O-GlcNAc glycosylation (blue).

Our study further explores the impact of GSK3β kinase activity on Tau aggregation mechanisms, particularly the phosphorylation-dependent changes in microtubule polymerization and seeding properties of Tau fragments. Our research focuses on Tau aggregation mechanisms, focusing on the effects of GSK3β phosphorylation on Taus aggregation and seeding behavior. We observed that Tau fragments, particularly those from the R2Ct and R3Ct regions, spanning the entire C-terminal domain starting from either the R2 or R3 repeats, exhibit altered microtubule polymerization and seeding activity depending on their phos- phorylation state. We have shown that R3Ct seeds can stimulate the aggregation of both R2Ct and R3Ct fragments while R2Ct preferentially promote its self-assembly indicating that the presence of the R2 repeat induces a cross-seeding barrier. We have proposed that R2 and R3 repeats could be the respective catalytic center for conformational selection of R2Ct and R3Ct during fibril assembly. Furthermore, PHF-1 hyperphosphorylation of both fragments provided by GSK3β, prevents tubulin polymerization and promotes a local conformational change. The latter results in an additional propensity to fold into an extended β-sheet conformation that extends over a sequence encompassing part of the PHF-1 motif (residues 392-402) in both fragments.

With regard to the aggregation of the full-length Tau 2N4R isoform, R2Ct and R3Ct seeds exhibit distinct behavior depending on their phosphorylation state or the presence of an aggregation-prone mutation (P301L) or not. R3Ct seeds are more efficient than R2Ct to seed Tau aggregation, and their seeding activity is independent of their phosphorylation state. In contrast, seeding of Tau-P301L aggregation is comparable with R2Ct and R3Ct seeds but is dependent on the PHF-1 phosphorylation

state with phosphorylated seeds exhibiting a stronger seeding activity over non-phosphorylated seeds. Although the R2Ct fragment contains a greater proportion of 2N4R Tau isoform than R3Ct (and both encompass the P301 site), the seeding barrier for R3Ct seeds to promote Tau aggregation appears to be lower than for R2Ct seeds, supporting the previous observation that R2 undergoes conformational dynamics into fibrils that has been shown to regulate fibrillar assembly. Moreover, phosphorylated seeds decrease the cross-seeding barrier to promote aggregation of the non-phosphorylated tau-P301L monomer. Overall, our study highlights that GSK3β phosphorylation of Tau fragments is able to decrease the seeding/cross-seeding barrier and/or change the conformational selection to recruit monomers into seeds. Moreover, it is likely that the seeding efficiency is an intricate cooperative mechanism that involved a complex interplay between the capacity of seeds to template conformational changes and the aggregation propensity of the monomers.

This study also underscores the challenges of studying the relationship between Tau phosphorylation and aggregation due to the limitations of specific tools for accurate analysis. We propose that semi-synthetic approaches, like those successfully used to address the role of PTMs in the aggregation process of α-synuclein, could enhance site-specific analysis of Tau PHF-1 phosphorylation (PHF1-2P or pS396/pS404, PHF1-3P or pS396/pS400/pS404) and tackle the phosphorylation/(dys)function relationships. We have explored the effect of different PHF-1 phosphorylation states on the (dys)functions of full-length Tau 2N4R taking advantage of the expressed protein ligation (EPL) approach to provide site-specific, homogenous phosphorylation in a collaboration with Prof. Christian P. Hackenberger (FMP, Humboldt-Universität zu Berlin). In this study, our group was involved in the functional characterization of the semi-synthetic Tau proteins. We have shown that increasing the number of phosphorylation sites within the PHF-1 epitope leads to a gradual loss on the activity of Tau in tubulin assembly. In an aggregation assay induced by heparin, a classical external inducer of Tau aggregation, phosphorylation reduces the formation of fibrils. However, this setup does not allow discriminating the intrisinc effect of phosphorylation on the aggregation capacity from the loss of heparin binding due to charge repulsion. Therefore, based on our previous study that has highlighted the seeding ability of the R3Ct fragment, we have further explored the effect of R3Ct seeds with different phosphorylation patterns on the aggregation of full-length Tau 2N4R in diverse combination of phosphorylation of PHF-1 taking advantage of the EPL approach. Interestingly, we demonstrated that GSK3β phosphorylation of R3Ct enables the aggregation of the semisynthetic Tau PHF1-3P more efficiently than non-phosphorylated seeds or those of non-phosphorylated Tau.

The marked differences we observed in the Tau cross-seeding aggregation assay, although contrasting with heparin-induced Tau aggregation, may prompt a re-evaluation of the use of heparin to study in vitro aggregation of phosphorylated Tau, as already suggested for acetylated Tau where lysine acetylation neutralizes the positive charges in the MTBD involved in heparin binding. Methods without the addition of aggregation initiators may be helpful for studying the effect of PTMs in the aggregation process to avoid interference with the inducer effect. However, aggregation of full-length Tau without external inducers proved to be hardly achieved and reproducible. Furthermore, the neuron-to-neuron prion-like propagation of Tau pathology has been described as an important mechanism involved in the progression of neurodegenerative diseases. The propagation, or spreading, is described as a process in which pathological Tau seeds from diseased neurons act as templates to promote misfolding of monomeric Tau proteins in healthy connected neurons, leading to their aggregation into fibrils. Thus, based on the rationale to study the molecular mechanisms at play in the seeding of Tau aggregation, we found here for the PHF-1 epitope that seeds of the R3Ct fragment, depending on their phosphorylation status, differentially seed the fibrillar aggregation of full-length Tau in a manner dependent on their phosphorylation, with phosphorylated seeds being more selective towards phosphorylated Tau. Together our results suggest that phosphorylation may provide a cross-seeding barrier, possibly through distinct strain conformation between phosphorylated and non-phosphorylated seeds. Phos-

phorylated seeds could preferentially recruit the corresponding phosphorylated protein, as exemplified by the preference in isoform recruitment between distinct tauopathy strains that are characterized by different proportions of 4R and 3R isoforms incorporated into fibrils. Such advancements would provide deeper insights into the role of Tau seeds in the propagation of tau pathology associated to neurodegenerative diseases and poten- tially uncover new therapeutic targets.

Appendices

Appendix A: Publications

List of Publications

Articles

1. Isabelle Landrieu, Elian Dupré, Davy Sinnaeve, **Léa El Hajjar**, Caroline Smet-Nocca. *Deciphering the Structure and Formation of Amyloids in Neurodegenerative Diseases with Chemical Biology Tools.* Frontiers in Chemistry, 2022, 10.

2. **Léa El Hajjar**, Adeline Page, Clarisse Bridot, François-Xavier Cantrelle, Isabelle Landrieu, Caroline Smet-Nocca. *Regulation of Glycogen Synthase Kinase-3β by Phosphorylation and O-β-Linked N-Acetylglucosaminylation: Implications on Tau Protein Phosphorylation.* Biochemistry, 2024, 63 (12), 1513-1533. DOI: 10.1021/acs.biochem.4c00095

3. **Léa El Hajjar**, Emmanuelle Boll, François-Xavier Cantrelle, Clarisse Bridot, Isabelle Landrieu, Caroline Smet-Nocca. *Effect of PHF-1 Hyperphosphorylation on the Seeding Activity of C-terminal Tau Fragments.* Submitted to Scientific Reports, August 2024.

4. Justine Mortelecque, Orgeta Zejneli, Séverine Bégard, Margarida C. Simões, **Lea ElHajjar**, Marine Nguyen, François-Xavier Cantrelle, Xavier Hanoulle, Jean-Christophe Rain, Morvane Colin, Cláudio M. Gomes, Luc Buée, Isabelle Landrieu, Clément Danis, Elian Dupré. *A Selection and Optimization Strategy for Single-Domain Antibodies Targeting the PHF6 Linear Peptide within the Tau Intrinsically Disordered Protein.* Journal of Biological Chemistry, Volume 300, Issue 4, 107163. DOI: 10.1016/j.jbc.2024.107163

Book Chapters

1. **Léa El Hajjar**, Clarisse Bridot, Marine Nguyen, François-Xavier Cantrelle, Isabelle Landrieu, Caroline Smet-Nocca. *The O-GlcNAc Modification of Recombinant Tau Protein and Characterization of the O-GlcNAc Pattern for Functional Study.* In: Smet-Nocca C (ed), *Tau Protein: Methods and Protocols.* Springer New York, New York, NY. (published, 2023).

2. **Léa El Hajjar**, Clarisse Bridot, Marine Nguyen, François-Xavier Cantrelle, Isabelle Landrieu, Caroline Smet-Nocca. *Phosphorylation of Tau Protein by CDK2/Cyclin A and GSK3β Recombinant Kinases: Analysis of Phosphorylation Patterns by Nuclear Magnetic Resonance Spectroscopy.* In: Smet-Nocca C (ed), *Tau Protein: Methods and Protocols.* Springer New York, New York, NY. (published, 2023).

Publications

width=!,height=!,pages=-
    width=!,height=!,pages=-

12 width=!,height=!,pages=- width=!,height=!,pages=- width=!,height=!,pages=- width=!,height=!,pages=-

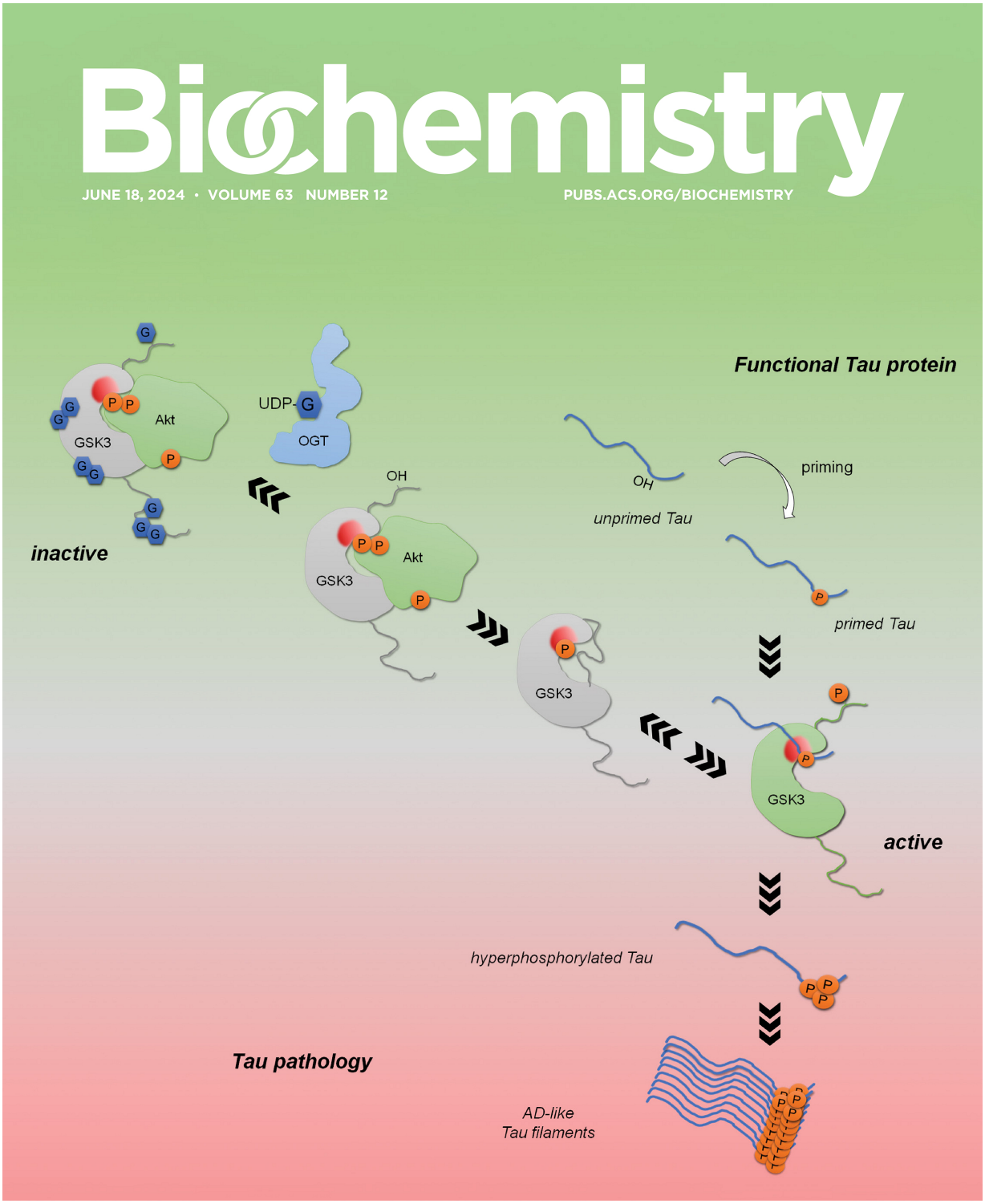
Biochemistry
JUNE 18, 2024 • VOLUME 63 NUMBER 12
PUBS.ACS.ORG/BIOCHEMISTRY
Functional Tau protein
UDP-G
OGT
Akt
GSK3
inactive
OH
unprimed Tau
priming
primed Tau
active
hyperphosphorylated Tau
Tau pathology
AD-like
Tau filaments
ACS Publications
Most Trusted. Most Cited. Most Read.
www.acs.org

Appendix B: Workshops, Conferences and other activities

Workshops and Conferences

Enrolled in the Graduate School for the Precision Health Master's Program in Lille for the entire duration of the PhD, with participation in 7 out of 10 seminars:

- Current Concepts in Precision Health - Pathophysiology and Molecular Basis of Diseases and Treatments Applied to Precision Health
- Current Concepts in Precision Health - From OMICS to Systems Biology
- Current Concepts in Precision Health - Ethics, Health, and Society
- Current Concepts in Precision Health - Public Policy and Health Economics
- Current Concepts in Precision Health - From Cohorts to Cutting-Edge Researches
- Current Concepts in Precision Health - Medical Devices and Precision Health
- Current Concepts in Precision Health - AI and Precision Health

Conferences and Training:

- **International EuroTau Conference:** Lille, October 25-26, 2021
- **Groupe Français des Peptides et Protéines (GFPP-22):** Port Leucat, May 29 - June 3, 2022
- **Practical Training on Liquid and Solid NMR:** NMR Platform, Lille, June 13-17, 2022
- **National Infranalytics Day (INFRANALYTICS: Support for Industry and Innovation):** Member of the organizing team responsible for badge printing, guest reception, and audio-visual management. Lille, June 23, 2022
- **Regional NMR-EPR Conference:** Lille, June 28, 2022
- **International AILM22 Conference (Advanced Isotopic Labelling Methods for Integrated Structural Biology):** Grenoble, September 13-16, 2022
- **Instruct Practical School AILM22:** Grenoble, September 16-23, 2022
- **Training on Effective Thesis Writing (and other documents) with LaTeX, Level Absolute Beginner**
- **Summer School of the Graduate Program in Precision Health:** July 3, 2023
- **International EuroTau Conference:** Lille, April 27-28, 2023

Supervision of Interns

During my PhD, I had the opportunity to supervise and mentor two interns, contributing to their academic training and research experience.

Observation Intern

I supervised a third-year observation intern for one week. This short-term internship provided the student with an introductory experience in a research environment.

Master 1 Intern

I supervised a Master 1 intern for a period of two months. During this time, the intern worked on a project related to post-translational modifications in the context of Alzheimer's disease.

Master 1 Intern

I supervised a Master 1 intern for a period of one and a half months. During this time, the intern worked on a project related to post-translational modifications and the seeding effect of fragments in the context of Alzheimer's disease.

Master 2 Intern

I also had the opportunity to supervise a Master 2 intern for six months. This intern worked on the study of post-translational modifications and the seeding effect of fragments in the context of Alzheimer's disease.

These supervision experiences were personally and professionally rewarding, allowing me to share my knowledge and expertise with future scientists and researchers.

Teaching

Second Year of PhD

During my second year of PhD, I participated in teaching activities as follows:

- Experimental Biochemistry Fundamentals: 28 hours of practical sessions (7 sessions of 4 hours each) and 6 hours of tutorials (4 sessions of 1 hour 30 minutes each), totaling 34 hours.
- Biochemistry: 20 hours of practical sessions (5 sessions of 4 hours each) and 6 hours of tutorials (4 sessions of 1 hour 30 minutes each), totaling 26 hours.

Third Year of PhD

In my third year of PhD, I will also participate in teaching activities as follows:

- Experimental Biochemistry Fundamentals: 16 hours of practical sessions (4 sessions of 4 hours each).
- Biochemistry: 16 hours of practical sessions (4 sessions of 4 hours each) and 6 hours of tutorials (4 sessions of 1 hour 30 minutes each), totaling 22 hours.

Bibliography

(15) Understanding Mass Spec Fragmentation Techniques | LinkedIn (2024). URL: https://www.linkedin.com/pulse/understanding-mass-spec-fragmentation-techniques-marcus-macht/.

A Armstrong, Richard (2019). "Risk Factors for Alzheimer's Disease". In: *Folia Neuropathologica* 57.2, pp. 87–105. ISSN: 1509-572X. DOI: 10.5114/fn.2019.85929. pmid: 31556570.

Abasi, Lannah S. et al. (Mar. 1, 2024). "Phosphorylation Regulates Tau's Phase Separation Behavior and Interactions with Chromatin". In: *Communications Biology* 7.1, pp. 1–17. ISSN: 2399-3642. DOI: 10.1038/s42003-024-05920-4.

Aβ Plaques: Breeding Ground for Toxic Tau? | ALZFORUM (2017). URL: https://www.alzforum.org/news/research-news/av-plaques-breeding-ground-toxic-tau.

Abskharon, Romany et al. (Oct. 10, 2023). "Structure-Based Design of Nanobodies That Inhibit Seeding of Alzheimer's Patient–Extracted Tau Fibrils". In: *Proceedings of the National Academy of Sciences* 120.41, e2300258120. DOI: 10.1073/pnas.2300258120.

Aducanumab to Be Discontinued as an Alzheimer's Treatment (2022). Alzheimer's Disease and Dementia. URL: https://alz.org/alzheimers-dementia/treatments/aducanumab.

Ahmed, Zeshan et al. (May 1, 2014). "A Novel in Vivo Model of Tau Propagation with Rapid and Progressive Neurofibrillary Tangle Pathology: The Pattern of Spread Is Determined by Connectivity, Not Proximity". In: *Acta Neuropathologica* 127.5, pp. 667–683. ISSN: 1432-0533. DOI: 10.1007/s00401-014-1254-6.

Ainani, Hassan et al. (Mar. 2023). "Liquid-Liquid Phase Separation of Protein Tau: An Emerging Process in Alzheimer's Disease Pathogenesis". In: *Neurobiology of Disease* 178, p. 106011. ISSN: 09699961. DOI: 10.1016/j.nbd.2023.106011.

Akhmanova, Anna and Michel O. Steinmetz (Apr. 2008). "Tracking the Ends: A Dynamic Protein Network Controls the Fate of Microtubule Tips". In: *Nature Reviews Molecular Cell Biology* 9.4, pp. 309–322. ISSN: 1471-0072, 1471-0080. DOI: 10.1038/nrm2369.

Albert, Marie et al. (June 2019). "Prevention of Tau Seeding and Propagation by Immunotherapy with a Central Tau Epitope Antibody". In: *Brain* 142.6, pp. 1736–1750. ISSN: 0006-8950. DOI: 10.1093/brain/awz100. pmid: 31038156.

Almeida, Zaida L. and Rui M. M. Brito (Jan. 2020). "Structure and Aggregation Mechanisms in Amyloids". In: *Molecules* 25.5 (5), p. 1195. ISSN: 1420-3049. DOI: 10.3390/molecules25051195.

Alonso, Alejandra D. et al. (Oct. 9, 2018). "Hyperphosphorylation of Tau Associates With Changes in Its Function Beyond Microtubule Stability". In: *Frontiers in Cellular Neuroscience* 12. ISSN: 1662-5102. DOI: 10.3389/fncel.2018.00338.

Alquezar, Carolina, Shruti Arya, and Aimee W. Kao (Jan. 7, 2021). "Tau Post-translational Modifications: Dynamic Transformers of Tau Function, Degradation, and Aggregation". In: *Frontiers in Neurology* 11, p. 595532. ISSN: 1664-2295. DOI: 10.3389/fneur.2020.595532. pmid: 33488497.

Alteen, Matthew G, Hong Yee Tan, and David J Vocadlo (June 1, 2021). "Monitoring and Modulating *O*-GlcNAcylation: Assays and Inhibitors of *O*-GlcNAc Processing Enzymes". In: *Current Opinion in Structural Biology*. Protein-Carbohydrate Complexes and Glycosylation 108 Sequences and Topology 68, pp. 157–165. ISSN: 0959-440X. DOI: 10.1016/j.sbi.2020.12.008.

Alzheimer's Disease (2018). nhs.uk. URL: https://www.nhs.uk/conditions/alzheimers-disease/.

Alzheimer's Disease (2017). *Alzheimer's Disease: The Great Morbidity of the 21st Century*. American Scientist. URL: https://www.americanscientist.org/article/alzheimers-disease-the-great-morbidity-of-the-21st-century.

Arnold, C. Shane et al. (Nov. 15, 1996). "The Microtubule-associated Protein Tau Is Extensively Modified with O-linked N-acetylglucosamine *". In: *Journal of Biological Chemistry* 271.46, pp. 28741–28744. ISSN: 0021-9258, 1083-351X. DOI: 10.1074/jbc.271.46.28741. pmid: 8910513.

Arrasate, M., M. Pérez, and J. Avila (Jan. 2000). "Tau Dephosphorylation at Tau-1 Site Correlates with Its Association to Cell Membrane". In: *Neurochemical Research* 25.1, pp. 43–50. ISSN: 0364-3190. DOI: 10.1023/a:1007583214722. pmid: 10685603.

Asai, Hirohide et al. (Nov. 2015). "Depletion of Microglia and Inhibition of Exosome Synthesis Halt Tau Propagation". In: *Nature Neuroscience* 18.11, pp. 1584–1593. ISSN: 1546-1726. DOI: 10.1038/nn.4132. pmid: 26436904.

Ashraf, Ghulam Md et al. (2014). "Protein Misfolding and Aggregation in Alzheimer's Disease and Type 2 Diabetes Mellitus". In: *CNS & neurological disorders drug targets* 13.7, pp. 1280–1293. ISSN: 1871-5273. pmid: 25230234. URL: https://www.ncbi.nlm.nih.gov/pmc/articles/PMC5193501/.

Audouard, Emilie et al. (Oct. 2016). "High-Molecular-Weight Paired Helical Filaments from Alzheimer Brain Induces Seeding of Wild-Type Mouse Tau into an Argyrophilic 4R Tau Pathology in Vivo". In: *The American Journal of Pathology* 186.10, pp. 2709–2722. ISSN: 1525-2191. DOI: 10.1016/j.ajpath.2016.06.008. pmid: 27497324.

Avila, Jesús (May 22, 2006). "Tau Phosphorylation and Aggregation in Alzheimer's Disease Pathology". In: *FEBS Letters*. Istanbul Special Issue 580.12, pp. 2922–2927. ISSN: 0014-5793. DOI: 10.1016/j.febslet.2006.02.067.

Avila, Jesús et al. (2012). "Tau Phosphorylation by GSK3 in Different Conditions". In: *International Journal of Alzheimer's Disease* 2012, p. 578373. ISSN: 2090-8024. DOI: 10.1155/2012/578373. pmid: 22675648.

Baars, Oliver and David H. Perlman (July 7, 2016). "Small Molecule LC-MS/MS Fragmentation Data Analysis and Application to Siderophore Identification". In: *Applications from Engineering with MATLAB Concepts*. Ed. by Jan Valdman. InTech. ISBN: 978-953-51-2459-7 978-953-51-2460-3. DOI: 10.5772/63018.

Ballatore, Carlo, Virginia M.-Y. Lee, and John Q. Trojanowski (Sept. 2007). "Tau-Mediated Neurodegeneration in Alzheimer's Disease and Related Disorders". In: *Nature Reviews Neuroscience* 8.9, pp. 663–672. ISSN: 1471-0048. DOI: 10.1038/nrn2194.

Bellenguez, Céline et al. (Apr. 2022). "New Insights into the Genetic Etiology of Alzheimer's Disease and Related Dementias". In: *Nature Genetics* 54.4, pp. 412–436. ISSN: 1546-1718. DOI: 10.1038/s41588-022-01024-z.

Beurel, Eleonore, Steven F. Grieco, and Richard S. Jope (Apr. 2015). "Glycogen Synthase Kinase-3 (GSK3): Regulation, Actions, and Diseases". In: *Pharmacology & therapeutics* 0, pp. 114–131. ISSN: 0163-7258. DOI: 10.1016/j.pharmthera.2014.11.016. pmid: 25435019.

Bhagat, Reshma et al. (Nov. 2023). "Long Non-Coding RNA SNHG8 Drives Stress Granule Formation in Tauopathies". In: *Molecular Psychiatry* 28.11, pp. 4889–4901. ISSN: 1476-5578. DOI: 10.1038/s41380-023-02237-2.

Biernat, Jacek and Eva-Maria Mandelkow (Mar. 1999). "The Development of Cell Processes Induced by Tau Protein Requires Phosphorylation of Serine 262 and 356 in the Repeat Domain and Is Inhibited by Phosphorylation in the Proline-rich Domains". In: *Molecular Biology of the Cell* 10.3, pp. 727–740. ISSN: 1059-1524. DOI: 10.1091/mbc.10.3.727.

Biernat, Jacek et al. (Nov. 2002). "Protein Kinase MARK/PAR-1 Is Required for Neurite Outgrowth and Establishment of Neuronal Polarity". In: *Molecular Biology of the Cell* 13.11, pp. 4013–4028. ISSN: 1059-1524. DOI: 10.1091/mbc.02-03-0046.

Bijttebier, Sebastiaan et al. (Apr. 7, 2023). "IP-LC-MSMS Enables Identification of Three Tau *O* -GlcNAcylation Sites as *O* -GlcNAcase Inhibition Pharmacodynamic Readout in Transgenic Mice Overexpressing Human Tau". In: *Journal of Proteome Research* 22.4, pp. 1309–1321. ISSN: 1535-3893, 1535-3907. DOI: 10.1021/acs.jproteome.2c00822.

Biogen Walks Away From Aducanumab to Prioritize Lecanemab and Alzheimer Disease Pipeline (Jan. 31, 2024). Neurology live. URL: https://www.neurologylive.com/view/biogen-walks-away-from-aducanumab-prioritize-lecanemab-alzheimer-disease-pipeline.

Biswas, Sayantanee and Katherine Kalil (Jan. 10, 2018). "The Microtubule-Associated Protein Tau Mediates the Organization of Microtubules and Their Dynamic Exploration of Actin-Rich Lamellipodia and Filopodia of Cortical Growth Cones". In: *Journal of Neuroscience* 38.2, pp. 291–307. ISSN: 0270-6474, 1529-2401. DOI: 10.1523/JNEUROSCI.2281-17.2017. pmid: 29167405.

Bloom, George S. (Apr. 1, 2014). "Amyloid-β and Tau: The Trigger and Bullet in Alzheimer Disease Pathogenesis". In: *JAMA Neurology* 71.4, pp. 505–508. ISSN: 2168-6149. DOI: 10.1001/jamaneurol.2013.5847.

Borghgraef, Peter et al. (Dec. 23, 2013). "Increasing Brain Protein O-GlcNAc-ylation Mitigates Breathing Defects and Mortality of Tau.P301L Mice". In: *PLoS ONE* 8.12. Ed. by Tsuneya Ikezu, e84442. ISSN: 1932-6203. DOI: 10.1371/journal.pone.0084442.

Bourré, Gwendoline et al. (2018). "Direct Crosstalk Between O-GlcNAcylation and Phosphorylation of Tau Protein Investigated by NMR Spectroscopy". In: *Frontiers in Endocrinology* 9. ISSN: 1664-2392. URL: https://www.frontiersin.org/articles/10.3389/fendo.2018.00595.

Bowne-Anderson, Hugo (2013). "Microtubule dynamic instability: A new model with coupled GTP hydrolysis and multistep catastrophe". In: 35.5, pp. 452–461. ISSN: 0265-9247. DOI: 10.1002/bies.201200131. pmid: 31556570.

Boyarko, Ben and Vivian Hook (Oct. 21, 2021). "Human Tau Isoforms and Proteolysis for Production of Toxic Tau Fragments in Neurodegeneration". In: *Frontiers in Neuroscience* 15. ISSN: 1662-453X. DOI: 10.3389/fnins.2021.702788.

Braak, H. and E. Braak (1991). "Neuropathological Stageing of Alzheimer-related Changes". In: *Acta Neuropathologica* 82.4, pp. 239–259. ISSN: 0001-6322. DOI: 10.1007/BF00308809. pmid: 1759558.

— (1995). "Staging of Alzheimer's Disease-Related Neurofibrillary Changes". In: *Neurobiology of Aging* 16.3, 271–278; discussion 278–284. ISSN: 0197-4580. DOI: 10.1016/0197-4580(95)00021-6. pmid: 7566337.

Braak, Heiko et al. (Oct. 2006). "Staging of Alzheimer Disease-Associated Neurofibrillary Pathology Using Paraffin Sections and Immunocytochemistry". In: *Acta Neuropathologica* 112.4, pp. 389–404. ISSN: 0001-6322. DOI: 10.1007/s00401-006-0127-z. pmid: 16906426.

Braithwaite, Steven P., Jeffry B. Stock, and M. Maral Mouradian (Apr. 1, 2012). "α-Synuclein Phosphorylation as a Therapeutic Target in Parkinson's Disease". In: *Reviews in the Neurosciences* 23.2, pp. 191–198. ISSN: 2191-0200. DOI: 10.1515/revneuro-2011-0067.

Brion, J P et al. (Jan. 1, 1985). "Neurofibrillary Tangles of Alzheimer's Disease: An Immunohistochemical Study". In: *Journal of submicroscopic cytology* 17.1, pp. 89–96. ISSN: 0022-4782. pmid: 3973960.

Brunello, Cecilia A. et al. (May 2020). "Mechanisms of Secretion and Spreading of Pathological Tau Protein". In: *Cellular and Molecular Life Sciences* 77.9, pp. 1721–1744. ISSN: 1420-682X, 1420-9071. DOI: 10.1007/s00018-019-03349-1.

Bukar Maina, Mahmoud, Youssra K. Al-Hilaly, and Louise C. Serpell (Mar. 2016). "Nuclear Tau and Its Potential Role in Alzheimer's Disease". In: *Biomolecules* 6.1 (1), p. 9. ISSN: 2218-273X. DOI: 10.3390/biom6010009.

Burt, Rajan A. et al. (May 19, 2022). "Mapping the O-GlcNAc Modified Proteome: Applications for Health and Disease". In: *Frontiers in Molecular Biosciences* 9. ISSN: 2296-889X. DOI: 10.3389/fmolb.2022.920727.

Butler, Morgane L M D et al. (Oct. 1, 2022). "Tau Pathology in Chronic Traumatic Encephalopathy Is Primarily Neuronal". In: *Journal of Neuropathology & Experimental Neurology* 81.10, pp. 773–780. ISSN: 0022-3069. DOI: 10.1093/jnen/nlac065.

Cabrera-Pastor, Andrea (June 27, 2024). "Extracellular Vesicles as Mediators of Neuroinflammation in Intercellular and Inter-Organ Crosstalk". In: *International Journal of Molecular Sciences* 25.13, p. 7041. ISSN: 1422-0067. DOI: 10.3390/ijms25137041. pmid: 39000150.

Caceres, A., S. Potrebic, and K. S. Kosik (June 1, 1991). "The Effect of Tau Antisense Oligonucleotides on Neurite Formation of Cultured Cerebellar Macroneurons". In: *Journal of Neuroscience* 11.6, pp. 1515–1523. ISSN: 0270-6474, 1529-2401. DOI: 10.1523/JNEUROSCI.11-06-01515.1991. pmid: 1904479.

Caceres, Alfredo and Kenneth S. Kosik (Feb. 1990). "Inhibition of Neurite Polarity by Tau Antisense Oligonucleotides in Primary Cerebellar Neurons". In: *Nature* 343.6257 (6257), pp. 461–463. ISSN: 1476-4687. DOI: 10.1038/343461a0.

Calle, Beatriz et al. (Sept. 1, 2021). "Benefits of Chemical Sugar Modifications Introduced by Click Chemistry for Glycoproteomic Analyses". In: *Journal of the American Society for Mass Spectrometry* 32.9, pp. 2366–2375. ISSN: 1879-1123. DOI: 10.1021/jasms.1c00084. pmid: 33871988.

Calvo-Rodriguez, Maria et al. (Nov. 8, 2019). "In Vivo Detection of Tau Fibrils and Amyloid β Aggregates with Luminescent Conjugated Oligothiophenes and Multiphoton Microscopy". In: *Acta Neuropathologica Communications* 7.1, p. 171. ISSN: 2051-5960. DOI: 10.1186/s40478-019-0832-1.

Cantrelle, François-Xavier et al. (2021). "Phosphorylation and O-GlcNAcylation of the PHF-1 Epitope of Tau Protein Induce Local Conformational Changes of the C-Terminus and Modulate Tau Self-Assembly Into Fibrillar Aggregates". In: *Frontiers in Molecular Neuroscience* 14. ISSN: 1662-5099. URL: https://www.frontiersin.org/articles/10.3389/fnmol.2021.661368.

Cardoso, Francisco Miguel Lopez et al. (Mar. 14, 2012). "Single Domain Camelid Antibodies That Neutralize Negative Strand Viruses". In: *Antiviral Drugs - Aspects of Clinical Use and Recent Advances*. IntechOpen. ISBN: 978-953-51-0256-4. DOI: 10.5772/34009.

Casamassimi, Amelia and Alfredo Ciccodicola (Mar. 14, 2019). "Transcriptional Regulation: Molecules, Involved Mechanisms, and Misregulation". In: *International Journal of Molecular Sciences* 20.6, p. 1281. ISSN: 1422-0067. DOI: 10.3390/ijms20061281. pmid: 30875728.

Causes and Risk Factors for Alzheimer's Disease (2024). Alzheimer's Disease and Dementia. URL: https://alz.org/alzheimers-dementia/what-is-alzheimers/causes-and-risk-factors.

Chakraborty, Pijush et al. (July 9, 2021). "Co-Factor-Free Aggregation of Tau into Seeding-Competent RNA-sequestering Amyloid Fibrils". In: *Nature Communications* 12.1 (1), p. 4231. ISSN: 2041-1723. DOI: 10.1038/s41467-021-24362-8.

Chakraborty, Pijush et al. (Dec. 19, 2023). *GSK3β Phosphorylation Catalyzes the Aggregation of Tau into Alzheimer's Disease-like Amyloid Strain*. DOI: 10.1101/2023.12.19.572292. Pre-published.

Chapuis, J. et al. (Nov. 2013). "Increased Expression of BIN1 Mediates Alzheimer Genetic Risk by Modulating Tau Pathology". In: *Molecular Psychiatry* 18.11, pp. 1225–1234. ISSN: 1476-5578. DOI: 10.1038/mp.2013.1. pmid: 23399914.

Chen, Dailu et al. (June 7, 2019). "Tau Local Structure Shields an Amyloid-Forming Motif and Controls Aggregation Propensity". In: *Nature Communications* 10.1 (1), p. 2493. ISSN: 2041-1723. DOI: 10.1038/s41467-019-10355-1.

Chen, J. et al. (Dec. 1992). "Projection Domains of MAP2 and Tau Determine Spacings between Microtubules in Dendrites and Axons". In: *Nature* 360.6405 (6405), pp. 674–677. ISSN: 1476-4687. DOI: 10.1038/360674a0.

Chen, Shufen et al. (2010). "MAPT Isoforms: Differential Transcriptional Profiles Related to 3R and 4R Splice Variants". In: *Journal of Alzheimer's Disease* 22.4, pp. 1313–1329. ISSN: 1387-2877. DOI: 10.3233/JAD-2010-101155. pmid: 20930284.

Chung, Chang Geon, Hyosang Lee, and Sung Bae Lee (Sept. 2018). "Mechanisms of Protein Toxicity in Neurodegenerative Diseases". In: *Cellular and molecular life sciences: CMLS* 75.17, pp. 3159–3180. ISSN: 1420-9071. DOI: 10.1007/s00018-018-2854-4. pmid: 29947927.

Chung, Dah-eun Chloe et al. (Aug. 23, 2021). "Cellular and Pathological Heterogeneity of Primary Tauopathies". In: *Molecular Neurodegeneration* 16.1, p. 57. ISSN: 1750-1326. DOI: 10.1186/s13024-021-00476-x.

Clavaguera, Florence et al. (July 2009). "Transmission and Spreading of Tauopathy in Transgenic Mouse Brain". In: *Nature Cell Biology* 11.7, pp. 909–913. ISSN: 1476-4679. DOI: 10.1038/ncb1901. pmid: 19503072.

Clavaguera, Florence et al. (June 4, 2013). "Brain Homogenates from Human Tauopathies Induce Tau Inclusions in Mouse Brain". In: *Proceedings of the National Academy of Sciences of the United States of America* 110.23, pp. 9535–9540. ISSN: 1091-6490. DOI: 10.1073/pnas.1301175110. pmid: 23690619.

Cohen, Todd J. et al. (2011). "The Acetylation of Tau Inhibits Its Function and Promotes Pathological Tau Aggregation". In: *Nature Communications* 2, p. 252. ISSN: 2041-1723. DOI: 10.1038/ncomms1255. pmid: 21427723.

Cole, Adam R. and Calum Sutherland (2008). "Measuring GSK3 Expression and Activity in Cells". In: *Methods in Molecular Biology (Clifton, N.J.)* 468, pp. 45–65. ISSN: 1064-3745. DOI: 10.1007/978-1-59745-249-6_4. pmid: 19099245.

Colin, Morvane et al. (Jan. 1, 2020). "From the Prion-like Propagation Hypothesis to Therapeutic Strategies of Anti-Tau Immunotherapy". In: *Acta Neuropathologica* 139. DOI: 10.1007/s00401-019-02087-9.

Colom-Cadena, Martí et al. (July 19, 2023). "Synaptic Oligomeric Tau in Alzheimer's Disease — A Potential Culprit in the Spread of Tau Pathology through the Brain". In: *Neuron* 111.14, 2170–2183.e6. ISSN: 0896-6273. DOI: 10.1016/j.neuron.2023.04.020.

Comtesse, N., E. Maldener, and E. Meese (May 11, 2001). "Identification of a Nuclear Variant of MGEA5, a Cytoplasmic Hyaluronidase and a Beta-N-acetylglucosaminidase". In: *Biochemical and Biophysical Research Communications* 283.3, pp. 634–640. ISSN: 0006-291X. DOI: 10.1006/bbrc.2001.4815. pmid: 11341771.

Cook, Casey et al. (2014). "Acetylation: A New Key to Unlock Tau's Role in Neurodegeneration". In: *Alzheimer's Research & Therapy* 6.3, p. 29. ISSN: 1758-9193. DOI: 10.1186/alzrt259. pmid: 25031639.

Coon, Keith D. et al. (Apr. 2007). "A High-Density Whole-Genome Association Study Reveals That APOE Is the Major Susceptibility Gene for Sporadic Late-Onset Alzheimer's Disease". In: *The Journal of Clinical Psychiatry* 68.4, pp. 613–618. ISSN: 1555-2101. DOI: 10.4088/jcp.v68n0419. pmid: 17474819.

Cooper, Geoffrey M. (2000). "Microtubules". In: *The Cell: A Molecular Approach. 2nd edition*. URL: https://www.ncbi.nlm.nih.gov/books/NBK9932/.

Coria, F., I. Rubio, and C. Bayón (1994). "Alzheimer's Disease, Beta-Amyloidosis, and Aging". In: *Reviews in the Neurosciences* 5.4, pp. 275–292. ISSN: 0334-1763. DOI: 10.1515/revneuro.1994.5.4.275. pmid: 7697197.

Crespo, Rosa, Wouter Koudstaal, and Adrian Apetri (Nov. 20, 2018). "In Vitro Assay for Studying the Aggregation of Tau Protein and Drug Screening". In: *Journal of Visualized Experiments: JoVE* 141. ISSN: 1940-087X. DOI: 10.3791/58570. pmid: 30531722.

Croft, Cara L. et al. (Mar. 2017). "Membrane Association and Release of Wild-Type and Pathological Tau from Organotypic Brain Slice Cultures". In: *Cell Death & Disease* 8.3, e2671–e2671. ISSN: 2041-4889. DOI: 10.1038/cddis.2017.97.

Cross, D. A. et al. (Dec. 21, 1995–28). "Inhibition of Glycogen Synthase Kinase-3 by Insulin Mediated by Protein Kinase B". In: *Nature* 378.6559, pp. 785–789. ISSN: 0028-0836. DOI: 10.1038/378785a0. pmid: 8524413.

Cuq, Professeur Jean-Louis (2024). "BIOCHIMIE DES PROTEINES". In.

Dahm, Ralf (Nov. 2006). "Alzheimer's Discovery". In: *Current Biology* 16.21, R906–R910. ISSN: 09609822. DOI: 10.1016/j.cub.2006.09.056.

Dajani, Rana et al. (June 15, 2001). "Crystal Structure of Glycogen Synthase Kinase 3β: Structural Basis for Phosphate-Primed Substrate Specificity and Autoinhibition". In: *Cell* 105.6, pp. 721–732. ISSN: 0092-8674. DOI: 10.1016/S0092-8674(01)00374-9.

Danis, Clément et al. (Apr. 6, 2022). "Inhibition of Tau Seeding by Targeting Tau Nucleation Core within Neurons with a Single Domain Antibody Fragment". In: *Molecular Therapy: The Journal of the American Society of Gene Therapy* 30.4, pp. 1484–1499. ISSN: 1525-0024. DOI: 10.1016/j.ymthe.2022.01.009. pmid: 35007758.

Dawson, P. E. and S. B. Kent (2000). "Synthesis of Native Proteins by Chemical Ligation". In: *Annual Review of Biochemistry* 69, pp. 923–960. ISSN: 0066-4154. DOI: 10.1146/annurev.biochem.69.1.923. pmid: 10966479.

De La-Rocque, Samantha et al. (Mar. 2021). "Knockin' on Heaven's Door: Molecular Mechanisms of Neuronal Tau Uptake". In: *Journal of Neurochemistry* 156.5, pp. 563–588. ISSN: 0022-3042. DOI: 10.1111/jnc.15144. pmid: 32770783.

De Rosa, Lucia et al. (Jan. 2, 2013). "Semi-Synthesis of Labeled Proteins for Spectroscopic Applications". In: *Molecules* 18.1, pp. 440–465. ISSN: 1420-3049. DOI: 10.3390/molecules18010440. pmid: 23282535.

Despres, Clément et al. (Aug. 22, 2017). "Identification of the Tau Phosphorylation Pattern That Drives Its Aggregation". In: *Proceedings of the National Academy of Sciences of the United States of America* 114.34, pp. 9080–9085. ISSN: 1091-6490. DOI: 10.1073/pnas.1708448114. pmid: 28784767.

DeTure, Michael et al. (Nov. 2002). "Tau Assembly in Inducible Transfectants Expressing Wild-Type or FTDP-17 Tau". In: *The American Journal of Pathology* 161.5, pp. 1711–1722. ISSN: 0002-9440. pmid: 12414518. URL: https://www.ncbi.nlm.nih.gov/pmc/articles/PMC1850799/.

DeTure, Michael A. and Dennis W. Dickson (Aug. 2, 2019). "The Neuropathological Diagnosis of Alzheimer's Disease". In: *Molecular Neurodegeneration* 14.1, p. 32. ISSN: 1750-1326. DOI: 10.1186/s13024-019-0333-5. pmid: 31375134.

Dickstein, D. L. et al. (Sept. 2016). "Cerebral [18 F]T807/AV1451 Retention Pattern in Clinically Probable CTE Resembles Pathognomonic Distribution of CTE Tauopathy". In: *Translational Psychiatry* 6.9, e900–e900. ISSN: 2158-3188. DOI: 10.1038/tp.2016.175.

Diez, Lisa and Susanne Wegmann (Sept. 25, 2020). "Nuclear Transport Deficits in Tau-Related Neurodegenerative Diseases". In: *Frontiers in Neurology* 11, p. 1056. ISSN: 1664-2295. DOI: 10.3389/fneur.2020.01056. pmid: 33101165.

Dignon, Gregory L., Robert B. Best, and Jeetain Mittal (Apr. 20, 2020). "Biomolecular Phase Separation: From Molecular Driving Forces to Macroscopic Properties". In: *Annual review of physical chemistry* 71, pp. 53–75. ISSN: 0066-426X. DOI: 10.1146/annurev-physchem-071819-113553. pmid: 32312191.

Dimou, Eleni et al. (July 2023). "Super-Resolution Imaging Unveils the Self-Replication of Tau Aggregates upon Seeding". In: *Cell Reports* 42.7, p. 112725. ISSN: 22111247. DOI: 10.1016/j.celrep.2023.112725.

Dissociation Technique Technology Overview | Thermo Fisher Scientific - FR (2023). URL: https://www.thermofisher.com/fr/fr/home/industrial/mass-spectrometry/mass-spectrometry-learning-center/mass-spectrometry-technology-overview/dissociation-technique-technology-overview.html.

Dominguez-Meijide, Antonio, Eftychia Vasili, and Tiago Fleming Outeiro (Nov. 13, 2020). "Pharmacological Modulators of Tau Aggregation and Spreading". In: *Brain Sciences* 10.11, p. 858. ISSN: 2076-3425. DOI: 10.3390/brainsci10110858. pmid: 33203009.

Donanemab Approved for Treatment of Early Alzheimer's Disease (2023). Alzheimer's Disease and Dementia. URL: https://alz.org/alzheimers-dementia/treatments/donanemab.

Downer, Brian et al. (Feb. 25, 2021). "Changes in Health Care Use by Mexican American Medicare Beneficiaries Before and After a Diagnosis of Dementia". In: *The Journals of Gerontology: Series A* 76.3. Ed. by Anne B Newman, pp. 534–542. ISSN: 1079-5006, 1758-535X. DOI: 10.1093/gerona/glaa236.

Duan, Pu et al. (Oct. 31, 2023). "Structure of the Nonhelical Filament of the Alzheimer's Disease Tau Core". In: *Proceedings of the National Academy of Sciences* 120.44, e2310067120. DOI: 10.1073/pnas.2310067120.

Dujardin, S., M. Colin, and L. Buée (Feb. 2015). "Invited Review: Animal Models of Tauopathies and Their Implications for Research/Translation into the Clinic". In: *Neuropathology and Applied Neurobiology* 41.1, pp. 59–80. ISSN: 1365-2990. DOI: 10.1111/nan.12200. pmid: 25428793.

Dujardin, Simon and Bradley T. Hyman (2019). "Tau Prion-Like Propagation: State of the Art and Current Challenges". In: *Advances in Experimental Medicine and Biology* 1184, pp. 305–325. ISSN: 0065-2598. DOI: 10.1007/978-981-32-9358-8_23. pmid: 32096046.

Duquette, Antoine et al. (Jan. 7, 2021). "Similarities and Differences in the Pattern of Tau Hyperphosphorylation in Physiological and Pathological Conditions: Impacts on the Elaboration of Therapies to Prevent Tau Pathology". In: *Frontiers in Neurology* 11. ISSN: 1664-2295. DOI: 10.3389/fneur.2020.607680.

Early-Onset Dementia and Alzheimer's Rates Grow for Younger American Adults (2021). URL: https://www.bcbs.com/the-health-of-america/reports/early-onset-dementia-alzheimers-disease-affecting-younger-american-adults.

El Hajjar, Léa et al. (June 18, 2024). "Regulation of Glycogen Synthase Kinase-3β by Phosphorylation and O-β-Linked N-Acetylglucosaminylation: Implications on Tau Protein Phosphorylation". In: *Biochemistry* 63.12, pp. 1513–1533. ISSN: 0006-2960. DOI: 10.1021/acs.biochem.4c00095.

El Mammeri, Nadia et al. (July 14, 2023). "Amyloid Fibril Structures of Tau: Conformational Plasticity of the Second Microtubule-Binding Repeat". In: *Science Advances* 9.28, eadh4731. DOI: 10.1126/sciadv.adh4731.

Elbaum-Garfinkle, Shana et al. (June 9, 2015). "The Disordered P Granule Protein LAF-1 Drives Phase Separation into Droplets with Tunable Viscosity and Dynamics". In: *Proceedings of the National Academy of Sciences of the United States of America* 112.23, pp. 7189–7194. ISSN: 1091-6490. DOI: 10.1073/pnas.1504822112. pmid: 26015579.

Eom, Tae-Yeon and Richard S. Jope (Mar. 5, 2009). "GSK3β N-terminus Binding to P53 Promotes Its Acetylation". In: *Molecular Cancer* 8.1, p. 14. ISSN: 1476-4598. DOI: 10.1186/1476-4598-8-14.

Falcon, Benjamin et al. (Jan. 9, 2015). "Conformation Determines the Seeding Potencies of Native and Recombinant Tau Aggregates". In: *The Journal of Biological Chemistry* 290.2, pp. 1049–1065. ISSN: 1083-351X. DOI: 10.1074/jbc.M114.589309. pmid: 25406315.

Falcon, Benjamin et al. (Sept. 2018a). "Structures of Filaments from Pick's Disease Reveal a Novel Tau Protein Fold". In: *Nature* 561.7721, pp. 137–140. ISSN: 1476-4687. DOI: 10.1038/s41586-018-0454-y.

Falcon, Benjamin et al. (Nov. 1, 2018b). "Tau Filaments from Multiple Cases of Sporadic and Inherited Alzheimer's Disease Adopt a Common Fold". In: *Acta Neuropathologica* 136.5, pp. 699–708. ISSN: 1432-0533. DOI: 10.1007/s00401-018-1914-z.

Falcon, Benjamin et al. (Apr. 2019). "Novel Tau Filament Fold in Chronic Traumatic Encephalopathy Encloses Hydrophobic Molecules". In: *Nature* 568.7752, pp. 420–423. ISSN: 0028-0836, 1476-4687. DOI: 10.1038/s41586-019-1026-5.

family=Canada given=Agence, prefix=de la santé publique du useprefix=false (Aug. 11, 2015). "Propagation de protéines mal repliées". In: URL: https://www.canada.ca/fr/sante-publique/services/rapports-publications/releve-maladies-transmissibles-canada-rmtc/numero-mensuel/2015-41/rmtc-volume-41-8-6-aout-2015-troubles-lies-proteines-repliees/rmtc-volume-41-8-6-aout-2015-troubles-lies-proteines-repliees-2.html.

Fang, X. et al. (Oct. 24, 2000). "Phosphorylation and Inactivation of Glycogen Synthase Kinase 3 by Protein Kinase A". In: *Proceedings of the National Academy of Sciences of the United States of America* 97.22, pp. 11960–11965. ISSN: 0027-8424. DOI: 10.1073/pnas.220413597. pmid: 11035810.

Fichou, Yann et al. (Dec. 26, 2018a). "Cofactors Are Essential Constituents of Stable and Seeding-Active Tau Fibrils". In: *Proceedings of the National Academy of Sciences* 115.52, pp. 13234–13239. DOI: 10.1073/pnas.1810058115.

Fichou, Yann et al. (May 1, 2018b). "Heparin-Induced Tau Filaments Are Structurally Heterogeneous and Differ from Alzheimer's Disease Filaments". In: *Chemical Communications* 54.36, pp. 4573–4576. ISSN: 1364-548X. DOI: 10.1039/C8CC01355A.

Fischer, Emil (1894). "Einfluss Der Configuration Auf Die Wirkung Der Enzyme. II". In: *Berichte der deutschen chemischen Gesellschaft* 27.3, pp. 3479–3483. ISSN: 1099-0682. DOI: 10.1002/cber.189402703169.

Fitzpatrick, Anthony W. P. et al. (July 2017). "Cryo-EM Structures of Tau Filaments from Alzheimer's Disease". In: *Nature* 547.7662 (7662), pp. 185–190. ISSN: 1476-4687. DOI: 10.1038/nature23002.

Flanagan, L. A. et al. (Sept. 1997). "The Structure of Divalent Cation-Induced Aggregates of PIP2 and Their Alteration by Gelsolin and Tau". In: *Biophysical Journal* 73.3, pp. 1440–1447. ISSN: 0006-3495. DOI: 10.1016/S0006-3495(97)78176-1. pmid: 9284311.

Fontaine, Sarah N. et al. (Feb. 11, 2015). "Cellular Factors Modulating the Mechanism of Tau Protein Aggregation". In: *Cellular and Molecular Life Sciences: CMLS* 72.10, pp. 1863–1879. ISSN: 1420-682X. DOI: 10.1007/s00018-015-1839-9. pmid: 25666877.

Förster, Sarah et al. (Sept. 1, 2014). "Increased O-GlcNAc Levels Correlate with Decreased O-GlcNAcase Levels in Alzheimer Disease Brain". In: *Biochimica et Biophysica Acta (BBA) - Molecular Basis of Disease* 1842.9, pp. 1333–1339. ISSN: 0925-4439. DOI: 10.1016/j.bbadis.2014.05.014.

Frame, S., P. Cohen, and R. M. Biondi (June 2001). "A Common Phosphate Binding Site Explains the Unique Substrate Specificity of GSK3 and Its Inactivation by Phosphorylation". In: *Molecular Cell* 7.6, pp. 1321–1327. ISSN: 1097-2765. DOI: 10.1016/s1097-2765(01)00253-2. pmid: 11430833.

Furman, Jennifer L. et al. (Jan. 1, 2017). "Widespread Tau Seeding Activity at Early Braak Stages". In: *Acta Neuropathologica* 133.1, pp. 91–100. ISSN: 1432-0533. DOI: 10.1007/s00401-016-1644-z.

Gandhi, Neha S. et al. (June 1, 2015). "A Phosphorylation-Induced Turn Defines the Alzheimer's Disease AT8 Antibody Epitope on the Tau Protein". In: *Angewandte Chemie* 127.23, pp. 6923–6927. ISSN: 00448249. DOI: 10.1002/ange.201501898.

Gao, Y. et al. (Mar. 30, 2001). "Dynamic O-glycosylation of Nuclear and Cytosolic Proteins: Cloning and Characterization of a Neutral, Cytosolic Beta-N-acetylglucosaminidase from Human Brain". In: *The Journal of Biological Chemistry* 276.13, pp. 9838–9845. ISSN: 0021-9258. DOI: 10.1074/jbc.M010420200. pmid: 11148210.

García-Morales, Victoria et al. (Dec. 2021). "Current Understanding of the Physiopathology, Diagnosis and Therapeutic Approach to Alzheimer's Disease". In: *Biomedicines* 9.12 (12), p. 1910. ISSN: 2227-9059. DOI: 10.3390/biomedicines9121910.

Gatta, Eleonora et al. (Mar. 1, 2016). "Evidence for an Imbalance between Tau *O*-GlcNAcylation and Phosphorylation in the Hippocampus of a Mouse Model of Alzheimer's Disease". In: *Pharmacological Research* 105, pp. 186–197. ISSN: 1043-6618. DOI: 10.1016/j.phrs.2016.01.006.

Gatz, Margaret et al. (Sept. 1, 2001). "Education and the Risk of Alzheimer's Disease: Findings From the Study of Dementia in Swedish Twins". In: *The Journals of Gerontology: Series B* 56.5, P292–P300. ISSN: 1079-5014. DOI: 10.1093/geronb/56.5.P292.

Gibbons, Garrett S., Virginia M. Y. Lee, and John Q. Trojanowski (Jan. 1, 2019). "Mechanisms of Cell-to-Cell Transmission of Pathological Tau". In: *JAMA neurology* 76.1, pp. 101–108. ISSN: 2168-6149. DOI: 10.1001/jamaneurol.2018.2505. pmid: 30193298.

Goedert, M and R Jakes (Dec. 1990). "Expression of Separate Isoforms of Human Tau Protein: Correlation with the Tau Pattern in Brain and Effects on Tubulin Polymerization." In: *The EMBO Journal* 9.13, pp. 4225–4230. ISSN: 0261-4189. pmid: 2124967. URL: https://www.ncbi.nlm.nih.gov/pmc/articles/PMC552204/.

Goedert, M. et al. (Oct. 1996a). "Assembly of Microtubule-Associated Protein Tau into Alzheimer-like Filaments Induced by Sulphated Glycosaminoglycans". In: *Nature* 383.6600, pp. 550–553. ISSN: 1476-4687. DOI: 10.1038/383550a0.

— (Oct. 10, 1996b). "Assembly of Microtubule-Associated Protein Tau into Alzheimer-like Filaments Induced by Sulphated Glycosaminoglycans". In: *Nature* 383.6600, pp. 550–553. ISSN: 0028-0836. DOI: 10.1038/383550a0. pmid: 8849730.

Goedert, Michel and Maria Grazia Spillantini (May 30, 2017). "Propagation of Tau Aggregates". In: *Molecular Brain* 10.1, p. 18. ISSN: 1756-6606. DOI: 10.1186/s13041-017-0298-7.

Goldberg, Howard J. et al. (Jan. 2006). "Posttranslational, Reversible O-glycosylation Is Stimulated by High Glucose and Mediates Plasminogen Activator Inhibitor-1 Gene Expression and Sp1 Transcriptional Activity in Glomerular Mesangial Cells". In: *Endocrinology* 147.1, pp. 222–231. ISSN: 0013-7227. DOI: 10.1210/en.2005-0523. pmid: 16365142.

Goldgaber, D. et al. (Feb. 20, 1987). "Characterization and Chromosomal Localization of a cDNA Encoding Brain Amyloid of Alzheimer's Disease". In: *Science (New York, N.Y.)* 235.4791, pp. 877–880. ISSN: 0036-8075. DOI: 10.1126/science.3810169. pmid: 3810169.

Gong, C.-X. and K. Iqbal (Oct. 1, 2008). "Hyperphosphorylation of Microtubule-Associated Protein Tau: A Promising Therapeutic Target for Alzheimer Disease". In: *Current Medicinal Chemistry* 15.23, pp. 2321–2328. ISSN: 09298673. DOI: 10.2174/092986708785909111.

Gonzalez-Rellan, Maria J. et al. (Apr. 22, 2022). "O-GlcNAcylation: A Sweet Hub in the Regulation of Glucose Metabolism in Health and Disease". In: *Frontiers in Endocrinology* 13. ISSN: 1664-2392. DOI: 10.3389/fendo.2022.873513.

Graham, Danielle L. et al. (Apr. 1, 2014). "Increased O-GlcNAcylation Reduces Pathological Tau without Affecting Its Normal Phosphorylation in a Mouse Model of Tauopathy". In: *Neuropharmacology* 79, pp. 307–313. ISSN: 0028-3908. DOI: 10.1016/j.neuropharm.2013.11.025.

Griebel, Guy et al. (Dec. 2, 2019). "The Selective GSK3 Inhibitor, SAR502250, Displays Neuroprotective Activity and Attenuates Behavioral Impairments in Models of Neuropsychiatric Symptoms of Alzheimer's Disease in Rodents". In: *Scientific Reports* 9.1, p. 18045. ISSN: 2045-2322. DOI: 10.1038/s41598-019-54557-5.

Grundke-Iqbal, I. et al. (July 1986). "Abnormal Phosphorylation of the Microtubule-Associated Protein Tau (Tau) in Alzheimer Cytoskeletal Pathology". In: *Proceedings of the National Academy of Sciences of the United States of America* 83.13, pp. 4913–4917. ISSN: 0027-8424. DOI: 10.1073/pnas.83.13.4913. pmid: 3088567.

Grupe, Andrew et al. (Apr. 15, 2007). "Evidence for Novel Susceptibility Genes for Late-Onset Alzheimer's Disease from a Genome-Wide Association Study of Putative Functional Variants". In: *Human Molecular Genetics* 16.8, pp. 865–873. ISSN: 0964-6906. DOI: 10.1093/hmg/ddm031. pmid: 17317784.

Guo, Jing L. et al. (Oct. 17, 2016). "Unique Pathological Tau Conformers from Alzheimer's Brains Transmit Tau Pathology in Nontransgenic Mice". In: *Journal of Experimental Medicine* 213.12, pp. 2635–2654. ISSN: 0022-1007. DOI: 10.1084/jem.20160833.

Guo, Tong, Wendy Noble, and Diane P. Hanger (May 2017). "Roles of Tau Protein in Health and Disease". In: *Acta Neuropathologica* 133.5, pp. 665–704. ISSN: 1432-0533. DOI: 10.1007/s00401-017-1707-9. pmid: 28386764.

Haass, Christian et al. (May 2012). "Trafficking and Proteolytic Processing of APP". In: *Cold Spring Harbor Perspectives in Medicine* 2.5, a006270. ISSN: 2157-1422. DOI: 10.1101/cshperspect.a006270. pmid: 22553493.

Habchi, Johnny et al. (July 9, 2014). "Introducing Protein Intrinsic Disorder". In: *Chemical Reviews* 114.13, pp. 6561–6588. ISSN: 0009-2665. DOI: 10.1021/cr400514h.

Haj-Yahya, Mahmood and Hilal A. Lashuel (May 30, 2018). "Protein Semisynthesis Provides Access to Tau Disease-Associated Post-translational Modifications (PTMs) and Paves the Way to Deciphering the Tau PTM Code in Health and Diseased States". In: *Journal of the American Chemical Society* 140.21, pp. 6611–6621. ISSN: 1520-5126. DOI: 10.1021/jacs.8b02668. pmid: 29684271.

Haj-Yahya, Mahmood et al. (Mar. 2, 2020). "Site-Specific Hyperphosphorylation Inhibits, Rather than Promotes, Tau Fibrillization, Seeding Capacity, and Its Microtubule Binding". In: *Angewandte Chemie (International Ed. in English)* 59.10, pp. 4059–4067. ISSN: 1433-7851. DOI: 10.1002/anie.201913001. pmid: 31863676.

Hampel, Harald et al. (Oct. 2021). "The Amyloid-β Pathway in Alzheimer's Disease". In: *Molecular Psychiatry* 26.10, pp. 5481–5503. ISSN: 1476-5578. DOI: 10.1038/s41380-021-01249-0.

Han, Zhuang Zhuang et al. (Apr. 1, 2023). "Prion-like Strain Effects in Tauopathies". In: *Cell and Tissue Research* 392.1, pp. 179–199. ISSN: 1432-0878. DOI: 10.1007/s00441-022-03620-1.

Hanger, D. P. et al. (Dec. 1998). "New Phosphorylation Sites Identified in Hyperphosphorylated Tau (Paired Helical Filament-Tau) from Alzheimer's Disease Brain Using Nanoelectrospray Mass Spectrometry". In: *Journal of Neurochemistry* 71.6, pp. 2465–2476. ISSN: 0022-3042. DOI: 10.1046/j.1471-4159.1998.71062465.x. pmid: 9832145.

Hanger, Diane P., Brian H. Anderton, and Wendy Noble (Mar. 2009). "Tau Phosphorylation: The Therapeutic Challenge for Neurodegenerative Disease". In: *Trends in Molecular Medicine* 15.3, pp. 112–119. ISSN: 1471-4914. DOI: 10.1016/j.molmed.2009.01.003. pmid: 19246243.

Harada, A. et al. (June 1994). "Altered Microtubule Organization in Small-Calibre Axons of Mice Lacking Tau Protein". In: *Nature* 369.6480 (6480), pp. 488–491. ISSN: 1476-4687. DOI: 10.1038/369488a0.

Harold, Denise et al. (Oct. 2009). "Genome-Wide Association Study Identifies Variants at CLU and PICALM Associated with Alzheimer's Disease, and Shows Evidence for Additional Susceptibility Genes". In: *Nature genetics* 41.10, pp. 1088–1093. ISSN: 1061-4036. DOI: 10.1038/ng.440. pmid: 19734902.

Hart, Gerald W. et al. (July 7, 2011). "Cross Talk Between O-GlcNAcylation and Phosphorylation: Roles in Signaling, Transcription, and Chronic Disease". In: *Annual Review of Biochemistry* 80 (Volume 80, 2011), pp. 825–858. ISSN: 0066-4154, 1545-4509. DOI: 10.1146/annurev-biochem-060608-102511.

Heiss, W. D. et al. (1991). "Abnormalities of Energy Metabolism in Alzheimer's Disease Studied with PET". In: *Annals of the New York Academy of Sciences* 640, pp. 65–71. ISSN: 0077-8923. DOI: 10.1111/j.1749-6632.1991.tb00192.x. pmid: 1776760.

Hernández-Vega, Amayra et al. (Sept. 2017). "Local Nucleation of Microtubule Bundles through Tubulin Concentration into a Condensed Tau Phase". In: *Cell Reports* 20.10, pp. 2304–2312. ISSN: 22111247. DOI: 10.1016/j.celrep.2017.08.042.

Hetman, Michal et al. (Apr. 1, 2000). "Role of Glycogen Synthase Kinase-3β in Neuronal Apoptosis Induced by Trophic Withdrawal". In: *Journal of Neuroscience* 20.7, pp. 2567–2574. ISSN: 0270-6474, 1529-2401. DOI: 10.1523/JNEUROSCI.20-07-02567.2000. pmid: 10729337.

Hick, Meike et al. (Jan. 2015). "Acute Function of Secreted Amyloid Precursor Protein Fragment APPsα in Synaptic Plasticity". In: *Acta Neuropathologica* 129.1, pp. 21–37. ISSN: 1432-0533. DOI: 10.1007/s00401-014-1368-x. pmid: 25432317.

"High Specificity of Widely Used Phospho-tau Antibodies Validated Using a Quantitative Whole-cell Based Assay" (2020). In: DOI: 10.1111/jnc.14830.

Höglinger, G. U., G. Respondek, and G. G. Kovacs (Nov. 1, 2018). "New Classification of Tauopathies". In: *Revue Neurologique*. INTERNATIONAL SFN /SOFMA MEETING 2018 174.9, pp. 664–668. ISSN: 0035-3787. DOI: 10.1016/j.neurol.2018.07.001.

Holmes, Brandon B. and Marc I. Diamond (July 18, 2014). "Prion-like Properties of Tau Protein: The Importance of Extracellular Tau as a Therapeutic Target". In: *The Journal of Biological Chemistry* 289.29, pp. 19855–19861. ISSN: 0021-9258. DOI: 10.1074/jbc.R114.549295. pmid: 24860099.

Holper, Sarah, Rosie Watson, and Nawaf Yassi (Jan. 2022). "Tau as a Biomarker of Neurodegeneration". In: *International Journal of Molecular Sciences* 23 (13, 13), p. 7307. ISSN: 1422-0067. DOI: 10.3390/ijms23137307.

Hooper, Claudie, Richard Killick, and Simon Lovestone (Mar. 2008). "The GSK3 Hypothesis of Alzheimer's Disease". In: *Journal of Neurochemistry* 104.6, pp. 1433–1439. ISSN: 0022-3042. DOI: 10.1111/j.1471-4159.2007.05194.x. pmid: 18088381.

Hou, Zhiqiang et al. (June 30, 2021). "Biophysical Properties of a Tau Seed". In: *Scientific Reports* 11.1, p. 13602. ISSN: 2045-2322. DOI: 10.1038/s41598-021-93093-z.

Hu, Jiaxin et al. (Jan. 2023). "Aggregation, Transmission, and Toxicity of the Microtubule-Associated Protein Tau: A Complex Comprehension". In: *International Journal of Molecular Sciences* 24.19 (19), p. 15023. ISSN: 1422-0067. DOI: 10.3390/ijms241915023.

Hu, Jinjian et al. (Mar. 27, 2024). "Phosphorylation and O-GlcNAcylation at the Same α-Synuclein Site Generate Distinct Fibril Structures". In: *Nature Communications* 15.1, p. 2677. ISSN: 2041-1723. DOI: 10.1038/s41467-024-46898-1.

Hu, Wen et al. (Oct. 2016). "Hyperphosphorylation Determines Both the Spread and the Morphology of Tau Pathology". In: *Alzheimer's & Dementia* 12.10, pp. 1066–1077. ISSN: 1552-5260. DOI: 10.1016/j.jalz.2016.01.014.

Hu, Wen et al. (Mar. 16, 2022). "Does Proteopathic Tau Propagate Trans-Synaptically in the Brain?" In: *Molecular Neurodegeneration* 17.1, p. 21. ISSN: 1750-1326. DOI: 10.1186/s13024-022-00527-x.

Huang, Yi-Hung, Peter W. Rose, and Chun-Nan Hsu (Aug. 28, 2015). "Citing a Data Repository: A Case Study of the Protein Data Bank". In: *PLOS ONE* 10.8, e0136631. ISSN: 1932-6203. DOI: 10.1371/journal.pone.0136631.

Huynh, Duc Tan and Michael Boyce (2023). "Chemical Biology Approaches to Understanding Neuronal O-GlcNAcylation". In: *Israel Journal of Chemistry* 63.1-2, e202200071. ISSN: 1869-5868. DOI: 10.1002/ijch.202200071.

Irwin, David J. (Jan. 2016). "Tauopathies as Clinicopathological Entities". In: *Parkinsonism & Related Disorders* 22 Suppl 1 (0 1), S29–33. ISSN: 1873-5126. DOI: 10.1016/j.parkreldis.2015.09.020. pmid: 26382841.

Ishihara, T. et al. (Nov. 1999). "Age-Dependent Emergence and Progression of a Tauopathy in Transgenic Mice Overexpressing the Shortest Human Tau Isoform". In: *Neuron* 24.3, pp. 751–762. ISSN: 0896-6273. DOI: 10.1016/s0896-6273(00)81127-7. pmid: 10595524.

Jackson, Samuel J. et al. (Jan. 20, 2016). "Short Fibrils Constitute the Major Species of Seed-Competent Tau in the Brains of Mice Transgenic for Human P301S Tau". In: *The Journal of Neuroscience: The Official Journal of the Society for Neuroscience* 36.3, pp. 762–772. ISSN: 1529-2401. DOI: 10.1523/JNEUROSCI.3542-15.2016. pmid: 26791207.

Jeganathan, Sadasivam et al. (Nov. 14, 2008). "Proline-Directed Pseudo-phosphorylation at AT8 and PHF1 Epitopes Induces a Compaction of the Paperclip Folding of Tau and Generates a Pathological (MC-1) Conformation*". In: *Journal of Biological Chemistry* 283.46, pp. 32066–32076. ISSN: 0021-9258. DOI: 10.1074/jbc.M805300200.

Jellinger, Kurt A. (Nov. 11, 2020). "Neuropathology of the Alzheimer's Continuum: An Update". In: *Free Neuropathology* 1, pp. 32–32. ISSN: 2699-4445. DOI: 10.17879/freeneuropathology-2020-3050.

Jie, Caitlin et al. (Jan. 30, 2021). "Tauvid: The First FDA-Approved PET Tracer for Imaging Tau Pathology in Alzheimer's Disease". In: *Pharmaceuticals* 14, p. 110. DOI: 10.3390/ph14020110.

Johnson, Gail V. W. and William H. Stoothoff (Nov. 15, 2004). "Tau Phosphorylation in Neuronal Cell Function and Dysfunction". In: *Journal of Cell Science* 117.24, pp. 5721–5729. ISSN: 0021-9533. DOI: 10.1242/jcs.01558.

Joiner, Cassandra M. et al. (Mar. 23, 2021). "Protein Substrates Engage the Lumen of O-GlcNAc Transferase's Tetratricopeptide Repeat Domain in Different Ways". In: *Biochemistry* 60.11, pp. 847–853. ISSN: 0006-2960. DOI: 10.1021/acs.biochem.0c00981. pmid: 33709700.

Kamah, Amina et al. (May 13, 2014). "Nuclear Magnetic Resonance Analysis of the Acetylation Pattern of the Neuronal Tau Protein". In: *Biochemistry* 53.18, pp. 3020–3032. ISSN: 0006-2960. DOI: 10.1021/bi500006v.

Kanaan, Nicholas M. et al. (July 6, 2011). "Pathogenic Forms of Tau Inhibit Kinesin-Dependent Axonal Transport through a Mechanism Involving Activation of Axonal Phosphotransferases". In: *Journal of Neuroscience* 31.27, pp. 9858–9868. ISSN: 0270-6474, 1529-2401. DOI: 10.1523/JNEUROSCI.0560-11.2011. pmid: 21734277.

Kanaan, Nicholas M. et al. (June 4, 2020). "Liquid-Liquid Phase Separation Induces Pathogenic Tau Conformations in Vitro". In: *Nature Communications* 11.1, p. 2809. ISSN: 2041-1723. DOI: 10.1038/s41467-020-16580-3.

Kang, J. et al. (Feb. 19, 1987–25). "The Precursor of Alzheimer's Disease Amyloid A4 Protein Resembles a Cell-Surface Receptor". In: *Nature* 325.6106, pp. 733–736. ISSN: 0028-0836. DOI: 10.1038/325733a0. pmid: 2881207.

Kaniyappan, Senthilvelrajan et al. (July 16, 2020). "FRET-based Tau Seeding Assay Does Not Represent Prion-like Templated Assembly of Tau Filaments". In: *Molecular Neurodegeneration* 15.1, p. 39. ISSN: 1750-1326. DOI: 10.1186/s13024-020-00389-1.

Kara, Eleanna, Jordan D. Marks, and Adriano Aguzzi (Dec. 2018). "Toxic Protein Spread in Neurodegeneration: Reality versus Fantasy". In: *Trends in Molecular Medicine* 24.12, pp. 1007–1020. ISSN: 1471-499X. DOI: 10.1016/j.molmed.2018.09.004. pmid: 30442495.

Katsikoudi, Antigoni et al. (Sept. 11, 2020). "Quantitative Propagation of Assembled Human Tau from Alzheimer's Disease Brain in Microfluidic Neuronal Cultures". In: *The Journal of Biological Chemistry* 295.37, pp. 13079–13093. ISSN: 0021-9258. DOI: 10.1074/jbc.RA120.013325. pmid: 32699110.

Kaufman, Sarah K. et al. (June 7, 2017). "Characterization of Tau Prion Seeding Activity and Strains from Formaldehyde-Fixed Tissue". In: *Acta Neuropathologica Communications* 5, p. 41. ISSN: 2051-5960. DOI: 10.1186/s40478-017-0442-8. pmid: 28587664.

Khlistunova, Inna et al. (Jan. 13, 2006). "Inducible Expression of Tau Repeat Domain in Cell Models of Tauopathy: AGGREGATION IS TOXIC TO CELLS BUT CAN BE REVERSED BY IN-

HIBITOR DRUGS*". In: *Journal of Biological Chemistry* 281.2, pp. 1205–1214. ISSN: 0021-9258. DOI: 10.1074/jbc.M507753200.

Kidd, M. (Jan. 12, 1963). "Paired Helical Filaments in Electron Microscopy of Alzheimer's Disease". In: *Nature* 197, pp. 192–193. ISSN: 0028-0836. DOI: 10.1038/197192b0. pmid: 14032480.

Kim, Dong Kyu et al. (July 2024). "FGFR3 Drives Aβ-induced Tau Uptake". In: *Experimental & Molecular Medicine* 56.7, pp. 1631–1642. ISSN: 2092-6413. DOI: 10.1038/s12276-024-01274-3.

Kim, Eun J. (Mar. 2011). "Chemical Arsenal for the Study of O-GlcNAc". In: *Molecules* 16.3 (3), pp. 1987–2022. ISSN: 1420-3049. DOI: 10.3390/molecules16031987.

Kim, Mingeun et al. (June 26, 2023). *Coupling the Coupling: Dissecting the Role of Tau's Microtubule-Binding Repeats in Modulating Amyloid-beta Aggregation and Toxicity Profiles in Alzheimer's Disease*. DOI: 10.26434/chemrxiv-2023-n5fv2. Pre-published.

Ko, Ryeojin et al. (Apr. 1, 2015). "Glycogen Synthase Kinase 3β Ubiquitination by TRAF6 Regulates TLR3-mediated pro-Inflammatory Cytokine Production". In: *Nature Communications* 6.1, p. 6765. ISSN: 2041-1723. DOI: 10.1038/ncomms7765.

Kojro, Elzbieta and Falk Fahrenholz (2005). "The Non-Amyloidogenic Pathway: Structure and Function of Alpha-Secretases". In: *Sub-Cellular Biochemistry* 38, pp. 105–127. ISSN: 0306-0225. DOI: 10.1007/0-387-23226-5_5. pmid: 15709475.

Koshland, D. E. (Feb. 1958). "Application of a Theory of Enzyme Specificity to Protein Synthesis". In: *Proceedings of the National Academy of Sciences of the United States of America* 44.2, pp. 98–104. ISSN: 0027-8424. DOI: 10.1073/pnas.44.2.98. pmid: 16590179.

Kosik, Kenneth S. et al. (Apr. 1, 1989). "Developmentally Regulated Expression of Specific Tau Sequences". In: *Neuron* 2.4, pp. 1389–1397. ISSN: 0896-6273. DOI: 10.1016/0896-6273(89)90077-9.

Kositzke, Adam et al. (Feb. 1, 2021). "Elucidating the Protein Substrate Recognition of O-GlcNAc Transferase (OGT) toward O-GlcNAcase (OGA) Using a GlcNAc Electrophilic Probe". In: *International Journal of Biological Macromolecules* 169, pp. 51–59. ISSN: 0141-8130. DOI: 10.1016/j.ijbiomac.2020.12.078.

Kouri, Naomi et al. (May 2011). "Corticobasal Degeneration: A Pathologically Distinct 4R Tauopathy". In: *Nature Reviews. Neurology* 7.5, pp. 263–272. ISSN: 1759-4766. DOI: 10.1038/nrneurol.2011.43. pmid: 21487420.

Krishnaswamy, Senthilkumar et al. (2018). "In Vivo Imaging of Tauopathy in Mice". In: *Amyloid Proteins: Methods and Protocols*. Ed. by Einar M. Sigurdsson, Miguel Calero, and María Gasset. New York, NY: Springer, pp. 513–526. ISBN: 978-1-4939-7816-8. DOI: 10.1007/978-1-4939-7816-8_32.

Ksiezak-Reding, H., W. K. Liu, and S. H. Yen (Dec. 4, 1992). "Phosphate Analysis and Dephosphorylation of Modified Tau Associated with Paired Helical Filaments". In: *Brain Research* 597.2, pp. 209–219. ISSN: 0006-8993. DOI: 10.1016/0006-8993(92)91476-u. pmid: 1472994.

Ksiezak-Reding, Hanna and Joseph S. Wall (2005). "Characterization of Paired Helical Filaments by Scanning Transmission Electron Microscopy". In: *Microscopy Research and Technique* 67.3-4, pp. 126–140. ISSN: 1097-0029. DOI: 10.1002/jemt.20188.

Lai, Robert Y. K., Charles R. Harrington, and Claude M. Wischik (June 2016). "Absence of a Role for Phosphorylation in the Tau Pathology of Alzheimer's Disease". In: *Biomolecules* 6.2 (2), p. 19. ISSN: 2218-273X. DOI: 10.3390/biom6020019.

Lambert, Jean-Charles et al. (Oct. 2009). "Genome-Wide Association Study Identifies Variants at CLU and CR1 Associated with Alzheimer's Disease". In: *Nature Genetics* 41.10, pp. 1094–1099. ISSN: 1546-1718. DOI: 10.1038/ng.439. pmid: 19734903.

Landrieu, Isabelle et al. (2022). "Deciphering the Structure and Formation of Amyloids in Neurodegenerative Diseases With Chemical Biology Tools". In: *Frontiers in Chemistry* 10. ISSN: 2296-

2646. URL: https://www.frontiersin.org/articles/10.3389/fchem.2022.886382.

Langui, Dominique, Fran¸cois Lachapelle, and Charles Duyckaerts (Feb. 1, 2007). "Modèles animaux des maladies neuro-dégénératives". In: *médecine/sciences* 23.2 (2), pp. 180–186. ISSN: 0767-0974, 1958-5381. DOI: 10.1051/medsci/2007232180.

Lasagna-Reeves, Cristian A. et al. (Oct. 3, 2012). "Alzheimer Brain-Derived Tau Oligomers Propagate Pathology from Endogenous Tau". In: *Scientific Reports* 2.1, p. 700. ISSN: 2045-2322. DOI: 10.1038/srep00700.

Lathuiliere, Aurelien and Bradley T. Hyman (Mar. 19, 2021). "Quantitative Methods for the Detection of Tau Seeding Activity in Human Biofluids". In: *Frontiers in Neuroscience* 15, p. 654176. ISSN: 1662-4548. DOI: 10.3389/fnins.2021.654176. pmid: 33828458.

Lauretti, Elisabetta, Ozlem Dincer, and Domenico Praticò (May 2020). "Glycogen Synthase Kinase-3 Signaling in Alzheimer's Disease". In: *Biochimica et biophysica acta. Molecular cell research* 1867.5, p. 118664. ISSN: 0167-4889. DOI: 10.1016/j.bbamcr.2020.118664. pmid: 32006534.

Lazarus, Michael B. et al. (Jan. 27, 2011). "Structure of Human O-GlcNAc Transferase and Its Complex with a Peptide Substrate". In: *Nature* 469.7331, pp. 564–567. ISSN: 0028-0836. DOI: 10.1038/nature09638. pmid: 21240259.

Lebouvier, Thibaud et al. (Jan. 1, 2009). "The Microtubule-Associated Protein Tau Is Also Phosphorylated on Tyrosine". In: *Journal of Alzheimer's Disease* 18.1, pp. 1–9. ISSN: 1387-2877. DOI: 10.3233/JAD-2009-1116.

Lecanemab Approved for Treatment of Early Alzheimer's Disease (2021). Alzheimer's Disease and Dementia. URL: https://alz.org/alzheimers-dementia/treatments/lecanemab-leqembi.

Lee, Byeong Eun, Pann-Ghill Suh, and Jae-Ick Kim (Nov. 2021). "O-GlcNAcylation in Health and Neurodegenerative Diseases". In: *Experimental & Molecular Medicine* 53.11, pp. 1674–1682. ISSN: 2092-6413. DOI: 10.1038/s12276-021-00709-5.

Lefebvre, Tony et al. (Jan. 2003). "Evidence of a Balance between Phosphorylation and O-GlcNAc Glycosylation of Tau Proteins—a Role in Nuclear Localization". In: *Biochimica et Biophysica Acta (BBA) - General Subjects* 1619.2, pp. 167–176. ISSN: 03044165. DOI: 10.1016/S0304-4165(02)00477-4.

Leney, Aneika C. et al. (Aug. 29, 2017). "Elucidating Crosstalk Mechanisms between Phosphorylation and O-GlcNAcylation". In: *Proceedings of the National Academy of Sciences of the United States of America* 114.35, E7255–E7261. ISSN: 1091-6490. DOI: 10.1073/pnas.1620529114. pmid: 28808029.

Leroy, Arnaud et al. (Oct. 22, 2010). "Spectroscopic Studies of GSK3β Phosphorylation of the Neuronal Tau Protein and Its Interaction with the N-terminal Domain of Apolipoprotein E". In: *Journal of Biological Chemistry* 285.43, pp. 33435–33444. ISSN: 0021-9258, 1083-351X. DOI: 10.1074/jbc.M110.149419. pmid: 20679343.

Leszek, Jerzy et al. (Feb. 2021). "The Links between Cardiovascular Diseases and Alzheimer's Disease". In: *Current Neuropharmacology* 19.2, pp. 152–169. ISSN: 1570-159X. DOI: 10.2174/1570159X18666200729093724. pmid: 32727331.

Li, Baobin et al. (Sept. 22, 2017a). "Structural Insights into the Substrate Binding Adaptability and Specificity of Human O-GlcNAcase". In: *Nature Communications* 8.1, p. 666. ISSN: 2041-1723. DOI: 10.1038/s41467-017-00865-1.

Li, Baobin et al. (Apr. 2017b). "Structures of Human O-GlcNAcase and Its Complexes Reveal a New Substrate Recognition Mode". In: *Nature structural & molecular biology* 24.4, pp. 362–369. ISSN: 1545-9993. DOI: 10.1038/nsmb.3390. pmid: 28319083.

Li, Guibin, Haishan Yin, and Jeff Kuret (Apr. 16, 2004). "Casein Kinase 1 Delta Phosphorylates Tau and Disrupts Its Binding to Microtubules *". In: *Journal of Biological Chemistry* 279.16,

pp. 15938–15945. ISSN: 0021-9258, 1083-351X. DOI: 10.1074/jbc.M314116200. pmid: 14761950.

Li, Ping et al. (July 2023a). "Liquid - Liquid Phase Separation of Tau: Driving Forces, Regulation, and Biological Implications". In: *Neurobiology of Disease* 183, p. 106167. ISSN: 1095-953X. DOI: 10.1016/j.nbd.2023.106167. pmid: 37230179.

Li, Yang et al. (Feb. 24, 2023b). "OGT Binding Peptide-Tagged Strategy Increases Protein O-GlcNAcylation Level in E. Coli". In: *Molecules* 28.5, p. 2129. ISSN: 1420-3049. DOI: 10.3390/molecules28052129. pmid: 36903375.

Liautard, Jean-Pierre et al. (Jan. 1, 2002). "La protéine prion : structure, dynamique et conversion in vitro". In: *médecine/sciences* 18.1 (1), pp. 62–69. ISSN: 0767-0974, 1958-5381. DOI: 10.1051/medsci/200218162.

Lim, Sungsu et al. (Nov. 1, 2014). "Cell-Based Models To Investigate Tau Aggregation". In: *Computational and Structural Biotechnology Journal* 12. DOI: 10.1016/j.csbj.2014.09.011.

Lim, Yehjun and Yanmei Li (Apr. 1, 2022). "Chemical Synthesis/Semisynthesis of Post-Translational Modified Tau Protein". In: *Progress in Chemistry* 34.8 (8), pp. 1645–1660. ISSN: 1005-281X. DOI: 10.7536/PC211012.

Limorenko, Galina and Hilal A. Lashuel (2022). "Revisiting the Grammar of Tau Aggregation and Pathology Formation: How New Insights from Brain Pathology Are Shaping How We Study and Target Tauopathies". In: *Chemical Society Reviews* 51.2, pp. 513–565. DOI: 10.1039/D1CS00127B.

Limorenko, Galina and Hilal A. Lashuel (Dec. 1, 2021). "To Target Tau Pathologies, We Must Embrace and Reconstruct Their Complexities". In: *Neurobiology of Disease* 161, p. 105536. ISSN: 0969-9961. DOI: 10.1016/j.nbd.2021.105536.

Linding, Rune et al. (Jan. 1, 2008). "NetworKIN: A Resource for Exploring Cellular Phosphorylation Networks". In: *Nucleic Acids Research* 36 (suppl_1), pp. D695–D699. ISSN: 0305-1048. DOI: 10.1093/nar/gkm902.

Linse, Sara (Feb. 1, 2019). "Mechanism of Amyloid Protein Aggregation and the Role of Inhibitors". In: *Pure and Applied Chemistry* 91.2, pp. 211–229. ISSN: 1365-3075. DOI: 10.1515/pac-2018-1017.

Lippens, Guy et al. (June 2016). "NMR Meets Tau: Insights into Its Function and Pathology". In: *Biomolecules* 6.2 (2), p. 28. ISSN: 2218-273X. DOI: 10.3390/biom6020028.

Liu, C. W., G. Lee, and D. G. Jay (1999). "Tau Is Required for Neurite Outgrowth and Growth Cone Motility of Chick Sensory Neurons". In: *Cell Motility and the Cytoskeleton* 43.3, pp. 232–242. ISSN: 0886-1544. DOI: 10.1002/(SICI)1097-0169(1999)43:3<232::AID-CM6>3.0.CO;2-7. pmid: 10401579.

Liu, Fei et al. (July 20, 2004). "O-GlcNAcylation Regulates Phosphorylation of Tau: A Mechanism Involved in Alzheimer's Disease". In: *Proceedings of the National Academy of Sciences* 101.29, pp. 10804–10809. DOI: 10.1073/pnas.0400348101.

Liu, Fei et al. (July 2009). "Reduced O-GlcNAcylation Links Lower Brain Glucose Metabolism and Tau Pathology in Alzheimer's Disease". In: *Brain: A Journal of Neurology* 132 (Pt 7), pp. 1820–1832. ISSN: 1460-2156. DOI: 10.1093/brain/awp099. pmid: 19451179.

Liu, Li et al. (Feb. 1, 2012). "Trans-Synaptic Spread of Tau Pathology In Vivo". In: *PLOS ONE* 7.2, e31302. ISSN: 1932-6203. DOI: 10.1371/journal.pone.0031302.

Liu, Yu-Qing et al. (Apr. 5, 2023). "14-3-3ζ Participates in the Phase Separation of Phosphorylated and Glycated Tau and Modulates the Physiological and Pathological Functions of Tau". In: *ACS Chemical Neuroscience* 14.7, pp. 1220–1225. DOI: 10.1021/acschemneuro.3c00034.

Lloret, Ana et al. (2011). "Amyloid-β Toxicity and Tau Hyperphosphorylation Are Linked via RCAN1 in Alzheimer's Disease". In: *Journal of Alzheimer's disease: JAD* 27.4, pp. 701–709. ISSN: 1875-8908. DOI: 10.3233/JAD-2011-110890. pmid: 21876249.

Lo, Chih Hung (June 1, 2021a). "Recent Advances in Cellular Biosensor Technology to Investigate Tau Oligomerization". In: *Bioengineering & Translational Medicine* 6.3, e10231. ISSN: 2380-6761. DOI: 10.1002/btm2.10231. pmid: 34589603.

— (2021b). "Recent Advances in Cellular Biosensor Technology to Investigate Tau Oligomerization". In: *Bioengineering & Translational Medicine* 6.3, e10231. ISSN: 2380-6761. DOI: 10.1002/btm2.10231.

Loughlin, Fionna E. and Jacqueline A. Wilce (Dec. 2019). "TDP-43 and FUS-structural Insights into RNA Recognition and Self-Association". In: *Current Opinion in Structural Biology* 59, pp. 134–142. ISSN: 1879-033X. DOI: 10.1016/j.sbi.2019.07.012. pmid: 31479821.

Lövestam, Sofia et al. (Mar. 4, 2022). "Assembly of Recombinant Tau into Filaments Identical to Those of Alzheimer's Disease and Chronic Traumatic Encephalopathy". In: *eLife* 11. Ed. by Edward H Egelman et al., e76494. ISSN: 2050-084X. DOI: 10.7554/eLife.76494.

Lu, Ping et al. (Oct. 31, 2023). "Cryo-EM Structure of Human O-GlcNAcylation Enzyme Pair OGT-OGA Complex". In: *Nature Communications* 14.1, p. 6952. ISSN: 2041-1723. DOI: 10.1038/s41467-023-42427-8.

Ma, Bo et al. (July 23, 2020). "Protein Glycoengineering: An Approach for Improving Protein Properties". In: *Frontiers in Chemistry* 8. ISSN: 2296-2646. DOI: 10.3389/fchem.2020.00622.

Ma, Junfeng and Gerald W. Hart (Feb. 2, 2017). "Analysis of Protein O-GlcNAcylation by Mass Spectrometry". In: *Current protocols in protein science* 87, pp. 24.10.1–24.10.16. ISSN: 1934-3655. DOI: 10.1002/cpps.24. pmid: 28150883.

Maccora, Janet, Ruth Peters, and Kaarin J. Anstey (Dec. 1, 2020). "What Does (Low) Education Mean in Terms of Dementia Risk? A Systematic Review and Meta-Analysis Highlighting Inconsistency in Measuring and Operationalising Education". In: *SSM - Population Health* 12, p. 100654. ISSN: 2352-8273. DOI: 10.1016/j.ssmph.2020.100654.

Macedo, Arthur C. et al. (Aug. 1, 2023). "The Use of Tau PET to Stage Alzheimer Disease According to the Braak Staging Framework". In: *Journal of Nuclear Medicine* 64.8, pp. 1171–1178. ISSN: 0161-5505, 2159-662X. DOI: 10.2967/jnumed.122.265200. pmid: 37321820.

Mackenzie, Ian R. A. and Manuela Neumann (2016). "Molecular Neuropathology of Frontotemporal Dementia: Insights into Disease Mechanisms from Postmortem Studies". In: *Journal of Neurochemistry* 138.S1, pp. 54–70. ISSN: 1471-4159. DOI: 10.1111/jnc.13588.

Maina, Mahmoud B. et al. (July 31, 2018). "The Involvement of Tau in Nucleolar Transcription and the Stress Response". In: *Acta Neuropathologica Communications* 6.1, p. 70. ISSN: 2051-5960. DOI: 10.1186/s40478-018-0565-6.

Mair, Waltraud et al. (Apr. 5, 2016). "FLEXITau: Quantifying Post-translational Modifications of Tau Protein in Vitro and in Human Disease". In: *Analytical Chemistry* 88.7, pp. 3704–3714. ISSN: 1520-6882. DOI: 10.1021/acs.analchem.5b04509. pmid: 26877193.

Makrinou, Eleni, John Collinge, and Michael Antoniou (Dec. 1, 2002). "Genomic Characterization of the Human Prion Protein (PrP) Gene Locus". In: *Mammalian Genome* 13.12, pp. 696–703. ISSN: 1432-1777. DOI: 10.1007/s00335-002-3043-0.

Mandelkow, Eva-Maria and Eckhard Mandelkow (July 2012). "Biochemistry and Cell Biology of Tau Protein in Neurofibrillary Degeneration". In: *Cold Spring Harbor Perspectives in Medicine* 2.7, a006247. ISSN: 2157-1422. DOI: 10.1101/cshperspect.a006247. pmid: 22762014.

Mandell, James W. and Gary A. Banker (Sept. 15, 1996). "A Spatial Gradient of Tau Protein Phosphorylation in Nascent Axons". In: *Journal of Neuroscience* 16.18, pp. 5727–5740. ISSN: 0270-6474, 1529-2401. DOI: 10.1523/JNEUROSCI.16-18-05727.1996. pmid: 8795628.

Mann, Jacob R. et al. (Apr. 17, 2019). "RNA Binding Antagonizes Neurotoxic Phase Transitions of TDP-43". In: *Neuron* 102.2, 321–338.e8. ISSN: 1097-4199. DOI: 10.1016/j.neuron.2019.01.048. pmid: 30826182.

Mann, Matthias and Ole N. Jensen (Mar. 2003). "Proteomic Analysis of Post-Translational Modifications". In: *Nature Biotechnology* 21.3, pp. 255–261. ISSN: 1546-1696. DOI: 10.1038/nbt0303-255.

Martin, Erik W. and Alex S. Holehouse (Dec. 11, 2020). "Intrinsically Disordered Protein Regions and Phase Separation: Sequence Determinants of Assembly or Lack Thereof". In: *Emerging Topics in Life Sciences* 4.3, pp. 307–329. ISSN: 2397-8554. DOI: 10.1042/ETLS20190164. pmid: 33078839.

Masters, C. L. et al. (June 1985). "Amyloid Plaque Core Protein in Alzheimer Disease and Down Syndrome". In: *Proceedings of the National Academy of Sciences of the United States of America* 82.12, pp. 4245–4249. ISSN: 0027-8424. DOI: 10.1073/pnas.82.12.4245. pmid: 3159021.

Mate De Gerando, Anastasie et al. (Aug. 2023). "Tau Seeding and Spreading in Vivo Is Supported by Both AD-derived Fibrillar and Oligomeric Tau". In: *Acta Neuropathologica* 146.2, pp. 191–210. ISSN: 1432-0533. DOI: 10.1007/s00401-023-02600-1. pmid: 37341831.

Matsuno, Mahito et al. (Mar. 22, 2023). "O-GlcNAcylation-induced GSK-3β Activation Deteriorates Pressure Overload-Induced Heart Failure via Lack of Compensatory Cardiac Hypertrophy in Mice". In: *Frontiers in Endocrinology* 14. ISSN: 1664-2392. DOI: 10.3389/fendo.2023.1122125.

Maury, Julien Jean Pierre et al. (Jan. 7, 2014). "Multiple Reaction Monitoring Mass Spectrometry for the Discovery and Quantification of O-GlcNAc-Modified Proteins". In: *Analytical Chemistry* 86.1, pp. 395–402. ISSN: 0003-2700. DOI: 10.1021/ac401821d.

Maziuk, Brandon F. et al. (Aug. 1, 2018). "RNA Binding Proteins Co-Localize with Small Tau Inclusions in Tauopathy". In: *Acta Neuropathologica Communications* 6.1, p. 71. ISSN: 2051-5960. DOI: 10.1186/s40478-018-0574-5.

McGeer, Patrick L. and John C. Steele (Dec. 1, 2011). "The ALS/PDC Syndrome of Guam: Potential Biomarkers for an Enigmatic Disorder". In: *Progress in Neurobiology*. Biological Markers for Neurodegenerative Diseases 95.4, pp. 663–669. ISSN: 0301-0082. DOI: 10.1016/j.pneurobio.2011.04.001.

McMillan, Pamela J et al. (Feb. 3, 2023a). "Tau–RNA Complexes Inhibit Microtubule Polymerization and Drive Disease-Relevant Conformation Change". In: *Brain* 146.8, pp. 3206–3220. ISSN: 0006-8950. DOI: 10.1093/brain/awad032. pmid: 36732296.

— (Feb. 3, 2023b). "Tau–RNA Complexes Inhibit Microtubule Polymerization and Drive Disease-Relevant Conformation Change". In: *Brain* 146.8, pp. 3206–3220. ISSN: 0006-8950. DOI: 10.1093/brain/awad032. pmid: 36732296.

Meisl, Georg et al. (Feb. 2016). "Molecular Mechanisms of Protein Aggregation from Global Fitting of Kinetic Models". In: *Nature Protocols* 11.2, pp. 252–272. ISSN: 1750-2799. DOI: 10.1038/nprot.2016.010. pmid: 26741409.

Meng, Jonathan X. et al. (May 16, 2022). "Hyperphosphorylated Tau Self-Assembles into Amorphous Aggregates Eliciting TLR4-dependent Responses". In: *Nature Communications* 13.1, p. 2692. ISSN: 2041-1723. DOI: 10.1038/s41467-022-30461-x.

Mirbaha, Hilda et al. (June 12, 2015). "Tau Trimers Are the Minimal Propagation Unit Spontaneously Internalized to Seed Intracellular Aggregation". In: *The Journal of Biological Chemistry* 290.24, pp. 14893–14903. ISSN: 1083-351X. DOI: 10.1074/jbc.M115.652693. pmid: 25887395.

Mirbaha, Hilda et al. (July 10, 2018). "Inert and Seed-Competent Tau Monomers Suggest Structural Origins of Aggregation". In: *eLife* 7. Ed. by Anna Akhmanova, e36584. ISSN: 2050-084X. DOI: 10.7554/eLife.36584.

Möller, H. J. and M. B. Graeber (1998). "The Case Described by Alois Alzheimer in 1911. Historical and Conceptual Perspectives Based on the Clinical Record and Neurohistological Sections". In: *European Archives of Psychiatry and Clinical Neuroscience* 248.3, pp. 111–122. ISSN: 0940-1334. DOI: 10.1007/s004060050027. pmid: 9728729.

Molliex, Amandine et al. (Sept. 24, 2015). "Phase Separation by Low Complexity Domains Promotes Stress Granule Assembly and Drives Pathological Fibrillization". In: *Cell* 163.1, pp. 123–133. ISSN: 0092-8674. DOI: 10.1016/j.cell.2015.09.015.

Montgomery, Kelly M. et al. (Feb. 22, 2023). "Chemical Features of Polyanions Modulate Tau Aggregation and Conformational States". In: *Journal of the American Chemical Society* 145.7, pp. 3926–3936. ISSN: 0002-7863, 1520-5126. DOI: 10.1021/jacs.2c08004.

Morgan-Smith, Meghan et al. (July 29, 2014). "GSK-3 Signaling in Developing Cortical Neurons Is Essential for Radial Migration and Dendritic Orientation". In: *eLife* 3. Ed. by Freda Miller, e02663. ISSN: 2050-084X. DOI: 10.7554/eLife.02663.

Morishima-Kawashima, M. et al. (1995). "Hyperphosphorylation of Tau in PHF". In: *Neurobiology of Aging* 16.3, 365–371; discussion 371–380. ISSN: 0197-4580. DOI: 10.1016/0197-4580(95)00027-c. pmid: 7566346.

Morozova, Viktoriya et al. (Sept. 4, 2019). "Normal and Pathological Tau Uptake Mediated by M1/M3 Muscarinic Receptors Promotes Opposite Neuronal Changes". In: *Frontiers in Cellular Neuroscience* 13. ISSN: 1662-5102. DOI: 10.3389/fncel.2019.00403.

Morris, Meaghan et al. (Aug. 2015). "Tau Post-Translational Modifications in Wild-Type and Human Amyloid Precursor Protein Transgenic Mice". In: *Nature Neuroscience* 18.8, pp. 1183–1189. ISSN: 1546-1726. DOI: 10.1038/nn.4067. pmid: 26192747.

Mortelecque, Justine et al. (Apr. 2024). "A Selection and Optimization Strategy for Single-Domain Antibodies Targeting the PHF6 Linear Peptide within the Tau Intrinsically Disordered Protein". In: *Journal of Biological Chemistry* 300.4, p. 107163. ISSN: 00219258. DOI: 10.1016/j.jbc.2024.107163.

Mroczko, Barbara, Magdalena Groblewska, and Ala Litman-Zawadzka (Sept. 20, 2019). "The Role of Protein Misfolding and Tau Oligomers (TauOs) in Alzheimer's Disease (AD)". In: *International Journal of Molecular Sciences* 20.19, p. 4661. ISSN: 1422-0067. DOI: 10.3390/ijms20194661. pmid: 31547024.

Mudher, Amrit et al. (Dec. 19, 2017). "What Is the Evidence That Tau Pathology Spreads through Prion-like Propagation?" In: *Acta Neuropathologica Communications* 5.1, p. 99. ISSN: 2051-5960. DOI: 10.1186/s40478-017-0488-7. pmid: 29258615.

Mufson, Elliott et al. (Mar. 12, 2015). "Hippocampal Plasticity During the Progression of Alzheimer's Disease". In: *Neuroscience* 309. DOI: 10.1016/j.neuroscience.2015.03.006.

Mukrasch, Marco D. et al. (Feb. 17, 2009). "Structural Polymorphism of 441-Residue Tau at Single Residue Resolution". In: *PLOS Biology* 7.2, e1000034. ISSN: 1545-7885. DOI: 10.1371/journal.pbio.1000034.

Murthy, Anastasia C. et al. (July 2019). "Molecular Interactions Underlying Liquid-Liquid Phase Separation of the FUS Low Complexity Domain". In: *Nature structural & molecular biology* 26.7, pp. 637–648. ISSN: 1545-9993. DOI: 10.1038/s41594-019-0250-x. pmid: 31270472.

Nagel, Alexis K. et al. (Apr. 2013). "Identification of O-Linked N-Acetylglucosamine (O-GlcNAc)-Modified Osteoblast Proteins by Electron Transfer Dissociation Tandem Mass Spectrometry Reveals Proteins Critical for Bone Formation". In: *Molecular & Cellular Proteomics : MCP* 12.4, pp. 945–955. ISSN: 1535-9476. DOI: 10.1074/mcp.M112.026633. pmid: 23443134.

Nam, Won-Hee and Young Pyo Choi (Nov. 14, 2018). "In Vitro Generation of Tau Aggregates Conformationally Distinct from Parent Tau Seeds of Alzheimer's Brain". In: *Prion* 13.1, pp. 1–12. ISSN: 1933-6896. DOI: 10.1080/19336896.2018.1545524. pmid: 30422056.

Narasimhan, Sneha et al. (Nov. 22, 2017). "Pathological Tau Strains from Human Brains Recapitulate the Diversity of Tauopathies in Nontransgenic Mouse Brain". In: *Journal of Neuroscience* 37.47, pp. 11406–11423. ISSN: 0270-6474, 1529-2401. DOI: 10.1523/JNEUROSCI.1230-17.2017. pmid: 29054878.

Neddens, Joerg et al. (June 29, 2018). "Phosphorylation of Different Tau Sites during Progression of Alzheimer's Disease". In: *Acta Neuropathologica Communications* 6, p. 52. ISSN: 2051-5960. DOI: 10.1186/s40478-018-0557-6. pmid: 29958544.

Ng, Bryan et al. (Feb. 15, 2024). "Tau Depletion in Human Neurons Mitigates Aβ-driven Toxicity". In: *Molecular Psychiatry*, pp. 1–12. ISSN: 1476-5578. DOI: 10.1038/s41380-024-02463-2.

Ngandu, T. et al. (Oct. 2, 2007). "Education and Dementia". In: *Neurology* 69.14, pp. 1442–1450. DOI: 10.1212/01.wnl.0000277456.29440.16.

Nott, Timothy J. et al. (Mar. 5, 2015). "Phase Transition of a Disordered Nuage Protein Generates Environmentally Responsive Membraneless Organelles". In: *Molecular Cell* 57.5, pp. 936–947. ISSN: 1097-4164. DOI: 10.1016/j.molcel.2015.01.013. pmid: 25747659.

O'Brien, Richard J. and Philip C. Wong (2011). "Amyloid Precursor Protein Processing and Alzheimer's Disease". In: *Annual Review of Neuroscience* 34, pp. 185–204. ISSN: 1545-4126. DOI: 10.1146/annurev-neuro-061010-113613. pmid: 21456963.

O'Donnell, Niall et al. (Feb. 2004). "Ogt-Dependent X-chromosome-linked Protein Glycosylation Is a Requisite Modification in Somatic Cell Function and Embryo Viability". In: *Molecular and Cellular Biology* 24.4, pp. 1680–1690. ISSN: 0270-7306. DOI: 10.1128/MCB.24.4.1680-1690.2004. pmid: 14749383.

O'Neal, Mary A. (Jan. 5, 2024). "Women and the Risk of Alzheimer's Disease". In: *Frontiers in Global Women's Health* 4. ISSN: 2673-5059. DOI: 10.3389/fgwh.2023.1324522.

Ozawa, Yuhei et al. (Dec. 28, 2022). "Classification of Proteins Inducing Liquid–Liquid Phase Separation: Sequential, Structural and Functional Characterization". In: *Journal of Biochemistry* 173.4, pp. 255–264. ISSN: 0021-924X. DOI: 10.1093/jb/mvac106. pmid: 36575582.

Pádua, Mafalda Soares et al. (Jan. 2024). "Insights on the Use of Transgenic Mice Models in Alzheimer's Disease Research". In: *International Journal of Molecular Sciences* 25.5 (5), p. 2805. ISSN: 1422-0067. DOI: 10.3390/ijms25052805.

Park, Jinsu et al. (June 2020). "O-GlcNAcylation as a Therapeutic Target for Alzheimer's Disease". In: *Neuromolecular Medicine* 22.2, pp. 171–193. ISSN: 1559-1174. DOI: 10.1007/s12017-019-08584-0. pmid: 31894464.

Park, Seoyoung et al. (June 2018). "Degradation or Aggregation: The Ramifications of Post-Translational Modifications on Tau". In: *BMB reports* 51.6, pp. 265–273. ISSN: 1976-670X. DOI: 10.5483/bmbrep.2018.51.6.077. pmid: 29661268.

Patel, Avinash et al. (Aug. 27, 2015). "A Liquid-to-Solid Phase Transition of the ALS Protein FUS Accelerated by Disease Mutation". In: *Cell* 162.5, pp. 1066–1077. ISSN: 1097-4172. DOI: 10.1016/j.cell.2015.07.047. pmid: 26317470.

Pathak, Shalini et al. (Sept. 2015). "The Active Site of O-GlcNAc Transferase Imposes Constraints on Substrate Sequence". In: *Nature structural & molecular biology* 22.9, pp. 744–750. ISSN: 1545-9993. DOI: 10.1038/nsmb.3063. pmid: 26237509.

Paul, Pallabi Sil et al. (Jan. 2, 2024). "Native PLGA Nanoparticles Attenuate Aβ-seed Induced Tau Aggregation under in Vitro Conditions: Potential Implication in Alzheimer's Disease Pathology". In: *Scientific Reports* 14.1, p. 144. ISSN: 2045-2322. DOI: 10.1038/s41598-023-50465-x.

Pelech, S. L. (1995). "Networking with Proline-Directed Protein Kinases Implicated in Tau Phosphorylation". In: *Neurobiology of Aging* 16.3, 247–256; discussion 257–261. ISSN: 0197-4580. DOI: 10.1016/0197-4580(94)00187-6. pmid: 7566335.

Peng, Pei-Hua, Kai-Wen Hsu, and Kou-Juey Wu (Aug. 15, 2021). "Liquid-Liquid Phase Separation (LLPS) in Cellular Physiology and Tumor Biology". In: *American Journal of Cancer Research* 11.8, pp. 3766–3776. ISSN: 2156-6976. pmid: 34522448. URL: https://www.ncbi.nlm.nih.gov/pmc/articles/PMC8414392/.

Perea, Juan Ramón, Marta Bolós, and Jesús Avila (Oct. 14, 2020). "Microglia in Alzheimer's Disease in the Context of Tau Pathology". In: *Biomolecules* 10.10, p. 1439. ISSN: 2218-273X. DOI: 10.3390/biom10101439. pmid: 33066368.

Perry, G et al. (May 1987). "Ubiquitin Is Detected in Neurofibrillary Tangles and Senile Plaque Neurites of Alzheimer Disease Brains." In: *Proceedings of the National Academy of Sciences* 84.9, pp. 3033–3036. ISSN: 0027-8424, 1091-6490. DOI: 10.1073/pnas.84.9.3033.

Piguet, O. et al. (Aug. 2009). "White Matter Loss in Healthy Ageing: A Postmortem Analysis". In: *Neurobiology of Aging* 30.8, pp. 1288–1295. ISSN: 1558-1497. DOI: 10.1016/j.neurobiolaging.2007.10.015. pmid: 18077060.

Pippin, Micah M. and Vikas Gupta (2024). "Pick Disease". In: *StatPearls*. Treasure Island (FL): StatPearls Publishing. pmid: 32965897. URL: http://www.ncbi.nlm.nih.gov/books/NBK562226/.

Podcasy, Jessica L. and C. Neill Epperson (Dec. 2016). "Considering Sex and Gender in Alzheimer Disease and Other Dementias". In: *Dialogues in Clinical Neuroscience* 18.4, pp. 437–446. ISSN: 1294-8322. pmid: 28179815. URL: https://www.ncbi.nlm.nih.gov/pmc/articles/PMC5286729/.

Pooler, Amy M. and Diane P. Hanger (July 26, 2010). "Functional Implications of the Association of Tau with the Plasma Membrane". In: *Biochemical Society Transactions* 38.4, pp. 1012–1015. ISSN: 0300-5127. DOI: 10.1042/BST0381012.

Pooler, Amy M. et al. (Feb. 1, 2012). "Dynamic Association of Tau with Neuronal Membranes Is Regulated by Phosphorylation". In: *Neurobiology of Aging* 33.2, 431.e27–431.e38. ISSN: 0197-4580. DOI: 10.1016/j.neurobiolaging.2011.01.005.

Pothin, Elodie, Dominique Lesuisse, and Pierre Lafaye (Sept. 30, 2020). "Brain Delivery of Single-Domain Antibodies: A Focus on VHH and VNAR". In: *Pharmaceutics* 12.10, p. 937. ISSN: 1999-4923. DOI: 10.3390/pharmaceutics12100937. pmid: 33007904.

Poudyal, Manisha et al. (Oct. 4, 2023). "Intermolecular Interactions Underlie Protein/Peptide Phase Separation Irrespective of Sequence and Structure at Crowded Milieu". In: *Nature Communications* 14.1, p. 6199. ISSN: 2041-1723. DOI: 10.1038/s41467-023-41864-9.

Powell, Wyatt C. et al. (Mar. 12, 2024). *Post-Translational Modifications Control Phase Transitions of Tau*. DOI: 10.1101/2024.03.08.583040. Pre-published.

Pratt, Matthew R. and David J. Vocadlo (Dec. 1, 2023). "Understanding and Exploiting the Roles of O-GlcNAc in Neurodegenerative Diseases". In: *Journal of Biological Chemistry* 299.12. ISSN: 0021-9258, 1083-351X. DOI: 10.1016/j.jbc.2023.105411. pmid: 37918804.

Probst, A. et al. (Mar. 1, 2000). "Axonopathy and Amyotrophy in Mice Transgenic for Human Four-Repeat Tau Protein". In: *Acta Neuropathologica* 99.5, pp. 469–481. ISSN: 1432-0533. DOI: 10.1007/s004010051148.

Protein Structural Analysis (2019). URL: https://www.sigmaaldrich.com/LB/en/applications/protein-biology/protein-structural-analysis.

Protéine globulaire (2024). *Protéine globulaire : définition et explications*. AquaPortail. URL: https://www.aquaportail.com/dictionnaire/definition/6982/proteine-globulaire.

Qiang, Liang et al. (July 9, 2018). "Tau Does Not Stabilize Axonal Microtubules but Rather Enables Them to Have Long Labile Domains". In: *Current Biology* 28.13, 2181–2189.e4. ISSN: 0960-9822. DOI: 10.1016/j.cub.2018.05.045. pmid: 30008334.

Raber, Jacob, Yadong Huang, and J. Wesson Ashford (2004). "ApoE Genotype Accounts for the Vast Majority of AD Risk and AD Pathology". In: *Neurobiology of Aging* 25.5, pp. 641–650. ISSN: 0197-4580. DOI: 10.1016/j.neurobiolaging.2003.12.023. pmid: 15172743.

Ramírez-Clavijo, Sandra and Gladis Montoya-Ortíz (July 18, 2013). "Gene Expression and Regulation". In: *Autoimmunity: From Bench to Bedside [Internet]*. El Rosario University Press. URL: https://www.ncbi.nlm.nih.gov/books/NBK459456/.

Ramirez-Rios, Sacnicte et al. (Oct. 2016). "Tau Antagonizes End-Binding Protein Tracking at Microtubule Ends through a Phosphorylation-Dependent Mechanism". In: *Molecular Biology of the Cell* 27.19, pp. 2924–2934. ISSN: 1059-1524. DOI: 10.1091/mbc.E16-01-0029.

Rankin, Carolyn A, Qian Sun, and Truman C Gamblin (June 28, 2007). "Tau Phosphorylation by GSK-3β Promotes Tangle-like Filament Morphology". In: *Molecular Neurodegeneration* 2, p. 12. ISSN: 1750-1326. DOI: 10.1186/1750-1326-2-12. pmid: 17598919.

Rawat, Priyanka et al. (Jan. 2022). "Phosphorylated Tau in Alzheimer's Disease and Other Tauopathies". In: *International Journal of Molecular Sciences* 23.21 (21), p. 12841. ISSN: 1422-0067. DOI: 10.3390/ijms232112841.

rédaction, la (2019). *Définition | Prion | Futura Santé*. Futura. URL: https://www.futura-sciences.com/sante/definitions/medecine-prion-234/.

Reynolds, C. H. et al. (Apr. 2000). "Phosphorylation Sites on Tau Identified by Nanoelectrospray Mass Spectrometry: Differences in Vitro between the Mitogen-Activated Protein Kinases ERK2, c-Jun N-terminal Kinase and P38, and Glycogen Synthase Kinase-3beta". In: *Journal of Neurochemistry* 74.4, pp. 1587–1595. ISSN: 0022-3042. DOI: 10.1046/j.1471-4159.2000.0741587.x. pmid: 10737616.

Riley, Kalen J., Brian D. Graner, and Michael C. Veronesi (July–Aug. 2022). "The Tauopathies: Neuroimaging Characteristics and Emerging Experimental Therapies". In: *Journal of Neuroimaging* 32.4, p. 565. DOI: 10.1111/jon.13001. pmid: 35470528.

Risk Factors for Alzheimer's Disease | Alzheimer's Society (Apr. 13, 2023). URL: https://www.alzheimers.org.uk/about-dementia/types-dementia/who-gets-alzheimers-disease.

Ross, Kerry L., Charity N. Davis, and Judith L. Fridovich-Keil (Sept. 1, 2004). "Differential Roles of the Leloir Pathway Enzymes and Metabolites in Defining Galactose Sensitivity in Yeast". In: *Molecular Genetics and Metabolism*. ASHG 2004 Meeting Toronto 83.1, pp. 103–116. ISSN: 1096-7192. DOI: 10.1016/j.ymgme.2004.07.005.

Saito, Taro et al. (Nov. 1, 2021). "Disulfide Bond Formation in Microtubule-Associated Tau Protein Promotes Tau Accumulation and Toxicity in Vivo". In: *Human Molecular Genetics* 30.21, pp. 1955–1967. ISSN: 0964-6906. DOI: 10.1093/hmg/ddab162.

Sala-Jarque, Julia et al. (Jan. 2022). "Towards a Mechanistic Model of Tau-Mediated Pathology in Tauopathies: What Can We Learn from Cell-Based In Vitro Assays?" In: *International Journal of Molecular Sciences* 23.19 (19), p. 11527. ISSN: 1422-0067. DOI: 10.3390/ijms231911527.

Sanvictores, Terrence and Fabiola Farci (2024). "Biochemistry, Primary Protein Structure". In: *StatPearls*. Treasure Island (FL): StatPearls Publishing. pmid: 33232013. URL: http://www.ncbi.nlm.nih.gov/books/NBK564343/.

Saraceno, G. Ezequiel et al. (Apr. 9, 2018). "Estradiol Activates PI3K/Akt/GSK3 Pathway Under Chronic Neurodegenerative Conditions Triggered by Perinatal Asphyxia". In: *Frontiers in Pharmacology* 9. ISSN: 1663-9812. DOI: 10.3389/fphar.2018.00335.

Savastano, Adriana et al. (Dec. 3, 2020). "Solid-State NMR Investigation of the Involvement of the P2 Region in Tau Amyloid Fibrils". In: *Scientific Reports* 10, p. 21210. ISSN: 2045-2322. DOI: 10.1038/s41598-020-78161-0. pmid: 33273615.

Sayas, C. L, J Ávila, and F Wandosell (May 23, 2002). "Regulation of Neuronal Cytoskeleton by Lysophosphatidic Acid: Role of GSK-3". In: *Biochimica et Biophysica Acta (BBA) - Molecular and Cell Biology of Lipids*. Lysolipid Mediators in Cell Signalling and Disease 1582.1, pp. 144–153. ISSN: 1388-1981. DOI: 10.1016/S1388-1981(02)00149-X.

Sayas, C. Laura et al. (Jan. 22, 2019). "Role of Tau N-terminal Motif in the Secretion of Human Tau by End Binding Proteins". In: *PLOS ONE* 14.1, e0210864. ISSN: 1932-6203. DOI: 10.1371/journal.pone.0210864.

Sayas, Carmen Laura and Jesús Ávila (Apr. 2021). "GSK-3 and Tau: A Key Duet in Alzheimer's Disease". In: *Cells* 10.4 (4), p. 721. ISSN: 2073-4409. DOI: 10.3390/cells10040721.

Schmand, Ben et al. (Sept. 1, 1997). "Low Education Is a Genuine Risk Factor for Accelerated Memory Decline and Dementia". In: *Journal of Clinical Epidemiology* 50.9, pp. 1025–1033. ISSN: 0895-4356. DOI: 10.1016/S0895-4356(97)00121-2.

Schneider, A. et al. (Mar. 1, 1999). "Phosphorylation That Detaches Tau Protein from Microtubules (Ser262, Ser214) Also Protects It against Aggregation into Alzheimer Paired Helical Filaments". In: *Biochemistry* 38.12, pp. 3549–3558. ISSN: 0006-2960. DOI: 10.1021/bi981874p.

Schoonhoven, Deborah N et al. (June 5, 2023). "Tau Protein Spreads through Functionally Connected Neurons in Alzheimer's Disease: A Combined MEG/PET Study". In: *Brain* 146.10, pp. 4040–4054. ISSN: 0006-8950. DOI: 10.1093/brain/awad189. pmid: 37279597.

Scialò, Carlo et al. (Mar. 2019). "Prion and Prion-Like Protein Strains: Deciphering the Molecular Basis of Heterogeneity in Neurodegeneration". In: *Viruses* 11.3 (3), p. 261. ISSN: 1999-4915. DOI: 10.3390/v11030261.

Serrano-Pozo, Alberto et al. (Sept. 2011). "Neuropathological Alterations in Alzheimer Disease". In: *Cold Spring Harbor Perspectives in Medicine* 1.1, a006189. ISSN: 2157-1422. DOI: 10.1101/cshperspect.a006189. pmid: 22229116.

Shafi, R. et al. (May 23, 2000). "The O-GlcNAc Transferase Gene Resides on the X Chromosome and Is Essential for Embryonic Stem Cell Viability and Mouse Ontogeny". In: *Proceedings of the National Academy of Sciences of the United States of America* 97.11, pp. 5735–5739. ISSN: 0027-8424. DOI: 10.1073/pnas.100471497. pmid: 10801981.

Shamir, Dov B. et al. (Nov. 26, 2020). "Dynamics of Internalization and Intracellular Interaction of Tau Antibodies and Human Pathological Tau Protein in a Human Neuron-Like Model". In: *Frontiers in Neurology* 11. ISSN: 1664-2295. DOI: 10.3389/fneur.2020.602292.

Shammas, Sarah L. et al. (Apr. 30, 2015). "A Mechanistic Model of Tau Amyloid Aggregation Based on Direct Observation of Oligomers". In: *Nature Communications* 6.1, p. 7025. ISSN: 2041-1723. DOI: 10.1038/ncomms8025.

Shen, Yufeng et al. (Sept. 2, 2011). "Effectiveness of CID, HCD, and ETD with FT MS/MS for Degradomic-Peptidomic Analysis: Comparison of Peptide Identification Methods". In: *Journal of proteome research* 10.9, pp. 3929–3943. ISSN: 1535-3893. DOI: 10.1021/pr200052c. pmid: 21678914.

Shi, Jianhua et al. (July 30, 2012). "Diverse Regulation of AKT and GSK-3β by O-GlcNAcylation in Various Types of Cells". In: *FEBS letters* 586.16, pp. 2443–2450. ISSN: 0014-5793. DOI: 10.1016/j.febslet.2012.05.063. pmid: 22687243.

Shi, Yang et al. (May 1, 2021a). "Cryo-EM Structures of Tau Filaments from Alzheimer's Disease with PET Ligand APN-1607". In: *Acta Neuropathologica* 141.5, pp. 697–708. ISSN: 1432-0533. DOI: 10.1007/s00401-021-02294-3.

Shi, Yang et al. (Oct. 2021b). "Structure-Based Classification of Tauopathies". In: *Nature* 598.7880, pp. 359–363. ISSN: 1476-4687. DOI: 10.1038/s41586-021-03911-7. pmid: 34588692.

Shulman, Joshua M. et al. (Feb. 11, 2011). "Functional Screening of Alzheimer Pathology Genome-Wide Association Signals in Drosophila". In: *American Journal of Human Genetics* 88.2, pp. 232–238. ISSN: 1537-6605. DOI: 10.1016/j.ajhg.2011.01.006. pmid: 21295279.

Siddiqua, Ayisha et al. (June 20, 2012). "Conformational Basis for Asymmetric Seeding Barrier in Filaments of Three- and Four-Repeat Tau". In: *Journal of the American Chemical Society* 134.24, pp. 10271–10278. ISSN: 0002-7863. DOI: 10.1021/ja303498q.

Sigurdsson, Einar M. (2018). "Tau Immunotherapies for Alzheimer's Disease and Related Tauopathies: Progress and Potential Pitfalls." In: *Journal of Alzheimer's disease : JAD* 64 (Suppl 1), S555–S565. ISSN: 1387-2877. DOI: 10.3233/JAD-179937. pmid: 29865056.

Sillen, Alain (2007). "NMR investigation of the interaction between the neuronal protein tau and the microtubules". In: 46.11, pp. 3055–3064. ISSN: 0006-2960. DOI: 10.1021/bi061920i. pmid: 31556570.

Silva, Marcos Vinícius Ferreira et al. (May 9, 2019). "Alzheimer's Disease: Risk Factors and Potentially Protective Measures". In: *Journal of Biomedical Science* 26.1, p. 33. ISSN: 1423-0127. DOI: 10.1186/s12929-019-0524-y.

Singh, Toolsee J. et al. (Sept. 1, 1996). "Non-Proline-Dependent Protein Kinases Phosphorylate Several Sites Found in Tau from Alzheimer Disease Brain". In: *Molecular and Cellular Biochemistry* 154.2, pp. 143–151. ISSN: 1573-4919. DOI: 10.1007/BF00226782.

Smet-Nocca, Caroline et al. (May 2011). "Identification of O-GlcNAc Sites within Peptides of the Tau Protein and Their Impact on Phosphorylation". In: *Molecular bioSystems* 7.5, pp. 1420–1429. ISSN: 1742-2051. DOI: 10.1039/c0mb00337a. pmid: 21327254.

Sonenberg, Nahum and Alan G. Hinnebusch (Feb. 20, 2009). "Regulation of Translation Initiation in Eukaryotes: Mechanisms and Biological Targets". In: *Cell* 136.4, pp. 731–745. ISSN: 0092-8674. DOI: 10.1016/j.cell.2009.01.042. pmid: 19239892.

Song, Ha-Lim et al. (Apr. 17, 2023). "Monoclonal Antibody Y01 Prevents Tauopathy Progression Induced by Lysine 280–Acetylated Tau in Cell and Mouse Models". In: *The Journal of Clinical Investigation* 133.8. ISSN: 0021-9738. DOI: 10.1172/JCI156537. pmid: 0.

Spittaels, Kurt et al. (Dec. 1, 1999). "Prominent Axonopathy in the Brain and Spinal Cord of Transgenic Mice Overexpressing Four-Repeat Human Tau Protein". In: *The American Journal of Pathology* 155.6, pp. 2153–2165. ISSN: 0002-9440. DOI: 10.1016/S0002-9440(10)65533-2.

Stambolic, V. and J. R. Woodgett (Nov. 1, 1994). "Mitogen Inactivation of Glycogen Synthase Kinase-3 Beta in Intact Cells via Serine 9 Phosphorylation". In: *The Biochemical Journal* 303 (Pt 3) (Pt 3), pp. 701–704. ISSN: 0264-6021. DOI: 10.1042/bj3030701. pmid: 7980435.

Stamos, Jennifer L et al. (Mar. 18, 2014). "Structural Basis of GSK-3 Inhibition by N-terminal Phosphorylation and by the Wnt Receptor LRP6". In: *eLife* 3, e01998. ISSN: 2050-084X. DOI: 10.7554/eLife.01998. pmid: 24642411.

Stephen, Hannah M, Trevor M Adams, and Lance Wells (Jan. 22, 2021). "Regulating the Regulators: Mechanisms of Substrate Selection of the O-GlcNAc Cycling Enzymes OGT and OGA". In: *Glycobiology* 31.7, pp. 724–733. ISSN: 0959-6658. DOI: 10.1093/glycob/cwab005. pmid: 33498085.

Strang, Kevin H., Todd E. Golde, and Benoit I. Giasson (July 1, 2019). "MAPT Mutations, Tauopathy, and Mechanisms of Neurodegeneration". In: *Laboratory Investigation* 99.7, pp. 912–928. ISSN: 0023-6837, 1530-0307. DOI: 10.1038/s41374-019-0197-x.

Stroo, Esther et al. (Feb. 14, 2017). "Cellular Regulation of Amyloid Formation in Aging and Disease". In: *Frontiers in Neuroscience* 11. ISSN: 1662-453X. DOI: 10.3389/fnins.2017.00064.

Structure des protéines (2024). URL: https://fr.wikipedia.org/w/index.php?title=Structure_des_prot%C3%A9ines&oldid=216698463.

Sui, Dexin, Mengyu Liu, and Min-Hao Kuo (Jan. 2, 2015). "In Vitro Aggregation Assays Using Hyperphosphorylated Tau Protein". In: *Journal of Visualized Experiments : JoVE* 95, p. 51537. ISSN: 1940-087X. DOI: 10.3791/51537. pmid: 25590418.

Sun, Emily et al. (Jan. 2022). "The Pivotal Role of NF-kB in the Pathogenesis and Therapeutics of Alzheimer's Disease". In: *International Journal of Molecular Sciences* 23.16 (16), p. 8972. ISSN: 1422-0067. DOI: 10.3390/ijms23168972.

Sutherland, Calum (2011). "What Are the Bona Fide GSK3 Substrates?" In: *International Journal of Alzheimer's Disease* 2011, p. 505607. ISSN: 2090-0252. DOI: 10.4061/2011/505607. pmid: 21629754.

Tagai, Kenji et al. (Jan. 6, 2021). "High-Contrast *In Vivo* Imaging of Tau Pathologies in Alzheimer's and Non-Alzheimer's Disease Tauopathies". In: *Neuron* 109.1, 42–58.e8. ISSN: 0896-6273. DOI: 10.1016/j.neuron.2020.09.042.

Tak, HyeJin et al. (Dec. 2, 2013). "Bimolecular Fluorescence Complementation; Lighting-Up Tau-Tau Interaction in Living Cells". In: *PLoS ONE* 8.12, e81682. ISSN: 1932-6203. DOI: 10.1371/journal.pone.0081682. pmid: 24312574.

Takeda, Shuko et al. (Oct. 13, 2015). "Neuronal Uptake and Propagation of a Rare Phosphorylated High-Molecular-Weight Tau Derived from Alzheimer's Disease Brain". In: *Nature Communications* 6.1, p. 8490. ISSN: 2041-1723. DOI: 10.1038/ncomms9490.

Tamvaka, Nicole et al. (June 2023). "Pick's Disease, Seeding an Answer to the Clinical Diagnosis Conundrum". In: *Biomedicines* 11.6 (6), p. 1646. ISSN: 2227-9059. DOI: 10.3390/biomedicines1106164

The McGurk Lab (2018). The McGurk Lab. URL: https://leeannemcgurk.wordpress.com/liquid-liquid-phase-separation/.

Theillet, Francois-Xavier et al. (Nov. 1, 2012). "Cell Signaling, Post-Translational Protein Modifications and NMR Spectroscopy". In: *Journal of Biomolecular NMR* 54.3, pp. 217–236. ISSN: 1573-5001. DOI: 10.1007/s10858-012-9674-x.

Therapeutics Search | ALZFORUM (2019). URL: https://www.alzforum.org/therapeutics/search?fda_statuses=&target_types%5B%5D=177&therapy_types%5B%5D=161&therapy_types%5B%5D=162&conditions%5B%5D=145&keywords-entry=&keywords=.

Therriault, Joseph et al. (June 2022). "Biomarker Modeling of Alzheimer's Disease Using PET-based Braak Staging". In: *Nature Aging* 2.6, pp. 526–535. ISSN: 2662-8465. DOI: 10.1038/s43587-022-00204-0.

Toleman, Clifford et al. (Dec. 17, 2004). "Characterization of the Histone Acetyltransferase (HAT) Domain of a Bifunctional Protein with Activable *O*-GlcNAcase and HAT Activities*169". In: *Journal of Biological Chemistry* 279.51, pp. 53665–53673. ISSN: 0021-9258. DOI: 10.1074/jbc.M410406200.

Tomé, Sandra O. et al. (Apr. 29, 2020). "Distinct Molecular Patterns of TDP-43 Pathology in Alzheimer's Disease: Relationship with Clinical Phenotypes". In: *Acta Neuropathologica Communications* 8, p. 61. ISSN: 2051-5960. DOI: 10.1186/s40478-020-00934-5. pmid: 32349792.

Tong, Xuhui et al. (July 8, 2022). "Liquid–Liquid Phase Separation in Tumor Biology". In: *Signal Transduction and Targeted Therapy* 7.1, pp. 1–22. ISSN: 2059-3635. DOI: 10.1038/s41392-022-01076-x.

Toral-Rios, Danira et al. (Mar. 17, 2020). "GSK3β and Tau Protein in Alzheimer's Disease and Epilepsy". In: *Frontiers in Cellular Neuroscience* 14. ISSN: 1662-5102. DOI: 10.3389/fncel.2020.00019.

Torres, C. R. and G. W. Hart (Mar. 10, 1984). "Topography and Polypeptide Distribution of Terminal N-acetylglucosamine Residues on the Surfaces of Intact Lymphocytes. Evidence for O-linked GlcNAc". In: *The Journal of Biological Chemistry* 259.5, pp. 3308–3317. ISSN: 0021-9258. pmid: 6421821.

Townsend, David et al. (Oct. 20, 2020). "Aggregation Kinetics and Filament Structure of a Tau Fragment Are Influenced by the Sulfation Pattern of the Cofactor Heparin". In: *Biochemistry* 59.41, pp. 4003–4014. ISSN: 0006-2960. DOI: 10.1021/acs.biochem.0c00443. pmid: 32954725.

Transmission Electron Microscopy | Nanoscience Instruments (2024). URL: https://www.nanoscience.com/techniques/transmission-electron-microscopy/.

Tripathi, Timir and Heena Khan (Feb. 4, 2020). "Direct Interaction between the β-Amyloid Core and Tau Facilitates Cross-Seeding: A Novel Target for Therapeutic Intervention". In: *Biochemistry* 59.4, pp. 341–342. ISSN: 0006-2960. DOI: 10.1021/acs.biochem.9b01087.

Trivedi, Rakesh and Hampapathalu Adimurthy Nagarajaram (Nov. 14, 2022). "Intrinsically Disordered Proteins: An Overview". In: *International Journal of Molecular Sciences* 23.22, p. 14050. ISSN: 1422-0067. DOI: 10.3390/ijms232214050. pmid: 36430530.

Tseng, Jui-Heng et al. (Apr. 27, 2021). "Tau Seeds Are Subject to Aberrant Modifications Resulting in Distinct Signatures". In: *Cell Reports* 35.4, p. 109037. ISSN: 2211-1247. DOI: 10.1016/j.celrep.2021.109037. pmid: 33910013.

Tsitokana, Mireille Elodie et al. (Jan. 2023). "Targeting the Brain with Single-Domain Antibodies: Greater Potential Than Stated So Far?" In: *International Journal of Molecular Sciences* 24.3 (3), p. 2632. ISSN: 1422-0067. DOI: 10.3390/ijms24032632.

Tsui, Ka Chun et al. (July 28, 2022). "Distribution and Inter-Regional Relationship of Amyloid-Beta Plaque Deposition in a 5xFAD Mouse Model of Alzheimer's Disease". In: *Frontiers in Aging Neuroscience* 14, p. 964336. ISSN: 1663-4365. DOI: 10.3389/fnagi.2022.964336. pmid: 35966777.

Ulrich, Giorgio et al. (Dec. 7, 2018). "Phosphorylation of Nuclear Tau Is Modulated by Distinct Cellular Pathways". In: *Scientific Reports* 8.1 (1), p. 17702. ISSN: 2045-2322. DOI: 10.1038/s41598-018-36374-4.

Vernon, Robert M. and Julie D. Forman-Kay (Oct. 2019). "First-Generation Predictors of Biological Protein Phase Separation". In: *Current Opinion in Structural Biology* 58, pp. 88–96. ISSN: 1879-033X. DOI: 10.1016/j.sbi.2019.05.016. pmid: 31252218.

Walsh, Dominic M. and Dennis J. Selkoe (Apr. 2016). "A Critical Appraisal of the Pathogenic Protein Spread Hypothesis of Neurodegeneration". In: *Nature Reviews. Neuroscience* 17.4, pp. 251–260. ISSN: 1471-0048. DOI: 10.1038/nrn.2016.13. pmid: 26988744.

Wang, Y. P. et al. (June 12, 2007). "Stepwise Proteolysis Liberates Tau Fragments That Nucleate the Alzheimer-like Aggregation of Full-Length Tau in a Neuronal Cell Model". In: *Proceedings of the National Academy of Sciences* 104.24, pp. 10252–10257. DOI: 10.1073/pnas.0703676104.

Wang, Yipeng and Eckhard Mandelkow (Jan. 2016). "Tau in Physiology and Pathology". In: *Nature Reviews. Neuroscience* 17.1, pp. 5–21. ISSN: 1471-0048. DOI: 10.1038/nrn.2015.1. pmid: 26631930.

Wang, Yipeng et al. (Nov. 1, 2009). "Tau Fragmentation, Aggregation and Clearance: The Dual Role of Lysosomal Processing". In: *Human Molecular Genetics* 18.21, pp. 4153–4170. ISSN: 0964-6906. DOI: 10.1093/hmg/ddp367. pmid: 19654187.

Wang, Yipeng et al. (Jan. 13, 2017a). "The Release and Trans-Synaptic Transmission of Tau via Exosomes". In: *Molecular Neurodegeneration* 12.1, p. 5. ISSN: 1750-1326. DOI: 10.1186/s13024-016-0143-y.

— (Jan. 13, 2017b). "The Release and Trans-Synaptic Transmission of Tau via Exosomes". In: *Molecular Neurodegeneration* 12.1, p. 5. ISSN: 1750-1326. DOI: 10.1186/s13024-016-0143-y.

Wang, Zihao, Marjan Gucek, and Gerald W. Hart (Sept. 16, 2008). "Cross-Talk between GlcNAcylation and Phosphorylation: Site-Specific Phosphorylation Dynamics in Response to Globally Elevated O-GlcNAc". In: *Proceedings of the National Academy of Sciences of the United States of America* 105.37, pp. 13793–13798. ISSN: 1091-6490. DOI: 10.1073/pnas.0806216105. pmid: 18779572.

Wang, Zihao, Akhilesh Pandey, and Gerald W. Hart (Aug. 2007). "Dynamic Interplay between O-linked N-acetylglucosaminylation and Glycogen Synthase Kinase-3-Dependent Phosphorylation". In: *Molecular & cellular proteomics: MCP* 6.8, pp. 1365–1379. ISSN: 1535-9476. DOI: 10.1074/mcp.M600453-MCP200. pmid: 17507370.

Wang, Zihao et al. (Jan. 1, 2010a). "Enrichment and Site Mapping of *O*-Linked *N*-Acetylglucosamine by a Combination of Chemical/Enzymatic Tagging, Photochemical Cleavage, and Electron Transfer Dissociation Mass Spectrometry*". In: *Molecular & Cellular Proteomics* 9.1, pp. 153–160. ISSN: 1535-9476. DOI: 10.1074/mcp.M900268-MCP200.

Wang, Zihao et al. (Jan. 12, 2010b). "Extensive Crosstalk Between O-GlcNAcylation and Phosphorylation Regulates Cytokinesis". In: *Science Signaling* 3.104, ra2–ra2. DOI: 10.1126/scisignal.2000526.

Wegmann, Susanne et al. (Jan. 22, 2013). "The Fuzzy Coat of Pathological Human Tau Fibrils Is a Two-Layered Polyelectrolyte Brush". In: *Proceedings of the National Academy of Sciences* 110.4, E313–E321. DOI: 10.1073/pnas.1212100110.

Wegmann, Susanne et al. (Dec. 14, 2015). "Removing Endogenous Tau Does Not Prevent Tau Propagation yet Reduces Its Neurotoxicity". In: *The EMBO journal* 34.24, pp. 3028–3041. ISSN: 1460-2075. DOI: 10.15252/embj.201592748. pmid: 26538322.

Wegmann, Susanne et al. (Apr. 3, 2018). "Tau Protein Liquid–Liquid Phase Separation Can Initiate Tau Aggregation". In: *The EMBO Journal* 37.7, e98049. ISSN: 0261-4189. DOI: 10.15252/embj.201798049. pmid: 29472250.

Weickert, S. et al. (Mar. 13, 2020). "The Mechanism of Hsp90-induced Oligomerizaton of Tau". In: *Science Advances* 6.11, eaax6999. DOI: 10.1126/sciadv.aax6999.

Wells, L., K. Vosseller, and G. W. Hart (Mar. 23, 2001). "Glycosylation of Nucleocytoplasmic Proteins: Signal Transduction and O-GlcNAc". In: *Science (New York, N.Y.)* 291.5512, pp. 2376–2378. ISSN: 0036-8075. DOI: 10.1126/science.1058714. pmid: 11269319.

Wen, Jitao et al. (Aug. 25, 2021). "Conformational Expansion of Tau in Condensates Promotes Irreversible Aggregation". In: *Journal of the American Chemical Society* 143.33, pp. 13056–13064. ISSN: 0002-7863. DOI: 10.1021/jacs.1c03078.

Wenger, Kathrin et al. (Feb. 2, 2023). "Common Mouse Models of Tauopathy Reflect Early but Not Late Human Disease". In: *Molecular Neurodegeneration* 18.1, p. 10. ISSN: 1750-1326. DOI: 10.1186/s13024-023-00601-y.

What Is Alzheimer's Disease? (2019). National Institute on Aging. URL: https://www.nia.nih.gov/health/alzheimers-and-dementia/what-alzheimers-disease.

Wischik, C M et al. (June 1988). "Isolation of a Fragment of Tau Derived from the Core of the Paired Helical Filament of Alzheimer Disease." In: *Proceedings of the National Academy of Sciences* 85.12, pp. 4506–4510. DOI: 10.1073/pnas.85.12.4506.

Women and Alzheimer's (2019). Alzheimer's Disease and Dementia. URL: https://alz.org/alzheimers-dementia/what-is-alzheimers/women-and-alzheimer-s.

Women and Alzheimer's Disease | Lifespan (2024). URL: https://www.lifespan.org/lifespan-living/women-and-alzheimers-disease.

Woodgett, James R. (Sept. 18, 2001). "Judging a Protein by More Than Its Name: GSK-3". In: *Science's STKE* 2001.100, re12–re12. DOI: 10.1126/stke.2001.100.re12.

Wouters, Yessica et al. (Oct. 3, 2022). "VHHs as Tools for Therapeutic Protein Delivery to the Central Nervous System". In: *Fluids and Barriers of the CNS* 19.1, p. 79. ISSN: 2045-8118. DOI: 10.1186/s12987-022-00374-4.

Wu, Hsin-Yi et al. (Dec. 8, 2014). "Characterization and Identification of Protein O-GlcNAcylation Sites with Substrate Specificity". In: *BMC Bioinformatics* 15.16, S1. ISSN: 1471-2105. DOI: 10.1186/1471-2105-15-S16-S1.

Wu, Jessica W. et al. (Aug. 2016). "Neuronal Activity Enhances Tau Propagation and Tau Pathology in Vivo". In: *Nature Neuroscience* 19.8, pp. 1085–1092. ISSN: 1546-1726. DOI: 10.1038/nn.4328. pmid: 27322420.

Wulff-Fuentes, Eugenia et al. (Jan. 21, 2021). "The Human O-GlcNAcome Database and Meta-Analysis". In: *Scientific Data* 8.1, p. 25. ISSN: 2052-4463. DOI: 10.1038/s41597-021-00810-4.

Xia, Yuxing, Stefan Prokop, and Benoit I. Giasson (Dec. 2021). ""Don't Phos Over Tau": Recent Developments in Clinical Biomarkers and Therapies Targeting Tau Phosphorylation in Alzheimer's Disease and Other Tauopathies". In: *Molecular Neurodegeneration* 16.1 (1), pp. 1–19. ISSN: 1750-1326. DOI: 10.1186/s13024-021-00460-5.

Xu, Senhan et al. (2021). "MS-based Proteomics for Comprehensive Investigation of Protein *O* -GlcNAcylation". In: *Molecular Omics* 17.2, pp. 186–196. ISSN: 2515-4184. DOI: 10.1039/D1MO00025J.

Xu, Yin, Heidi Martini-Stoica, and Hui Zheng (Apr. 26, 2016). "A Seeding Based Cellular Assay of Tauopathy". In: *Molecular Neurodegeneration* 11.1, p. 32. ISSN: 1750-1326. DOI: 10.1186/s13024-016-0100-9.

Yang, Shuai et al. (May 10, 2023). "Molecular Mechanisms and Cellular Functions of Liquid-Liquid Phase Separation during Antiviral Immune Responses". In: *Frontiers in Immunology* 14. ISSN: 1664-3224. DOI: 10.3389/fimmu.2023.1162211.

Yang, Xiaoyong et al. (Feb. 21, 2008). "Phosphoinositide Signalling Links O-GlcNAc Transferase to Insulin Resistance". In: *Nature* 451.7181, pp. 964–969. ISSN: 1476-4687. DOI: 10.1038/nature06668. pmid: 18288188.

Ye, Haiqiong et al. (Aug. 2022). "The Role of Post-Translational Modifications on the Structure and Function of Tau Protein". In: *Journal of Molecular Neuroscience* 72.8, pp. 1557–1571. ISSN: 0895-8696, 1559-1166. DOI: 10.1007/s12031-022-02002-0.

Yuzwa, Scott A. et al. (Aug. 2008). "A Potent Mechanism-Inspired O-GlcNAcase Inhibitor That Blocks Phosphorylation of Tau in Vivo". In: *Nature Chemical Biology* 4.8, pp. 483–490. ISSN: 1552-4469. DOI: 10.1038/nchembio.96. pmid: 18587388.

Yuzwa, Scott A. et al. (Feb. 26, 2012). "Increasing O-GlcNAc Slows Neurodegeneration and Stabilizes Tau against Aggregation". In: *Nature Chemical Biology* 8.4, pp. 393–399. ISSN: 1552-4469. DOI: 10.1038/nchembio.797. pmid: 22366723.

Yuzwa, Scott A. et al. (Apr. 2014). "O-GlcNAc Modification of Tau Directly Inhibits Its Aggregation without Perturbing the Conformational Properties of Tau Monomers". In: *Journal of Molecular Biology* 426.8, pp. 1736–1752. ISSN: 00222836. DOI: 10.1016/j.jmb.2014.01.004.

Zabik, Nicole L., Matthew M. Imhof, and Sanela Martic-Milne (June 2017). "Structural Evaluations of Tau Protein Conformation: Methodologies and Approaches". In: *Biochemistry and cell biology = Biochimie et biologie cellulaire* 95.3, pp. 338–349. ISSN: 0829-8211. DOI: 10.1139/bcb-2016-0227. pmid: 28278386.

Zeidan, Quira and Gerald W. Hart (Jan. 1, 2010). "The Intersections between O-GlcNAcylation and Phosphorylation: Implications for Multiple Signaling Pathways". In: *Journal of Cell Science* 123.1, pp. 13–22. ISSN: 0021-9533. DOI: 10.1242/jcs.053678.

Zhang, Huiqin et al. (May 27, 2021). "Interaction between Aβ and Tau in the Pathogenesis of Alzheimer's Disease". In: *International Journal of Biological Sciences* 17.9, pp. 2181–2192. ISSN: 1449-2288. DOI: 10.7150/ijbs.57078.

Zhang, Wenjuan et al. (Feb. 5, 2019). "Heparin-Induced Tau Filaments Are Polymorphic and Differ from Those in Alzheimer's and Pick's Diseases". In: *eLife* 8. Ed. by Nikolaus Grigorieff et al., e43584. ISSN: 2050-084X. DOI: 10.7554/eLife.43584.

Zhang, Wenjuan et al. (Apr. 9, 2020). "Novel Tau Filament Fold in Corticobasal Degeneration". In: *Nature* 580.7802, pp. 283–287. ISSN: 0028-0836, 1476-4687. DOI: 10.1038/s41586-020-2043-0.

Zhang, Yi et al. (Apr. 7, 2022). "Tauopathies: New Perspectives and Challenges". In: *Molecular Neurodegeneration* 17.1, p. 28. ISSN: 1750-1326. DOI: 10.1186/s13024-022-00533-z.

Zhao, Boxuan Simen, Ian A. Roundtree, and Chuan He (Jan. 2017). "Post-Transcriptional Gene Regulation by mRNA Modifications". In: *Nature reviews. Molecular cell biology* 18.1, pp. 31–42. ISSN: 1471-0072. DOI: 10.1038/nrm.2016.132. pmid: 27808276.

Zhao, Jianfeng, Hongrong Wu, and Xiao-Qing Tang (May 2021). "Tau Internalization: A Complex Step in Tau Propagation". In: *Ageing Research Reviews* 67, p. 101272. ISSN: 1872-9649. DOI: 10.1016/j.arr.2021.101272. pmid: 33571704.

Zheng, Hui and Edward H. Koo (Apr. 28, 2011). "Biology and Pathophysiology of the Amyloid Precursor Protein". In: *Molecular Neurodegeneration* 6.1, p. 27. ISSN: 1750-1326. DOI: 10.1186/1750-1326-6-27.

Zheng, Huiting et al. (Jan. 2024). "The Enigma of Tau Protein Aggregation: Mechanistic Insights and Future Challenges". In: *International Journal of Molecular Sciences* 25.9 (9), p. 4969. ISSN: 1422-0067. DOI: 10.3390/ijms25094969.

Zhou, Juan et al. (May 2010). "Divergent Network Connectivity Changes in Behavioural Variant Frontotemporal Dementia and Alzheimer's Disease". In: *Brain: A Journal of Neurology* 133 (Pt 5), pp. 1352–1367. ISSN: 1460-2156. DOI: 10.1093/brain/awq075. pmid: 20410145.

Zhou, Qiuzhi et al. (Apr. 1, 2022). "Human Tau Accumulation Promotes Glycogen Synthase Kinase-3β Acetylation and Thus Upregulates the Kinase: A Vicious Cycle in Alzheimer Neurodegeneration". In: *eBioMedicine* 78. ISSN: 2352-3964. DOI: 10.1016/j.ebiom.2022.103970. pmid: 35339896.

Zhu, Yanping et al. (Dec. 12, 2014). "The Emerging Link between O-GlcNAc and Alzheimer Disease". In: *The Journal of Biological Chemistry* 289.50, pp. 34472–34481. ISSN: 1083-351X. DOI: 10.1074/jbc.R114.601351. pmid: 25336656.

Zhu, Yi and Gerald W. Hart (June 1, 2021). "Targeting O-GlcNAcylation to Develop Novel Therapeutics". In: *Molecular Aspects of Medicine*. Pathophysiological Significance of Glycans and Glycosylation 79, p. 100885. ISSN: 0098-2997. DOI: 10.1016/j.mam.2020.100885.

Zupancic, Jennifer M. et al. (Aug. 9, 2023). "Quantitative Flow Cytometric Selection of Tau Conformational Nanobodies Specific for Pathological Aggregates". In: *Frontiers in Immunology* 14. ISSN: 1664-3224. DOI: 10.3389/fimmu.2023.1164080.